THE YAWING OF WIND TURBINES WITH BLADE CYCLIC PITCH VARIATION

Final Report

By
K. H. Hohenemser
A. H. P. Swift
D. A. Peters

August 1981

Washington University Technology Associates, Inc.
St. Louis, Missouri

U.S. Department of Energy

Solar Energy

DISCLAIMER

THE YAWING OF WIND TURBINES
WITH BLADE CYCLIC PITCH VARIATION

FINAL REPORT.
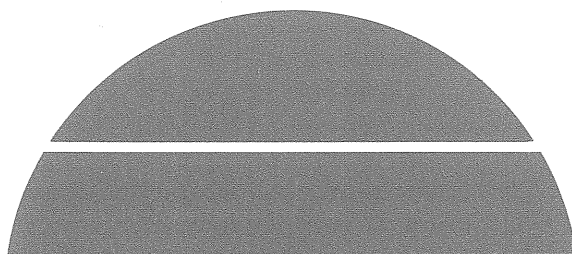
K. H. HOHENEMSER
A. H. P. SWIFT
D. A. PETERS

AUGUST 1981

WASHINGTON UNIVERSITY TECHNOLOGY
ASSOCIATES, INC., ST. LOUIS, MISSOURI

FOREWORD

Washington University Technology Associates is pleased to submit this Final Report on The Yawing of Wind Turbines With Blade Cyclic Pitch Variation under Solar Energy Research Institute Division, Subcontract No. XH-9-8085-3 and Midwest Research Institute Prime Contract No. EG-77C-01-4042.

We wish to thank the Solar Energy Research Institute for awarding the subcontract for this work to the WUTA Corporation. This work was directed and administered for SERI by Dr. Irwin Vas, Branch Chief--Wind Energy Branch. Mr. Richard Mitchell had program management responsibility for the work and was assisted by Mr. Peter South, acting as Principal Engineer. The subcontract was administered by Ms. Lori Miranda.

The report covers the Contract and Amendment One performance period of September 15, 1979 to December 15, 1980. The principal investigator for this program was Dr. Kurt H. Hohenemser. Mr. Andrew H. P. Swift designed the wind tunnel model, performed part of the analytical work and all of the experimental work including its evaluation. Dr. David A. Peters served as coinvestigator for dynamics analysis. Mr. Patrick F. Rice, in addition to administering the project, contributed to the instrumentation design and to its implementation. Mr. William Stein of Astral Wilcon replaced the late Mr. Warren A. Strutman for the design and construction of the 7.6-m-diameter test wind turbine which has many components in common with the Astral Wilcon 10B machine.

According to the original contract, the work was to be completed by October 15, 1980. Amendment One to the contract extended the performance period to December 15, 1980 and increased the funding level in order to enhance the instrumentation to include measurements of critical dynamic loads of the test wind turbine. It was believed that the measurement of performance as well as of dynamic loads would facilitate determining whether the new concept has the potential of cost-effective wind energy conversion.

On June 28, 1980, after 15 hours of operation of the test turbine over a five-day period, lightning strikes severely damaged the instrumentation and recording system. It took over a month to repair the damage and to replace the destroyed components of the instrumentation system. Despite the time lost in July and despite the unusually hot and windless month of August, the contract goal to analyze and verify by atmospheric experiments the yaw characteristics and power output of a wind turbine with blade cyclic pitch variation has been achieved. The development of an automatic rotor speed control system has not been initiated as yet and was not called for in the contract and its amendment.

Richard Mitchell
SERI Technical Monitor

iii

SUMMARY

The horizontal axis wind turbine under study incorporates two features: The application of blade cyclic pitch variation adopted from rotorcraft technology, and the use of yaw angle control, not only for wind direction following, but also for rotor speed or torque control. Cyclic pitch variation in a two-bladed rotor relieves the blades of all the gyroscopic and odd harmonic aerodynamic root moments. It makes rapid yaw rates of a two-bladed rotor possible without causing vibratory hub moments and without causing appreciable angular excursions of the blade tip path plane. Due to the allowable rapid yaw rates of wind turbines with blade cyclic pitch variation, the two conventional separate control systems - yaw control for wind direction following and blade feathering control for regulating rotor speed and torque - can be replaced by a system with only a single control variable, the rotor yaw angle.

The concept can be implemented in various ways. One way is to use an active blade cyclic pitch control adopted from rotorcraft technology in combination with a freely yawing nacelle. Another way is to use passive blade cyclic pitch variation in combination with a yaw gear drive. A third way is to use passive cyclic pitch variation in combination with an adjustable tail vane for the freely yawing nacelle. The last method has been selected for this study as being the simplest and most reliable. Passive cyclic pitch variation is particularly simple for a two-bladed rotor. The blade pair is free to pitch about the common cyclic pitch axis without the need of a linkage. The blade axes have a small built-in prelag angle with respect to the cyclic pitch axis so that imbalancing gyroscopic or aerodynamic moments cause cyclic pitch variation that removes the imbalance.

The concept was first studied with a small scale wind tunnel model operating without power extraction. The model test results showed that the two-bladed rotor operated smoothly at yaw angles up to 50°, that it started easily at 3.5 m/s tunnel speed, and that the rotor speed could be precisely controlled by yaw angle variation. It was then decided to design, analyze and build a two-bladed 7.6 m diameter wind rotor of this type for atmospheric testing. Astral Wilcon performed the design and construction of the machine using many components of their Model 10B wind turbine.

The machine was mounted on a Unarco Rhon SSV steel tower which was made tiltable to facilitate installation and maintenance of the instrumentation. A careful dynamic analysis of the rotor and its support was performed including a check for potential aeroelastic instabilities. After the assembly of the machine on the tower, dynamic tests were performed to check the analysis. The structure was thoroughly instrumented to obtain performance, dynamic load and vibration data during operation. Analog data were taken of performance and load parameters for nearly steady conditions and for transients. Digital data were taken and processed in an Apple II microcomputer system to obtain means and standard deviations of the measured variables.

The machine was operated between May 23 and October 25, 1980 during 41 days for 96 hours. The operational envelope extended to 16 m/s wind velocity, 360 rotor rpm, 45° yaw angle power-on and 80° yaw angle power-off. For most tests the nacelle was automatically furled when 228 rpm at 10 kW rotor power was exceeded. Unfurling was performed manually. When dividing the total rotor energy output

iv

by the total wind energy flow through the rotor disk during a test run, power coefficients C_p of over 0.4 were obtained. This is based data from an anemometer located 13.4 m above ground and 5.5 m below the rotor center. Winds were never sufficiently high to obtain full power or full rotor speed at 45° yaw angle. Thus, the power cut-off wind speed limit above which loads would become excessive could not be determined. It also was not possible, for lack of steady wind speeds above 13 m/s, to obtain high yaw angle power-off operation at rated rotor speed. Within the operational envelope, dynamic loads and vibrations were low. The highest loads were recorded at the overspeed power-on condition with 16 m/s wind velocity and 360 rpm. This condition is far outside the normal operational envelope.

The atmospheric tests have proven the passive blade cyclic pitch variation concept to be viable. A full evaluation requires the development and testing of a completely automatic rotor speed control system to replace the overspeed furling system presently installed. In a prototype, a number of modifications are necessary. The blades with their long retention box should be replaced by slightly longer blades and extended airfoil sections closer to the hub. This will gain, according to analysis, about 10% in performance and about 50% in starting torque. The generator in its present configuration has good efficiencies only at high power and poor efficiency at the more frequently used lower power outputs. For electric grid connection, either a synchronous inverter must be added or an induction or synchronous generator must be used. A preliminary study has shown that the concept should be readily applicable to larger machine sizes. The simplicity, ruggedness and reliability of a two-bladed, tail vane stabilized, furl angle controlled machine with passive cyclic pitch variation may make this concept attractive for quite large horizontal axis wind turbines. Tail vane stabilization is used for the largest airplanes. There is no compelling reason not to consider tail vanes for large wind turbines. The usual objection against tail vane stabilization — the high gyroscopic loads on the rapidly yawing wind direction following rotor — is not valid for the yawing of wind turbines with blade cyclic pitch variation, no matter how large the machine.

TABLE OF CONTENTS

TABLE OF CONTENTS
(continued)

TABLE OF CONTENTS
(continued)

LIST OF FIGURES

LIST OF FIGURES
(continued)

LIST OF FIGURES
(continued)

LIST OF FIGURES
(continued)

LIST OF TABLES

A	Rotor Disk Area
A_V	Tail Vane Planform Area
I	Machine Yawing Moment of Inertia
M_α	Tail Vane stability Derivative
$M_{\dot{\alpha}}$	Tail Vane Damping Derivative
N	Number of Sample Sets
P	Rotor Power Output
Q	Rotor Torque
R	Rotor Radius
R_e	Reynolds number
T	Rotor Thrust
V	Wind Velocity
a	Lift Slope of Airfoil
a_V	Lift Slope of Tail Vane
C_{do}	Profile Drag Coefficient
$C_{0.7}$	Blade Chord at 0.7 R
$C_P = P/A(\rho/2)V^3$	Power Coefficient
$C_Q = Q/A\rho R(\Omega R)^2$	Torque Coefficient
$C_T = T/A\rho(\Omega R)^2$	Thrust Coefficient
h	Vane Moment Arm to Yaw Axis
q	Dynamic Pressure ($\rho V^2/2$)
$U(t)$	Unit Step Function
α_{Vo}	Angle of Instantaneous Wind Direction Change
α	Rotor Angle of Attack ($90^{\circ} - \alpha$ = Yaw Angle)
α_B	Blade Angle of Attack
α_V	Tail Vane Angle of Attack
β	Cyclic Pitch Amplitude
ζ	Damping Over Critical Damping Ratio
$\lambda = \Omega R/V$	Tip Speed Ratio
$\lambda_A = (V/\Omega R)\sin\alpha$	Axial Flow Component
$\mu = (V/\Omega R)\cos\alpha$	Edgewise Flow Component

$\tilde{}_{0.7}$ Blade Aerodynamic Pitch Angle at 0.7 R

ρ Air Density

$\sigma_{0.7} = 2\ C_{0.7}/R$ Rotor Solidity Ratio

Ω Angular Speed of Rotation

ω Natural Frequency Without Damping

ω_n Damped Natural Frequency

ω_T Natural Tower Frequency

$V/\Omega R$ Wind Speed Ratio

$\sigma =$ Blade Solidity Ratio
CPM   Rotor Mode Frequency

INTRODUCTION

The term "cyclic pitch variation" is taken from rotorcraft technology. It is applied when, in a rotating frame of reference, the blade pitch angle changes periodically with the period of the rotor revolution. For rotorcraft with cantilever blades, cyclic pitch variation removes the aerodynamic and gyroscopic pitching and rolling moments on the airframe which otherwise would be very high. For rotorcraft with hinged or teetering blades, cyclic pitch variation compensates blade flapping and keeps the blade tip path plane approximately normal to the rotor shaft in addition to providing the means for rotorcraft control.

Except for two vertical axis wind turbine types, cyclic pitch variation has not been applied to wind rotors. The lack of cyclic pitch variation in horizontal axis wind turbines with cantilever blades exposes these machines to higher aerodynamic and gyroscopic loads than necessary. These loads are particularly evident in two-bladed wind turbines with cantilever blades since the imbalanced aerodynamic and gyroscopic blade moments produce substantial two per revolution loads and vibrations of the nonrotating structure. For this reason most wind turbine designers have selected three or four-bladed rotors rather than the more cost effective two-bladed rotor. The NASA MOD-OA and MOD-1 two-bladed wind turbines with cantilever blades avoid excessive gyroscopic effects by using a slow yaw gear drive. As a consequence, the machines cannot follow rapid wind direction changes. Edgewise wind components of substantial magnitude can then occur and can cause increased dynamic blade loads. To relieve the ill effects of edgewise wind components, individual blades or pairs of opposing blades have been occasionally hinged to the hub to allow out-of-plane blade motions. Hinges have been used in large two-bladed wind turbines built in the forties and fifties. They are again incorporated in the latest US, German and Swedish designs of megawatt size two-bladed wind turbines.

Horizontal axis wind turbines need means for wind direction following and for automatic rotor speed or torque control. Wind direction following is accomplished either by a tail vane, or by a yaw gear drive, or by the inherent yaw stability of a wind rotor located down wind of the yaw axis, (self-yawing wind turbine). Rotor speed or torque control is usually accomplished by a blade feathering mechanism adopted from propeller technology. In Ref. 1 some cost saving alternatives to the current technology are discussed. For one of the alternatives, both the yaw gear drive and the blade feathering mechanism are omitted and replaced by a blade cyclic pitch control mechanism adopted from rotorcraft technology. It is then possible to use a single control variable – the blade cyclic pitch input – both for rotor speed or torque control and for wind direction following. With cyclic pitch variation, yaw control can be made precise. In contrast, self-yawing wind turbines tend to overshoot in yaw angle, and conventional yaw gear drives are too slow to adapt to rapid wind direction changes.

Figures 1-1a and 1-1b, taken from Ref. 1, show typical steady state rotor power curves for a chart of control angle vs. tip speed ratio. Figure 1-1a represents blade feathering angle control, Fig. 1-1b represents rotor yaw angle control achieved by blade cyclic pitch variation. Constant rotor speed operation with a

1

synchronous generator is assumed. Synchronization (SYNC) occurs with zero power at the tip speed ratio for operational rotor speed over cut-in wind velocity (vertical line with arrow). With increasing wind speed the power rises to the rated value (horizontal line with arrow). Above rated wind speed, rated power is kept constant up to cut-out wind speed (rising curve with arrow). The two sets of steady state power curves shown in Fig. 1-1a and 1-1b are similar, therefore blade feathering angle control can be replaced by rotor yaw angle control provided that sufficiently rapid yaw angle changes are feasible.

Ref. 1 explains that the time constant of yaw response to a cyclic pitch input for a ratio of nacelle over blade moment of inertia of 3.4 (MOD-0) is approximately $1.7/\Omega$, where Ω is the angular rotor speed in rad/sec. The response of rotor speed to a torque input has a time constant of about $20/\Omega$ for a MOD-0 type wind rotor. Therefore one can expect a satisfactory rotor speed control with cyclic pitch inputs if the servo-actuator has a matching time constant of say $5/\Omega$. The MOD-0 machine has a higher moment of inertia ratio than necessary, and therefore even shorter yaw response times are feasible.

The purpose of the present study is to determine by analysis, by small scale wind tunnel model testing, and by atmospheric testing, whether blade cyclic pitch variation, adopted from rotorcraft technology, can be beneficially applied to the yawing of horizontal axis wind turbines.
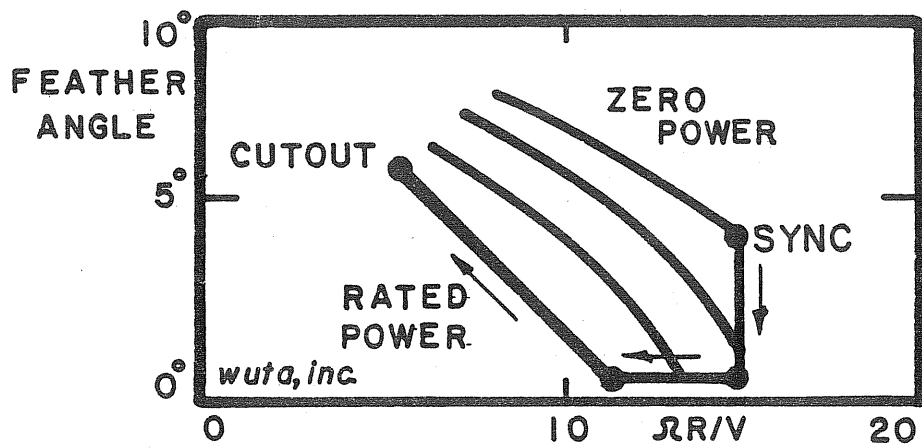
Figure 1-1a.   POWER CURVES FOR CONSTANT ROTOR SPEED VS. TIP SPEED RATIO,
WITH BLADE FEATHERING ANGLE CONTROL AT ZERO YAW ANGLE
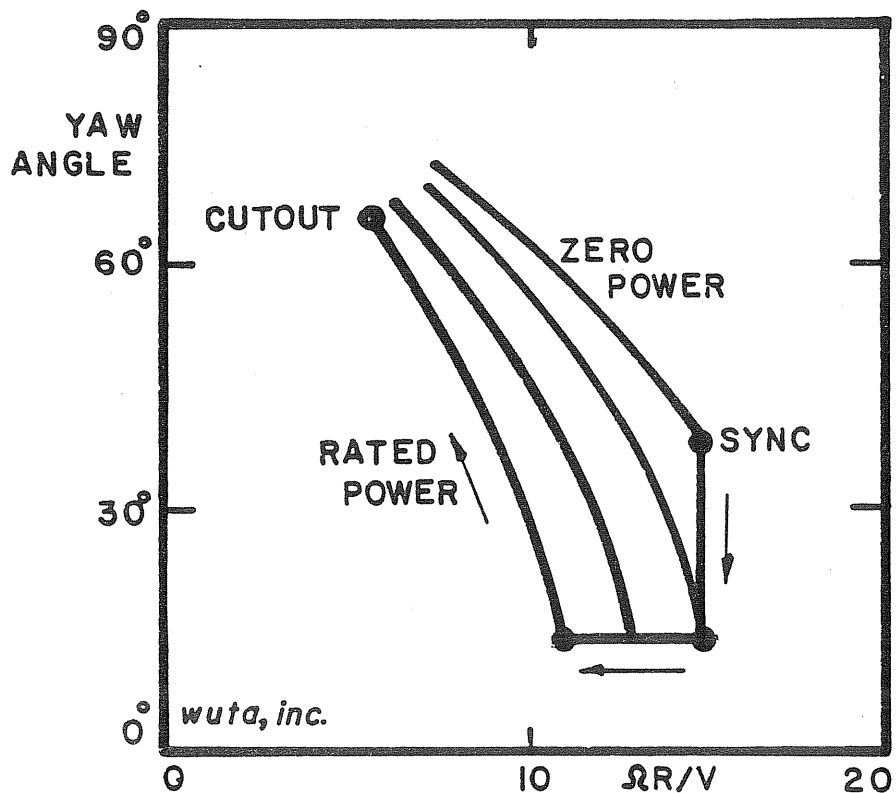
Figure 1-1b.   POWER CURVES FOR CONSTANT ROTOR SPEED VS. TIP SPEED RATIO,
WITH ROTOR YAW ANGLE CONTROL AT ZERO BLADE FEATHERING ANGLE

SECTION 2.0

APPLICABLE ROTOR CRAFT EXPERIENCE

Before discussing the reasons for selecting the wind turbine configuration used for this study, a brief summary of applicable rotorcraft experience will be given.

2.1 DIRECTION OF FLOW THROUGH ROTOR

In a rotorcraft it is unavoidable that upflow as well as downflow through the rotor must be used. In powered flight the direction of the flow through the rotor disk is downward, in autorotational flight it is upward. Dynamic loads and vibrations are higher for upflow when the rotor operates in the wake of the fuselage. In a wind turbine one has a choice of upwind or downwind rotor location with respect to the mast. From the point of view of dynamic loads and vibrations, the upwind location of the rotor is better. Propeller type turbines have shown substantial dynamic rotor load increases from the wake of the mast. Although this effect will be alleviated by cyclic pitch variation, the nacelle wake is of greater importance in oblique flow.

2.2 ROTOR STABILITY DERIVATIVES

The two rotor stability derivatives of interest for wind turbines are rotor angle of attack stability and rotor damping. For a wind turbine the rotor angle of attack is equal to 90° minus the yaw angle. A rotor is stable with respect to angle of attack changes if an increase in angle of attack produces a hub moment that tends to restore the original rotor angle of attack. A rotor has positive damping if a rate of change of rotor angle of attack produces a hub moment that resists the rate of change. Lifting rotors have negative angle of attack stability, and they usually have inadequate rotor damping. In rotorcraft, tail surfaces and rate gyros acting on the controls compensate for the inadequate rotor stability derivatives. For an upwind location of a wind turbine with blade cyclic pitch variation the damping about the yaw axis may be negative. In this case a tail surface or rate gyro damping is a necessity.

2.3 ACTIVE BLADE CYCLIC PITCH CONTROL

In rotorcraft one distinguishes cyclic pitch moment control from cyclic pitch thrust vector control. Often a combination of both is used. Moment control is best suited for rotors with more than two blades, since in a two-bladed rotor the hub moment varies twice per revolution from a maximum value to zero. The cyclic pitch thrust vector control system for a two-bladed rotor has been extensively researched and applied in thousands of two-bladed Bell Helicopters. This control technology could be directly transferred to wind turbines.

5

2.4 ROTOR EMASCULATION

In compound rotorcraft where the lift in hovering is provided by a lifting rotor, and where the lift in cruising flight is mainly generated by a fixed wing, rotor controls are not useful in cruising. In order to eliminate undesirable rotor stability derivatives in cruising flight, the rotor can be "emasculated" as was done for the US Army XV-1 compound rotorcraft, Ref. 2 and 3. The method of emasculation used was passive cyclic pitch variation whereby a small up blade flapping angle produced a large down blade pitch angle. The rotor of the XV-1 compound rotorcraft had a three to one pitch-flap ratio in cruising flight and flew to advance ratios (flow component in the rotor plane over blade rotational tip speed) of over one without difficulties, whereby the rotorcraft was controlled and stabilized by aerodynamic surfaces. The emasculation by a large blade pitch-flap coupling practically eliminates angle of attack instability and negative rotor damping. It makes the rotor easy to control by external means.

2.5 VIBRATIONS

Two-bladed rotors with active cyclic pitch variation from thrust vector control achieve a reasonably low vibration level. The XV-1 compound rotorcraft with its passive cyclic pitch variation was almost vibration free in cruising flight. The rotor was three-bladed. For a two-bladed rotor a higher vibration level can be expected. However, it should not exceed that of the two-bladed rotor with cyclic pitch thrust vector control. In contrast to rotorcraft, vibratory gravity loads do occur in two-bladed horizontal axis wind turbines. In the nonrotating frame of reference they have a frequency of twice per revolution. They can be kept small by designing the blades with an in-plane bending natural frequency which is at least two times the frequency of rotor revolution.

6

SECTION 3.0

CONFIGURATION SELECTION

The wind tunnel model and the atmospheric test equipment together with the test results will be described later. Some of the reasons for selecting the configuration for these tests will be discussed here. It should be noted that this selection had to be made at the beginning of the research period before any experience with the wind turbine with cyclic blade pitch variation was available. Thus, only qualitative arguments could be applied.

3.1 TWO OR MORE-BLADED ROTOR

In rotorcraft developments, two-bladed rotors were successful when rotor hub pitching and rolling moments were avoided. The two-bladed emasculated rotor with passive cyclic pitch variation is hub moment free and can be expected to operate with a low vibration level. The same is true for the two-bladed rotor with cyclic pitch thrust vector control. The two-bladed wind turbine is for various reasons more cost effective than a three or four-bladed wind turbine. A two-bladed hub moment free rotor has been selected for this study.

3.2 UPWIND OR DOWNWIND ROTOR

From the previous discussion it is evident that dynamic loads and vibrations are alleviated when an upwind rotor location is used. The disadvantage of negative yaw damping is overcome by using a tail surface to provide rotor angle of attack stability and damping, or, in the absence of a tail vane, by using artificial stabilizing and damping means. An upwind rotor location has been selected.

3.3 ACTIVE OR PASSIVE CYCLIC PITCH VARIATION

Cyclic pitch thrust vector control is suitable for a two-bladed rotor and results in a low vibration level. When used in an upwind rotor, artificial stabilizing and damping means are needed. Since the cyclic pitch input must be responsive to wind direction and rotor speed or torque signals, artifical stabilization amounts merely to a conditioning of these signals.

A substantial simplification of the two-bladed wind rotor can be obtained by applying passive blade cyclic pitch variation instead of active blade cyclic pitch control. Such a rotor can be rapidly yawed without resistance and without transferring gyroscopic moments to the hub. Figure 4-1a shows a two-bladed rotor design of this kind used for a small scale wind tunnel test model. The hub can swivel freely about the two pins that form the cyclic pitch axis. The blades are attached to the hub with a small fixed prelag angle with respect to this axis. Any imbalanced out-of-plane blade forces cause a rotation of the blade pair about the two pins which tends to restore the balance. For example, a rate of yaw will produce an oscillatory gyroscopic moment in the rotating frame of reference. Cyclic pitch motion of adequate amplitude and phase will balance the gyroscopic moment. The cyclic pitching motion is coupled with a small teetering motion which is hardly noticeable. Because of its simple and rugged design, a

wind rotor with passive blade cyclic pitch variation has been selected for this study.

3.4 YAW GEAR DRIVE OR TAIL VANE

The rotor with passive cyclic pitch variation must be yawed by external means; for example, by a yaw gear drive. Contrary to usual systems with blade feathering control, the input to the yaw gear drive is the only control variable. It responds to wind direction and to rotor speed signals. Wind direction following can also be accomplished by a tail vane. To yaw a tail vane stabilized wind rotor, the tail boom is swivelled from its normal position in line with the rotor axis to a "furled" position. The furl angle is approximately equal to the rotor yaw angle, Fig. 4-3b. To obtain precise rotor speed or torque control, a furl actuator must be used that is responsive to speed or torque signals. Figure 1-1b is valid no matter whether rotor yawing is achieved by active cyclic pitch control, or by passive cyclic pitch variation in combination with a yaw gear drive or in combination with a tail vane and a furl mechanism.

A yaw gear drive adds to the dynamic complexity of a wind turbine and requires a torsionally stiff tower. It also adds to the complexity of the automatic control system because it requires wind direction inputs in addition to rotor speed or rotor torque inputs. Furl control of a vane stabilized wind rotor with passive blade cyclic pitch variation appears to be the simplest approach promising the greatest reliability of the end product, and has, therefore, been selected for this study.

3.5 DEPENDENCE OR INDEPENDENCE FROM ELECTRICAL GRID

Induction and synchronous wind turbine generators have a near constant operational speed, determined by the electrical grid. Beyond cut-out and in case of grid failure, automatic overspeed limitation must be provided. In the case of synchronous generators, automatic rotor speed regulation must be adequate for the process of synchronization. Beyond rated wind speed, automatic torque limitation is required for both induction and synchronous generators. Since the speed varies somewhat with torque for induction generators, the overspeed limitation, if sufficiently accurate, may also serve as a torque limitation. A self-excited generator or alternator operating with a constant electric load independent of an electrical grid develops a torque that steeply rises with rotor speed. Therefore rotor speed limitation also serves as torque limitation. This simplifies the requirements for the automatic control system. For the atmospheric test wind turbine, a self-excited alternator with grid independent stand alone operation has been selected for this study. An automatic overspeed limitation for the wind turbine is adequate for this configuration.

3.6 CONFIGURATION SUMMARY

- A two-bladed, emasculated, hub moment free rotor with passive cyclic pitch variation, located upwind of the mast.

- A movable tail boom that can be rotated from a position essentially perpendicular to the rotor plane (zero furl angle) to a position essentially parallel to the rotor plane (90° furl angle).

- A power actuator that can adjust the tail boom furl angle (the angle between rotor axis and tail boom) in response to rotor speed signals.

- A self-excited alternator with constant electric load for stand alone grid independent operation.

SECTION 4.0

SMALL SCALE WIND TUNNEL MODEL STUDIES

The purpose of the first series of small scale wind tunnel model tests, conducted in October, 1979, was to gain initial yawing experience with a wind rotor having passive cyclic pitch variation. A second series of tests was conducted in April, 1980 to obtain quantitative data on starting capability and to determine operating parameters at higher wind speed.

4.1 THE MODEL

The axial view of the model rotor, Fig. 4-1a, has been described before. Blade and blade retentions with their flexures have been adopted from an existing lifting rotor model. The side view of the complete model is shown in Fig. 4-1b. The tail boom can be adjusted for various furl angles between runs. Only autorotational conditions can be tested. High blade drag due to the small Reynolds number is, however, the equivalent of extracting power from a larger rotor. The following table summarizes pertinent data for the model and for the full scale machine.

Table 4-1. COMPARISON OF MODEL AND FULL SCALE PARAMETERS

	Model	Full Scale Machine
Rotor Diameter, inch (meter)	17.2(0.437)	300(7.62)
Blade Chord, inch (meter)	1.0(0.0254)	12 to 4(0.30 to 0.10)
Blade solidity ratio	0.075	0.032(at .7R)
Blade Twist, degrees	0.0	9.5
Blade Airfoil	0015	4425 to 4412
Blade Lock Number	6.4	7.0
Blade Prelag Angle, degrees	23	23
Cyclic Pitch Stops, degrees	+9	+13
Reference Rotor rpm	1800	225
Reynolds Number for 0.7 R	50,000	640,000
Vane Area, ft^2, (meter^2)	0.026(0.0024)	12.5(1.16)
Vane Arm, inch (meter)	12.5(0.317)	204(5.18)
Vane Aspect Ratio	2.4	5.5

Although the model and the full scale machine are not geometrically similar, the near equality of the blade prelag angles and of the blade Lock numbers results in the same ratio (1.7) of rigid blade body mode frequencies over rotational frequencies. Thus the blade cyclic pitch dynamics of model and full scale rotor are the same outside of the blade stall regime except that the cyclic pitch stops for the model are narrower than for the full scale rotor.

BLADE

FLEXURE

HUB

SHAFT

1.2 IN

1.0 IN

BLADE
PRELAG ANGLE
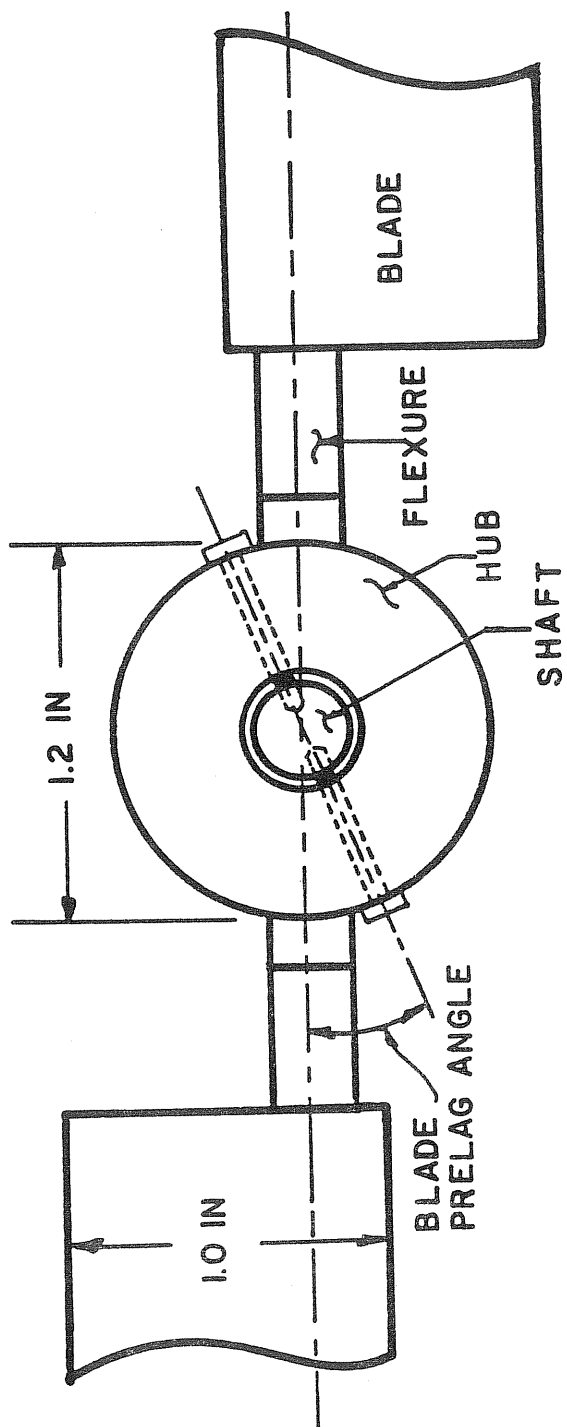
Figure 4-la.   WIND TUNNEL MODEL, AXIAL VIEW OF HUB

TUNNEL
FLOOR

YAW ANGLE
ADJUSTOR

Figure 4-lc.   WIND TUNNEL MODEL, FIXED YAW MODE,
SIDE VIEW

12.5 IN

3 IN

17.2 IN

YAW BEARING

TUNNEL FLOOR

wuta, Inc.
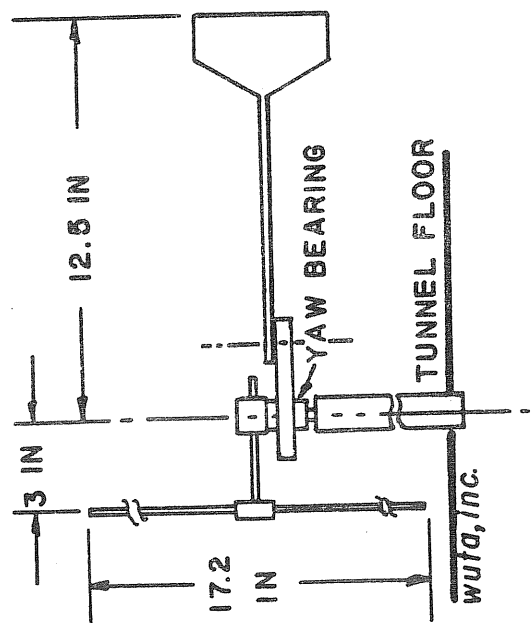
Figure 4-lb.   WIND TUNNEL MODEL, FREE YAW MODE,
SIDE VIEW

12

The model can be tested in a free yaw mode with tail vane, in a fixed yaw mode without tail vane, and the yaw angle can be changed during test runs by a yaw angle adjuster below the lower tunnel wall, see Fig. 4-1c.

4.2 FIRST TEST SERIES RESULTS

The rotor speed, measured with a stroboscope, is determined as a function of wind tunnel speed and yaw angle. For zero yaw angle Figure 4-2 shows wind speed ratio V/ R vs. rotor speed with the blade Reynolds number scale for 0.7 R superimposed. Blade pitch angle is about zero. The wind speed ratio varies from 0.2 to 0.3 depending on rotor rpm. The relation shown in Fig. 4-2a is used to correct the data for nonzero yaw conditions to a "reference" rpm of 1800. The corrected result of the yaw tests is shown in Fig. 4-3a. For the free yawing tests the furl angle has been assumed equal to the rotor yaw angle (Fig. 4-3b) although there may be some small difference between the two angles. As seen in Fig. 4-3a the wind speed ratio is minimum at about 20° yaw angle. The discontinuity in slope at about 50° yaw angle is presumably caused by blade stall. This discontinuity should not occur for larger rotors with higher Reynolds number. Some insight into the characteristics of larger rotors is given by the dash line. It represents the results of autorotational tests of a 3 meter diameter rotor with four hinged blades tested by NACA at a blade Reynolds number for 0.7 R of 620,000, Ref. 4. One can expect the atmospheric test rotor with a blade Reynolds number for 0.7 R of 640,000 to follow the dash curve rather than the solid curve found for the small scale model at a Reynolds number of 50,000.

In the fixed yaw mode where the yaw angle can be varied while the rotor is autorotating, it was observed that rotor rpm could be easily controlled by yawing. The rotor self-started soon after starting the wind tunnel and ran smoothly without visible flapping in both yawed and unyawed positions, except that beyond 50° yaw angle some cyclic pitch stop pounding occurred for high wind speeds and rotor speeds. This is presumably related to the slope discontinuity seen in Fig. 4-3a and caused by progressing blade stall. The full scale rotor did not produce this phenomenon because of the much higher stall margin.

In the free yaw mode, the model started easily and demonstrated a high degree of stability about the yaw axis. Transient testing was performed by forcibly yawing the model 20° away from equilibrium and then releasing it. The model returned rapidly to the equilibrium position with almost no overshoot. The cyclic pitch amplitude remained within the $\pm 9^{o}$ limit during the rapid yaw rate test.

4.3 SECOND TEST SERIES RESULTS

During the second series of tests conducted in April, 1980 the model reliably started with zero yaw angle at about 8 mph wind speed. When running, it could be quickly stopped by using 90° yaw angle. It did not start at this yaw angle up to the highest tested wind speed of 24 mph. The blades showed no motions up to 15 mph when stopped with 90° yaw angle but flapped in an irregular manner at 24 mph. The rotor started at 20 mph for 80° yaw angle but did not go beyond the stop pounding phase. This can be explained by looking at Fig. 4-3a. A yaw angle of

13
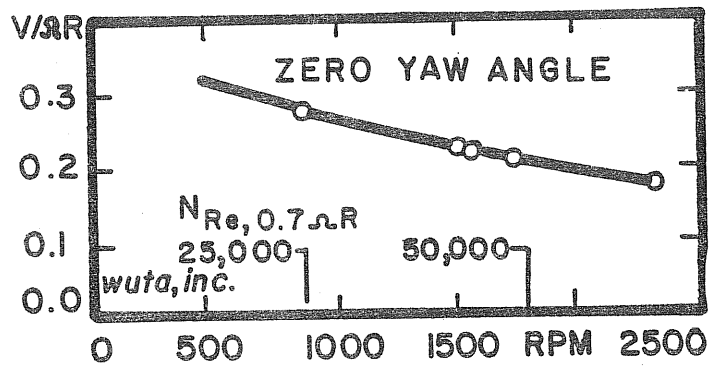
Figure 4-2.   EFFECT OF ROTOR SPEED OR REYNOLDS NUMBER ON WIND SPEED RATIO
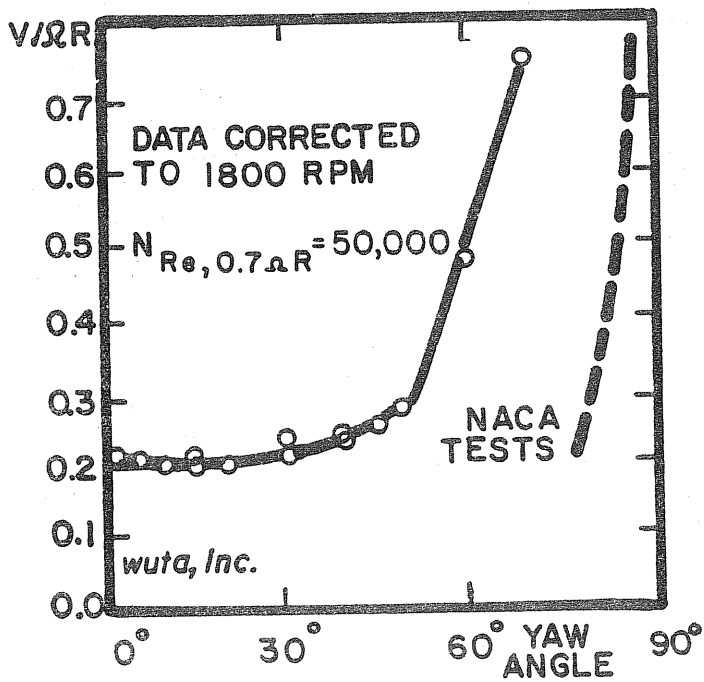
Figure 4-3a.   WIND SPEED RATIO VS.
YAW ANGLE
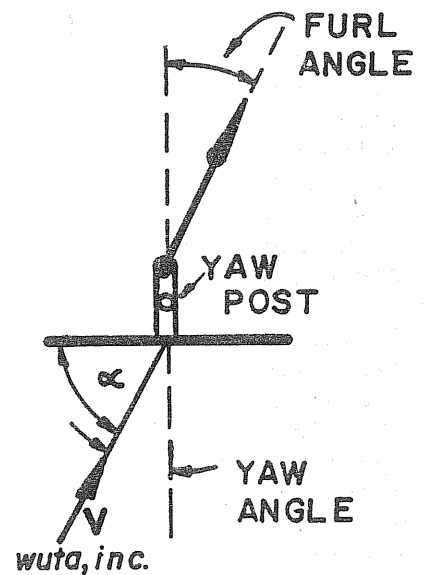
Figure 4-3b.   DEFINITION OF YAW
ANGLE, FURL ANGLE
AND ALPHA

14

80° for the model is not attainable without severe stall, as can be presumed from the difference between the dash line and the solid line. One can expect the full scale rotor to start at 80° yaw angle and to pass through the initial brief stop pounding phase to normal operation as characterized by the dash line in Fig. 4-3a.

The maximum wind speed at zero yaw angle was 20 mph during the first series of tests. It was increased to 24 mph for the second test series. At this wind speed and at 2100 rpm ($V/\Omega R = 0.21$), a striking rotor instability occurred. Just prior to the onset of the instability the cyclic pitch amplitude was small and the rotor ran smoothly. Suddenly cyclic pitch stop pounding was observed with an estimated frequency of 10 to 20 Hz. The rpm rapidly dropped to about one-third its initial value and the tip path plane was strongly warped, indicating that the cyclic pitch frequency was different from the usual 1P. This condition persisted until the tunnel speed was reduced to under 12 mph. In repeated tests, the onset of the instability was always exactly at 24 mph wind speed. The instability occurred at somewhat lower tunnel speed when the rotor was yawed.

It was suspected that the instability for the model was related to the fact that at 2100 rpm the blade coning frequency was much lower than the rigid body frequency. The opposite relation holds for the full scale rotor. Figure 4-4, for the model, shows the coning frequency and the rigid body frequency vs. rotational frequency $\Omega/2\pi$ Hz. The coning frequency for zero rotor speed was measured; the change with rotor speed was computed. The rigid body frequency was also computed. The crossover point for the full scale rotor is above the overspeed limit at 360 rpm. The crossover point for the model is far below 2100 rpm (35 Hz) when the instability set in. The two blade modes cannot couple in the linear range since the rigid body mode is asymmetrical and the coning mode is symmetrical. However, in the stalled regime the modes do couple and may produce an unstable coupled mode. The model rotor is operating close to stall in autorotation. Any cyclic pitch variation will bring one blade deeper into stall, the other out of stall. It may be significant that instability occurs when the rigid body mode frequency is 1.5 times that of the coning mode frequency.

An analysis of this phenomenon would be quite difficult since non-linear equations are involved. Also, little is known about dynamic stall at low Reynolds number and no attempt was made to develop a theory of the observed instability. The blade flexures were subsequently reinforced in order to appreciably raise the coning frequency. The model was then operated at zero yaw angle up to 28 mph wind speed and 2500 rpm without encountering instability. At 28 mph the model was yawed to 45° yaw angle whereby the rotor speed dropped to 1450 rpm. When yawing further to 50°, the stop pounding instability occurred and could be removed by yawing the rotor back to smaller angles. The observed effect of the coning mode frequency on the instability proves that a coupling between rigid body mode and coning mode is in fact involved. Blade stall must also be involved, otherwise the two modes would not couple. Since the full scale rotor is much further removed from stall than the model rotor, and since its ratio of coning mode frequency over rigid body mode frequency is always larger than one, one can expect the full scale rotor to be free of the stop pounding instability if adequate stall margins are preserved.

15
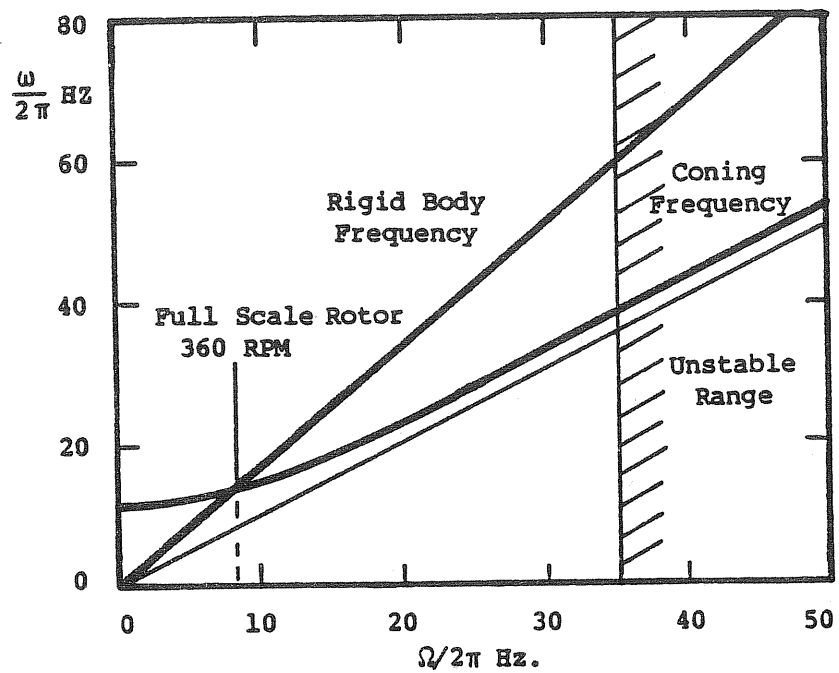
Figure 4-4.   RIGID BODY AND CONING FREQUENCIES FOR MODEL VS. FREQUENCY OF
ROTATION

A paper by Glasgow and Miller, Ref. 5, shows that the NASA DOE MOD-0 machine in the configuration with teetering untwisted blades can also exhibit stop pounding. Stop pounding occurred repeatedly in this configuration after encountering a gust of wind. The stop pounding condition persisted after the passing of the gust and could only be removed by feathering the blades ten degrees. No explanation is given for this phenomenon in the paper. Upon contacting the authors it was learned that the MOD-0 with the teetering blades, could not be operated with the normal rotor speed of 40 rpm. Because of a dynamic condition it could only operate with a reduced rotor speed of 33 rpm where stall is imminent. The gusts brought the blades deeper into stall so that stop pounding set in which did not disappear at lower wind speed. Only unstalling of the blades by feathering terminated the stop pounding condition. The behavior of the MOD-0 with teetering blades is similar to that of the model rotor with reinforced blade retention flexures. Stop pounding occurred for the model rotor at a high yaw angle with imminent blade stall, and stop pounding conditions disappeared when the rotor was yawed back to positions with a higher blade stall margin.

The presumed role of blade stall in the stop pounding incidents of the MOD-0 machine has not been suggested by the authors of Ref. 5, but is our own interpretation. Assuming that this interpretation is correct, the experience with the small scale model and with the MOD-0 machine with teetering blades teaches an important lesson: Rotors with teetering blades or with passive cyclic pitch variation should not be operated close to operational regions where a gust could precipitate blade stall. In case this presumable stall-related stop pounding condition should occur in the atmospheric test rotor, the blades should be unstalled by either reducing the rotor yaw angle or by shedding the alternator electric load. For the full scale rotor, contrary to the model rotor, autorotational conditions are far removed from stall and shedding of the electric alternator load should terminate the stop pounding condition if it occurs.

In summary, the small scale model tests demonstrated smooth operation of the rotor with passive cyclic pitch variation up to yaw angles of 50°, good controllability of rotor speed by yawing, easy starting between 0 and 80° yaw angle, good damping of yaw transients, and capability of high yaw rates without vibrations. The model also demonstrated that blade-stall-related stop pounding may occur with involvement of the blade coning mode. The blade airfoil and its pitch settings were not too well defined; the tunnel wall effect was substantial. For these reasons only a qualitative evaluation of the model tests was made and no attempt was made to compare the model test results with the results of an analysis.

SECTION 5.0

ANALYTICAL STUDIES

The analytical studies were conducted in support of the design of the atmos-pheric test turbine. The performance analysis for zero yaw angle uses conven-tional methods assuming steady wind speed and wind direction. The emphasis is on establishing trends with configuration changes. With respect to the steady state yaw characteristics, rough estimates had to be made because of the lack of an accepted analytical method applicable to yawed conditions. The prediction of natural frequencies was hampered by ill-defined structural properties of blades, nacelle and tower. Tests were used to correct the original assumptions. Potential linear aeroelastic instabilities have been analyzed with the originally assumed structural properties. Corrections were believed to be unnecessary since no linear aeroelastic instabilities have been uncovered up to very high rotor overspeed. Analysis has not been performed on the stall related nonlinear cyclic pitch stop pounding condition observed during the second wind tunnel model test series.

5.1 PERFORMANCE ANALYSIS FOR ZERO YAW ANGLE

The purpose of the performance analysis for zero yaw angle was to establish the effect of blade pitch setting, the effect of the number of blades (two and three) and the effect of blade solidity ratio on the rotor performance. The method used was taken from Ref. 6. The details of the analysis are given in Appendix A. The results should only be used for comparisons and not for the prediction of the actual performance which depends on neglected details such as blade shank loss, blade surface roughness, deviations of the actual blade airfoil from the ideal airfoil shape, and varying Reynolds number over blade span and wind speed. The blade airfoil characteristics for all blade stations have been taken from the "standard roughness" curves of Ref. 7 which are valid for 3×10^6 Reynolds number. This corresponds approximately to the characteristics of a smooth airfoil at the much lower Reynolds number for the 0.7R blade span station when operating at rated rotor speed.

Figure 5-1 shows the blade planform with airfoil sections along the span and the distribution of chord and section thickness. The blade is tapered from 12 in chord at the root to 4 in chord at the tip. The section thickness varies from 25% at the root to 12% at the tip. The twist is nonlinear and amounts to a total of 9.5^o. The long blade shank section is needed for the three-bladed Astral Wilcon 10B machine but is not needed for the two-bladed lifting rotor wind turbine with cyclic pitch variation. The long blade shank with its aerodynamic losses has been adopted for the atmospheric test rotor in order to avoid the high costs of a special blade design. The blade shank would be shortened to about one-half its present length in a prototype design, whereby the aerodynamic shank loss would be reduced by much more than one-half.

Figure 5-2 shows the performance coefficient of the two-bladed atmospheric test rotor defined by $C_p = 2P/\rho V^3 \pi R^2$ vs. tip speed ratio $\Omega R/V$. The four curves are for blade pitch settings at 0.7R of -4°, -2°, 0, and $+2^o$. As usual in the wind rotor literature, the plus sign applies toward blade feathering, the minus sign applies toward blade unfeathering. In the rotorcraft literature the pitch

Radius Station, %	20.0	32.0	34.7	43.0	56.0	73.3	100.0
Radius Station, inch	30.0	48.0	52.0	65.0	84.0	110.0	150.0
Chord, inch	--	12.0	11.7	10.6	9.2	7.2	4.2
Thickness, inch	--	3.0	2.8	2.2	1.6	1.1	0.5
Section	--	0025	4424	4421	4418	4415	4412
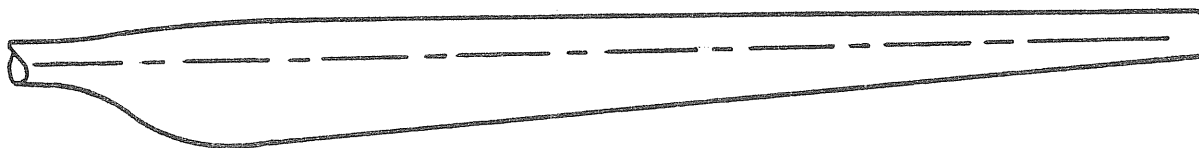
Figure 5-1.   BLADE GEOMETRY, ATMOSPHERIC TEST ROTOR
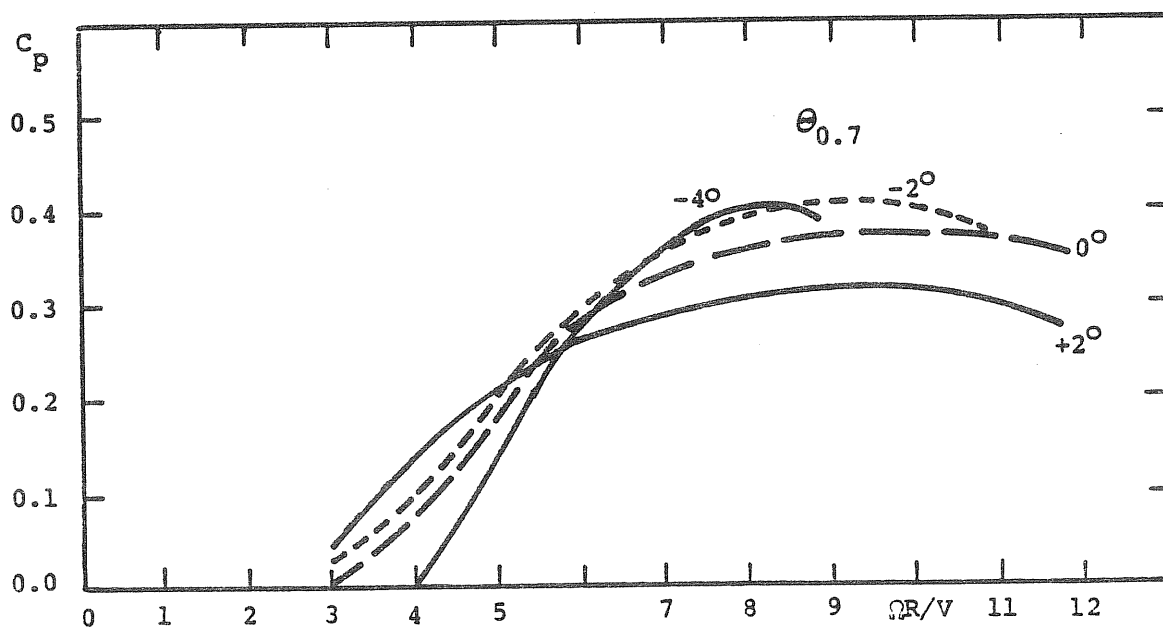
Figure 5-2.   COEFFICIENT OF PERFORMANCE VS. TIP SPEED RATIO FOR TWO-BLADED TEST ROTOR

angles have opposite signs. The angles are measured from the zero lift chord line of the airfoil. As will be seen later, the atmospheric test rotor will operate up to rated wind speed with a tip speed ratio close to the maximum value of C_p. We are, therefore, interested in finding the blade pitch setting for the highest value of C_p. According to Fig. 5-2 this setting is -2°. The yawing characteristics in the subsequent section have been established on the assumption of a blade pitch setting at 0.7R of -2°.

Figure 5-3 shows the equivalent curves for a three-bladed rotor using the same blade design. The optimum C_{pmax} is again obtained for a blade pitch setting of -2°. The value of C_{pmax} for -2° is now somewhat above 0.4 while, for the two-bladed rotor, it is somewhat below 0.4. In order to find out whether or not the improvement in C_{pmax} of the three-bladed rotor over the two-bladed rotor was caused by the higher solidity of 0.048 vs. 0.032, an analysis was made for a two-bladed rotor with 0.048 solidity ratio. As Fig. 5-4 shows, the increased blade solidity did not result in an increased C_{pmax}, merely in a shift of the optimum tip speed ratio value from 9.8 to 7.7, same as for the three-bladed rotor. This shows that the slender blades of the two-bladed atmospheric test rotor do not have a performance penalty. They are less costly than wider blades and allow cost savings from a lower gear ratio as compared to wider blades.

Figure 5-5 shows a comparison between the performance of a three-bladed rotor and a two-bladed rotor with a 4% larger diameter, as would be used for a prototype version of the test rotor. The details of the blade geometry are given in Fig. 6-33. The loss in performance from having two rather than three blades is now fully compensated. A third blade adds 50% to the cost of two blades, while a 4% larger blade span adds at most 8% to the cost. Quite apart from the much simpler hub of a two-bladed rotor, the blade cost savings alone are substantial, and they are obtained without a loss in rotor power. The optimum tip speed ratio is about 9.8 vs. 7.7 for the three-bladed rotor. Thus the two-bladed rotor will have a higher rotor speed and will require a lower gear ratio when operating with C_{pmax}.

One may suspect that the higher blade centrifugal force from the higher rotor speed will require reinforcements of the blade structure. Actually the strength margin with respect to blade centrifugal force is usually quite high, particularly for fiberglass blades. Critical stresses are in bending, and a higher centrifugal force reduces the bending stresses because of centrifugal relief. For the two-bladed atmospheric test rotor the centrifugal force is directly transmitted from one blade to the opposite blade without thrust bearings used in conventional propeller rotors. The increase in centrifugal force for a two-bladed rotor compared to the three-bladed rotor does not present a problem.

5.2 STEADY STATE YAW CHARACTERISTICS

A simple estimate of steady state yaw characteristics is possible when blade stall effects are neglected, a constant blade angle of attack is assumed, and a uniform inflow through the rotor disk is stipulated. For zero blade pitch setting and rectangular untwisted blades one has from axial momentum theory

$$\lambda = \tan \alpha - C_T/2\mu(1 + (\lambda/\mu)^2)^{\frac{1}{2}} \tag{5-1}$$
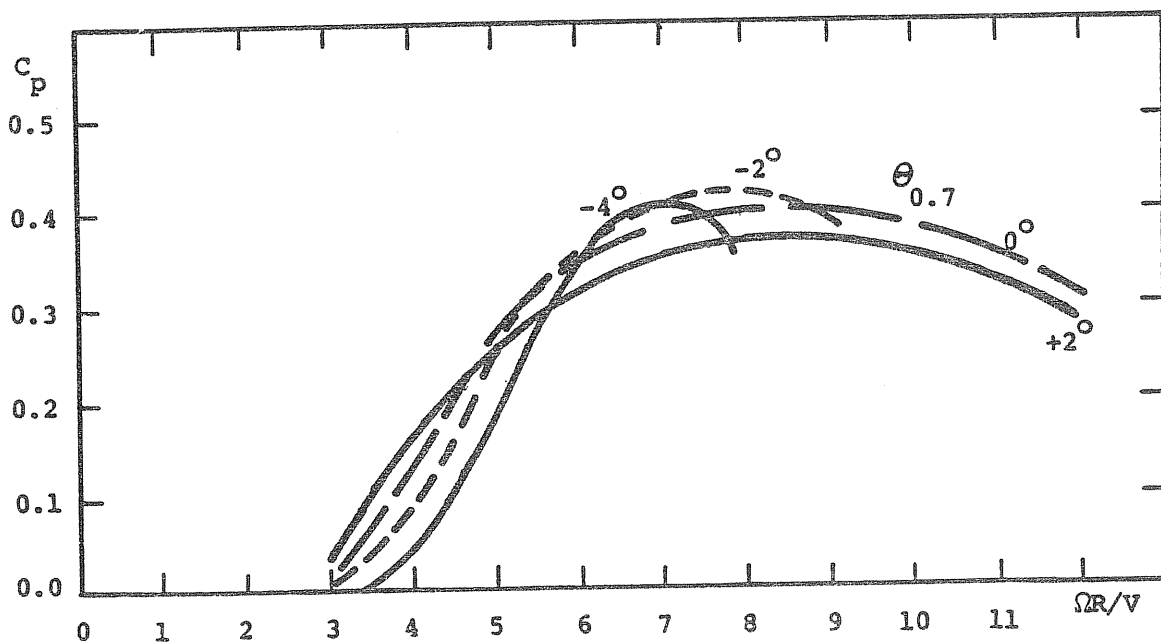
Figure 5-3.   COEFFICIENT OF PERFORMANCE VS. TIP SPEED RATIO FOR THREE-
BLADED ROTOR
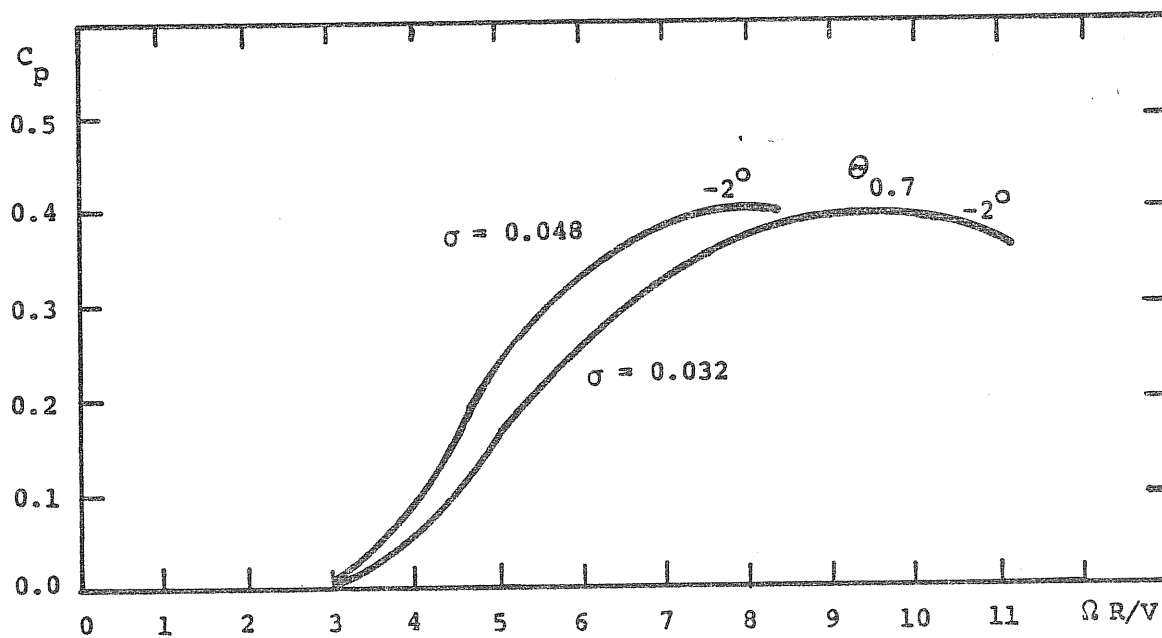
Figure 5-4.   COEFFICIENT OF PERFORMANCE VS. TIP SPEED RATIO OF TWO-BLADED
ROTOR FOR TWO BLADE SOLIDITY RATIOS
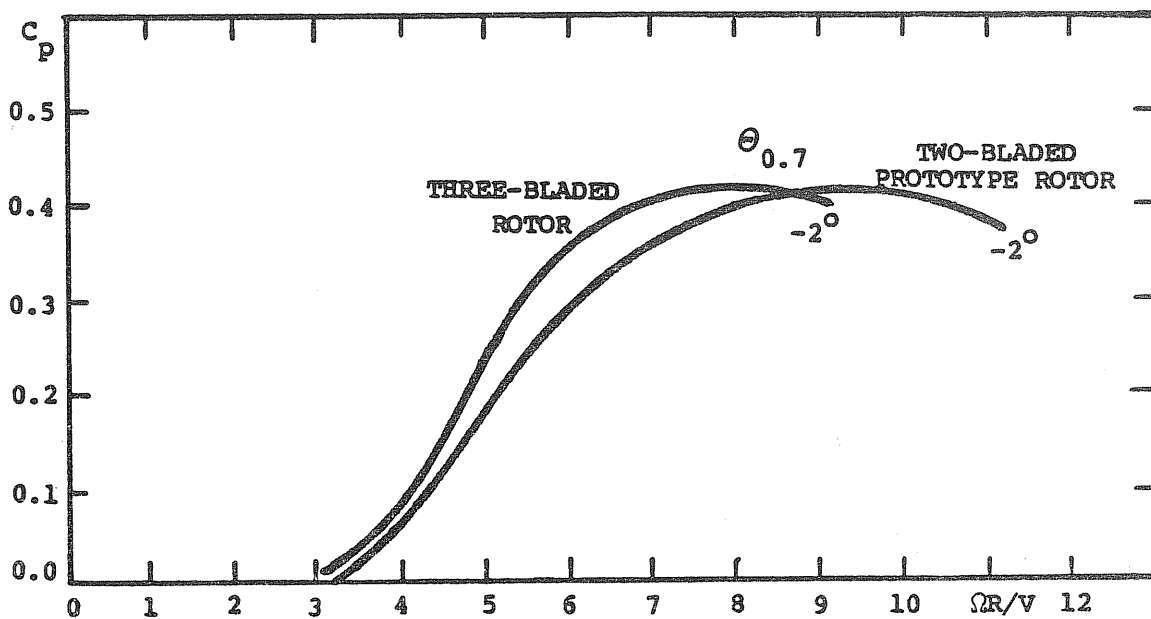
Figure 5-5.   COEFFICIENT OF PERFORMANCE VS. TIP SPEED RATIO COMPARISON
FOR THREE-BLADED ROTOR AND TWO-BLADED PROTOTYPE ROTOR

From blade element theory $\qquad C_T = \lambda \sigma a/4 \qquad\qquad$ (5-2)

From energy balance $\qquad\qquad C_Q = \lambda C_T - \sigma C_{do}/8 \qquad$ (5-3)

Equations 5-1 to 5-3 have been evaluated for $= 0.032$, $C_{do} = 0.01 + 0.5\alpha^2 B$ and $a = 2\pi$.

Figure 5-6 shows the results in terms of a C_p vs. $\Omega R/V$ chart with lines of constant rotor angle of attack α.

The results of a more refined analysis that includes rotors with hinged blades and stall effects are presented in Ref. 8. Only Eq. 5-1 and Eq. 5-3 need to be evaluated. The equivalent blade profile drag coefficient C_{do} and the axial flow component λ are given as a function of C_T/σ and μ in the form of tables and charts. These tables have been somewhat modified for the atmospheric test rotor to account for the higher stall angles. Fig. 5-7 shows the results in the same form as Fig. 5-6. The slanting line represents a constant rotor speed and constant rotor torque condition which results in constant torque coefficient C_Q/σ. Curves similar to those in Fig. 5-7 have been obtained by analysis in Ref. 9 and by wind tunnel tests in Ref. 10. These rotors have cantilever blades while Fig. 5-7 is based on a rotor with hinged blades. The rotor with passive cyclic pitch variation probably has characteristics not too different from those shown in Fig. 5-7.

To apply Fig. 5-7 to a particular wind rotor, the torque characteristics of the load must be known. The atmospheric test equipment has a three- phase ac brushless alternator with rectifier for dc output. It is operated with a constant resistance. The electrical dc power output vs. rpm was measured in a bench test and the mechanical rotor torque input was estimated, considering gearing and electrical losses. The result is the steeply rising curve shown in Fig. 5-8a and 5-8b which represents rotor power required in kW vs. rotor rpm for a 22.5:1 alternator to rotor gear ratio. The rotor power available in kW vs. rotor rpm at various wind velocities has been obtained from Fig. 5-7, assuming sea level standard atmosphere. Figure 5-8a for $\alpha = 90^o$ (zero yaw angle) shows that, for all wind speeds, the intersection of power required and power available curves occurs nearly at the maximum of the power available. Figure 5-8b for $\alpha = 60^o$ (30° yaw angle) shows that higher wind speeds are required to obtain the same power output. For example, at $\alpha = 90^o$ the rotor power output is 7.8 kW at 20 miles per hour and 195 rpm, at $\alpha = 60^o$ the rotor power output is 7.6 kW at 24 miles per hour and 190 rpm. The maximum available power no longer occurs at the intersection with the power required curve but occurs at higher rotor speed. This fact is of no concern since the purpose of yawing the wind turbine is to dissipate the excess power over the rated power. However, the intersection of the two curves is now at an acute angle which reduces the rpm stability at constant wind speed; that is the driving torque increment per unit rpm decrement.

5.3 DYNAMIC ANALYSIS AND COMPARISON WITH TEST RESULTS

Detail drawings of the various components of the Astral Wilcon Model 10B machine, from which the structural properties could be determined, were not available. Therefore, the dynamic characteristics of the experimental wind

24
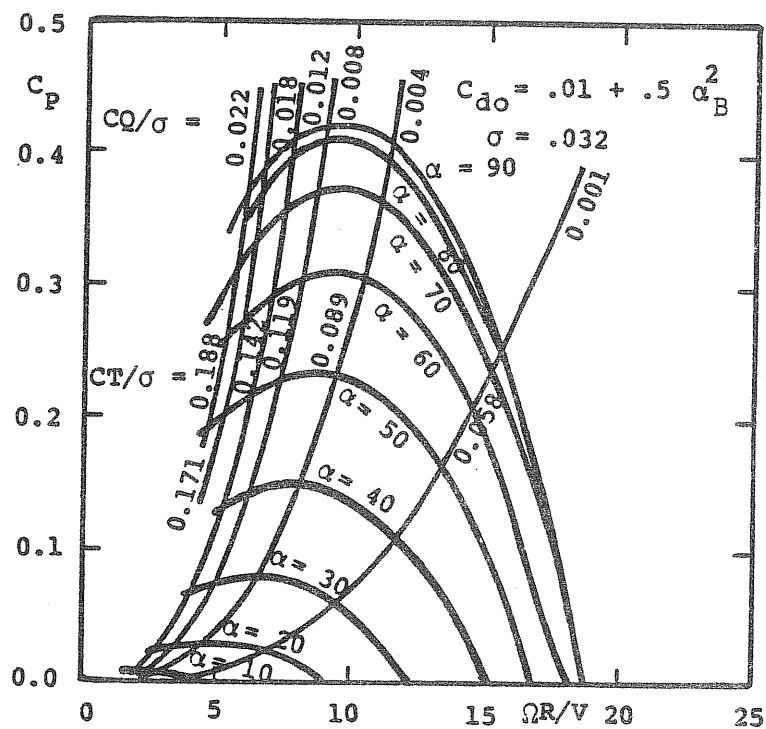
Figure 5-6.   POWER COEFFICIENT VS. TIP SPEED RATIO FOR CONSTANT ROTOR
                ANGLE OF ATTACK VALUES ALPHA, Eq. (5-1) to (5-3)
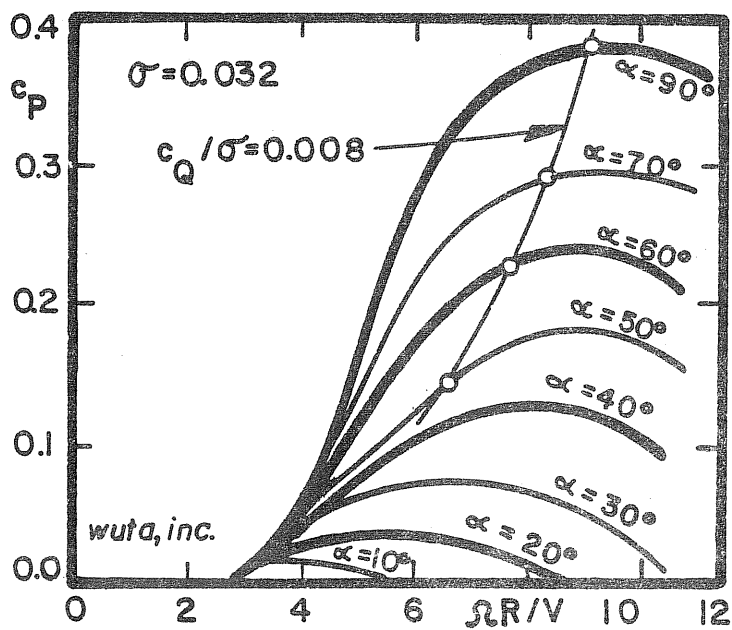
Figure 5-7.   POWER COEFFICIENT VS. TIP SPEED RATIO FOR CONSTANT ROTOR
                ANGLE OF ATTACK VALUES ALPHA, Reference 8.

25
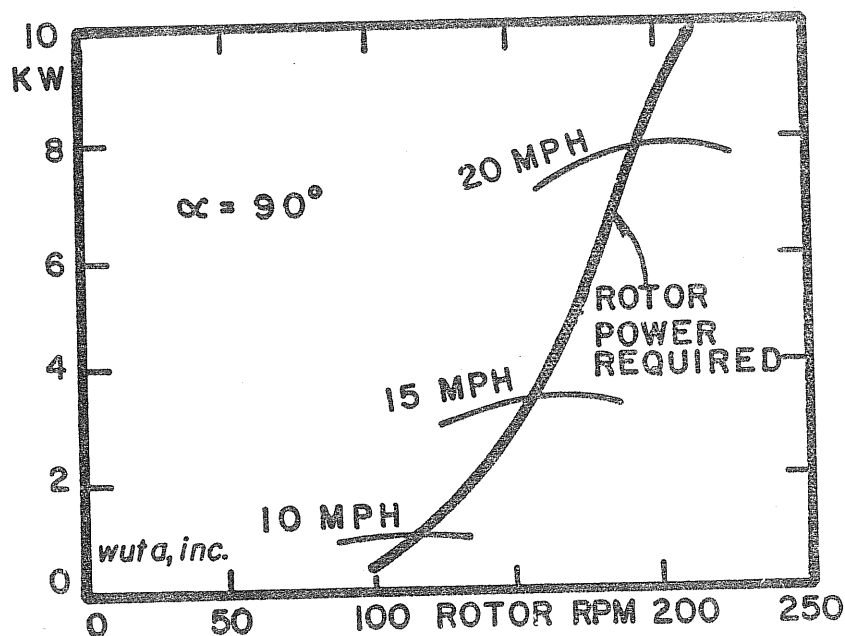
Figure 5-8a.   ROTOR POWER REQUIRED VS. ROTOR RPM FOR VARIOUS WIND SPEEDS
WITH 90 DEGREE ROTOR ANGLE OF ATTACK, GEAR RATIO 22.5/1
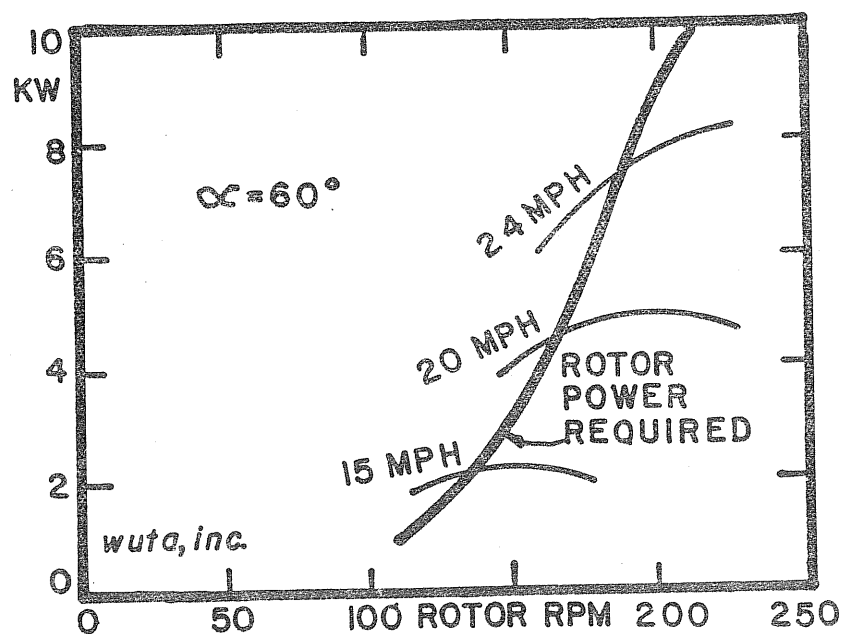
Figure 5-8b.   ROTOR POWER REQUIRED VS. ROTOR RPM FOR VARIOUS WIND SPEEDS
WITH 60 DEGREE ROTOR ANGLE OF ATTACK, GEAR RATIO 22.5/1

turbine had to be determined by a combination of testing and analysis. Tapered and twisted finite blade elements were used for the analysis. The development of the method and its application to the test turbine are described in Ref. 11.

5.3.1 Rotor Natural Frequencies

The fiberglass blades have been modified from those for the three-bladed Astral Wilcon 10B wind machine by shortening the tubular shank at the blade root. The blade has a spar of I-beam shape made of longitudinal fibers, a skin laid up from commercially available fiberglass sheets, and epoxy and expanded foam filler in between. There were insufficient data on the structural design to deduce stiffness or dynamic properties. One blade of the set of three was shipped to Washington University in October 1979. At that time the blade retention design had not been developed. The blade was clamped at the tubular shank with two different cantilever blade lengths (141.5 and 125 in). The natural frequencies for both clamping configurations were measured by an impulse test and by a frequency response test with an intermittent airjet impinging on the blade tip. The first and second flap-bending frequencies of 7.6 Hz and 24 Hz measured for the short shank length were exactly the same as those measured in May 1980 for the complete rotor installed on the machine. The first in-plane frequency of the single blade test was close to 7.6 Hz as indicated by slow beats between the flapping and in-plane mode. The fully assembled rotor did not show these beats and had a clearly separable in-plane blade frequency of 8.0 Hz. The first blade torsional frequency was difficult to measure and has a value of about 30 Hz. Except for the second coning mode, no higher mode frequencies could be measured with the method applied.

The blade was weighed, its center of gravity was determined, and it was swung as a physical pendulum to determine the pendulum frequency. From these data and from the blade shape, the mass distribution was estimated. The stiffness distribution was first assumed and then varied until the analytical values of the two first flap-bending frequencies agreed with the measured values. The bending stiffness at 0.7R was measured by a static deflection test. It agreed quite well with the final blade stiffness assumptions for the dynamic analysis. Next, the frequencies for the other modes and the effects of centrifugal force on the frequencies were analytically determined together with the aerodynamic damping of the two most important modes. The analysis and its results are described in Appendix B.

Figure 5-9a and 5-9b show the natural rotor frequencies in a rotating frame of reference for symmetrical and asymmetrical modes in the form of fan diagrams. The lines for the various harmonics (1P, 2P, etc.) are superimposed on the frequency vs. rotor speed curves. The corresponding mode shapes are sketched in Fig. 5-10. The rigid body mode which represents rotation about the cyclic pitch axis (see Fig. 4-1a), is not sketched. According to Fig. 5-9b, it has a frequency of 1.70Ω except when it couples with the asymmetrical in-plane mode in the 300 rpm region. In the coupling region it is slightly less than 1.70 . The in-plane frequency curve has been corrected somewhat from the curve given in Appendix B to account for the 8.0 Hz measured with the complete rotor when nonrotating. The asymmetrical flap-bending mode could not be excited. The values shown in Fig. 5-9b are from the analysis. The coning mode frequency curve of Fig. 5-9a is taken uncorrected from Appendix B and agrees with the measured value of 7.6 Hz at zero rpm. The symmetrical in-plane mode could not be
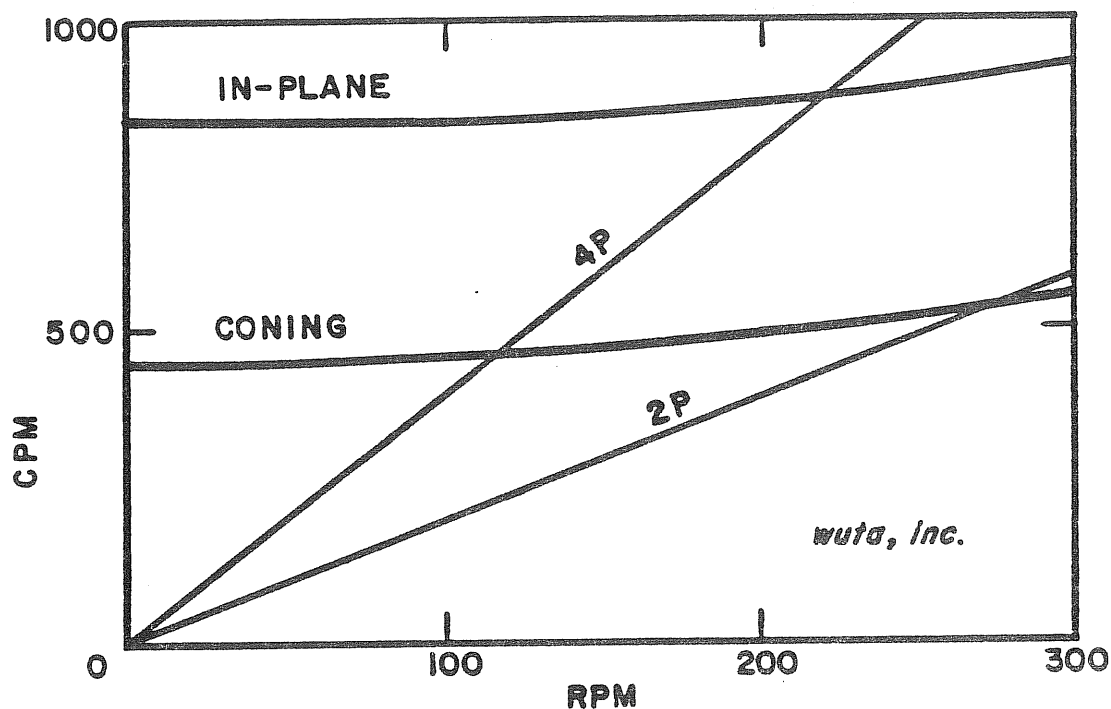
Figure 5-9a.   SYMMETRICAL ROTOR MODE FREQUENCIES VS. ROTOR SPEED
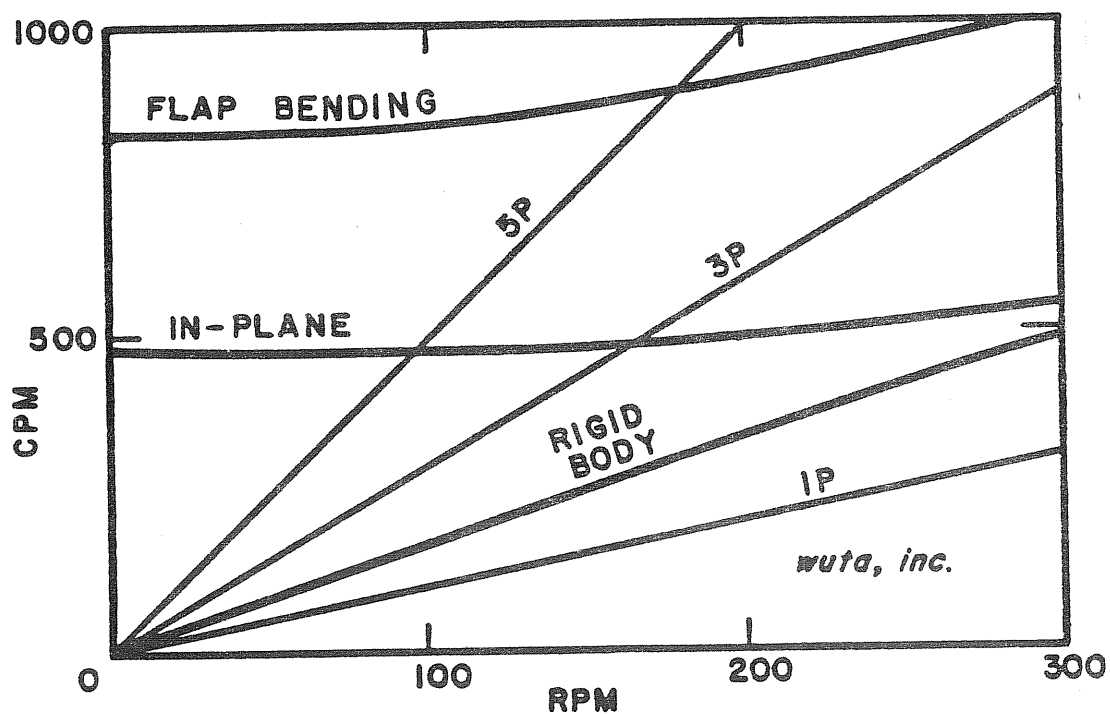
Figure 5-9b.   ASYMMETRICAL ROTOR MODE FREQUENCIES VS. ROTOR SPEED

28
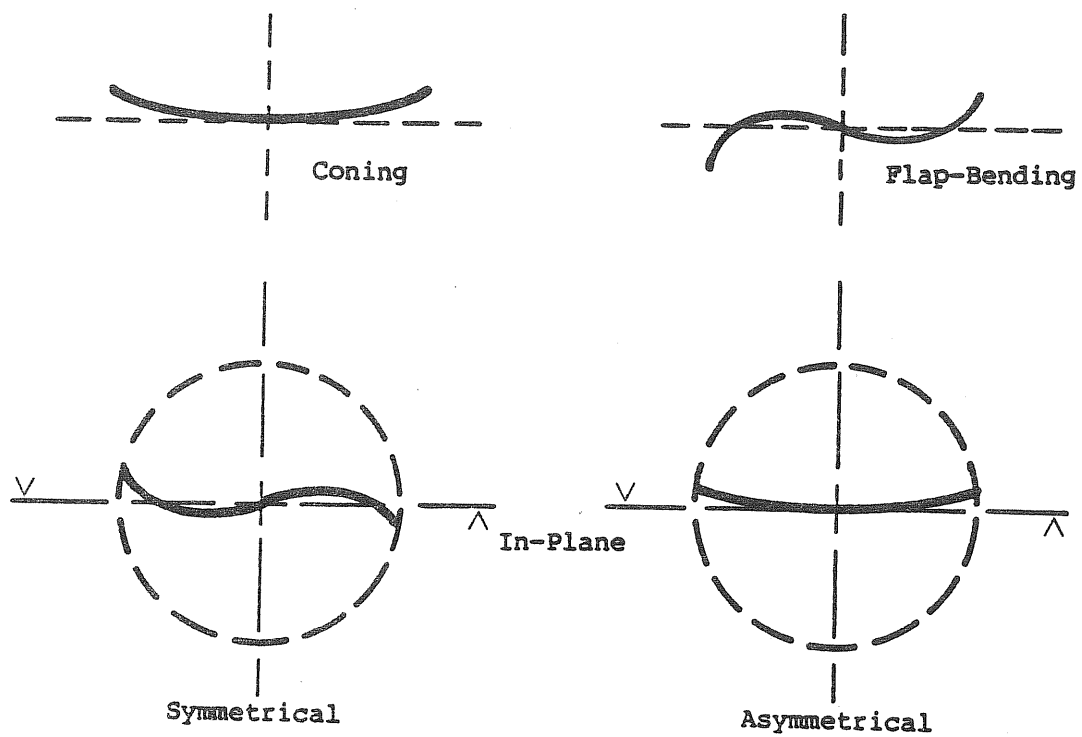
Figure 5-10.   ROTOR MODE SHAPES

excited. Its frequency curve is obtained from the analysis and is shown in Fig. 5-9a. The aerodynamic damping effect was computed for the two modes with the lowest frequency. The damping ratio for the rigid body mode is 0.26, for the coning mode 0.21. This result was obtained with the analysis method described in Ref. 11.

The frequencies in the nonrotating frame are obtained from those in the rotating frame shown in Fig. 5-9 by adding or subtracting the angular rotor speed. The gravity excitation is 1P (one per revolution) in the rotating system, far below the asymmetrical in-plane mode frequency. There is no appreciable resonance amplification of the gravity excitation. This fact was confirmed by atmospheric tests conducted up to 285 rpm. For exactly zero resonance amplification the rotor support of a two-bladed rotor is not excited at all by gravity loads. This is almost true for the two-bladed rotor of the atmospheric test equipment. The asymmetrical in-plane mode will be aerodynamically excited with 3P, 5P, etc. There is no resonance with 1P. The 5P resonance is below 100 rpm and of no significance. The 3P resonance is at 165 rpm where the extracted power is low and in normal operation (except for special tests) the rotor will have zero furl angle. The symmetrical in-plane mode is excited by 4P. It may be modified by the gear train effects which have not been included. The rigid out-of-plane mode is aerodynamically excited by 1P, 3P, etc. and is far removed from resonance. This mode is further well damped with 0.26 damping ratio. The coning mode is excited by 2P and 4P. The 2P resonance with the coning mode is at 280 rpm which can only occur in a transient condition without power extraction. This mode is also well damped with a damping ratio of 0.21. The higher modes are only excited by high harmonics which can be expected to be weak. Overall, (except for the 2P resonance with the coning mode) the natural rotor frequencies appear to be well placed and no severe resonances have been observed during atmospheric testing up to 285 rotor rpm.

5.3.2 Tower and Tail Boom Natural Frequencies

Tower modes and natural frequencies have been computed for the unfurled rotor position as discussed in Appendix B. The first analysis ignored the effect of the yaw post. Later it was found that the yaw post softens the structure considerably and lowers the tower frequency. While mass and stiffness distribution of the tower was reasonably well known from the manufacturers drawings (the tower consists of the upper three sections of the five section 100 ft. Unarco Rhon S.S.V. type), the boundary condition at the foundation was difficult to determine. A rigid cantilever condition was assumed which is apparently incorrect. The first tower mode in the direction of the rotor axis was computed to have a frequency of 158 cpm without including the yaw post and of 134 cpm with its inclusion, while the measured value is 112 cpm. The second tower mode was computed to have a frequency of 796 cpm vs. the measured value of 750 cpm. The frequencies of the lateral modes perpendicular to the rotor axis were computed to be even higher. They could not be measured and are apparently not excited by the rotor. Horizontal oscillatory rotor forces are absorbed by the inertia of the nacelle and damped by the horizontal tail vane motion. The 1P tower resonance at 112 rpm was noticeable during the atmospheric tests but not severe. The 2P tower resonances are at 56 rpm for the first mode and at 375 rpm for the second mode. Both are outside the operational rpm range. The 4P resonance with the second tower mode at 187 rpm appears to be mild. For the tower vibration analysis the rotor was assumed to act as a point mass. However, coupling

between blade and tower modes was considered in the aeroelastic analysis. No appreciable tower resonances occur except for the mild 4P resonance with the second tower mode, and mild 1P resonance with the first tower mode.

The vertical tail boom mode natural frequency was computed to be 280 cpm. The measured value with the tail boom installed on the machine is 160 cpm. The boundary condition at the root of the tail boom is far from being cantilever as assumed in the analysis. The lateral boom mode could not be excited and is strongly damped by the tail vane. Although the analysis was limited to the unfurled configuration, the dynamic tests showed that the natural frequencies of tower and tail boom are not measurably affected by the furl angle. The following table summarizes the natural frequencies obtained by the analysis described in Appendix B and by testing.

Table 5-1. COMPARISON OF ANALYSIS AND TEST NATURAL FREQUENCIES

	Analysis	Test
First Tower Mode	134	112 cpm
Vertical Tail Boom Mode	280	160 cpm
Second Tower Mode	796	750 cpm

The 1P, 2P and 4P resonances are shown in Table 5-2.

Table 5-2. TOWER AND TAIL BOOM RESONANCES

Excitation	First Tower Mode	Vertical Boom	Second Tower Mode
1P	112	160	---
2P	56	80	---
4P	28	40	180 rpm

Although mild, the 1P resonances are clearly seen in the oscillograph records. The 2P and 4P resonances below 90 rotor rpm are also clearly seen but they are not severe. The vertical boom resonances could be reduced by installing a horizontal damping surface at the aft end of the tail boom.

5.4 AEROELASTIC STABILITY ANALYSES

5.4.1 Flutter

Classical blade flutter can occur when the torsion mode frequency coalesces with a bending mode frequency. Torsion modes have been neglected in the preceding dynamic analysis since the lowest torsion mode frequency is much higher than the

bending mode frequencies of interest (30 Hz vs. 8 Hz). An analysis including blade torsion was performed and is described in Appendix B. It is found that a coalescence between the torsion mode frequency and the second flap-bending frequency would not occur below 1000 rpm and that even then the coalescence would not result in flutter. The coupled mode is always positively damped. While the computed 1000 rpm case is fictitious (due to the neglected Mach number effects the rotor could not reach this rpm anyway) the study does show that flutter cannot occur even at substantial overspeed due to the high blade torsional frequency.

5.4.2 Whirl Instability

A two-bladed rotor can exhibit whirl instability in the region where rotor rpm and tower natural frequency coincide. For equal rotor support stiffness in the vertical and horizontal direction, as could occur with a yaw gear drive, a whirl instability is in fact predicted. Due to free-yawing under the influence of the tail vane, the rotor support stiffness in the horizontal direction is zero. An analysis presented in Appendix C shows that no whirl instability exists for this case. The whirl analysis was performed prior to the inclusion of the softening effect of the yaw post in the analysis of the first tower mode natural frequency. The first tower mode natural frequency was initially computed to be 158 cpm as compared to 134 cpm for the improved analysis and a measured value of 112 cpm. The atmospheric tests showed no sign of a whirl instability.

5.4.3 Ground Resonance

What is misleadingly called ground resonance in rotorcraft technology has destroyed many helicopters. It occurs for our machine in the region where the uncoupled tower mode in the rotating frame with frequency $\Omega - \omega_T$ coalesces with the uncoupled asymmetrical in-plane mode frequency. This coalescence occurs far above the operational range at about 700 rpm. A weak instability with 0.02 negative damping ratio occurs in the rotor speed range between 420 and 500 rpm. The coalescence of the uncoupled tower mode frequency in the rotating frame $\Omega + \omega_T$ with the in-plane frequency takes place in this range. This instability is also far above the expected maximum overspeed of 300 rpm. Furthermore, the omitted tail vane damping and yaw bearing friction will most likely overcompensate the small negative damping found using the simplified mathematical model. The coupled mode shows substantial participation of rigid yawing, so that both of the two damping sources will be available. The analysis, using the method of Ref. 11, was again performed before the yaw post effect had been considered and uses 158 cpm as the frequency of the first tower mode.

5.4.4 Rotor Rigid Body Mode Instability

The rotor rigid body mode frequency of 1.7 coalesces with the asymmetrical in-plane mode frequency at about 350 rpm. A closed form approximate solution showed a negative damping ratio of the coupled mode of 0.001. However, the finite element analysis of Ref. 11 gave, positive damping of the coupled mode.

SECTION 6.0

FULL SCALE WIND TURBINE STUDIES

When considering the best approach to a quantitative experimental study of a wind turbine with blade cyclic pitch variation, the question arose whether to use wind tunnel tests with a large wind tunnel model with adequate Reynolds number or atmospheric tests. The advantage of wind tunnel tests is that the steady flow characteristics can be easily compared to analytical results. The disadvantage is that a realistic simulation of the effects of variable wind velocity and direction is not feasible. Also, under present conditions it was unlikely that we could have obtained an early time slot in one of the larger wind tunnels. Therefore, atmospheric testing appeared to be the only practical approach. Due to the random variability of wind speed and wind direction, statistical data collection and processing was the preferred method of atmospheric testing.

It would be desirable to use the average wind velocity and direction over the rotor disk as independent variables. However, the measurement of flow velocities near the rotor disk requires sophisticated equipment like laser velocimetry which so far has only been used in the laboratory, not in the field. In the absence of flow measurements at the rotor disk one has to relate the wind speed measured at some point near the rotor to the random performance or load measurements. For this purpose the method of wind speed "bins" developed at Sandia Laboratory is useful and can serve as a standard method to compare characteristics of different wind rotors for the same wind speed distribution, or the effects of different wind speed distributions on a particular type of wind rotor. A comparison with analytical data would require the use of random process theory. The mean value of a random measurement variable associated with a wind speed "bin" is not the same as the steady state value associated with the wind velocity at the center of the "bin". The location of the reference wind speed pick-up can also greatly influence the results. For all of these reasons atmospheric test data have to be carefully interpreted. A comparison with analytical steady state data or with atmospheric test data for other wind rotors at other locations is not at all straightforward. We have used rotor speed "bins" rather than wind speed bins for some of the statistical data presentation. The uncertainties in the relations are then reduced. Many of the dynamic variables depend primarily on rotor speed and only indirectly on wind speed.

6.1 ATMOSPHERIC TEST EQUIPMENT

The proposal for the research on the yawing of wind turbines with blade cyclic pitch requested a grid connected induction generator with 1.5 kW rated power driven by a 4 m diameter wind rotor. The proposal argued that the small test rotor would allow easier modifications than a more practical larger size. The proposal considered quite drastic configuration changes including a change from upwind to downwind rotor position and a change from passive to active cyclic pitch variation. Later considerations of the kind discussed in Section 3 made it evident that the selected configuration was superior to possible other configurations, so that no configuration changes need be considered for the atmospheric test equipment. Furthermore, it was found that for the slender

blades needed for the concept of autorotational storm survival, the blade Reynolds number for a 4 m diameter rotor would be rather low and not typical of more practical wind rotor sizes. For these reasons it was decided to conduct the atmospheric tests with a larger wind rotor with 8 to 10 kW rated power output.

In the search for an off-the-shelf machine of the size and configuration desired with upwind rotor location and variable tail boom position, two were found that looked promising: The Millville Model 10-3 and the Astral Wilcon Model 10B. The Millville machine was offered either with an induction generator for grid connection, or with a much heavier self excited generator for stand alone operation. As was explained in Section 3, the induction generator would require either a very accurate rotor speed limitation or a combination of rotor speed and torque limitation. The Millville machine with induction generator did not have torque control; it had merely a rotor speed control by blade feathering which is claimed to be sufficiently accurate to serve as torque limitation. Since we could not be sure that a yaw angle rpm control with sufficient accuracy for application to an induction generator could be easily developed, we preferred a self-excited generator where, for a constant electric load, a rotor speed limitation also serves as torque limitation.

When comparing the Millville Model 10-3 machine equipped with self excited generator to the Astral Wilcon Model 10B which was only offered with a self-excited generator, the Astral Wilcon machine appeared to be the better choice. The blades are molded using glass fiber reinforced resin, they are strongly tapered and twisted and they have a low blade solidity. The Millville blades are made of riveted aluminum sheet metal, have constant chord, have a much greater blade solidity and are much heavier. The rest of the Millville machine is also much heavier. The self-excited generator alone weighs 600 lb, close to the total weight of the Astral Wilcon 10B machine. A low moment of inertia about the yawing axis is desired since the load of the tail boom actuator is determined by this moment of inertia and by the bearing friction. A disadvantage of the Astral Wilcon 10B machine is that prior operation experience exists only with some components like the blades, the alternator and the tail boom with vane. Support beam, gear train and yaw bearings with yaw post are a new design with no prior experience. This led to certain problems to be discussed later. Also, no performance measurements had been made with the Astral Wilcon 10B wind turbine and therefore we did not know whether it was an efficient and cost effective wind energy conversion system. The purpose of the atmospheric tests was to establish the characteristics of the new wind rotor under study, not to develop an efficient prototype. Therefore, the uncertainties about the selected machine were not believed to be detrimental to the purpose of the study.

The Astral Wilcon 10B machine is standardly equipped with a three-bladed rotor with automatic feathering control whereby the blades themselves act as fly weights for the constant speed governor. They move radially outward under the influence of the centrifugal force and against the forces of heavy springs. The radial motion of the blades is coupled with collective blade pitch changes. The two-bladed rotor of the atmospheric test equipment with its passive cyclic pitch variation was designed in cooperation with Astral Wilcon, using modified Model 10B blades and modified blade retentions. The rotor was built at Astral Wilcon. The entire machine including rotor was received by WUTA in March 1980. It was mounted on a pedestal in the WUTA laboratory and subjected to numerous tests to

be described under the headings for the various components. Certain structural weaknesses were removed by appropriate modifications, also to be described later. After mounting the strain gages, all calibrations were performed in the laboratory.

An instrument shed was positioned just outside the laboratory with direct access from the laboratory. All required electrical circuitry was installed in the shed together with the recording equipment and associated electronics. Simultaneously the test site was prepared by constructing the tiltable tower with its cradle, working platform, power winch foundation and gin pole. In May, 1980 the machine and instrument shed were transported to the site and the machine was mounted on the tower. The first machine run was achieved on May 23, 1980. The various components will be described in the following subsections.

6.1.1 Site

The site for the atmospheric test equipment was in the the 2000 acre wooded Tyson Research Center owned by Washington University. Figure 6-1 is a topographical map of the site environment. The test turbine was located close to the high point of a ridge that extends in the north-south direction. The ridge was wooded, but a sufficient number of trees have been cut so that the site is now completely open between the southwest and northwest, the sector of the prevailing wind directions. In other directions there are trees which reach 25 ft above the base of the tower. However, the 25 ft diameter wind turbine is mounted on top of a 60 ft tower and therefore is effectively open to wind from all directions. The instrument shed, the power winch and gin pole for raising and lowering the tower are on the ridge to the north of the tower. The entire research park is enclosed by a fence and has only one access, controlled by a guard. Access to the site is via a 1.2 mile dirt road with a steep slope to the top of the ridge. The access road begins 1/3 mile from the gate down the paved road toward the administration building. After the initial steep slope the road follows the ridge with only minor up and down slopes. The access road is drivable the entire year except during times of solid snow cover. AC power and telephone service is available 500 ft to the north of the site.

Work at the site began in December, 1979 with the pouring of a 11 X 11 X 4 ft concrete foundation for the tower. It continued in January, 1980 with the erection of the first 20 ft tower section. Further work at the site was delayed until April, 1980 due to a solid snow cover during February and most of March. All installations at the site were completed in May, 1980. Various pieces of test equipment are described under their respective headings in following sections.

6.1.2 Rotor

The assembly drawing of the atmospheric test equipment (Appendix E) shows an axial and a side view of the rotor. The blade geometry has been discussed in Section 5.1 and the dynamic blade characteristics were discussed in Section 5.3.1. The blade spar material has 50% glass fiber content. The style 1600 glass fiber used in the blade spars has the following properties: tensile strength, 67 ksi; flexural strength, 150 ksi; modulus, 3,300 ksi. The fatigue strength is probably not more than 25% of the ultimate strength. The blades

RANGER STATIONS (500FT)

POWER LINE

LINE SHED (650FT)

EXPERIMENTAL SETUP AND INSTRUMENT SHED (700FT)

N

500 700 600

600 700 550

650 650

SITE ENTRANCE

HIGHWAY 44

wuta, inc.
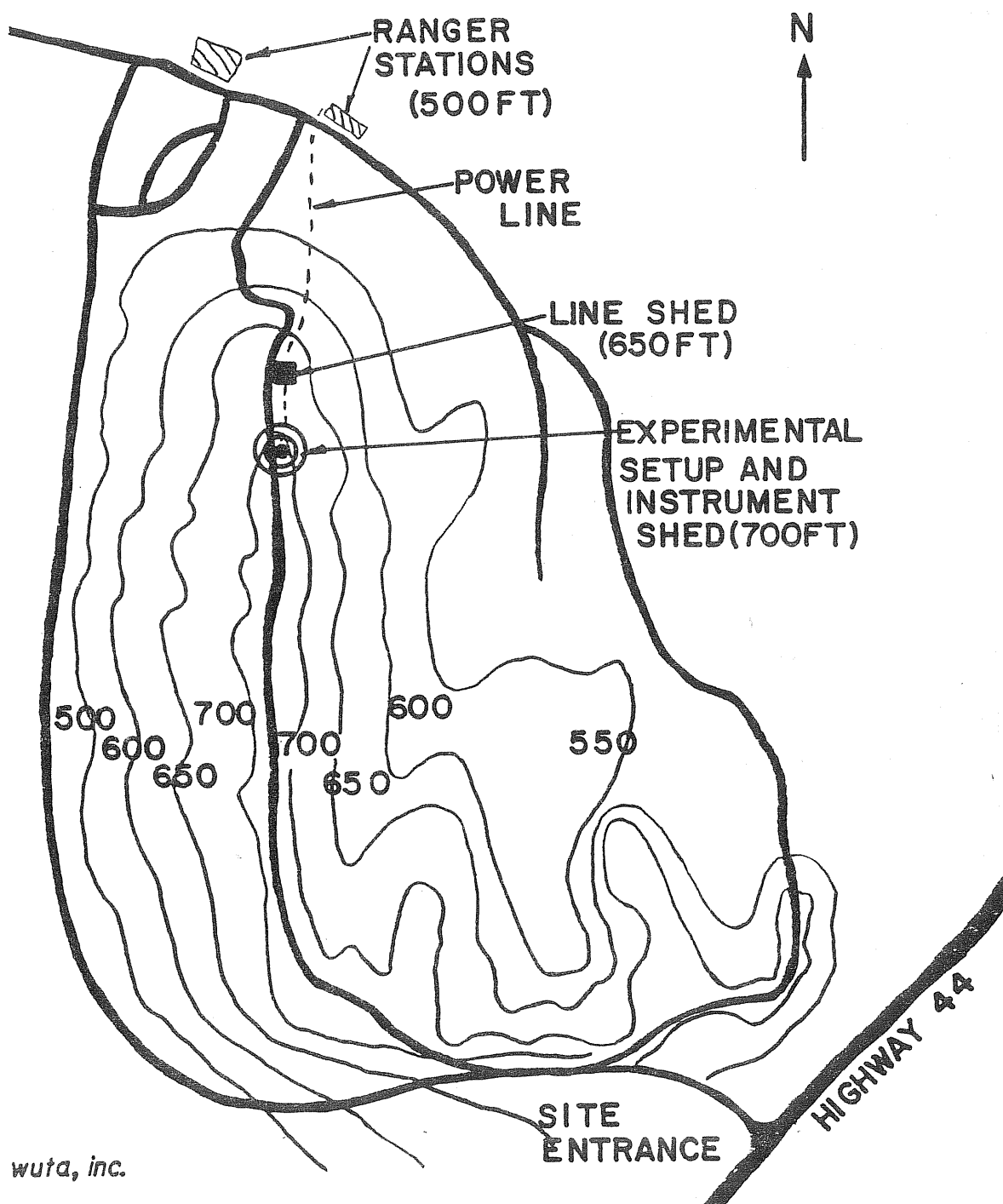
Figure 6-1.   CONTOUR MAP OF SITE ENVIRONMENT

have been operated in the first version of the Model 10B for several months without failure at a site in Chelmsford, MA. Astral Wilcon has not released a detail design drawing of the blades from which a structural analysis could be made. However it is believed that the sustained prior operational experience of the blades is sufficient to have confidence in their structural integrity for operation on the test rotor. A third blade, used for dynamic tests, is available for structural tests if so desired and could also be cut at various blade sections to determine the fiber structure.

As shown on the assembly drawing in Appendix E, each blade is retained by two clamps which are bolted to two aluminum channels. The clamps are made from modified cast aluminum bearing blocks used in the Model 10B rotor. These clamps were used as molds for the blade shanks and for the blade retention rings molded onto the shanks. They transfer the centrifugal force to the clamps in addition to force transfer by friction. By later using the molds as clamps a uniform fit was obtained. The penalty of this process is that the clamps are not exchangeable. While the centrifugal force is transferred both by friction and by the molded retention rings on the blade shank, torsion is transferred only by friction. After loosening the bolts that connect the blade clamps to the aluminum channels the blade can be rotated with respect to the clamps, and therefore blade pitch is adjustable. The blades were carefully adjusted for pitch setting when the rotor was assembled in the laboratory. When the rotor was run at the site, the blades tracked perfectly and required no further adjustment. This is quite unusual for wind rotors. It is believed that the ease of achieving good blade tracking is a beneficial side effect of the passive cyclic pitch arrangement; an arrangement which automatically compensates for most of the difference in pitch setting between the two blades. The blades carry a marker and the outer clamps carry a scale. This allows the pitch of both blades to be changed by the same amount in order to experimentally establish the optimum blade pitch angle. The blades weigh only 31 lb each, a very low weight compared to most wind turbine rotor blades of this size. One blade came with an external balance weight installed at 0.7R. It was replaced by an internal balance weight of 2.6 lb fastened to the blade shank between the two blade clamps.

The aluminum block retention channels are connected on both sides by bolted aluminum plates to form a closed box for greater stiffness. The center of the channels carry the aluminum bearing blocks for the cyclic pitch bearings. Rulon flange bearings are inserted between the bearing blocks and the steel pin welded to the hub. The axial view in Appendix E shows the cyclic pitch axis rotated from its normal position in line with the blade axis by 23° in the sense of a blade prelag as described for the rotor model in Section 3.3. The center of the rearward channel has a reinforced circular opening to insert the rotor shaft. The connection between rotor and shaft is made via a welded hub with taper lock, commercially available. The inner ring of the taper lock is fastened to the shaft by a key to transmit torque and by a drift pin to prevent forward motion in case of forward thrust. The normal rearward thrust is transmitted to the shaft by a sleeve. The rim of the reinforced circular opening in the rear channel forms a stop which limits cyclic pitch amplitude. Rubber pads are inserted at the contact location between the shaft and the rear channel. They provide a spring constant of 1200 in-lb flapping moment per degree.

Mounting the rotor to the shaft is a simple operation. Two horizontal screws, accessible from the rear of the hub, pull the outer taper lock ring against the inner taper lock ring fastened to the shaft by key and drift pin. There is a third screw for loosening the taper lock connection after removing the first two screws. The rotor can then be removed from the shaft. The holes for the tightening screws are one-half in the outer ring which has threads, and one-half in the inner ring which has no threads. These screws act as keys to transmit torque from the outer to the inner ring in addition to friction. The advantage of the taper lock connection is that there can be no play between hub and shaft which may cause fretting corrosion.

The retention structure and the hub weigh 80 lb. This high weight is necessary to adapt the long blade shank to the retention mechanism. The channels are 50 in long, much longer than would be required for a new blade design. Since the Model 10B blade bearing blocks were transformed to clamps, the retention structure has a greater cross section than would be necessary with a new blade design. Eliminating the heavy clamps with the many attachment bolts will also save weight and cost. A prototype machine having a known optimum blade pitch angle would not require adjustable clamps.

6.1.3 Power Transmission

The rotor drives a Morse 115D15 shaft-mounted two-stage speed reducer with a total gear ratio of 15:1. Astral Wilcon has no prior experience with this speed reducer. Morse did not know the operating characteristics of the 115D15 reducer when using it as a speed augmenter as is done in the wind machine. The speed reducer has spiral teeth which are torqued in the opposite direction in the AW10B application from that for which they were designed. The very low efficiency, measured as the ratio of electrical power output over rotor power input, during atmospheric testing at low rpm may have been in part caused by the low efficiency of the speed reducer used as a speed increaser. Monitoring the gear box temperature during extended operation at rated power is desirable. The torque link of the shaft-mounted speed reducer develops a load of 950 lb at rated power. The moment arm of this force to the rear shaft bearing is 4.3 in. The shaft bending moment (4100 in-lb) from the speed reducer torque link is the highest the shaft experiences and is very much higher than the bending moment from the rotor weight. The alternating stress in the 2 in diameter rotor shaft is ± 10.4 ksi. For this reason the shaft is made of high quality 160 ksi strength steel. It is expensive and difficult to machine. The rotor shaft could probably be made of lower quality steel to save machining and material costs in a prototype machine by moving the speed reducer closer to the rear shaft bearing.

There is no taper lock connection between rotor shaft and gear shaft, merely a key for transmitting torque. The torque link load apparently prevents play in the connection. The Morse speed reducer is widely used in industry and should represent a mature design. The speed reducer weighs 80 lb. The torque link connection to the carrier beam looked inadequate and has been reinforced. The speed reducer output shaft turns 15 times rotor speed and is located at the rear. It carries a pulley and timing belt which drives the alternator. The alternator is supported by a bracket bolted to the speed reducer rear face. The machine was delivered with a set of pulleys that gave a total alternator to

rotor gear ratio of 25:1. In order to make atmospheric testing more flexible, two new sets of pulleys were purchased to reduce or to increase the total gear ratio by ± 15%. The machine was delivered without a tach generator. A tach generator (also used as a starting motor) was shaft-mounted to the speed reducer output shaft. The rotor shaft extends through the speed reducer. A slipring unit with 12 silver sliprings is mounted to the extension of the rotor shaft at the rear of the speed reducer. The rotor shaft has a 0.5 in bore extending all the way from the rotor hub to the slipring unit to accept wires from the rotor strain gages. Since the timing belt provides a very soft connection between rotor and alternator, dynamic drive system problems are not anticipated. Drive system torsional vibrations were measured by a strain gage torque meter located behind the rotor hub.

6.1.4 Alternator

A Maremont Model E-95 12 volt brushless truck alternator was rewound by Astral Wilcon. It weighs 35 lb as compared to 600 lb for the Millville Model 10-3 self-excited generator. During a bench test with an electric resistance load of 5.5 ohm at 5500 rpm it delivered 220 V, corresponding to 8.8 kW. It has operated several months in the Chelmsford, MA machine. In order to limit the voltage to 200 V (needed for the installation of the 8 kW Gemini synchronous inverter) the number of stator windings was reduced from 34 to 28. This alternator version was used in a Model 10B machine erected in Harvard, MA in March, 1980. A similar alternator was delivered to WUTA.

Two field failures were experienced in the Harvard machine within a short time. It was not established whether the field wire breakage was caused by vibrations or by overheating. Astral Wilcon rewound the alternator field with thinner wire which increased the field resistance from 200 to 700 ohm. The windings were embedded in epoxy to prevent vibration damage. The original alternator was exchanged for one with the modified field. We checked this alternator in May, 1980 on a production test facility with a 5.15 ohm electric load. The voltage and power output vs. rpm curves begin to flatten out at 4500 rpm with output power of 4.6 kW. At 5500 rpm the output was 200 V, corresponding to 7.8 kW. All generator configurations tested had tuning capacitators, as shown in Fig. 6-2.

We were concerned about the early flattening of the output power vs. rpm curve. Astral Wilcon offered to exchange the first replacement alternator with a second replacement which had the original 34 stator windings but with the higher resistance field. We were advised to use 60μF tuning capacitors with this version rather than the 50μF installed before. The second replacement alternator was mounted in the machine without bench testing. During atmospheric testing the voltage vs. rpm curve peaked at 173 V at 4400 rpm, corresponding to 5 kW. At 5500 rpm the power output decreased to 4.2 kW. Apparently this version of the alternator was mistuned. In October, 1980 we replaced the latest alternator with the one previously used. With a 6 ohm load resistance and 50μF tuning capacitors it gave an output of 7.5 kW at 5500 rpm, somewhat less than obtianed for the bench tests. The various alternator configurations and their parameters are listed in Table 6-1.

Table 6-1. ALTERNATOR CONFIGURATIONS

Config.	Number of Stator Windings	Field Resistance, ohm	kW at 5500 rpm	Test	Comment
1	28	200	?	–	2 field failures
2	28	700	7.8	WUTA Bench	First replacement
			7.5	WUTA Atmosph.	
3	34	200	8.8	A.W. Bench	Chelmsford machine
4	34	700	4.2	WUTA Atmosph.	Second replacement

As mentioned before, the ratio of electrical power output over rotor power input as determined during atmospheric testing is very low, particularly in the middle and lower power range. Though we have no way to differentiate between electrical and mechanical losses in the transmission system, the alternator may experience high losses at low power. The tuning capacitors are designed to increase the maximum power output from about 5 kW to over 8 kW at rated speed. The effect of the tuning capacitors is likely to reduce alternator efficiency in the middle and low power range mostly used in the wind turbine.

Before designing a prototype with this alternator, the question of optimum configuration with respect to variables like number of stator windings, tuning capacitors and field should be established by bench tests. The test results may show that the alternator, even in its optimum configuration, is not suitable for an 8 kW wind turbine.

According to the manufacturer, the alternator can withstand an overspeed of 10,000 rpm which corresponds to 400 rotor rpm. Since the manufacturer could not give any information on maximum acceptable alternator gyroscopic loads, we ran a test where the alternator was subjected to a gyroscopic load that would occur at 6000 rpm for a yaw rate of 1 rad/sec. The alternator passed this test without any indication of damage to the rotor. The actual maximum yaw rate is expected to be about 0.5 rad/sec. The maximum yaw rate measured to date was 0.3 rad/sec. Figure 6-2 shows the wiring diagram for the alternator. The stator windings produce three-phase ac which is rectified by diodes to dc. The field and the dc load are in parallel.

While the principle of using automotive components in wind machines is very interesting because these components are cheap, light and easy to replace, much more experience must be accumulated with such components to be sure that this selection is more cost effective than using components that are designed for the long life required for wind turbines.

6.1.5 Tail Boom Vane

The 204 in long aluminum tail boom is adapted from a commercially available lamp post. The diameter reduces between root and tip from 7 to 6 in. It weighs 92 lb. The tail vane is made of fiberglass material, weighs 28 lb and is bolted to the tail boom. The geometry can be taken from the assembly drawing in Appendix E and also from the Table in Section 4.1. The furl bearings at the root of the tail boom are 3 in diameter Rulon flange bearings which are not obtainable off-the-shelf but are special made and very costly. When the decision to use Rulon bearings was made, the furl actuator had not as yet been selected. We were concerned that the higher friction of the less costly bronze bearings used for Model 10B may affect actuator operation. The friction of the Rulon bearings under the gravity load of the tail boom and vane were measured to be 80 ft-lb. The electric furl actuator can overcome 250 ft-lb. The furl actuator bracket is aluminum, welded to the top of the tail boom near its root.

For the Astral Wilcon Model 10B, the tail boom is elastically connected to the furl actuator to relieve the rotor of gyroscopic loads. These springs are omitted for the atmospheric test machine since the passive cyclic pitch rotor can accept high rates of yaw. One might suspect that the omission of the springs would lead to higher tail boom horizontal root moments. However the strain gage measurements showed small oscillatory moments, well within the estimated fatigue strength of the tail boom. The highest root moment occurred during the cut-in and cut-out of the furl actuator, which accelerates and decelerates quite rapidly. Although the aluminum tail boom when produced from a collision damaged lamp post is inexpensive, a fiberglass boom and vane produced in one mold would be more suitable for a prototype machine. The main load that the furl actuator must overcome is the tail boom bearing friction resulting from the gravity moment. Therefore, it is important that the boom and vane be as light as possible.

6.1.6 Carrier Beam and Yaw Post

As can be seen from the assembly drawing in Appendix E, the main structural element of the nacelle is the 8 by 5.3 in I-beam. The I-beam must transmit the gravity moment of the tail boom and vane, the rotor and rotor support, and the rotor thrust and torque to the yaw post. This is no problem in the unfurled position of the tail boom since the I-beam is subjected to bending. However, in the furled position of the tail boom its gravity moment loads the I-beam in torsion, causing high stresses and a lack of stiffness. This deficiency was determined at Astral Wilcon when the chassis was supported by the yaw post and the tail boom was furled. To correct the problem, 1/8 in steel plates were welded to each side of the I-beam over part of its length and delivered to WUTA in this configuration. An attempt to analyze the structure showed that the side plates are rather ineffective without bulkheads to close the box. A rear bulkhead was added, the side plates were extended all the way to the front of the I-beam, and the front end was closed. The I-beam was then completely boxed and the structure was capable of accepting the large gravity moment of the tail boom and vane in the furled position without excessive stresses and excessive torsional softness.

41

The yaw post is welded to a flange that is bolted to the lower I-beam flange. This is a rather soft connection even though it had been stiffened by boxing the I-beam. In a prototype a box beam should be used as the main structural element rather than an I-beam, and the yaw post should be welded or bolted to both the upper and the lower sides of the box beam. The yaw post is made from high quality seamless tubing having a 3 in diameter and one-half inch wall thickness.

6.1.7 Furl Control System

As seen from the assembly drawing in Appendix E, the furl actuator is located above the tail boom and extends between brackets on the tail boom and the carrier beam. Figure 6-3 shows the kinematic characteristics of the furl actuator. Extension and moment arm with respect to the tail boom bearing center are plotted vs. furl angle. The extension vs. furl angle curve is slightly nonlinear. The moment arm varies between 2.7 in in the furled position and 4.4 in at 30° furl angle and back to 3.7 in at zero furl angle. The actuator is a 12 V dc Saginaw Steering Gear "Performance Pak" with 12 in stroke, 750 lb maximum operating load and 3000 lb maximum static load. A ball screw is driven via a reduction gear by a 12 V dc motor. The actuator has a 30 percent duty cycle to prevent motor overheating. The irreversible actuator has a constant rate of 1.1 in/sec, almost independent of load. It accelerates and decelerates rapidly, and is mass produced for the automotive industry. It is inexpensive and easily replaced. As can be seen from Fig. 6-3, only one-half of the 12 in stroke is used in our application.

An actuator "proof test" was conducted with the machine installed in our laboratory on a pedestal. The time to 85° furling was 4.7 sec. Starting current was 60 amps. Steady state running current was 12 amps. Initial boom hinge moment was 150 ft-lb with 12 Hz oscillations and 75 ft-lb after 1 sec. When fully cycling the actuator five times per minute (0.78 use factor), the motor temperature rose from $21^\circ C$ to $70^\circ C$ in 18 minutes. Except for the statement that among many hundred-thousand actuators sold only a few were returned because of malfunctions, actuator reliability data could not be obtained from the manufacturer.

Figures 6-4a and 6-4b show the manual and automatic furl/unfurl control systems. The actuator motor was powered by two relays; one for furling, one for unfurling. The relays are tripped by a low voltage circuit a) in response to a manually operated toggle switch, b) in response to limit switches at both ends of the actuator travel, and c) in response to overspeed and underspeed voltage signals from the tach generator. An underspeed sensing relay is available but has not been used in our tests. When the overspeed signal trips the furl relay, the actuator travels toward the furl direction until rated rotor speed is established. In the event this system malfunctions, it can be overridden by a manual toggle switch which directly powers the actuator to furl or unfurl. The actuator was manually set to desired furl angles and statistical data were collected until overspeed furling occurred. After the wind speed had subsided below the value that caused the overspeed, the operator reset the machine to the proper furl angle. The microprocessor was programmed in a way such that furling due to overspeed interrupted data collection.
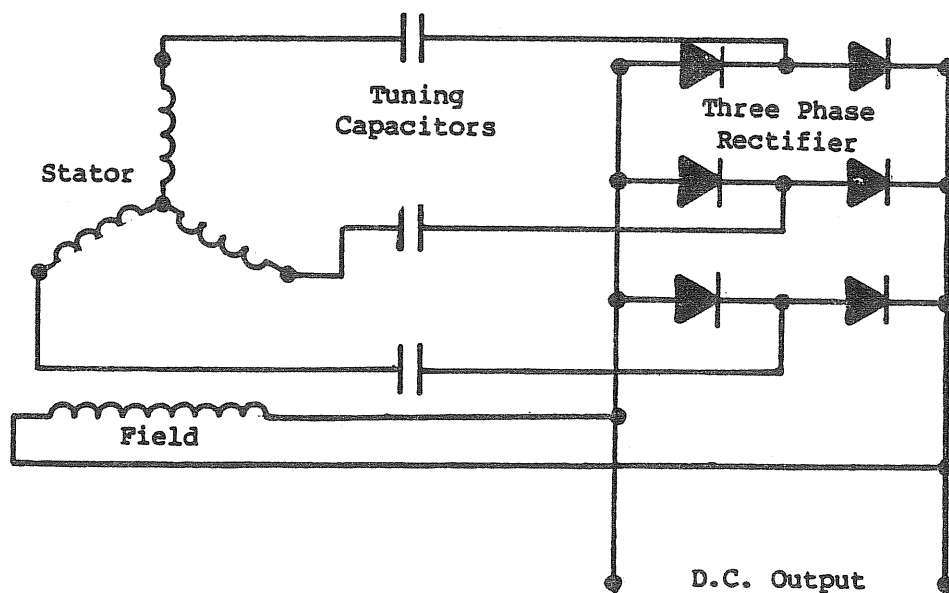
Figure 6-2.   ALTERNATOR WIRING DIAGRAM
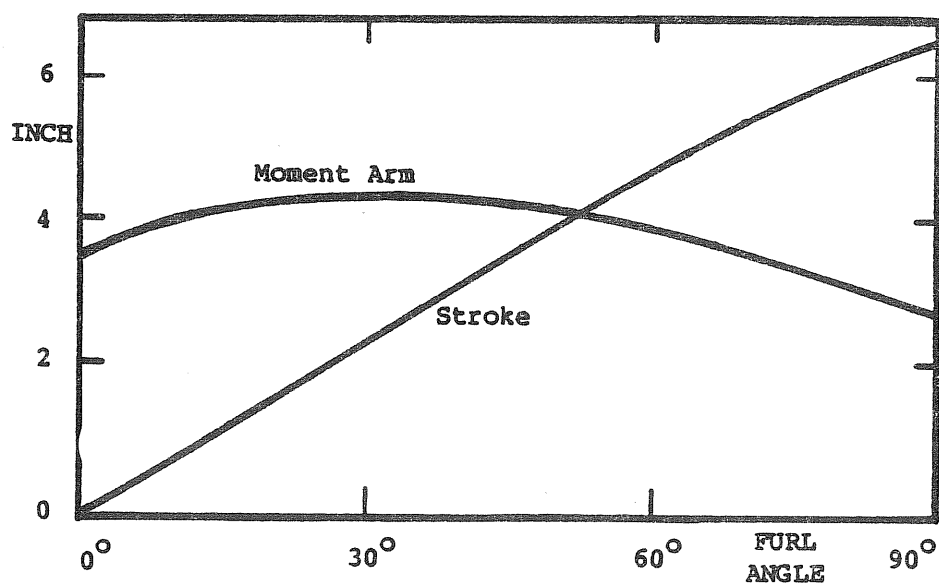
Figure 6-3.   FURL ACTUATOR KINEMATICS

43
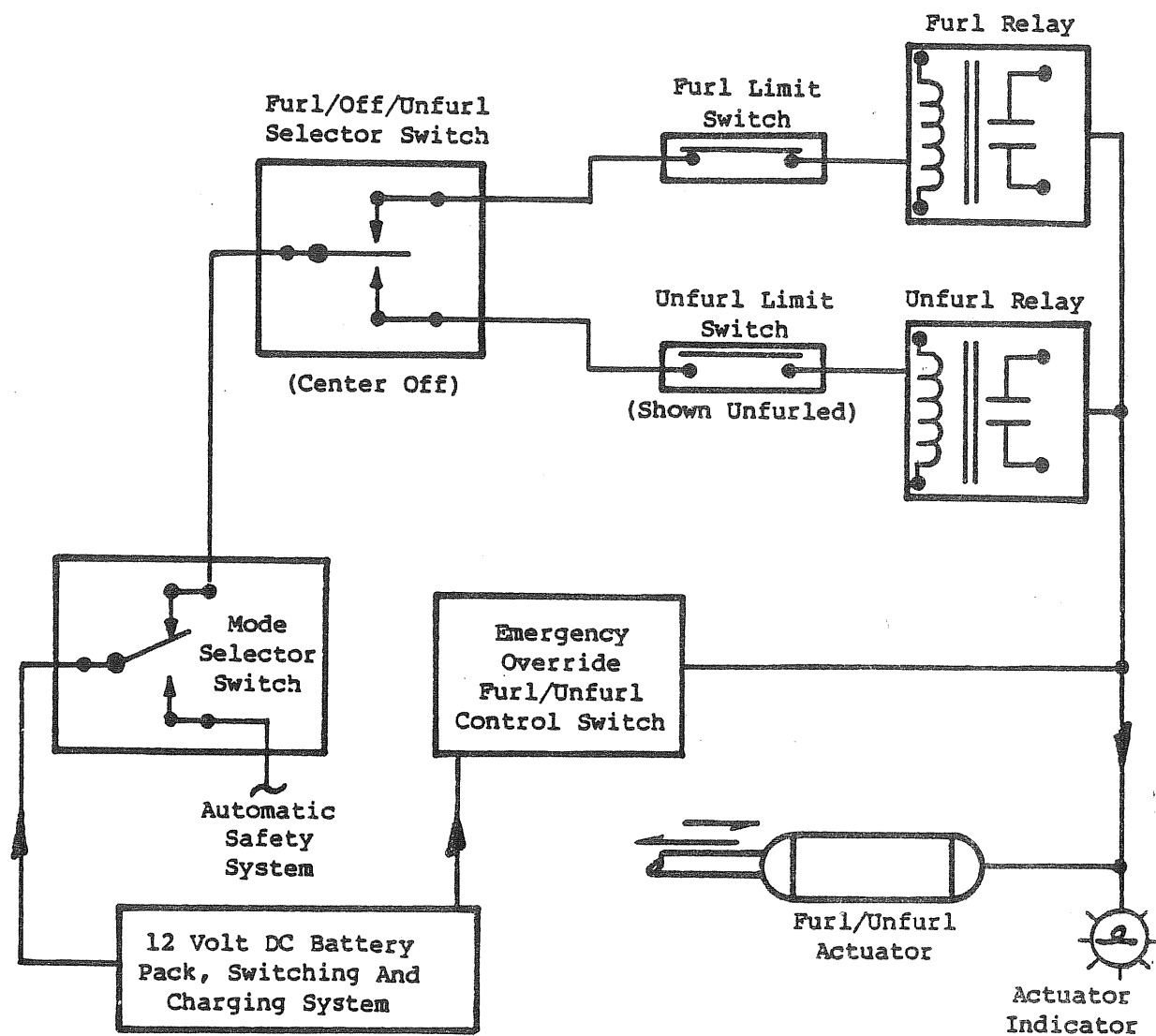
Figure 6-4a.   FURL/UNFURL MANUAL CONTROL SYSTEM
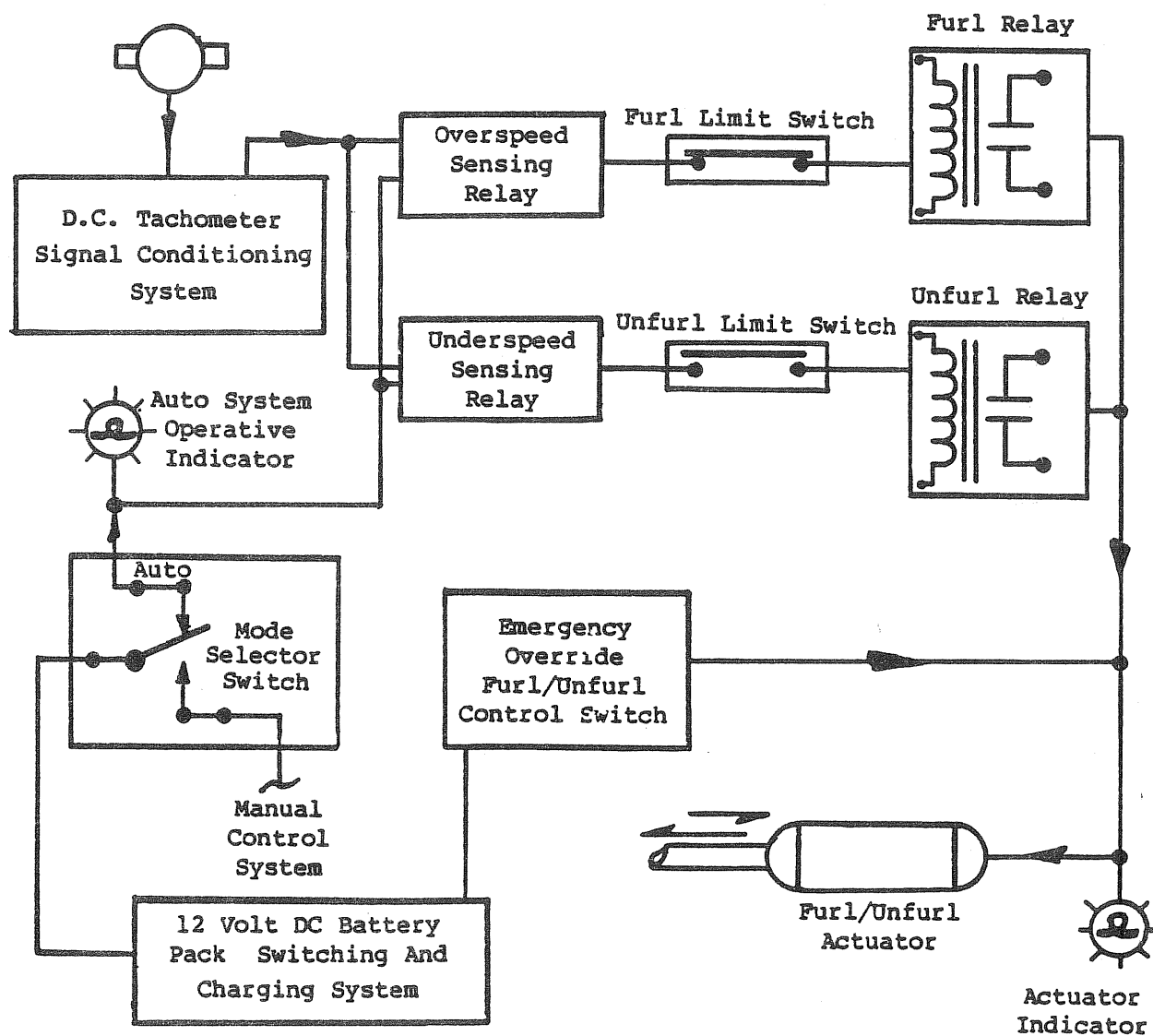
Figure 6-4b.   FURL/UNFURL AUTOMATIC SAFETY SYSTEM

The furl control system was designed to automatically furl the rotor in response to a rotor overspeed signal to relieve the operator of continuously monitoring rotor rpm. Resetting the desired furl angle after automatic furling resulting from overspeed is left to the operator.

In the Astral Wilcon Model 10B machine, the electrical actuator serves only as an emergency furling device in the event of failure of the automatic blade feathering control system. Its use for the automatic furl control of a wind turbine with blade cyclic pitch variation does not appear to be practical because of its 30 percent duty cycle and its constant rate of travel. A continuous automatic furl control system should be developed for prototype machine application.

6.1.8 Tiltable Tower

To facilitate maintenance and calibration of the instrumentation of rotor and nacelle we modified the Unarco-Rohn Type S.S.V. 60 ft (19.7 m) tower so that it could be tilted from the vertical position to a position about 6° from horizontal. Appendix E shows a side view of the tilting mechanism. Two of the three tower legs were hinged. Four clamps are shown in the drawing. Actually seven clamps per leg were used to attach two angle irons to each of the two legs. A test was performed in the Structures Laboratory of Washington University to determine the structural limit of the clamping arrangement Each clamp can transmit 1000 lb from the leg to the angle iron. However, the linear range of the force-deflection curve is only 300 lb. With seven clamps, 2100 lb can be transferred per leg without permanent deformation or slippage. The bearing block attachment was also tested. A 2000 lb horizontal force can be sustained without slippage in the elongated holes of the flanges.

Figure 6-5 shows the positions of tower, gin pole or boom and cables for a number of tower tilting angles. Tower plus machine weight is 2200 lb. The center of gravity is 35 ft above the tower hinge and the cable attachment is at this location. The gin pole weight is neglected. The tower boom and cable forces are given in Table 6-2.

Table. 6-2. TOWER, BOOM AND CABLE FORCES FOR TOWER TILTING

Tower Tilt, Degrees	Tower Force, k-1b	Boom Force, k-1b	Horizontal Tower Force, k-1b	Horizontal Boom Force, k-1b	Tower-Boom Cable Force, k-1b	Boom-Winch Cable Force, k-1b
90	2.2	0.0	0.0	0.0	0.0	0.0
69	2.6	0.6	1.0	0.4	1.1	0.8
48	2.7	1.4	1.9	0.7	1.8	1.6
27	2.6	2.6	2.3	0.4	2.6	2.4
6	2.0	3.7	2.0	0.8	2.9	3.3

Horizontal tower force and horizontal boom force at the hinges are given in the table. The tower and cable forces listed are distributed between two legs and two cables. The maximum boom force including the boom weight of 600 lb is 4300 lb. The winch and cables are designed for 8000 lb loads and have an ample safety margin. The gin pole has guy wires for lateral stabilization. The tower also has lateral guy wires which are normally loose but can take lateral forces if necessary. There are wooden cradles for both the tower and for the gin pole. The gin pole is in near vertical position when the tower is near horizontal position. The boom gravity moment balances the tower gravity moment about the tower hinge line when the tower is about 10° from vertical. The boom to winch cable becomes slack and the tower tends to drop on the leg opposite the hinged legs. An automatic hydraulic lift jack with a 14 in stroke supports the third tower leg during the final phase of tower raising in order to cushion this drop. When lowering the tower, the lift jack is raised until the boom winch cable becomes tight. From there on the winch controls the tower lowering process.

Figure 6-6 shows the tower leg foot before and after the modification. Before modification, the square leg flanges rest on four lower flange nuts which allow height adjustments for plumbing the tower. The upper flange nuts are tightened after plumbing. The anchor bolts extending through the flange holes also prevent the tower from tilting after removal of the upper flange nuts. The modified tower leg foot has shortened anchor bolts, long spacer nuts, and bolts that tie the leg flange to the spacer nuts. A ground plate carrying two bearing blocks is held down by four long spacer nuts. The tower can can be tilted about the two tower hinges without interference after removal of the flange bolts from all three leg flanges. The modified tower leg foot is not height adjustable.

The first of the three 20 ft long tower sections was built using the original tower leg foot with ground plate in place. Since this foot is height adjustable, the tower section could be plumbed. The distance between leg flange and ground plate was measured for each of the 12 anchor bolts. Spacer nuts of correct length were then made. The tower section was lifted off the anchor bolts, the anchor bolts were shortened, the long spacer nuts were installed, the tower section lowered, and the flange bolts were inserted and tightened. The leg clamps shown in Appendix E were attached and the angle irons bolted in place. The pins were inserted into the bearing blocks and through the holes in the angle irons after properly adjusting the angle irons. There are two bearing blocks per tower leg with angle irons in between the sets of blocks.

After removal of the leg flange bolts the lower tower section was tilted into a horizontal position, supported by a temporary cradle. The two upper 20 ft tower sections each were constructed, taking care that their axes coincided with that of the lower tower section to retain the tower plumb. The gin pole was attached to the bearing blocks on the ground plate under the tower leg opposite to the two hinged tower legs. Winch cables were installed and the tower was raised to the vertical position. The tower cradle and working platform were built, so that the tower, after lowering to the near horizontal position, was ready to receive the machine. The only minor mishap occurred when the gin pole cradle was damaged from sidewise swinging of the gin pole when it was lowered to its cradle. The sidewise swinging was possible because the guy wires were loose due to misalignment of their ground attachment points with the gin pole tilting axis. After correcting this condition, lowering and raising of the tower with the winch became routine.

47
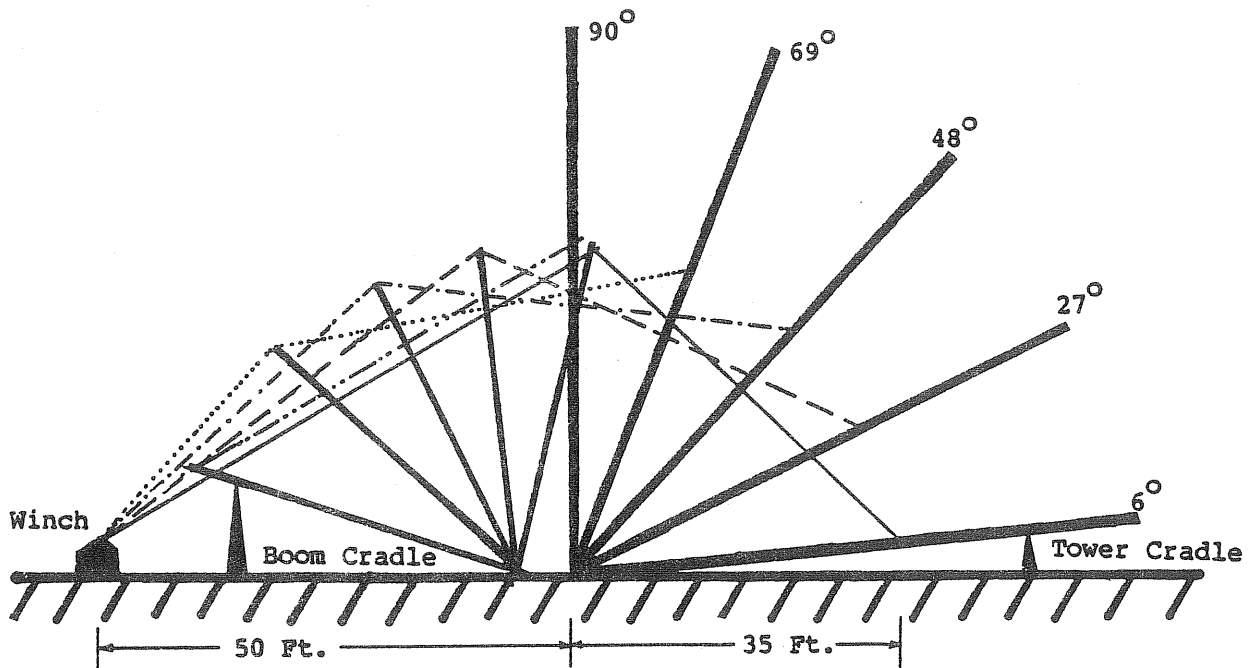
Figure 6-5.   TOWER AND BOOM POSITION DURING TILTING
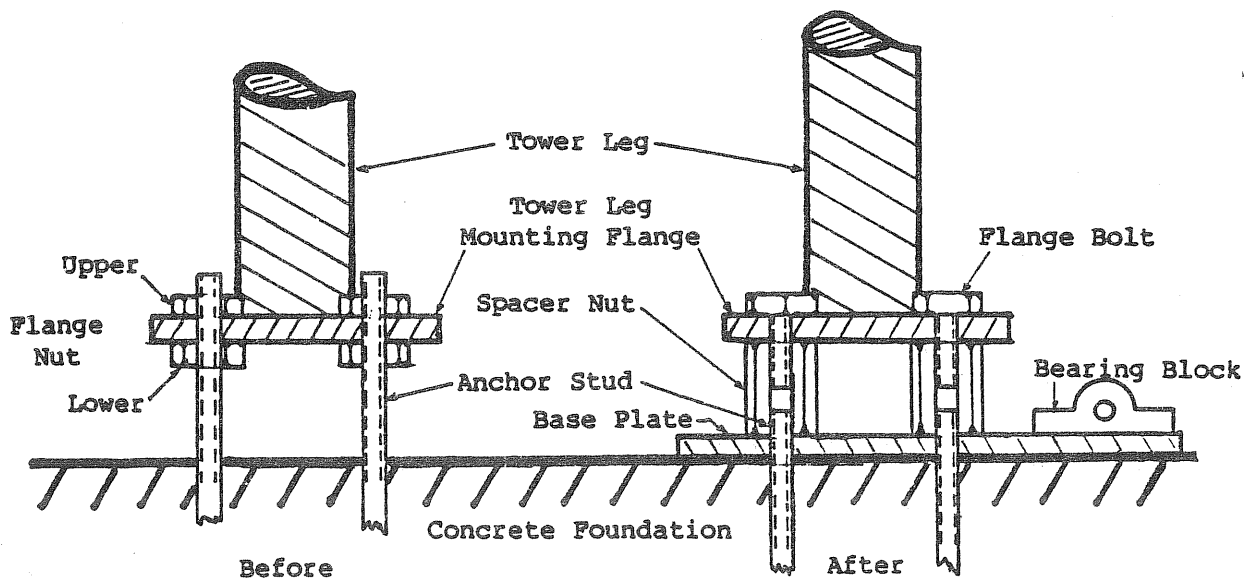
Figure 6-6.   TOWER LEG FOOT BEFORE AND AFTER MODIFICATION

Although the development of the tower tilting mechanism involved considerable effort and costs, substantial overall cost and time savings were achieved by using a tiltable tower. The ease of erecting the tower without a professional crew, installing the machine on the tower without a crane, installing the electrical system, and performing numerous instrumentation and maintenance tasks for the machine on the ground were accomplished without a costly "cherry picker". Tower tilting from horizontal to vertical position and vice versa takes about 15 minutes including insertion or removal of the 12 leg flange bolts. Two persons are needed for the operation. The machine is furled during tower tilting operation. As soon as the tower is tilted somewhat from vertical, the tail boom swings under the effect of gravity into its lowest possible position. When approaching the working platform, the tail boom, now in near vertical position, is manually lifted up to near horizontal position and lowered onto its cradle. It has been the policy to lower the tower to its cradle whenever the site is unattended. The tach generator, used as a motor and as a brake, is used to position the blades properly before the tower contacts its cradle. The rotor has the tendency to start when raising or lowering the tower when the wind is from the West of from the East. Using the tach generator as a brake, starting can be prevented. Raising and lowering the tower has been performed in wind speeds up to 15 miles per hour.

6.1.9   Starter Motor – Tach Generator

The starter motor, also used as rotor brake and as tach generator is a 12 V dc permanent magnet motor. It is connected to the output shaft of the gear box (see the drawing in Appendix E). During a proof test conducted in the WUTA laboratory when the machine was mounted on a pedestal, the starter motor drove the rotor shaft to an equilibrium speed of 50 rpm. The rotor shaft friction torque was 5 to 6 ft-lb, and its starting torque was 15 ft-lb. Its power at 50 rotor rpm is 60 watts.

The computed aerodynamic starting torque coefficient is shown in Fig. 6-7. The rpm and torque scales are shown for 9 mph wind speed. The curve has a minimum at about 20 rpm. If the wind speed is insufficient and the starter motor is not operating, the rotor speed will remain in the vicinity of 20 rpm without accelerating further. This characteristic has been clearly observed during atmospheric testing. Figure 6-7 indicates that, to achieve self-starting at 9 mph, the friction torque must be reduced to about 2.5 ft-lb. Since the starting torque increases with the square of the wind speed, a torque of 6 ft-lb will be overcome in a wind of 14 mph. These conclusions have been confirmed by starting tests, discussed later in this report.

The starter motor is also used as a brake when tilting the tower. Finally, it is used as a tach generator to provide the rpm input to the microcomputer and the overspeed relay. The starter motor is an inexpensive unreliable item and failed twice during the tests. It costs $12 and is widely available. It proved to be very useful for the tests but could be omitted for a prototype.

49
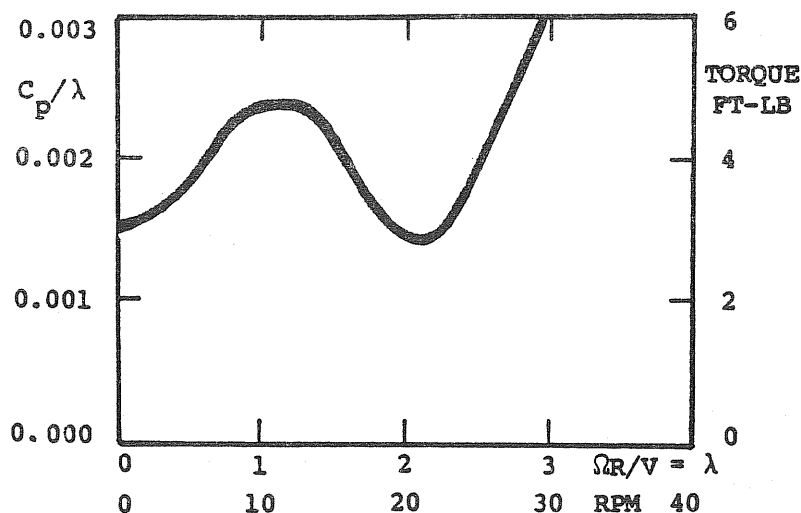
Figure 6-7.   COMPUTED STARTING TORQUE VS. RPM AT 9 MPH WIND SPEED

6.1.10 Instrumentation

Three kinds of instruments were used for recording the test data:

o   A multi-channel oscillograph recorder.

o   A microprocessor data acquisition system including analog to digital
     converters, internal clock, 12 in screen monitor, and printer-
     plotter.

o   Display instruments for monitoring and manual recording.

Auxiliary recording equipment included a twenty channel "Vishay" model 2100
strain gage conditioner and amplifier system, a twelve ring slip ring unit to
transmit signals from the rotating system, and various signal conditioning
filters and output buffers. All of the recording instrumentation used was on
loan from Washington University or WUTA. The recording instrumentation was in
use during June, 1980 and was destroyed or severely damaged during lightning
strikes on June 28, 1980. The instrumentation was repaired and returned to
service early in September, 1980.

The measured quantities are divided into slow varying quantities for which a sampling rate of one per second was adequate, and fast varying quantities which were sampled at a rate of 128 samples per second or continuously recorded on the oscillograph. The slow varying measured quantities were: wind speed, rotor speed, furl position, yaw post position, load voltage, alternator temperature, and ambient temperature. There were display instruments for all of these quantities. The first five quantities would be recorded simultaneously with the oscillograph and microprocessor. The signals were conditioned to vary between 0 and 5 V dc which is the range that the microprocessor accepts. The 5 V input range is divided into 255 intervals. The analog to digital converter assigns each measured voltage point to one of these intervals. The largest conversion error is $\pm$ 0.01 V or $\pm$ 0.2% of the total range of the measured quantity.

The oscillograph channels used a 470 ohm damping resistance and had a sensitivity of 4 V/in. The 5 V range of the measured quantities correspond to a 1.25 in range on the oscillograph record. The light sensitive paper speed was for either 0.25 or 1.00 in/sec. In the operating rotor speed regime between 100 and 225 rpm, the time for one rotor revolution corresponds to 0.15 to 0.066 or 0.6 to 0.267 in on the oscillograph record. The recording rolls were seven inches wide, so that five quantities could be recorded simultaneously without overlap. In addition, the rotor speed signal which consists of 0.1 in wide event marks in response to a magnetic pickup were displayed on the paper as a sixth channel. The rpm signal was taken for all oscillograph records.

The fast varying measured quantities for the rotor were: blade flap-bending, blade in-plane bending, shaft torque, and blade cyclic pitch variation. The signal wires from the strain gage bridges pass through the hollow rotor shaft to the silver slip ring assembly at the rear of the shaft and down the tower to the instrument shed located 70 ft (24 m) from the tower base. The fast varying measured quantities for the nonrotating structure are: vertical and sidewise tail boom bending, fore-aft and sidewise yaw post bending, fore-aft and sidewise linear accelerations of the rotor bearing block. The lightning strike on June 28, 1980 destroyed one of the linear accelerometers. Prior to the strike it had been found that the sidewise accelerations are always substantially smaller than the fore-aft accelerations. Therefore the destroyed expensive accelerometer was not replaced. After resumption of the atmospheric tests in September, 1980, only fore-aft accelerations were recorded. Detailed comments on each measured quantity in the sequence listed above are presented in the following sections.

6.1.10.1 Wind Speed

Until June 28, 1980 a model A7-104-4 anemometer sold by Natural Power, Inc. was used to measure wind speed. The signal frequency was proportional to wind speed (1.7 mph/Hz, or 0.76 m/s/Hz). A frequency to dc converter was adjusted during the wind tunnel calibration such that the display voltmeter and the microprocessor received 0.18 V/m/s. A "bin" of 1/2 m/s corresponded to 0.090 V. The 5 V range of the signal corresponded to a wind speed range of 0 to 27.8 m/s (62 mph). The anemometer was first installed on a horizontal boom attached to the tower at about 44 ft height. The anemometer boom had a natural frequency of 3 Hz (180 cpm) and was strongly excited by the rotor. To avoid reading errors and damage to the anemometer, it was relocated on a fixed mast of 40 ft (12 m) height installed 50 ft (15 m) to the north of the tower. During the transfer to

the fixed mast the anemometer was damaged beyond repair and was replaced. On June 28, 1980 the replacement anemometer was struck by lightning and destroyed, together with all of the recording equipment in the adjacent instrument shed. A separate mast for the anemometer increases the danger of a lightning strike and it was relocated to the tower attached boom. Since the A7-104-4 anemometer had been found to be sensitive to support boom vibrations, it was replaced with a TV 102 Texas Electronics anemometer which produced a dc voltage proportional to wind speed in the required range of 0-5 V. When checking out this instrument it was found that it produced a $\pm$ 1 V oscillation with the frequency of its rotation. It was returned to the manufacturer and was repaired under warranty without charge. The oscillation, after repair was reduced to $\pm$ 0.1 V. A wind speed signal conditioning circuit (Fig. 6-8) with active filter and three buffers was developed. The circuit completely removed the signal oscillations. It also provides three buffered outputs; one to the microcomputer, the oscillograph and to a dc meter for visual monitoring. Prior to the buffered output the signal to one of the recording instruments had some effect on the signals to the others. The TV 102 anemometer had a calibration constant of 15 mph/V and a range of 0 to 75 mph. The calibration constant is 60 mph/in on the oscillograph record.

The anemometer boom extended to the west of the tower and was not in the wake of obstacles for the prevailing wind direction. However, easterly winds produced a wake from the tower structure. The anemometer was located 18 ft (5.5 m) below the rotor center. Due to the upwind conditions from the ridge on which the wind turbine is located, the wind speed can be higher at the anemometer than at the rotor center. This appeared to be true for westerly winds. For northerly or southerly winds the speed at the anemometer location was expected to be lower than at the rotor center. Because of the uncertainty about the average wind speed over the rotor disk the performance coefficient C_p based on the anemometer readings was not a reliable efficiency measure.

6.1.10.2 Rotor Speed

There were two rotor speed signals available. One signal originated from a magnetic pickup which gave one impulse per rotor revolution. It was recorded by the oscillograph and allowed an accurate determination of the rotor speed by measuring the distance between impulses. The other signal originated from the tach generator which produced up to 17 V, contaminated by brush noise. During the initial statistical data taking, the signal was merely reduced in strength by a voltage divider, so that the standard deviation for the rotor speed included the brush noise. Later a rotor speed conditioning circuit shown in Fig. 6-9 was developed. The circuit had a low pass filter and three buffer amplifiers for the three outputs to the microcomputer, the dc meter and the oscillograph. This arrangement prevented interference errors from coupling to these three outputs as was originally experienced. The calibration constants were 1 V/60 rpm for the microcomputer to 300 rpm (3 V) maximum, 1 V/100 rpm for the dc meter, and 1 in/240 rpm for the oscillograph record.
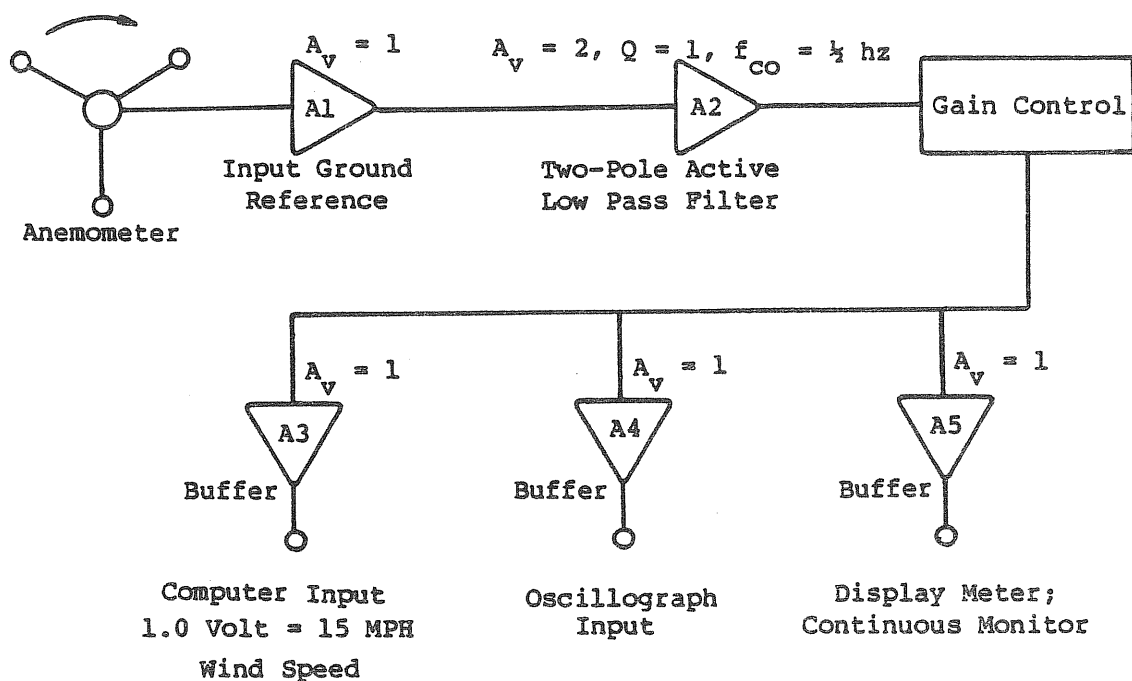
Figure 6-8.   WIND SPEED SIGNAL CONDITIONING CIRCUIT
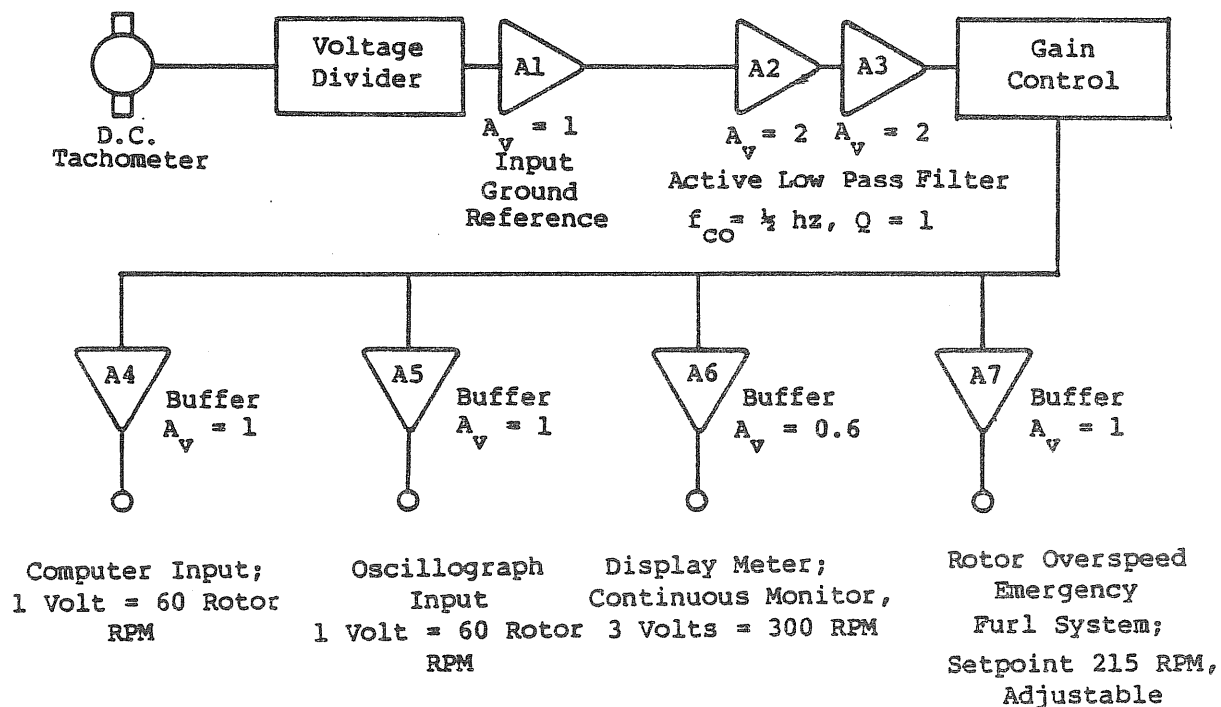
Figure 6-9.   ROTOR SPEED SIGNAL CONDITIONING CIRCUIT

53

6.1.10.3 Furl and Yaw Post Position

The electronic configuration of the Boom Position Detector (furl angle) and the Yaw Post Angular Position Detector circuits were essentially identical. Each consisted of a high quality rotating wire-wound potentiometer as the movable or sensing element. Each was excited from an adjustable voltage regulator having load regulation of ± 0.2% with noise and voltage ripple less than 2 mV maximum over the adjustable excitation range. Each position detector was excited at a dc voltage level in the range from five to eight volts, dependent upon the calibration constant of the given circuit. The input voltage to the Vishay Series 2100 Signal Conditioner was essentially potentiometric in nature. The input circuit configuration selected allowed high level voltage signals to be transmitted from the position detector to the signal conditioner rather than millivolt level signals. Since the transmission distance is approximately 150 ft, high level signals are desirable. Maximum current flow in the signal input circuit never exceeded 40μA, thereby assuring minimal line loss. Further, the ratio of detector resistance to transmission wire resistance was greater than 100,000/1. Measurement error resulting from line resistance was therefore not significant. The amplifier input after scaling varied from five through 20 mV. Scaling was accomplished directly at the amplifier input using 0.1% MIL-R-55182J divider networks. Amplifier input stability was ± 2μV RTI/^{o}C (maximum) with noise and drift of less than 10μV RTI/day. The amplifier input is common mode connected and has input impedance approaching 26 M ohms. Amplifier Gain (A_v) was set in the range from 100/1 to 300/1 depending upon the output maximum voltage level required. Amplifier linearity was ± 0.05% at dc. Circuit calibration and amplifier operational tests were performed at the control panel of the Vishay Signal Conditioner. Additionally, the circuit was configured to allow the "balance potentiometer" (normally used for strain gage circuit balance) to function as a voltage level offset control.

The Boom Position Detector was a 270 degree rotary linear wire-wound potentiometer, mounted on the underside of the tail boom pivot pin. The potentiometer slider (wiper) was driven by a linear mechanical linkage connected to the tail boom. Overall position sensitivity was 0.3 V per 10° of furl angle. Zero output voltage corresponded to the fully unfurled position.

The Yaw Post Angular Position Detector was a 360° linear wire-wound potentiometer mounted on a tower brace and the lower yaw post support plate. It was driven by a timing belt connected to the yaw post. Overall sensitivity was 1.00 V per 100 degrees of yaw post rotation. Zero output corresponded to a North position. The furl and yaw post position signal conditioning circuit is shown in Fig. 6-10.

6.1.10.4 Load Voltage

The alternator load voltage was measured across the resistive load bank which consisted of seven resistors having nominal resistance of 40 ohm each. The load resistors were located just outside the instrument shed. Since the voltage was used to compute the alternator power output by dividing the squared voltage voltage by the resistance, it was important to estimate the possible error from a change in resistance with temperature. One of the resistors was connected to a 250 V source and the resistance measured as it heated up to about 70°C.

Equilibrium temperature was reached in 10 minutes. The resistance increased from 40.84 to 41.46 ohm or a 1.5% increase. Since the alternator voltage was limited to 225 V and was mostly below this value, in atmospheric testing it was considered unnecessary to correct for the effect of temperature on the load resistance. The total load bank resistance was 5.8 ohm. Measured at the machine, the resistance including that of the dc cable to the shed, was 6.0 ohm. A correction of 6/5.8 = 1.03 was made to the voltage measured across the load resistors in order to obtain the voltage at the alternator location. The alternator power output is thus determined as $(1.03 \text{ X alternator voltage})^2/6.0$ ohm .

During initial tests, the three-phase current from the alternator was conducted down the tower to the shed, where the rectifier and tuning capacitors were located. The alternating current in the cables adjacent to the signal wires caused severe noise in all signals. Rectifier and tuning capacitors were then moved to the tower top and only dc voltage was transmitted to the shed. The signal noise was greatly reduced but still unacceptable. It was apparently caused by the ac ripple in the dc current. The dc cables were then inserted into a metal conduit that extended from the tower to the instrument shed. The noise in all signals was then substantially eliminated except that the dc load voltage still contained small ac ripples. A voltage signal conditioning circuit, shown in Fig. 6-11, was added. It had a low pass filter and buffer amplifiers for the microcomputer input and for the oscillograph input. The average calibration constant is 1 V/100 load volts. The visual display dc meter received the load voltage directly. The voltage signal conditioning unit produced some errors in the generator output measurements because the signal-voltage relationship was somewhat nonlinear at low power outputs, and because signal conditioner gain was temperature dependent. The meter readings were believed to be more accurate and have been used where available.

6.1.10.5 Strain Gage Circuits

Micro-Measurement 350 ohm strain gages Model CEA-06-250UW-350 were used for all bridge locations. Each bridge was made up of four gages; two in tension, two in compression. The gage factor for each gage was 2.1. For most bridges the gain in the Vishay 2100 was set for a 2020 amplification factor. The excitation level was 10 V. For a complete four gage bridge the strain is then given by

$$E = \text{Volt}/(10\text{X}2020\text{X}2.1)$$

The stress is $\sigma = E$, where E is the modulus of elasticity. $E = 10.4\text{X}10^6$ psi for the aluminum blade retention and the tail boom. $E = 30\text{X}10^6$ psi for the steel yaw post and cyclic pitch flexure. The moment calibrations were made in terms of nominal bending moments at the rotor center, at the tail boom hinge and at the upper yaw post bearing. The cyclic pitch flexure, driven by an eccentric, was calibrated in terms of degrees cyclic pitch deflection. Table 6-3 gives the Vishay 2100 gain, the volt/unit, the psi/unit, and the oscillograph inch/unit for the strain gage bridges. For the sake of completeness, the gains and calibration constants for the linear accelerometer, for the furl and yaw post potentiometers and for the load voltage are added to the table.
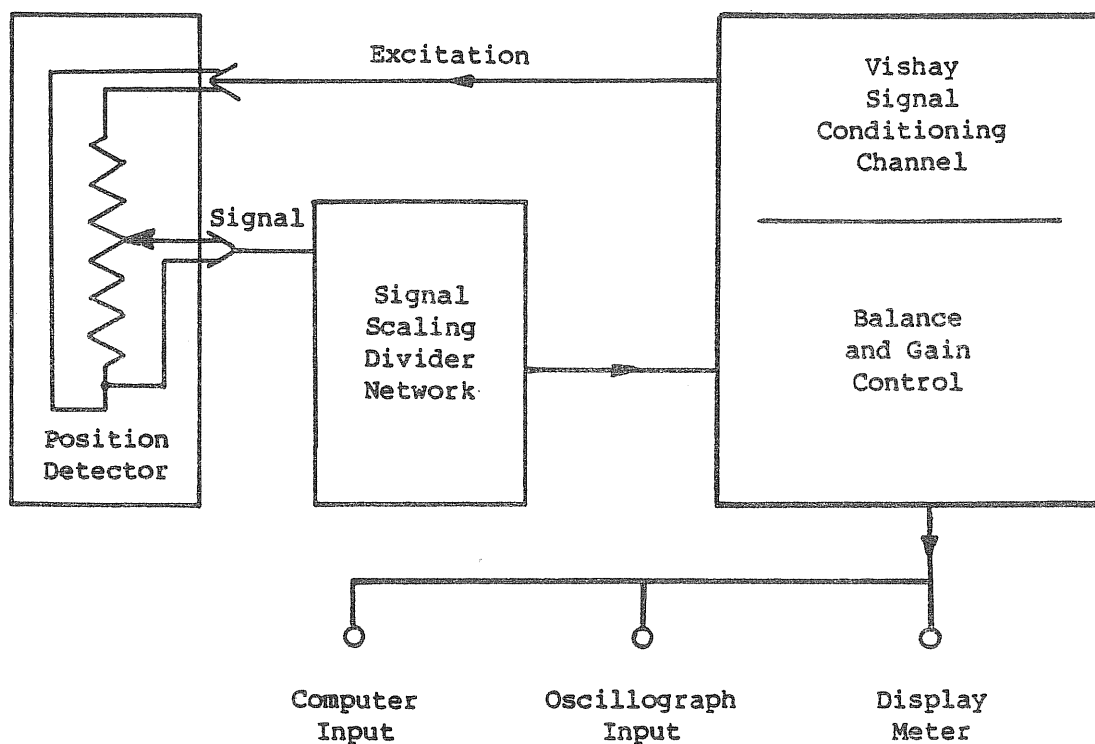
Figure 6-10.   FURL AND YAW POST POSITION SIGNAL CONDITIONING CIRCUIT
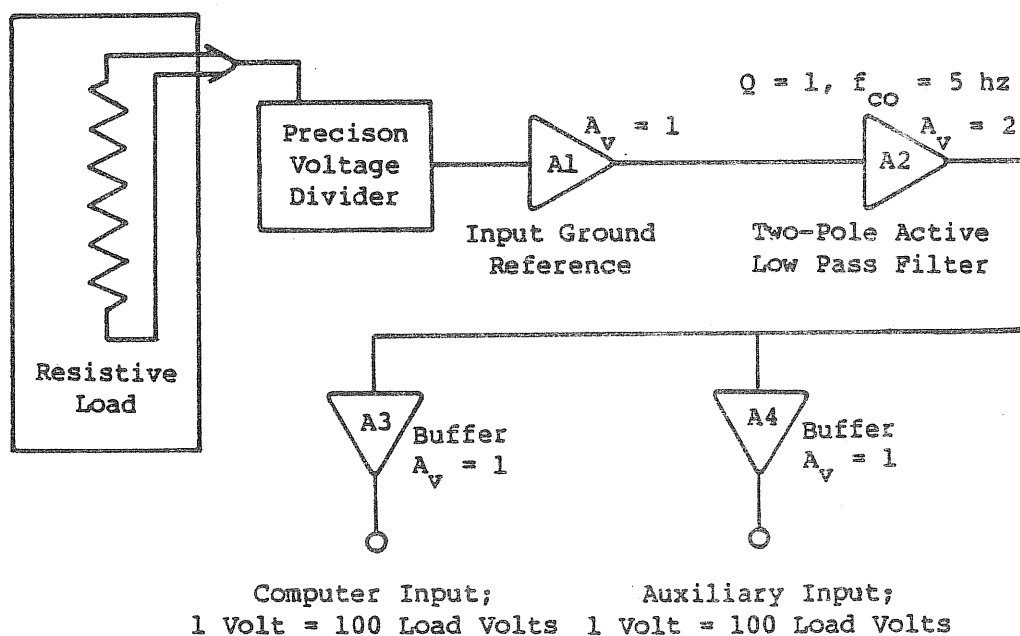
Figure 6-11.   LOAD VOLTAGE SIGNAL CONDITIONING CIRCUIT

56

Table 6-3. INSTRUMENT GAINS

Vishay Channel	Signal	Gain Setting	Volt/Unit	Psi/Unit	Oscillograph Inch/Unit
L	Cyclic Pitch	533/1	2V/10 degrees	10,100/10 degrees	0.5/10 degrees
2	Blade In-Plane Bending	2020/1	$4.6V/10^4$ in-lb	$1,120/10^4$ in-lb	$1.15/10^4$ in-lb
3	Blade Flap Bending	2020/1	$3.2V/10^4$ in-lb	$770/10^4$ in-lb	$0.80/10^4$ in-lb
4	Rotor Torque	2020/1	$1.2V/10^3$ in-lb	$840/10^3$ in-lb	$0.30/10^3$ in-lb
5	Accelerometer	1599/1	5V/g	N/A	1.25/g
6	Tail Boom Bending	2020/1	$3.9V/10^4$ in-lb	$950/10^4$ in-lb	$0.97/10^4$ in-lb
7	Yaw Post Position	512/1	1v/100 degrees	N/A	0.25/100 degrees
8	Yaw Post Bending,	2020/1	$5.8V/10^4$ in-lb	$4100/10^4$ in-lb	$1.45/10^4$ in-lb
8a	(Since Oct. '80)	517/1	$1/45V/10^4$ in-lb	$4100/10^4$ in-lb	$0.36/10^4$ in-lb
9	Furl Position	102/1	0.30V/10 degrees	N/A	0.075/10 degrees
10	Load Voltage	1/100	1v/100v	N/A	0.25/100v

Zero or 3.6 V for the yaw post position signal indicates that the rotor axis points north. Zero volt for the furl position signal indicates zero furl angle (90° rotor angle of attack). The magnetic pick-up signal for the rotor speed was always the bottom signal on the oscillograph record. Time moved from left to right. Positive voltage (there was no negative voltage) was from top to bottom of the oscillograph record. The yaw post bending gain had been reduced to one-quarter beginning in October, 1980, in order to limit the output to the 5 V level compatible with the microcomputer A/D input board.

6.1.10.6 Microcomputer System

The microcomputer system for statistical data processing consisted of:

- A 48K, 6502 microprocessor based, "Apple II Plus" Central Processing Unit;

- An AIO2, 16 channel analog to digital conversion module compatible with the "Apple II Plus" C.P.U.;

- A plug-in, "Mountain Hardware" real time clock;

- An "Apple" mini-disk drive unit;

- A "Trend Com 200" Thermal Printer; and,

- A black and white video monitor.

Some of the special features available with this system include floating point BASIC language capability incorporated in the read only memory; built in, high resolution graphics capability; and print-out capability of the graphics display in both standard and expanded scales.

Further details concerning the hardware are available in the "Apple II Plus" Hardware Manual and other product literature.

Several peripheral devices were added to integrate the computer system into the project instrumentation system. Three protective devices were added between the computer power supply and the available grid power. First, a 120 V constant voltage "Sola" transformer was installed to protect against power transients; second, filter and surge protection circuits were installed to protect against lightning and high voltage power surges; and third, a standby power source, purchased from the Apple Company, was added to provide reserve power to protect data and programs stored in computer memory in the event of line power failure.

It is significant to note that, although the constant voltage transformer and reserve power supply were installed at the time of the lightning strike described in Section 6.1.10.7, the computer was severely damaged by the strike, indicating the sensitive nature of these devices to electrical transients.

In addition to power supply protection devices, a special interface box was constructed for the 16 channel, 0 to 5 V dc A/D board. It consisted of self-grounding inputs (i.e. the input connections are automatically grounded when the patch plugs are removed to guard against static electric discharges across the input ports), and 10 V Zener diodes placed across each input to protect against reverse and over voltages. Use of 5.6 V Zener diodes was attempted, but the input signals became nonlinear at voltages in excess of 3 to 4 V.

Accuracy of the A/D interface board was determined using a "Fluke" digital voltmeter and reference voltage source. The board, which converts 0 to 5 V dc to a digital scale of 0 to 255 (0 to FF hexidecimal), read approximately 6% higher over its entire range. This error was compensated for during data processing by using 54 digital units per volt rather than 51, as required by the A/D board scaling factor. Although this limited the upper scale reading to approximately 4.6 V, it had little effect on data accuracy since most data were collected at values well below the 4.6 V dc limit.

Program and data storage was accomplished using the mini-disk system. One disk acted as an "operating disk" and contained the sampling programs; a second disk containing the graphical plotting routines. "Bin" data was stored on separate "data" disks.

All data and programs were copied onto separate back-up disks to protect against disk failure or operator errors, both of which occurred several times during the course of computer data sampling and analysis.

6.1.10.7 Lightning Protection

The wind turbine generator test site selected for this study was at an elevation of approximately 700 ft. It was an isolated wooded area and was without question the tallest conductive structure in the area. The test site was located 22 miles southwest of St. Louis, Missouri in an area prone to strong atmospheric disturbance. The test site was likely to be affected by three main disturbances; direct lightning strikes, main power surges and induced transients. Direct lightning strikes are the most severe source of atmospheric disturbance. The significant factors of concern for direct lightning strikes are the pulse rise time, current amplitude and current duration. The 50 percentile probabilistic stroke peak current is about 18,000 amp, with about one in one hundred strikes exceeding 120,000 peak amp. The stroke duration can persist up to 100 msec and the rise time of the pulse can approach a few nanoseconds. Most lightning strikes reach 90 percent of their peak current in less than one microsecond.*

A severe thunderstorm occurred in the area of the test site on June 28, 1980. The concentration of high frequency energy resulted in significant damage to the wind turbine instrumentation. The test site was so severely struck that the test equipment was subjected to direct strikes, power main surges and electromagnetic pulses from nearby lightning. The electrical storm lasted

---

*These data were obtained from Lightning Elimination Associates.

several hours and resulted in nearly 7000 dollars damage to instrumentation. Signal transducers including strain gage bridges, accelerometers, position sensing potentiometers and the site anemometer were destroyed by direct strikes. Computer and signal conditioning instrumentation integrated circuits were destroyed by line transients and electromagnetic pulses. Fortunately, the turbine hardware and generator did not sustain damage, although the fuse protecting the field winding of the generator was blown.

Lightning Elimination Associates carries a complete line of protective devices ideally suited to elimination of transients and damage from other disturbance causes. Our emphasis in providing additional lightning and surge protection hardware was centered on protection of the wind turbine hardware and transducers. Instrumentation was isolated from signal and power sources when unattended. This approach was taken because the cost of providing transient eliminators (TE's) for each signal system was prohibitive given the duration and funding level of this work. The following discussion describes the steps taken to insure safety to equipment from subsequent electrical storms.

The turbine generator was mounted on top of a 60 ft Rohn tower, modified to provide a tiltable function as described in Section 6.1.8. Each leg of the tower was connected by a large copper cable to individual grounding rods driven ten feet into the earth at the base of the tower. The tower was grounded to the wind turbine generator by three large carbon brushes which contacted the yaw post. The machine frame was grounded to the main shaft. The main shaft extended through the gear box to the rotor and passive cyclic pitch mechanism and was grounded by two large carbon brushes. The blade retention mechanism was grounded to the main shaft using woven copper straps. The cyclic pitch mechanism effectively isolates the blade retention box beam from the main shaft because Rulon bearings were used in the mechanism. The woven copper straps provided a flexible ground path around the Rulon bearings.

The grounding arrangement described above provided shunt paths around all mechanical components likely to sustain damage from a direct lightning strike. The key components protected were the cyclic pitch mechanism bearings, the gear box bearings and the yaw post bearings. The tail boom was effectively grounded to the machine frame through the shunt path of the furl actuator mechanism.

Site protection was further improved by installation of a lightning rod mounted to the top of the wooden tower tilt boom (gin pole). As shown in Fig. 6-5 and Appendix E, the boom was in the full upright position when the tower was lowered and resting in its cradle. The lightning rod was connected to two grounding rods at the base of the boom. The lightning rod was the preferred strike point for any lightning strikes in the vicinity of the test site and helped insure protection of the tower (lowered) and instrument shed during periods when testing was not in progress.

Metal Oxide Varistors (MOVS) (passive low cost devices) were used extensively on all tower instruments and power wiring. All MOVS were connected to grounding rods. They serve a dual function. During operational tests, they functioned as low energy high amplitude noise clamps, protecting signal conditioners and A/D computer input boards from excessive input voltage. They were very effective when used to bypass furl/unfurl actuator switching noise and commutator noise from the tach generator.

The MOVS provided a second protective function when the tower was in the lowered position and unattended. All signal inputs were disconnected from the signal conditioning equipment and the computer during unattended periods. The MOVS effectively tied the transducer signal wires to ground. In the event of a lightning strike or other atmospheric disturbance, the MOVS would break down and drain the voltage to ground. Breakdown occurred in nanoseconds. All conductors formed shunt drain paths to ground, helping to insure the survival of the transducers and the integrity of the wiring insulation.

During normal operation and data acquisition, the instrumentation power inputs were protected by Sola transformers and surge isolators. The surge isolators protected the instrumentation from power line surges caused by lightning strikes, earth currents, magnetic induction, switch arcing and inductive switching transients.

The main power was disconnected from the instrument shed by a large knife switch when the site was unattended. The power line ground connector was not disconnected by this switch. The power line ground connector was connected to an earth grounding rod at the instrument shed insuring power line ground conductor integrity.

6.2   DATA ACQUISITION AND PROCESSING METHODS

Two kinds of data acquisition methods were used: Analog data acquisition with an oscillograph, and digital data acquisition with a microcomputer. Approximations to steady state data were obtained both from oscillograph records and from meter readings. Data on transients were extracted from oscillograph records. Digital data acquisition and processing by the microcomputer were used to obtain statistics on performance parameters.

6.2.1   Analog Data

Steady state data were difficult to obtain during atmospheric testing since wind speed and rotor speed were continuously changing. All oscillograph records contained the traces of wind speed and rotor speed so that it was possible to judge when a more or less steady state occurred over several seconds.

Sometimes it was not possible to find a steady state record. For example, conditions with high wind speeds were only obtainable during gusts. In order to include the gust conditions in the steady state rotor power evaluation, the angular rotor acceleration was determined from the oscillograph record, and the inertia torque was added to the measured rotor shaft torque. The sum of rotor inertia torque and rotor shaft torque equals the aerodynamic torque. It was found that the inertia corrected rotor torque agreed with the steady state torque values and could be considered a quasi-steady aerodynamic torque. It was multiplied by the angular rotor speed to obtain rotor power.

The steady values of the measured quantities showed little scatter when plotted vs. rotor speed. The larger scatter when plotted vs. wind speed was caused by the difference between the wind speed reading from the anemometer located 13 ft (5.5 m) below the rotor center and the average wind speed seen by the rotor.

61

Scatter was also caused by the fact that the rotor speed, due to rotor inertia, follows wind speed changes only after a certain delay.

In addition to steady state evaluations vs. rotor speed and vs. wind speed, some time histories were extracted from the oscillograph records. They show starting and furling processes and responses to gusts.

6.2.2 Statistical Data Processing

Five computer programs were developed for statistical data sampling using the method of bins. The five programs sampled data as follows:

1. Two performance variables vs. wind speed, using only BASIC language;

2. One dynamic variable, (usually cyclic pitch amplitude) vs. yaw rate;

3 & 4. Two or six performance variables vs. wind speed using a high speed sampling machine language routine; and

5. Six dynamic load variables vs. rotor speed.

The first program collected the mean value, standard deviation, the global maximum and the global minimum of rotor speed and cyclic pitch amplitude for each wind speed bin. The second program collected the mean and standard deviation of the cyclic pitch amplitude for each yaw rate bin. From the oscillograph records a clear dependence of cyclic pitch amplitude on yaw rate was observed. It was decided to collect statistical data on this dependence. The third and fourth programs collected statistical data required for performance evaluation vs. wind speed bins. The fifth program collected statistical data for dynamic loads vs. rotor speed bins.

In addition to the five sampling programs, two analysis programs were developed. The first program converted the digital voltage data stored in each bin array into a graphical plot. The second program performed statistical data evaluation of the rotor power vs. wind speed data and calculated and plotted the rotor coefficient of performance as a function of average wind speed and for each wind speed bin.

A more detailed description of these programs is presented in the following sections. The documentation for these programs is presented in Appendix D.

6.2.2.1 Power-off Data vs. Wind Speed

The "Wind-2" program was developed to sample cyclic pitch amplitude and rotor rpm as a function of wind speed bin using only BASIC language programming commands. This was the first sampling program developed and was used to collect data in autorotation before a faster and more sophisticated machine language sampling program was developed. See Appendix D for details.

The program sampled wind speed and rotor rpm input ports twice using BASIC commands available in the Apple command structure and then took the average of each and stored the value. The program then sampled the cyclic pitch position for approximately 1 sec (47 times), stored the values, and, after sampling, determined the maximum and minimum value sampled. Next, the cyclic pitch amplitude was determined by calculating one-half of the difference of the maximum and minimum value. Using a 56 unit wind speed bin array based on a 0.5 m/sec bin width, values of the maximum, minimum, mean, standard deviation and number of samples were updated for the current wind speed bin number for both rpm and cyclic pitch amplitude.

The program had several control and monitoring features. The furl angle was tested to insure it was set properly and that automatic furling had not occurred. Since the rotor was tilted 8 degrees, actual furl angles were a geometric combination of rotor tilt and furl set angles. The program calculated the required furl set angle for a chosen furl angle and insured the angle was within limits for data sampling. The rpm was tested to insure the wind turbine was not in a starting mode which could bias the higher wind speed bins if gusts occurred during starting. Wind speed was tested to insure the winds were not zero. If any of these tests failed, a message was printed to the user and the bin arrays were not updated.

In addition, cyclic pitch amplitude was tested. If it approached the stop limits, the speaker was toggled providing an audible warning and a visual warning appeared on the screen. This alerted the operator to possible stop-pounding during operation.

Finally, machine performance was monitored by printing current values of wind speed, rpm, cyclic pitch amplitude and tip speed ratio on the screen.

At the conclusion of data sampling, as determined by the operator, the bin array data was output to a data disk and a "hard-copy" was produced on the thermal printer.

A plotting routine using the Apple high resolution graphics capability was used to present bin data for analysis. Elapsed time of the test and approximate rotor revolutions occurring during the test were also output.

The program was capable of sampling at a rate of about one sample for both variables every 3.5 sec.

6.2.2.2 Cyclic Pitch Amplitude vs. Yaw Rate

The "Yawrate" program was developed to relate a dynamic variable, usually cyclic pitch amplitude, to yaw rate using the method of bins based on yaw rate. The program began by sampling yaw position and then sampled the real-time clock, which read time in milliseconds and stored these values. Next, cyclic pitch position was sampled for approximately one-half second (24 times) and these values were also stored. Yaw position was then sampled again, followed by the clock and the elapsed time was calculated. Knowing the elapsed time and the yaw position before and after the cyclic pitch sampling, an approximate yaw rate in degrees per second was calculated. The yaw rate was an approximation since it assumed constant linear yaw rate over the 0.5 sec interval.

There were 35 yaw rate bins, 1 degree per second in width, for both positive (clockwise) and negative (counter clockwise) yaw rates.

After determining that the calculated yaw rate was within limits (i.e. between 0 and 36 degrees per second) the cyclic pitch amplitude was calculated and the yaw rate bin arrays were updated as was done for the "Wind-2" program.

At the conclusion of testing, as determined by the operator, both the positive and negative yaw rate bin arrays were output to data disk and then to the printer. The data was plotted for analysis using a graphical plotting routine.

The program monitored rotor rpm. Only data within specified rpm limits was accepted by the program since cyclic pitch amplitudes were a function of rpm as well as yaw rate.

Furl angle was set at the beginning of the test and held constant during the sampling.

Sampling was monitored during operation and current yaw rate and cyclic pitch amplitude were output to the video monitor.

6.2.2.3 Power-on Data vs. Wind Speed

The "Wind-6" program was developed and incorporates a machine language high speed sampling program developed through consultation with "Micro Systems Development" of St. Louis.

The high speed sampling program was developed using assembly language mnemonics for the Apple 6502-based microprocessor. Briefly, the program was used as a subroutine of the Wind-6 program and sampled five input channels 128 times in one second in a multiplexing fashion and then sampled eight more input channels at the end of the high speed sampling routine. These data were stored in the computer along with the 32 previous data sets (i.e. 32 previous seconds worth of data). Next, the amplitude and the mean value were calculated and stored for each "high speed" channel. In addition, the global maximums and minimums for all channels were stored as a function of bin number. Up to five rapidly varying high speed dynamic channels and eight slowly varying dynamic channels were sampled in approximately one second using BASIC to address the locations where the mean values and amplitudes of the current sample set were stored. The bin arrays were updated with data from each of the variables sampled. This was accomplished by calling this subroutine.

The "Wind-6" program was developed to provide a wind speed bin analysis on six variables using the high speed sampling routine. The variables chosen were rpm, cyclic pitch amplitude, rotor power output, generator power output, rotor-to-generator efficiency, and thrust loading. To determine instantaneous values of these variables, the following signals were sampled using the high speed subroutine. Rpm was sampled directly as a slowly changing variable, (i.e. once per second). Cyclic pitch was sampled as a "fast" variable (i.e. 128 times per second) and the current amplitude read at the stored address. Current rotor power was determined by sampling rotor torque as a "fast" variable and reading mean rotor torque at the stored address. This value, multiplied by present rpm,

provided rotor power data. Generator power was determined by sampling generator voltage as a "slow" variable (i.e. once per second), squaring the value and dividing by the resistive load. Efficiency was determined by taking the ratio of generator power to rotor power, while thrust was determined by sampling the fore-aft yaw post strain gage value and dividing by the moment arm to the rotor shaft.

Each of these quantities was sorted into appropriate wind speed bin arrays, and plotted in graphical form as described in the "Wind-2" program.

The "Wind-6" program incorporated all the testing procedures and performance monitoring features of the "Wind-2" program. In addition, atmospheric parameters for the test were input to the program and recorded so that the performance results could be corrected to standard conditions for nondimensional coefficient calculation.

6.2.2.4 Rpm and Rotor Torque vs. Wind Speed (Fast Sampling Rate)

The "Wind-2 Fast" program was developed to enhance rapid data collection of two significant variables as "fast" sampling variables. Although the machine language sampling subroutine, described above for the "Wind-6" program was quite fast, the time to sort the data in six bin arrays, perform the operational testing procedures and output performance parameters averaged about 3.5 sec per sample set. This resulted in rather lengthy tests to accumulate the data necessary to determine meaningful bin values, especially with rapidly changing wind conditions. Thus, the "Wind-2 Fast" program was an abbreviated version of the "Wind-6" program with all extraneous features deleted. The program was used to sample mean rpm and rotor power as fast variables (i.e. 128 times per second) and store these variables in bin arrays. All testing for furl angle, rpm, etc. was removed from the sampling iteration and video output was reduced to only the two parameters being sampled.

This resulted in a 1.4 second iteration time per sample set compared with the 3.5 sec previously. Otherwise, the program operated the same as the "Wind-6" program.

6.2.2.5 Load Amplitudes vs. Rpm

The "RPM-6" program, based on the high speed, machine language sampling subroutine, was developed to determine structural and cyclic pitch response to varying rpm. The program operated in a manner directly analagous to the "Wind-6" program with wind speed bins replaced by rpm bins and performance variables replaced by structural loads variables. The rpm bins were 8.8 rpm in width. The variables sampled and stored in the bin arrays included cyclic pitch amplitude, mean flap-bending amplitude and yaw post bending amplitude or front accelerometer amplitude.

Each of these variables were sorted and stored in bin arrays and then plotted in graphical form as described above.

The only data output during the test was rpm bin number and warnings if furl angle, rpm or cyclic pitch exceeded preset limits. These tests and warnings were the same as described in the "Wind-6" program.

6.2.2.6 Plotting Routines

Bin array data was stored on the data disks as digital voltage values determined directly from the A/D board output. These values were converted into appropriate units and plotted on axes stored in binary form on the bin plot disk. In addition, a plot was completed showing the log of the number of samples vs. wind speed so that the sample distribution of the test was known. The program used the high resolution graphics feature of the Apple computer system, and printed the graph as desired on the Thermal Printer in either a standard or expanded scale.

6.2.2.7 Coefficient of Performance Analysis

The "CP" program was developed to calculate rotor performance and mean wind speeds based on the results of a performance test.

Bin array data for the desired rotor power test were read into the program along with a standard atmospheric correction factor based on ambient pressure and temperature recorded during the data collection.

First, using the number of samples present in each bin, the mean wind speed occurring during the test was calculated. Next, using the number of samples in each bin, mean wind power during the test was calculated using a corrected air density (based on the atmospheric correction factor for the test period) and rotor disk area using the equation

$$P = 1/2 \; \rho_{corr.} \; A_{rotor} \; V_{wind}^{3} \qquad\qquad (6\text{-}1)$$

Then, the wind speed at mean power was calculated. Next, mean rotor power over all bins was calculated and an average coefficient of performance for the rotor during the test period was output. Finally, for each bin mean rotor power was compared with power available at that wind speed and a plot of performance coefficient vs. wind speed bin was output.

6.3 TEST RESULTS

6.3.1 Running Time

The following table indicates the number of days and hours the machine was operated each month. During unattended periods the tower was resting on its cradle in near horizontal position to protect the instrumentation from lightning strikes.

Table 6-4. LIST OF OPERATING DAYS AND HOURS

Month	May	June	July	August	September	October	Total
Test Days	3	3	-	8	13	14	41
Test Hours	3	12	-	11	22	48	96

To obtain the number of tower raisings, 5 must be added to the number of days, since the tower was raised and lowered 5 times without testing.

Atmospheric testing began on May 23, 1980 and was interrupted on June 28, 1980 by lightning strikes which destroyed or severely damaged the instrumentation despite the lowered position of the tower. Between May 23 and June 28, 1980 power-off conditions were tested. The month of July was spent repairing the instrumentation damage. The test runs in August were performed to check out repaired and additional new instrumentation. The first tests with power extraction were conducted during September. The test runs were completed on October 25, 1980. The figures which appear in the following sections include the date on which the information presented in the figure was obtained.

6.3.2 Starting

As discussed in Section 6.1.9, the wind velocity required for self-starting of the rotor depends on the system friction torque. The following values were measured without rotation and at an ambient temperature of 10°C.:

- Without alternator belt, without starting motor   3.5 ft-lb

- Starting motor added   4.0 ft-lb

- Alternator friction torque added   5.0 ft-lb

- Alternator belt added   6.0 ft-lb

Figure 6-12 shows the self-starting time history from an oscillograph record for wind speed in mph, rotor speed in rpm, rotor power in kW and cyclic pitch amplitude in degrees. The dips in wind speed are followed a few seconds later by dips in rpm.

The acceleration between 30 and 120 rpm occurred in 30 sec at wind speeds between 6 and 9 pmh (average 7 mph). The acceleration between 20 and 45 rpm was accomplished in 20 sec at wind speeds between 4 and 12 mph (average 8 mph). The initial acceleration to 20 rpm, not shown in Fig. 6-12, took several minutes. The rotor could not get over 10 rpm at a wind speed of 12 mph. Finally a gust with a 16 mph peak accelerated the rotor beyond the negative "hump" seen in Fig. 6-7.

67

As shown in Fig. 6-12, a lull of wind speed to 2 mph extending over more than 10 sec lowered the rotor speed from 45 to 30 rpm. When the wind speed rose up to 8 mph, the rotor accelerated rapidly to 100 rpm and, after a dip to 80 rpm caused by the dip in wind speed to 5 mph, accelerated further to 120 rpm. Rotor power was negligible up to 80 rpm but reached almost 1 kW at 120 rpm. The cyclic pitch amplitude $\pm \beta^{o}$ which was initially between stops ($\pm 11.5^{o}$) began to rapidly drop above 60 rpm, and was only $\pm 2^{o}$ at 120 rpm. As will be shown later, it also varied systematically with yaw rates resulting from wind direction changes. The electric resistance load of the alternator of 6 ohm was present during the entire test. Below 80 rpm it had almost no effect on alternator torque.

Though it would normally not be needed, starting has also been investigated in furled positions. The larger the furl angle, the higher the wind speed required for starting. Since power would not be extracted for the higher furl angles, the starting tests were performed power-off. Figure 6-13 shows a time history of power-off starting at 60° furl angle. The average wind speed was 15 mph. The rotor speed rose rapidly to its equilibrium value of about 130 rpm. The cyclic pitch amplitude was at the stop limit up to 50 rpm and then declined to a value of 2° to 3° beyond 100 rpm.

The generator belt and the starting motor were taken off in order to determine the effect of a lower friction torque for rotor speed. The friction torque was reduced from 6 ft-lb 3.5 ft-lb. Figure 6-14 shows one of several self-starting time histories taken in this configuration. The rotor accelerated promptly from standstill and reached 40 rpm in 40 sec, in wind which varied between 6 and 12 mph (average 9 mph). It then rapidly accelerated to 160 rpm in 20 sec in a wind of 10 mph average. This test showed that a reduction in friction torque from 6 to 3.5 ft-lb would be very effective in reducing the required starting wind velocity. For the prototype blade version to be discussed later, analysis indicates almost twice the starting torque would be available compared to Fig. 6-7.

When adding automatic furl control, it may be practical to use a spring for furling and hydraulic pressure from a constant speed hydraulic governor for unfurling. In case of oil pressure loss the rotor would be furled by the spring. After stopping, the oil pressure would go to zero and the rotor would assume the furled postion. For the purpose of starting, the turbine must be motored until the oil pressure is sufficient to unfurl the machine. This procedure has been simulated and the result is shown in Fig. 6-15. The starter motor was turned on in the furled position. After 30 sec when 20 rpm had been reached, the rotor was slowly unfurled at a rate of 3°/sec. The rotor began to rapidly accelerate at about 30° furl angle and the starter was turned off when the fully unfurled position was attained. The wind speed varied between 9 and 10 mph throughout the starting procedure. This test showed that motored starting from a furled postion is possible in a 9 mph wind provided that sufficient oil pressure for unfurling would be available at about 20 rpm. If a spring were used for unfurling and oil pressure for furling, a starter may not be necessary. To protect against loss of oil pressure, an emergency furling device or a rotor brake would be desirable. The advantage of an unfurling spring is that the hydraulic governor could be driven through a centrifugal clutch so that it would not cause a power loss until needed for overspeed prevention.

68
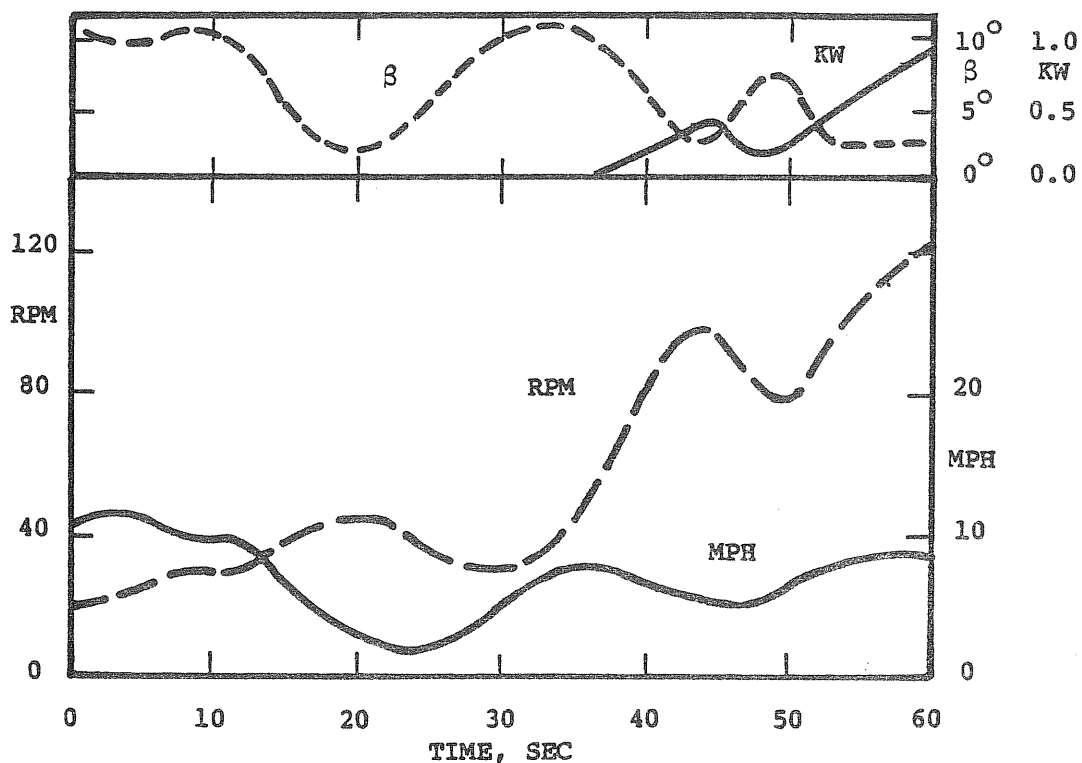
Figure 6-12.   POWER-ON STARTING AT 15 DEGREE FURL ANGLE; ROTOR SPEED, ROTOR POWER, WIND SPEED AND CYCLIC PITCH AMPLITUDE VS. TIME, 14 October 1980
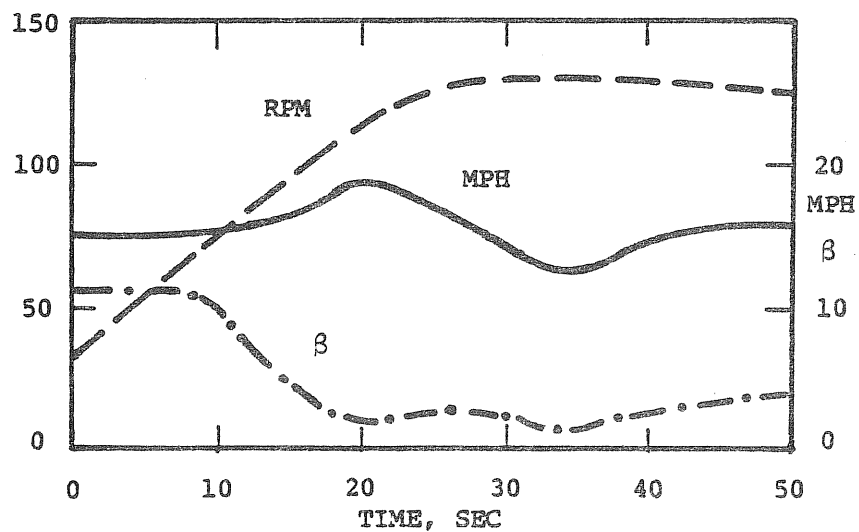
Figure 6-13.   POWER-OFF STARTING AT 60 DEGREE FURL ANGLE; ROTOR SPEED, WIND SPEED AND CYCLIC PITCH AMPLITUDE VS. TIME, 22 September 1980

69
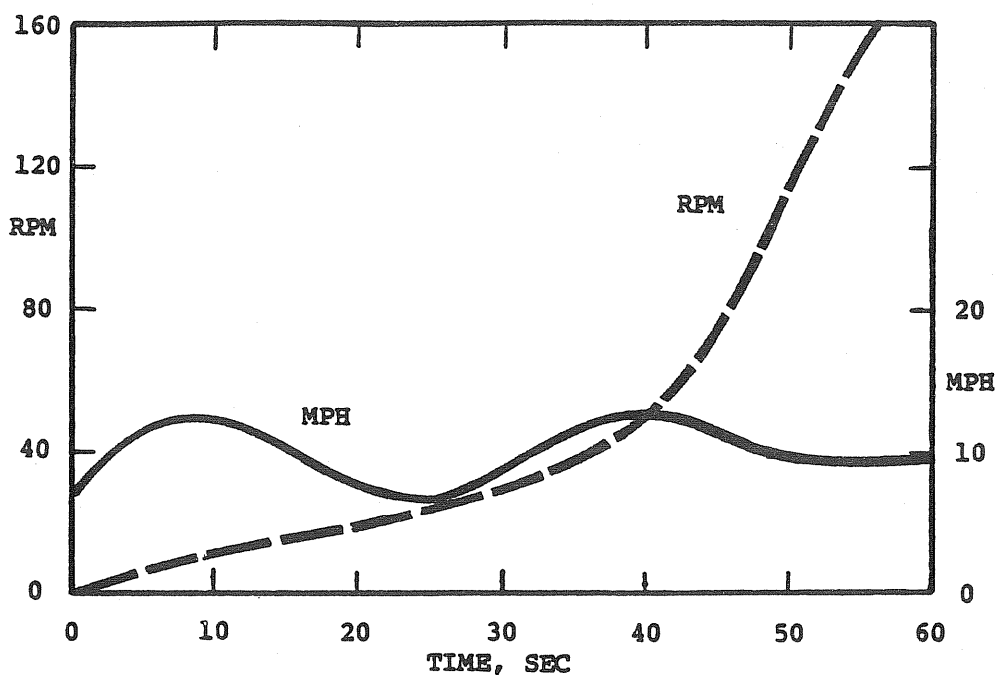
Figure 6-14.   GENERATOR-OFF STARTING AT 15 DEGREE FURL ANGLE; ROTOR SPEED
AND WIND SPEED VS. TIME, 17 October 1980
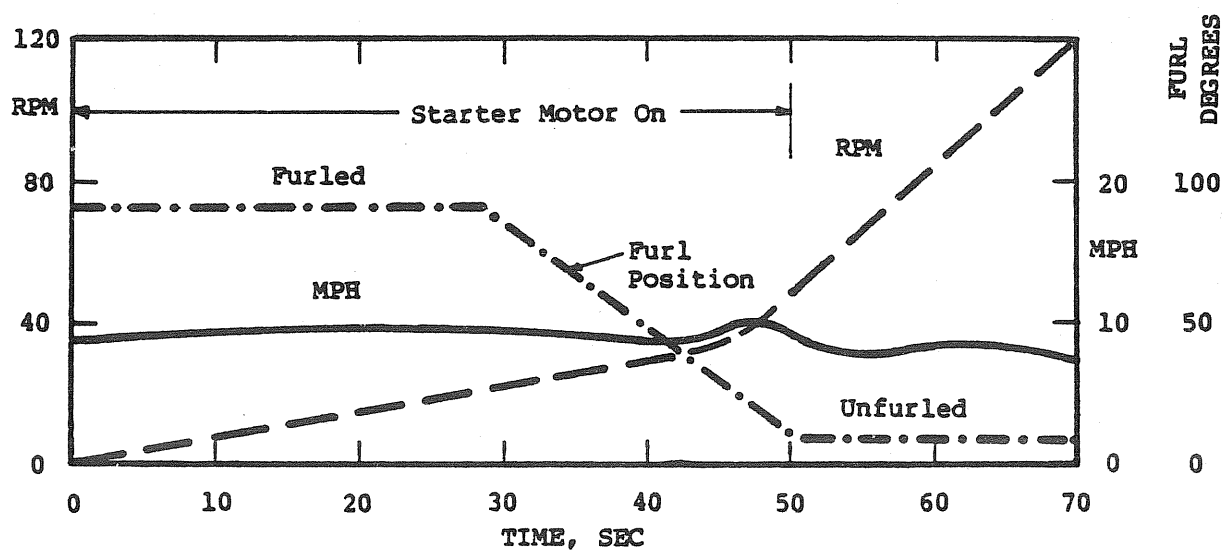
Figure 6-15.   POWER-OFF STARTING FROM THE FULL FURL POSITION; ROTOR SPEED,
WIND SPEED AND FURL POSITION VS. TIME, 12 September 1980

70

Finally, a time history of motored starting in the unfurled position is shown in Fig. 6-16. The wind speed is low and varies between 3 and 6 mph. The starter was on during the first 40 sec up to about 40 rpm. Then the rotor accelerated quite rapidly to 80 rpm driven only by the low wind speed. Over the last 40 sec the average wind speed was 4.7 mph, the average rotor speed was 75 rpm resulting in an average tip speed ratio of $\Omega R/V = 14.2$. The data were taken during the first run of the wind turbine on May 23, 1980.

In summary, the wind turbine accelerates rapidly at wind speeds as low as 5 mph once the negative "hump" shown in Fig. 6-7 at 10 to 20 rpm has been overcome. To produce power, the average wind speed must be over 8 mph. There may always be gusts above this average wind speed of sufficient magnitude to get the turbine across the negative "hump". Once this is accomplished, there can be temporary wind lulls down to very low wind velocities without reducing the rpm below the "hump", and rotor speed will pick up rapidly when the wind speed returns. In a prototype a starting motor may not be needed, particularly if the initial friction torque of the system can be reduced. Due to the much reduced shank length and the wider inboard chord, the prototype blade version has almost twice the aerodynamic starting torque as the present blades according to the analysis.

6.3.3 Power-off Tests

Analog data taken with the oscillograph have been used to extract approximate steady state conditions and to obtain time histories of furling processes and gust responses. Digital data have been processed to obtain statistical aerodynamic and load parameters during extended runs of one hour or more.

6.3.3.1 Power-off Analog Data

Figure 6-17 shows the speed ratio $V/\Omega R$ vs. yaw angle (assumed equal to the furl angle). The model test results and NACA test results from Fig. 4-3a are superimposed. The full scale rotor autorotates at much lower speed ratios than the model. In part this is caused by the lower blade solidity ratio, and in part by the higher Reynolds number. The discontinuity of the model curve at 50° yaw angle, interpreted as a stall effect, is not seen for the full scale rotor curve. The measured speed ratio curve blends into the NACA curve, which probably is approximately representative also for the wind rotor. The measurements were taken at 14 to 27 mph wind speed corresponding to 160 to 250 rotor rpm.

Figure 6-17 illustrates the difficulty of power-off rotor speed control at small yaw angles. For example, a gust at zero yaw angle which doubles the wind velocity would require a change in yaw angle (equal to furl angle) of 70°. The first 30° of yaw angle change will not change $V/\Omega R$ and is thus ineffective for the purpose of rotor speed control. In normal operation there is no need for a power-off rotor speed control at low yaw angle. For power-off operation at high yaw angle, required for storm survival, rotor speed control requires only small yaw angle changes. For example, a doubling of the wind velocity from 60° yaw angle operation at zero power would, according to Fig. 6-17, require a change of yaw angle of only 20° and would be immediately effective. As will be shown below, the automatic furl control was not capable of preventing sizeable
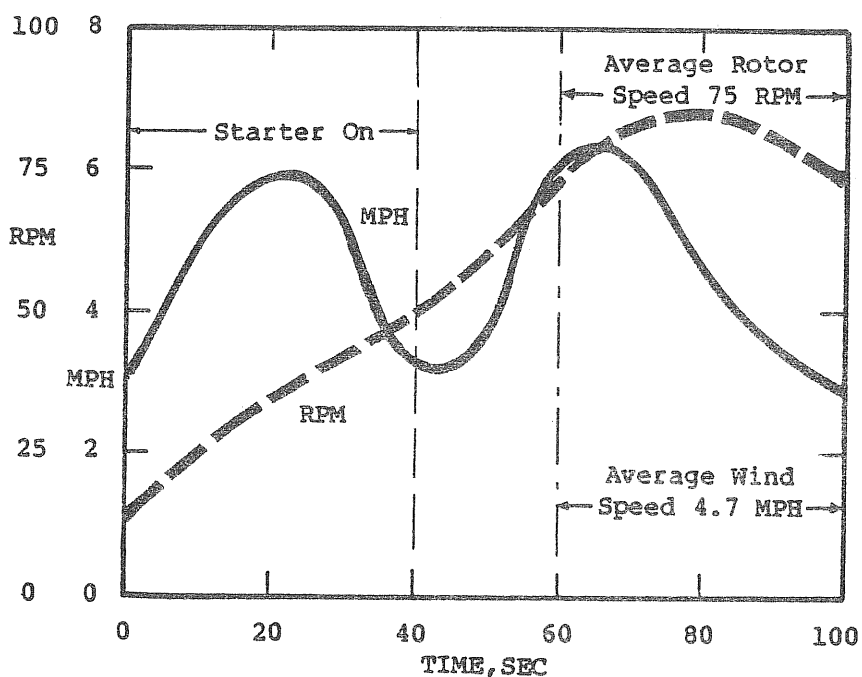
Figure 6-16.   POWER-OFF MOTORED STARTING IN THE UNFURLED POSITION,
ROTOR SPEED AND WIND SPEED VS. TIME, 23 MAY 1980
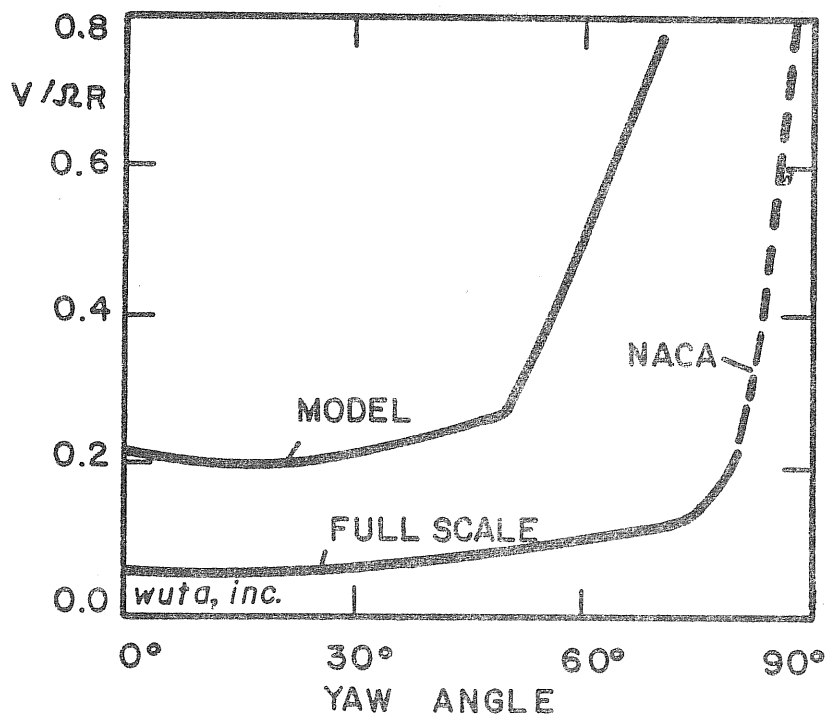
Figure 6-17.   STEADY STATE AUTOROTATION TEST RESULTS FOR MODEL AND FULL
SCALE MACHINE,   2-11 October 1980

72

overspeed from a gust when the unfurled rotor was operated power-off in autorotation. This characteristic is evident from Fig. 6-17. Unfurled power-off operation can and should be avoided except in the case of power failure.

Along the power-off operational line in Fig. 6-17 the flap-bending amplitude increases from $\pm$ 1500 in-lb at 15° yaw angle to $\pm$ 3100 in-lb at 80° yaw angle. The in-plane amplitude remains nearly constant at $\pm$ 1800 in-lb. The stresses in the blade retention are quite low, up to $\pm$ 240 psi for flap-bending, and $\pm$ 190 psi for in-plane bending. The cyclic pitch amplitude is $\pm$ 2° to $\pm$ 4° and is affected by yaw rates resulting from wind direction changes.

To establish the autorotational characteristics shown in Fig. 6-17, some low furl angle tests were conducted power-off. The automatic furl control was set to trip at 228 rpm. Figure 6-18a shows an automatic furling process initiated by strong gusts that increased the wind speed at the anemometer location from 14 to 30 mph in 6 sec. Automatic furling began at 228 rpm and stopped 4 sec later at 85° furl angle. The maximum rotor speed was 310 rpm at 45° furl angle. Without furling, the equilibrium rotor speed for 30 mph wind velocity would be 540 rpm. A tip speed ratio of $\Omega R/V = 16$ is assumed. The maximum flap bending amplitude occurred directly after the initiation of furling and was a 2P oscillation of $\pm$ 10,000 in-lb, coresponding to a stress of $\pm$ 772 psi.

The maximum rotor torque amplitude occurring at the same time was a 4P oscillation with $\pm$ 1660 in-lb corresponding to $\pm$ 1400 psi shear stress in the rotor shaft. The maximum rotor thrust was about 320 lb estimated from a static flap-bending moment of 16,000 in-lb. An overspeed condition can occur in power-on operation if the power suddenly fails. The test results prove that the overspeed condition is benign. Damage was not caused to any component, and the dynamic loads and stresses remained well within allowable limits.

Figure 6-18b shows automatic furling in a mild gust that increased the wind speed from 12 to 15 mph in 7 sec. The overspeed limit was set at 215 rpm and the rotor speed reached a maximum of 225 rpm. Furling stopped at 60° furl angle when the rotor speed was crossing the 215 rpm limit.

In another test the power was cut off at 165 rpm and simultaneous furling was initiated. Figure 6-19 shows the time histories of wind speed, rpm and furl angle. The rpm increased from 165 to 225 in 3 sec and reached its maximum at about 50° furl angle. 80° furl angle was obtained after 4.3 sec. From then on the rpm steadily declined despite a brief gust from 16 to 21 mph. During this gust the power was inadvertently turned on for 2 sec without arresting the decline in rpm. In both cases, that of Fig. 6-18 and that of Fig. 6-19, the rpm increased power-off by 35% during furling and reached its maximum at about two-thirds of the way to complete furling. To cover the emergency case of sudden loss of power, the machine must be capable of withstanding, without damage, a power-off overspeed of at least 35%.

6.3.3.2 Power-off Digital Data

Figure 6-20 shows results of digital data acquisition for power-off conditions. Figures 6-20a is for 15° furl angle, Fig. 6-20b is the result for 45° furl angle. The first graph in each figure gives log N vs. wind speed bin, where N is the

Figure 6-18a.   POWER-OFF AUTOMATIC FURLING RESPONSE TO STRONG WIND GUSTS;
                 ROTOR SPEED, WIND SPEED AND FURL ANGLE VS. TIME,
                 16 October 1980
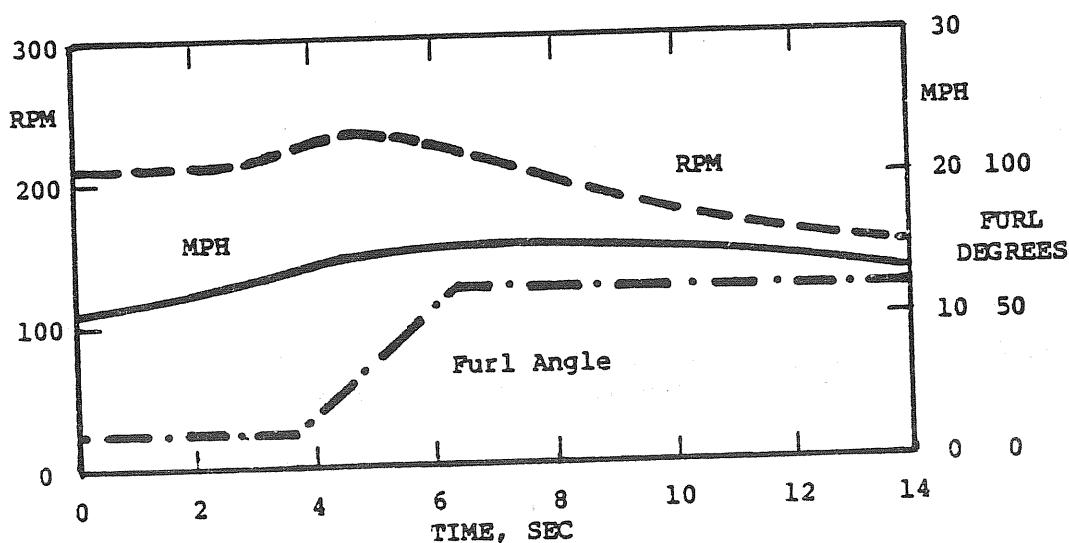
Figure 6-18b.   POWEROFF AUTOMATIC FURLING RESPONSE TO MILD WIND GUSTS;
                 ROTOR SPEED, WIND SPEED AND FURL ANGLE VS. TIME, 20 Sept '80

74
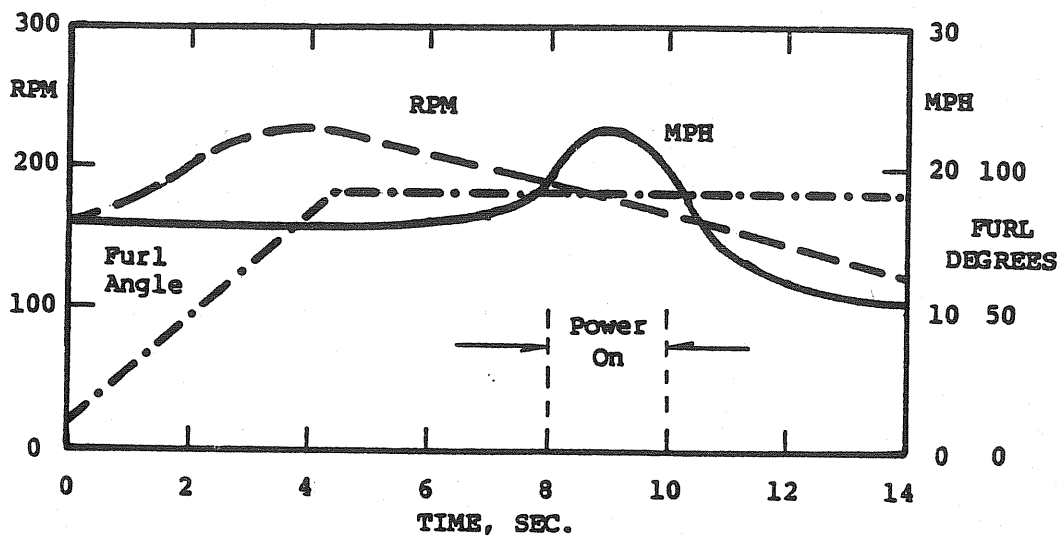
Figure 6-19.   SIMULTANEOUS POWER CUT AND FURLING; ROTOR SPEED, WIND SPEED
AND FURL POSITION VS. TIME, 10 October 1980
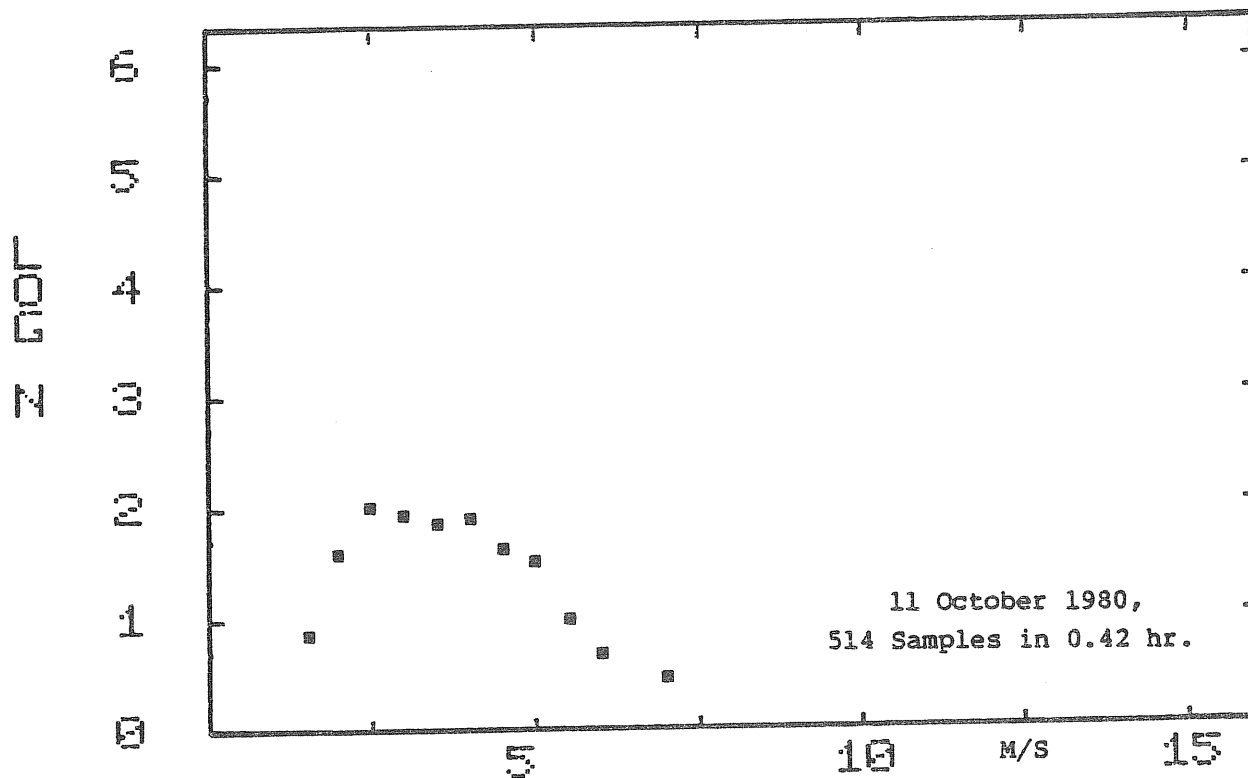
Figure 6-20al.   POWER-OFF RUN, SAMPLE DISTRIBUTION, LOG (N) SAMPLES VS.
WIND SPEED FOR 15 DEGREE FURL ANGLE
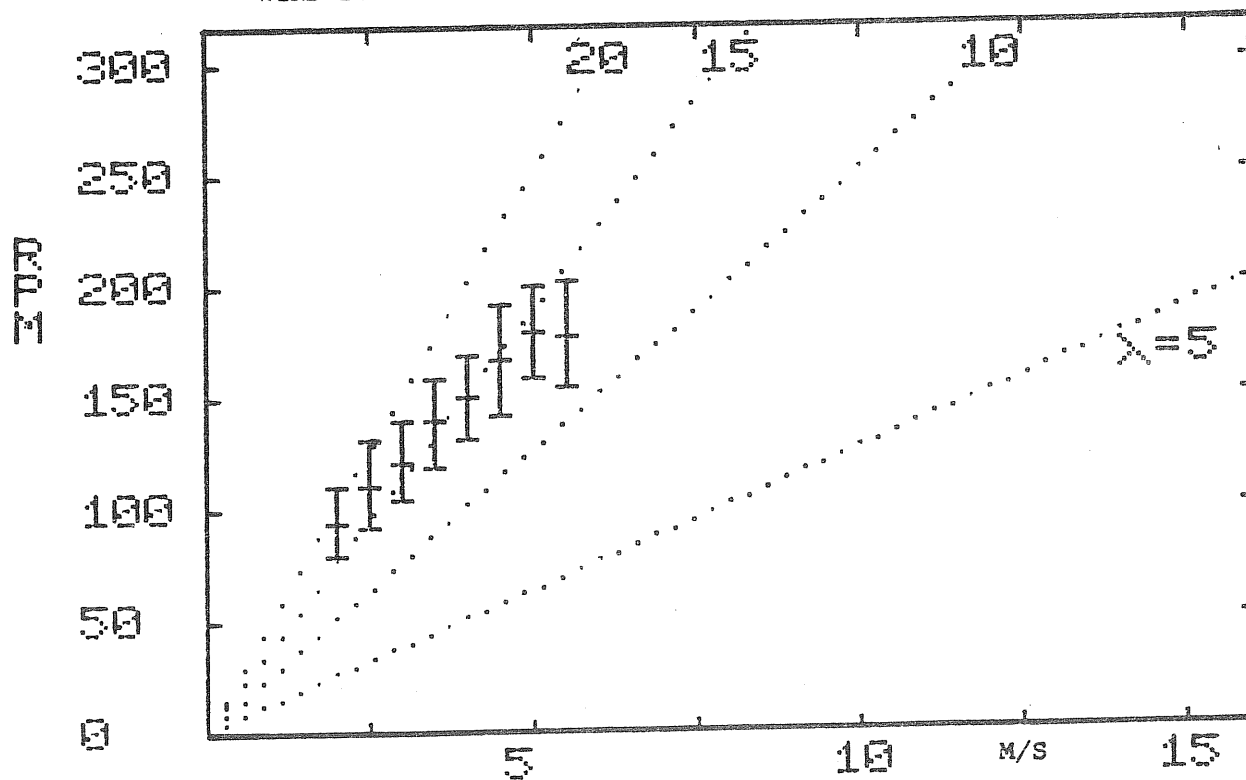
Figure 6-20a2.   POWER-OFF RUN, RPM VS. WIND SPEED FOR 15 DEGREE FURL ANGLE,
11 October 1980,   514 Samples in 0.42 hr.

number of samples in the bin. The bin midpoints are at 0.5, 1.0, 1.5, 2.0, etc. m/s wind speed. One or two points farthest to the right have been neglected because they represent very few samples. The statistics are not meaningful for these bins.

The second graph of each figure gives the mean and standard deviation of rotor speed for each wind speed bin. The dotted lines represent constant tip speed ratios $\Omega R/V = 5, 10, 15,$ and 20. In Fig. 6-20a, valid for 15° furl angle, the mean values of rpm represent tip speed ratios of more than 15 at the low end, and tip speed ratios of less than 15 at the high end of wind speed and rpm. For a steady wind the tip speed ratio is constant and, according to Fig. 6-17, has for 15° furl angle the value of $\Omega R/V = 16$. For fluctuating wind speed, the tip speed ratio varies because the inertia of the rotor keeps the rpm lower than equilibrium for gust peaks and higher than equilibrium for gust valleys. If one computes the wind speed which represents the mean power in the wind,

$$V_{MP} = \left(\Sigma(V^3 N)/\Sigma N \right)^{1/3} \qquad\qquad (6-2)$$

one obtains a tip speed ratio close to that found in a steady wind for the corresponding bin. For example, V_{MP} for the sample distribution of Fig. 6-20a has the value 3.6 m/s. For this velocity the tip speed ratio is in fact close to 16, while at the low end it is 18 and at the high end it is 13.

The third graph of Fig. 6-20a shows cyclic pitch amplitude vs. wind speed. The mean, standard deviation and global maximum and minimum for each wind speed bin are plotted. For low wind speed the mean values are about $\pm 3°$; for high wind speeds they are about one-half this value.

Figure 6-20b, (a furl angle of 45°) shows a lower tip speed ratio of about 12. For steady conditions the tip speed ratio should be about 12.5 according to Fig. 6-17, and the digital data agree with the analog data. The trend toward higher tip speed ratios at lower wind speed is also recognizable from Fig. 6-20b. The trend is not as pronounced as in Fig. 6-20a, possibly because of the higher number of samples taken or possibly because of the relative absence of fast gusts. The third graph of Fig. 6-20b shows rotor power vs. wind speed. The appreciable power at higher wind speed and higher rotor speed is either caused by air pumping losses of the generator (windage loss) or by the tightening of the belt from centrifugal forces. Without the alternator belt the rotor power is quite small.

Loads are not presented for power-off conditions although they have been measured. The power-on dynamic loads at the same furl angle and rpm were found to be either the same or somewhat higher than power-off.

6.3.4 Power-on Tests

Analog data taken with the oscillograph served the dual purpose of estimating steady state characteristics and of obtaining time histories of special events. Digital data were used to obtain the "bin" statistics over extended runs.
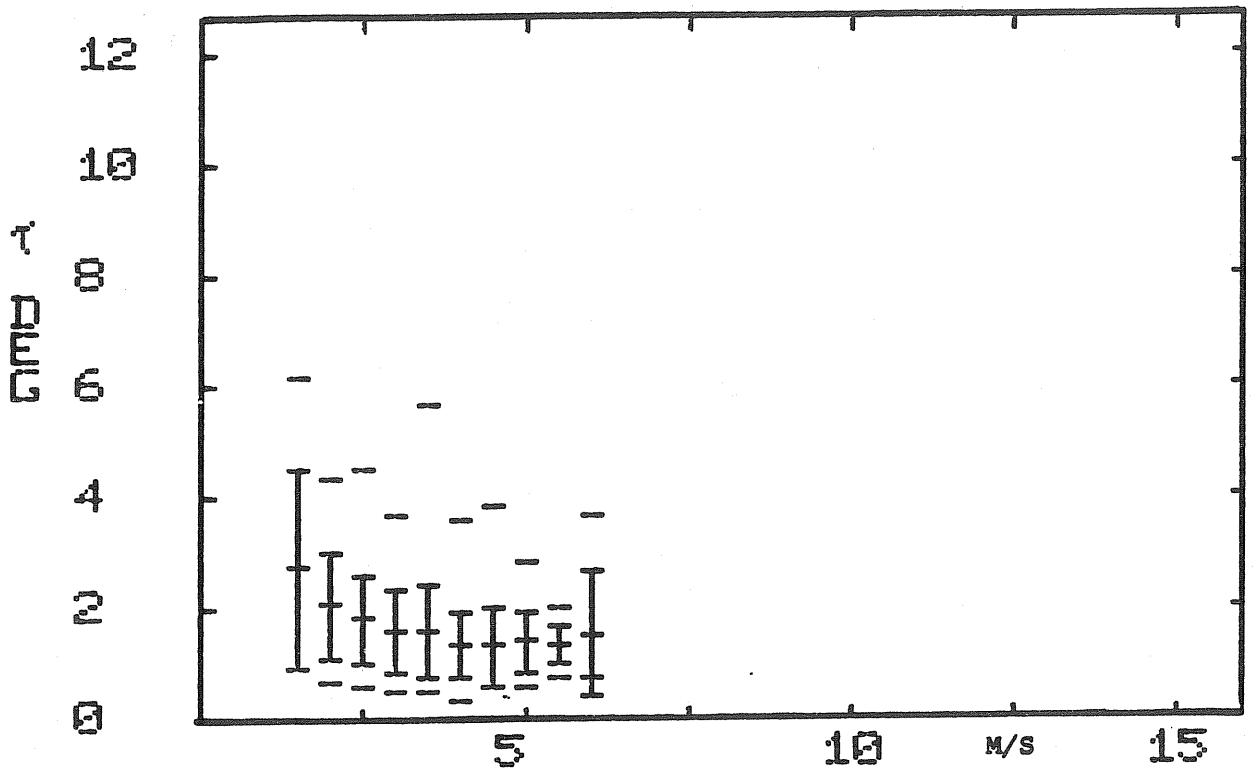
Figure 6-20a3. POWER-OFF RUN, CYCLIC PITCH AMPLITUDE VS. WIND SPEED FOR 15
DEGREE FURL ANGLE, 11 October 1980, 514 Samples in 0.42 hr.

Figure 6-20b1. POWER-OFF RUN, SAMPLE DISTRIBUTION, LOG (N) SAMPLES VS.
WIND SPEED FOR 45 DEGREE FURL ANGLE, 24 October 1980

Figure 6-20b2.   POWER-OFF RUN, RPM VS. WIND SPEED FOR 45 DEGREE FURL ANGLE

Figure 6-20b3.   POWER-OFF RUN, ROTOR POWER VS. WIND SPEED FOR 45 DEGREE FURL
                  ANGLE, 24 October 1980, 1000 Samples

6.3.4.1 Power-on Analog Data

A considerable amount of time and effort was lost while taking performance data with the second replacement alternator which was the first to be tested on the wind turbine. According to the test data sent by Astral Wilcon, the second replacement alternator compared to the first replacement alternator bench tested by WUTA as shown in Table 6-5.

Table 6-5. ALTERNATOR POWER OUTPUT

RPM	Second Replacement watt, A.W.	First Replacement watt, WUTA
2000	200	11
3000	1100	680
4000	4000	2530
4500	6600	4600
5000	8500	6500
5500	9600	7780

The rotor to alternator gear ratio for the second replacement alternator was selected as 21.4:1 instead of the original 25:1 ratio due to the higher power output at a given rpm. Figure 6-21 shows a comparison of alternator power vs. rotor rpm for the A.W. bench test and for the installation in the wind turbine.

The oscillograph reading for the alternator load voltage was checked against the meter reading whenever a steady condition was obtained for a few seconds. The alternator power reached a maximum of 5 kW with increasing rpm. Beyond 5 kW the power decreased rapidly with rpm. This contrasts with the power curve obtained by Astral Wilcon, also shown in Fig. 6-21. The rotor power reaches a maximum of 6 kW at 220 rpm and follows the trend of the alternator power. The stator and field windings, capacitor and diodes were checked for shorts, but none could be detected. According to Astral Wilcon, the alternator should have a maximum power of 5 kW without the tuning capacitor. The second version alternator may have been mistuned. An overall system efficiency at the upper end of the power curve of 0.75 to 0.80 was obtained by comparing the rotor power input from the strain gage torque meter with the electrical alternator power output. This efficiency includes the mechanical and electrical losses.

The early drop of rotor power with increasing rpm produced overspeed at relatively low wind speed. Figure 6-22 shows a case where a power-on overspeed of 282 rpm was reached at only 21 mph wind speed. The furl signal was not recorded. The start of automatic furling is recognizeable by an increase in dynamic loads. It appears that furling was delayed, probably due to a malfunction of the tach generator signal. Nevertheless, the rotor speed at 21 mph should not have exceeded 210 rpm with a normal alternator.

Despite extensive checks of all components involved in the alternator output, the cause for early peaking of the power curve could not be determined. A
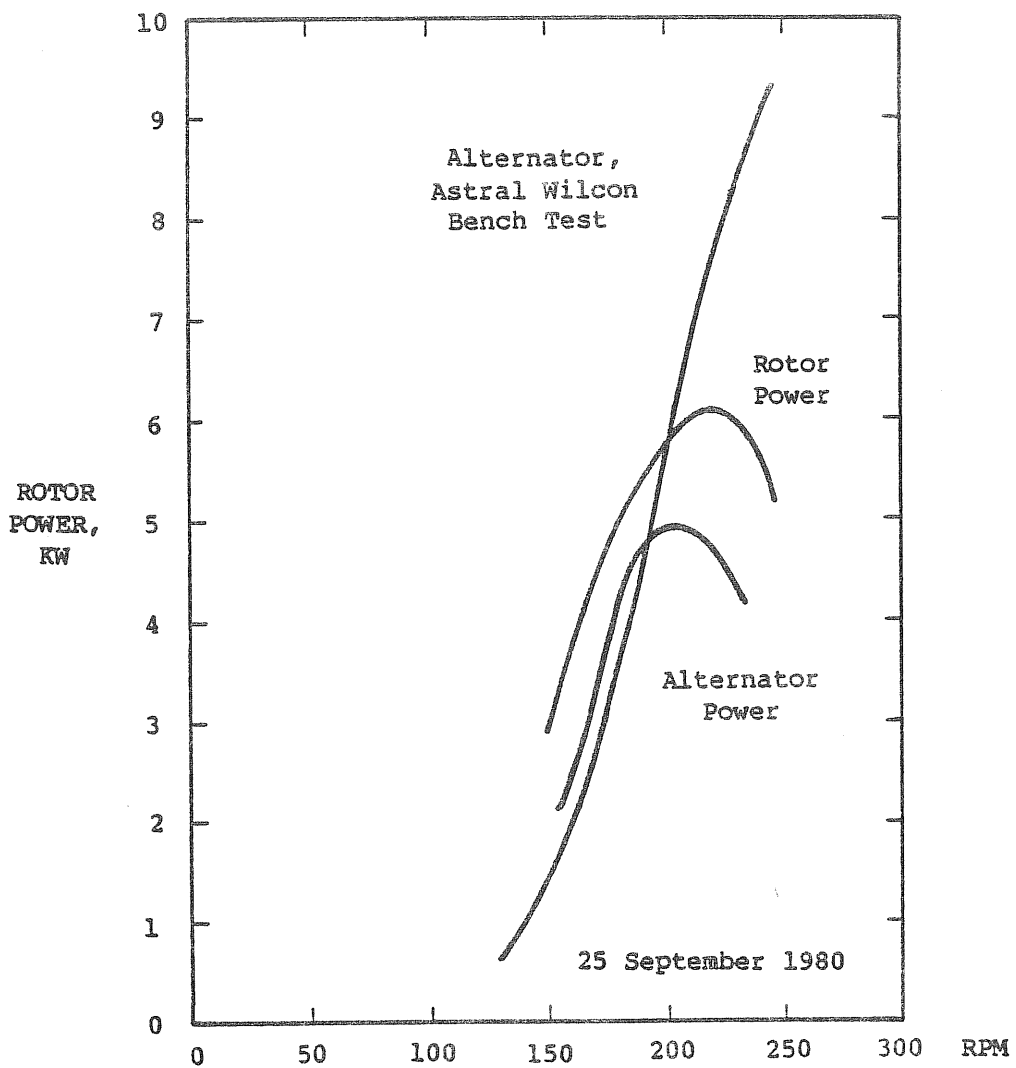
Figure 6-21.   SECOND REPLACEMENT ALTERNATOR POWER CURVES; ROTOR POWER AND
GENERATOR POWER VS. ROTOR SPEED, 21.4/1 GEAR RATIO
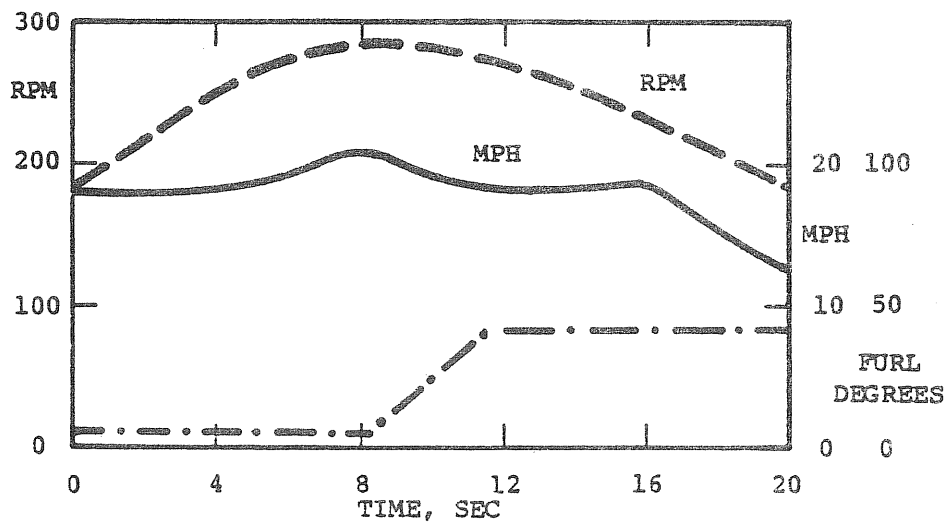
Figure 6-22.   POWER-ON OVERSPEED WITH FAULTY ALTERNATOR; WIND SPEED, ROTOR
SPEED AND FURL POSITION VS. TIME, 25 September 1980

magnetic pick-up to measure alternator speed was then installed. This made it possible to check for belt slippage, which was found not to occur. The faulty alternator was exchanged for the first replacement alternator, bench tested in May 1980 by WUTA. Power-on tests with this alternator began on October 10, 1980, using the original overall gear ratio of 25:1.

First the effect of alternator resistance load was determined. Figure 6-23 shows the electrical power output vs. rotor rpm for 8.2, 6.0 and 5.3 ohm load resistance together with the WUTA bench test result for 5.1 ohm resistance. At the upper end of the power curve a 6 ohm load produces the maximum power, though 5.3 ohm gives only slightly less power. 8.2 ohm resistance is much worse at the upper end of the curve, though there is a crossover at about 4 kW, so that a 8.2 ohm resistance is somewhat better at the low end of the power curve. The agreement of the wind turbine tests with the WUTA bench test is good. It was then decided to conduct the remaining power-on atmospheric test with the first replacement alternator. This alternator had the following configuration: 700 ohm field resistance, 28 stator windings, 50μF tuning capacitors, and a gear ratio of 25:1.

Figure 6-24 shows rotor power vs. rotor speed for the unfurled position (actually 15° yaw angle) and for 40° furl angle. The data were taken from oscillograph records at periods where the rotor speed was approximately constant over a few seconds. The solid line corresponds to a torque coefficient of $C_Q/\sigma = 0.0080$, also shown in the analytical data of Fig. 5-7. With two exceptions, the measured rotor power points were reasonably well represented by the constant torque coefficient line. This illustrates that the rotor power varied with the cube of the rotor speed. The two highest rotor power points were taken during a period of rotor acceleration. When the measured shaft torque was corrected by the inertia torque from the angular rotor acceleration, the corrected rotor power values agreed with the cubic power curve. For example, at 250 rpm the acceleration was 15 rpm/sec or 1.57 rad/sec^2. The torque correction is,

$$\Delta Q = 1.57 \times 65 \times 12 = 1200 \text{ in-1b} \qquad (6-3)$$

where a rotor moment of inertia of 65 slug ft^2 is used. The shaft torque was 3660 in-1b. The corrected torque is 3660 + 1220 = 4880 in-1b. The rotor power computed with this torque is 14.6 kW at 250 rpm rather than 11 kW found without the inertia torque correction. In the same way the second point was corrected, increasing the rotor power at 230 rpm from 6.6 to 11.4 kW.

Figure 6-25 shows the same measurements including the two corrected values in a graph of rotor power vs. wind speed at the anemometer site. Again the unfurled condition (15° furl angle) is compared to the condition with 40° furl angle. The two solid lines represent $C_p = 0.38$ and $C_p = 0.14$ which one would expect from the analytical graphs of Fig. 5-7 for $\alpha = 90^\circ$ and $\alpha = 50^\circ$ respectively. although there is more scatter in Fig. 6-25 than in Fig. 6-24, the two analytical curves are a reasonable representation of the measured values. This will become more evident from Table 6-6. The values of mph in brackets are those on the curves of Fig. 6-25 for the measured rotor power. The difference between the measured and analytical wind speed values for each measured rotor power was in most cases small. The last two rows for 15° furl angle data include the rotor power corrected for inertia rotor torque. The efficiencies for these two conditions were low since the alternator power input was only from the shaft torque, not from the corrected torque.
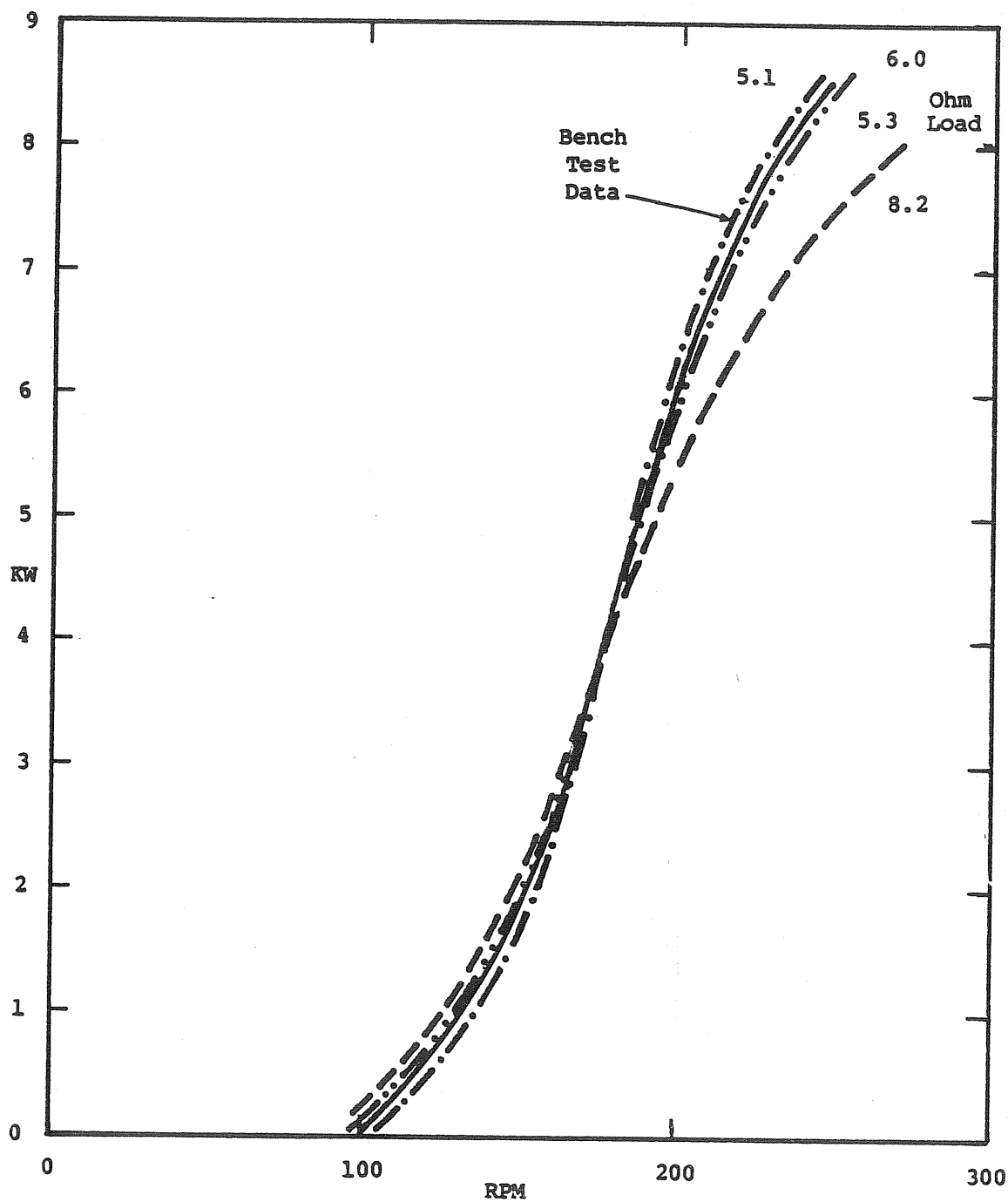
Figure 6-23.   FIRST REPLACEMENT ALTERNATOR; ELECTRIC POWER VS. ROTOR SPEED, 25/1 GEAR RATIO, 10 OCTOBER 1980
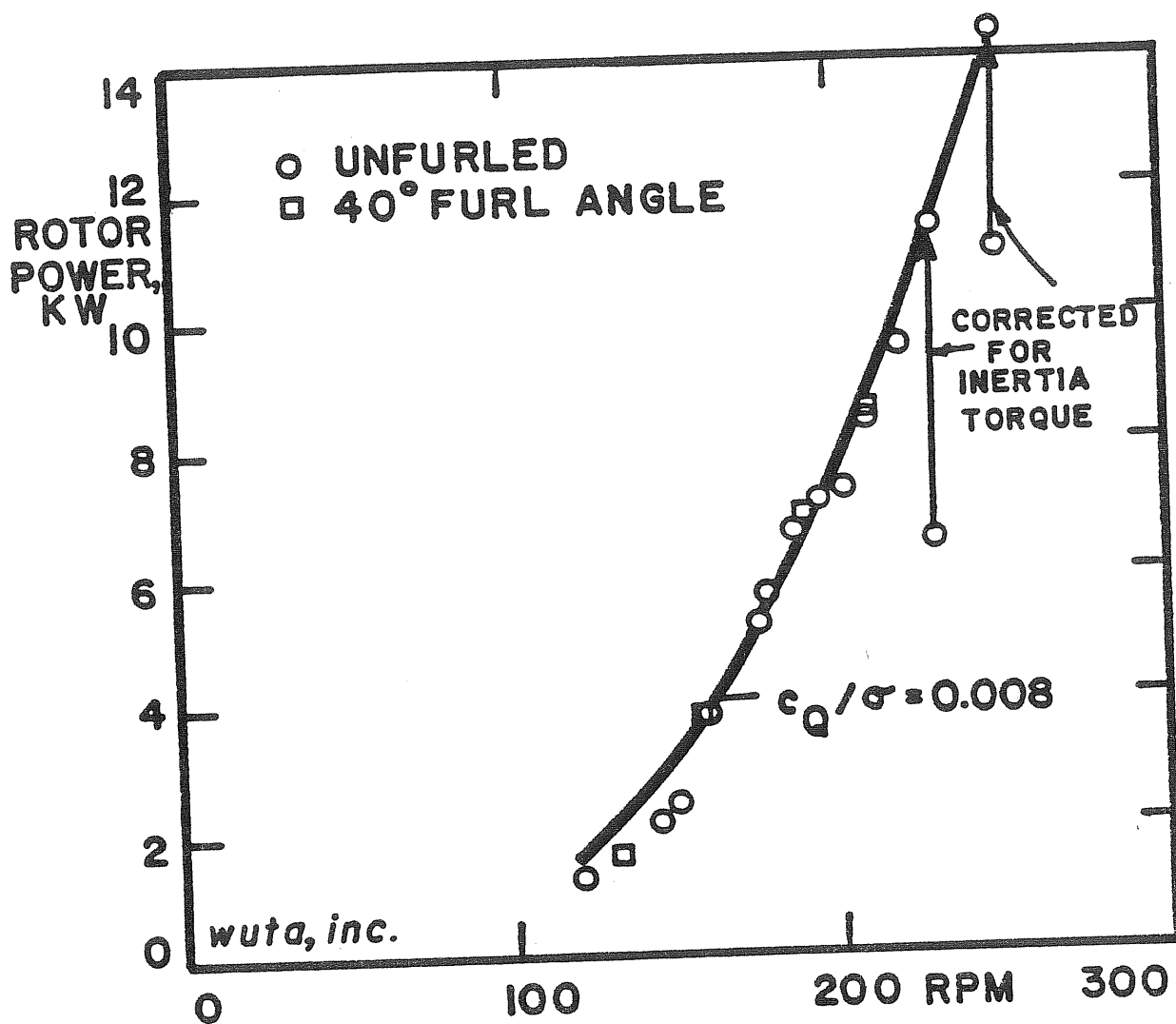
Figure 6-24.   ROTOR POWER VS. ROTOR SPEED; 25/1 GEAR RATIO, 11 October 1980
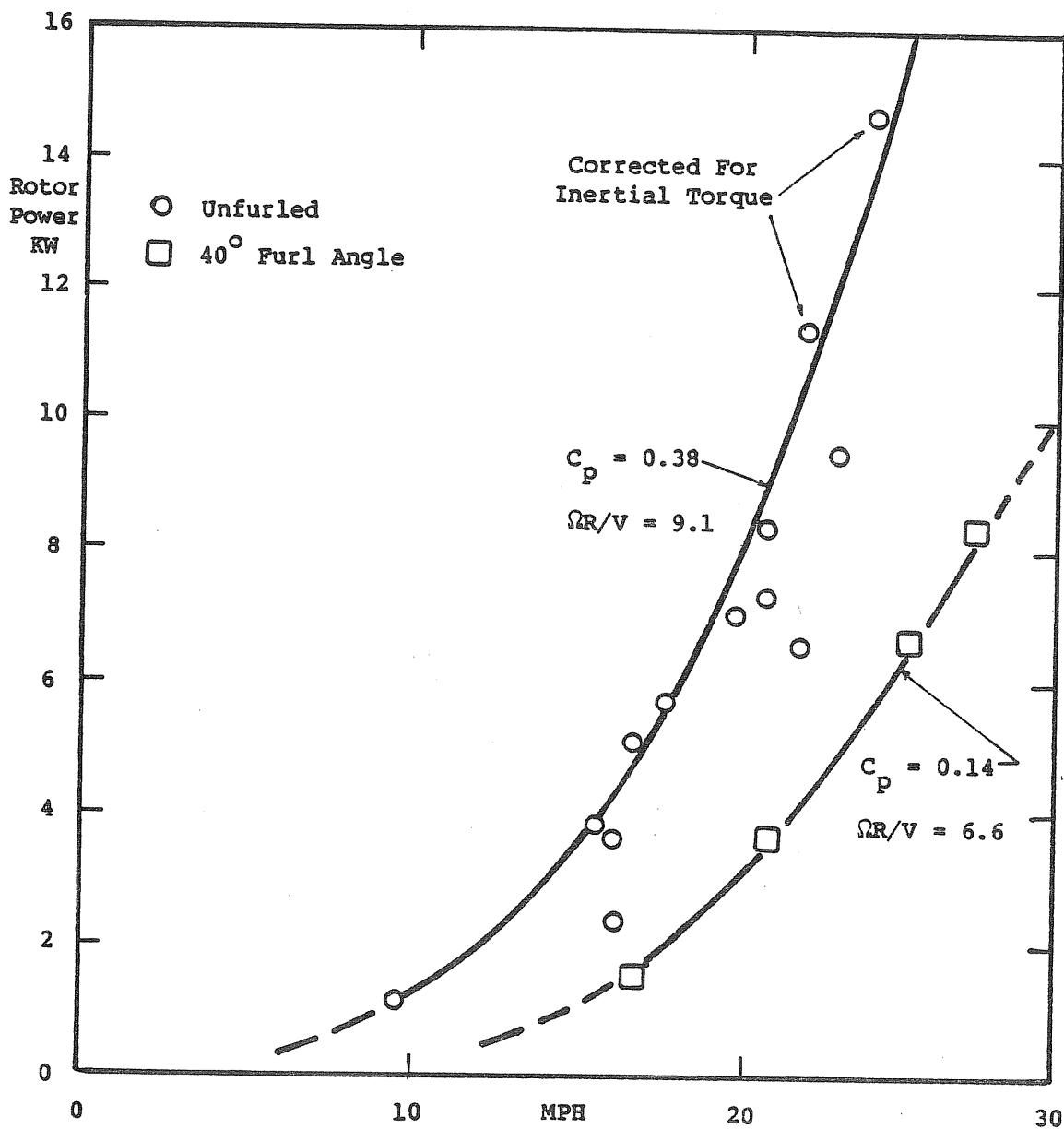
Figure 6-25.   ROTOR POWER VS. WIND SPEED FOR UNFURLED POSITION AND 40
DEGREE FURL ANGLE, 11 October 1980

Table 6-6. ANALOG PERFORMANCE DATA

UNFURLED (15°)

rpm	mph	(mph)	Rotor Power kW	Alt. Power kW	Efficiency
120	10	(10.4)	1.2	.6	.50
150	16.5	(13.6)	2.4	1.7	.71
160	16.5	(16.5)	3.8	2.3	.61
174	17	(17)	5.2	3.7	.72
177	18	(18)	5.7	4.1	.72
186	22	(19)	6.7	5.0	.75
195	20	(19.3)	7.0	5.8	.82
202	21	(21.5)	7.3	6.2	.84
210	21	(20.4)	8.4	6.9	.82
220	23	(21.2)	9.5	7.7	.81
230	22	(22.5)	11.4	8.0	.70
250	24	(24.5)	14.6	8.7	.60

FURLED (40°)

rpm	mph	(mph)	Rotor Power kW	Alt. Power kW	Efficiency
135	17	(17)	1.6	1.1	.68
160	21	(21.5)	3.8	2.3	.61
190	25	(26.4)	6.9	5.4	.80
210	27	(28.4)	8.4	6.8	.81

In summary, the steady state analog data up to 40° furl angle indicate that the wind rotor had characteristics close to those that would be predicted by Fig. 5-7. Note, for example, that 8.4 kW rotor power was produced for 210 rpm unfurled at 21 mph and 40° furled at 27 mph. The efficiency for those conditions was about 80%. The losses included mechanical friction from bearings, gears and belt and the electrical alternator losses. At lower rotor speed and rotor power the efficiency was much lower. The analog data will be substantiated and expanded by the digital data presented in Section 6.3.4.2

Figure 6-26 shows one of the many recorded time histories of power-on automatic furling. The initiation of furling was set at 228 rpm and gust wind rising to 30 mph tripped the furling relays. The rotor speed reached 250 rpm. The furl actuator stopped at 70° furl angle when the rpm decreased to the 228 rpm set point.

Figure 6-27 shows the time history of a power-on gust wind peaking at 36 mph. The automatic furling device had been switched off, so that the machine was in a manual furling mode. The operator, not expecting the strong gust which doubled the wind speed from 18 to 36 mph at the anemomenter site within 4 sec delayed manual furling by about 4 sec. Furling came too late to prevent a rotor
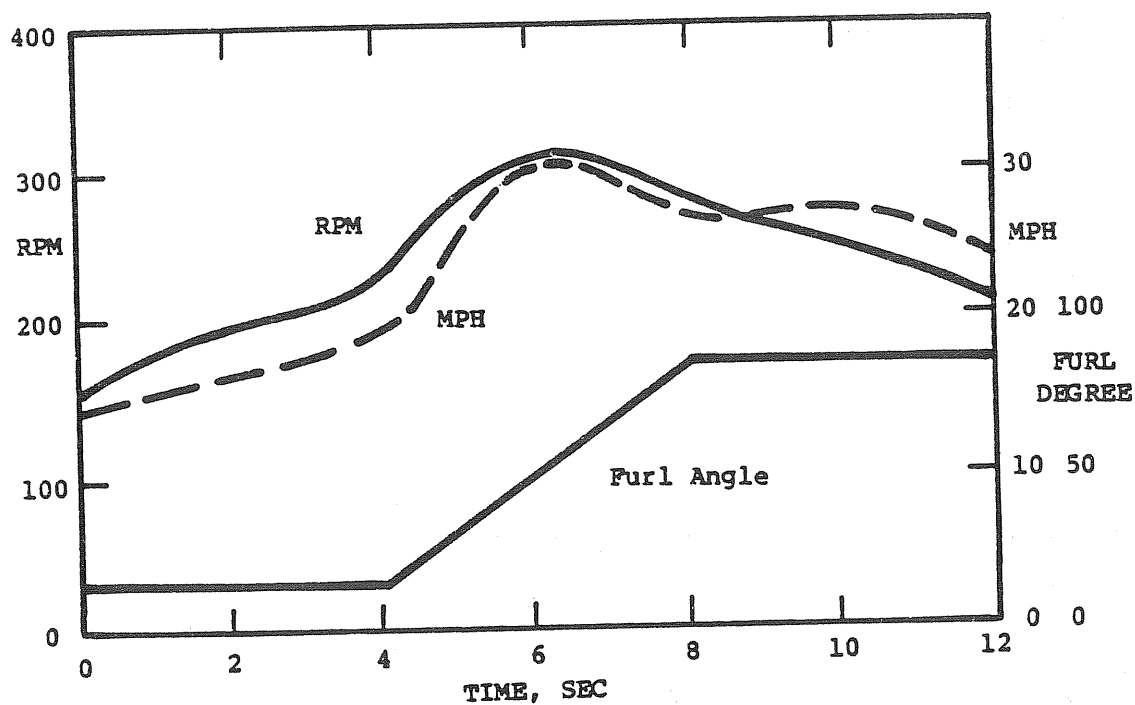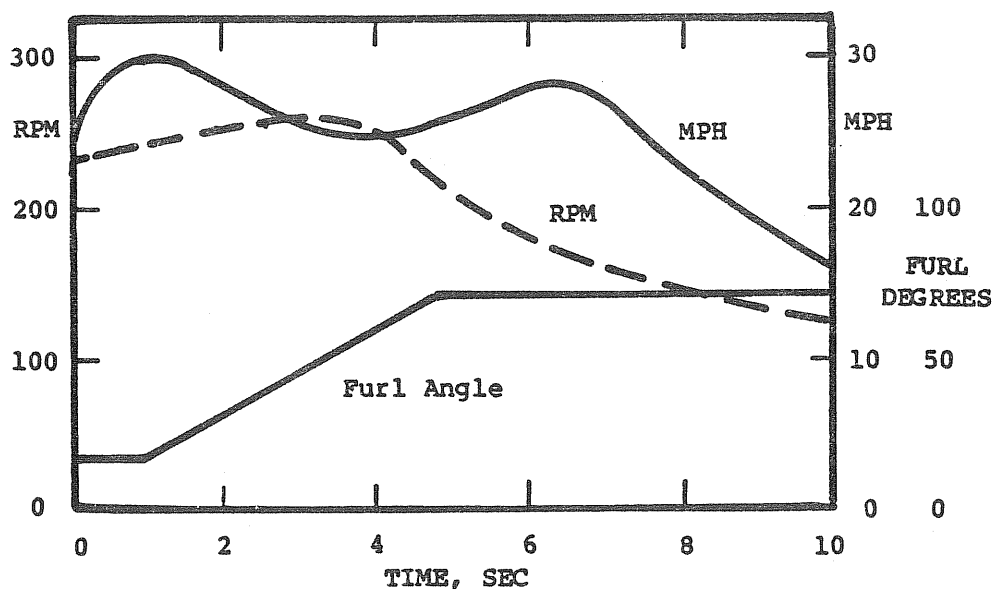
Figure 6-26.   POWER-ON AUTOMATIC FURLING RESPONSE TO WIND GUSTS; ROTOR
SPEED, WIND SPEED AND FURL ANGLE VS. TIME, 16 October 1980
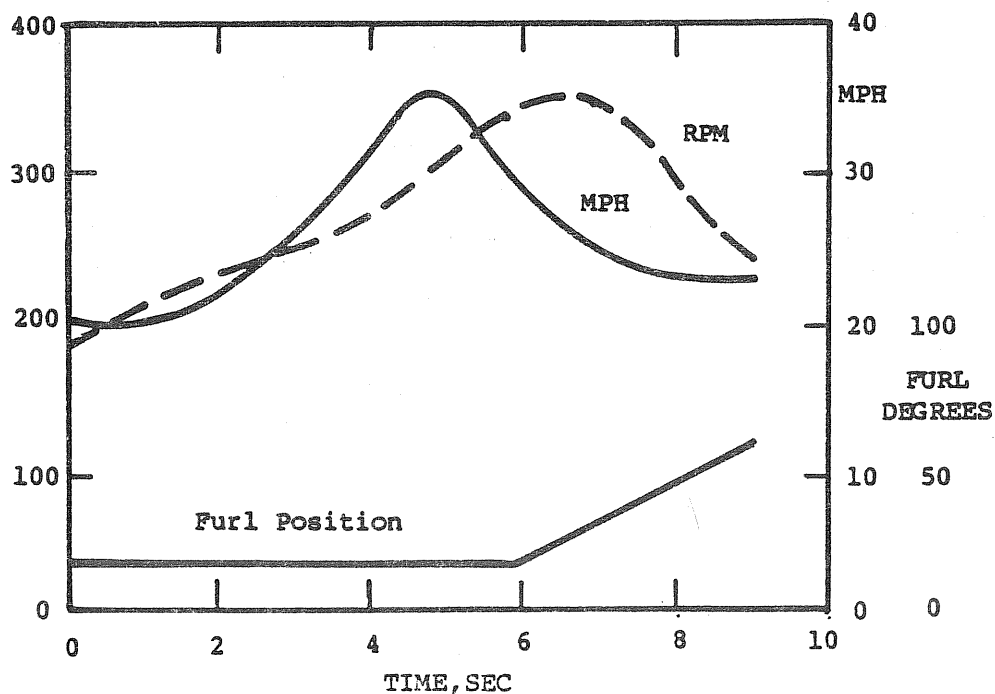
Figure 6-27.   POWER-ON ROTOR RPM RESPONSE TO WIND GUST AND DELAYED FURL-
ING; ROTOR SPEED, WIND SPEED AND FURL ANGLE VS. TIME,
11 October 1980

overspeed to 360 rpm which occurred 2 sec after the peaking of the gust. This was the highest wind velocity and the highest overspeed encountered. A careful check after the event revealed no damage. The alternator experienced an overspeed to 9000 rpm. According to the manufacturer it is designed for 10,000 rpm. The tach generator experienced 5400 rpm; it is designed for 4000 rpm. The aerodynamic rotor power including rotor inertia torque nearly reached 30 kW. The alternator power output at 9000 rpm was only 5.5 kW which explains the rapid increase in rotor speed. The alternator power probably peaks at about 7000 rpm and then rapidly declines with increasing rpm. During the delayed furling the cyclic pitch amplitude went up from 3° to 11°; the shaft torque 4P amplitude went up from 660 to 3300 in-lb.

6.3.4.2 Power-on Digital Data

Figures 6-28 and 6-29 show the performance sampling results of power-on runs in the unfurled position (15°) and in the 45° furl position respectively, in winds from the northwest and west. The data for the upper end of the wind speed scale were biased if frequent automatic furlings occurred during the test run. Sampling was interrupted during furling and unfurling. The two runs presented in Fig. 6-28 and 6-29 were performed in wind conditions without automatic furling. Figure 6-28a and 6-29a show the smooth sampling distributions for both runs. In contrast, sampling distributions taken in south wind were ragged with substantial differences in the number of samples for adjacent wind speed bins. The other measured variables also showed much more scatter and the average C_p values were substantially lower with southerly winds. The wind reaching the site from the south passes over woods that extend close to the site. Apparently the wind from the south is quite turbulent and degrades machine performance. Only tests in winds from the west or northwest are presented for performance evaluation. Winds from the south are included for load data. The point to the farthest right in Fig. 6-28a and 6-29a has been neglected because it represents too few samples.

Figures 6-28b and 6-29b show a similar pattern for rpm vs. wind speed to those discussed for the power-off test results, Fig. 6-20. Toward the high end of the wind speed scale the tip speed ratio is lower, and toward the low end of the scale the tip speed ratio is higher. The rotor power shown in Fig. 6-28c and 6-29c has a substantial standard deviation in each wind speed bin caused by rpm variation and by the sensitivity of rotor power to rpm indicated by Fig. 6-24. The generator to rotor efficiency of Fig. 6-28d shows efficiencies of over 0.80 for the higher wind speeds, but very low efficiencies for lower wind speeds. Much of the wind turbine operation will be at wind speeds of 5 to 6 meter per second (11 to 13 mph) where the generator to rotor efficiency is only 40%. Although the distribution between mechanical and electrical losses is not known, it is likely that most of the loss is electrical and caused by the tuning capacitors needed to increase the peak power output from 5 kW to 8 kW. Obviously a prototype should not use the alternator in its present configuration. Subsequently, we will ignore the alternator performance and only present the rotor performance.

Figure 6-28e shows the rotor thrust in newtons. To obtain pound force divide the number of newtons by 4.45. The rotor thrust is obtained by dividing the yaw
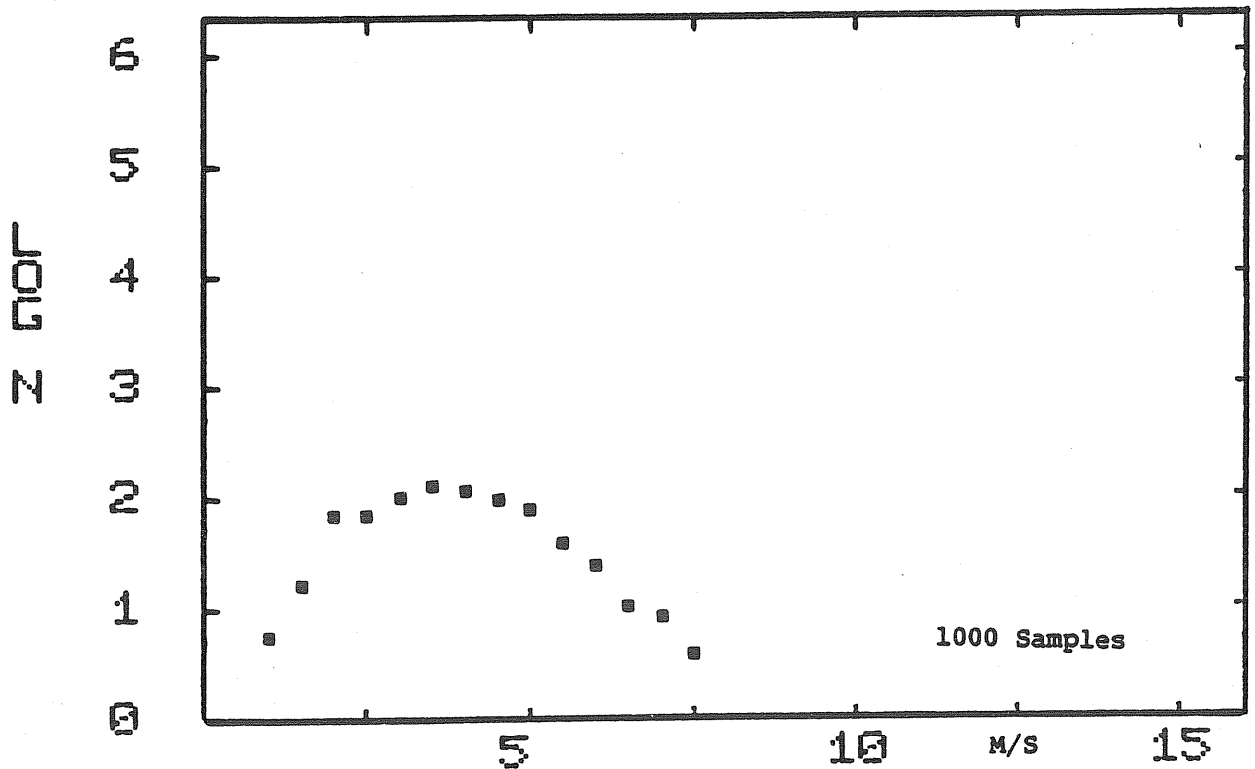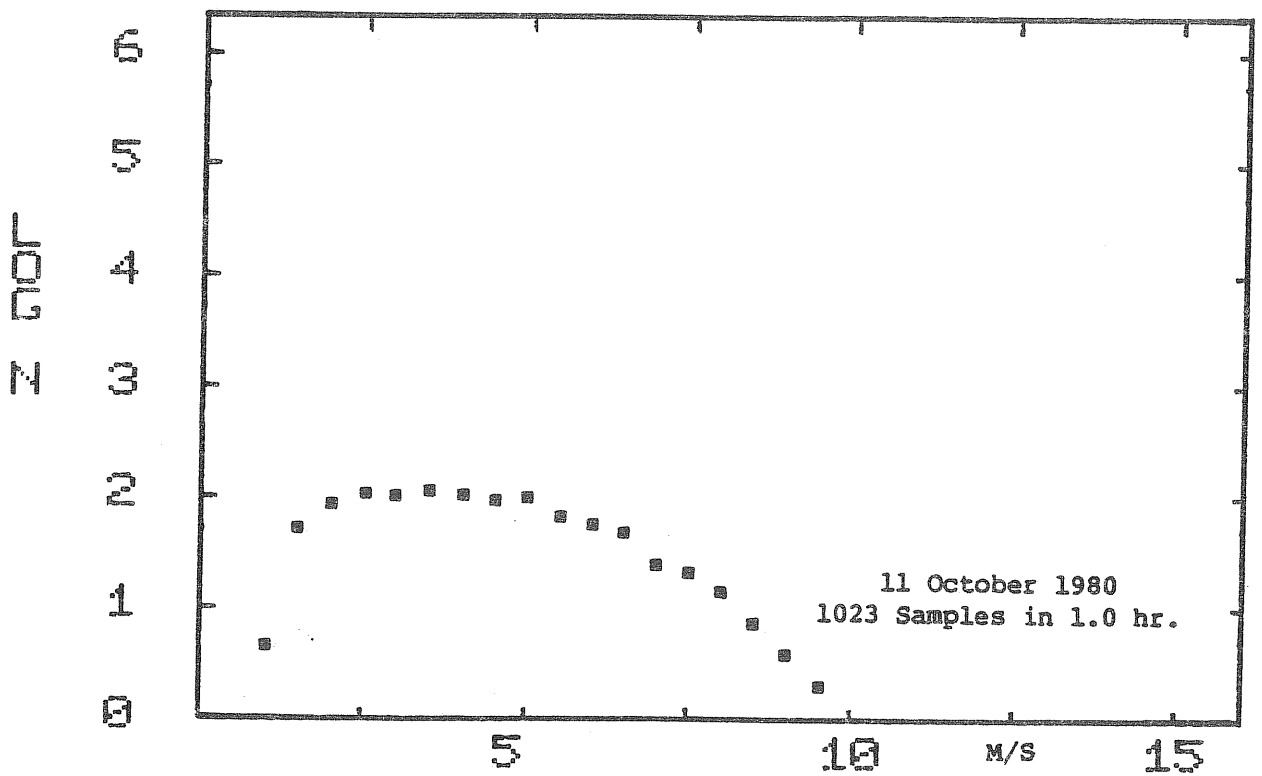
Figure 6-28a.   POWER-ON RUN, SAMPLE DISTRIBUTION, LOG (N) SAMPLES VS. WIND
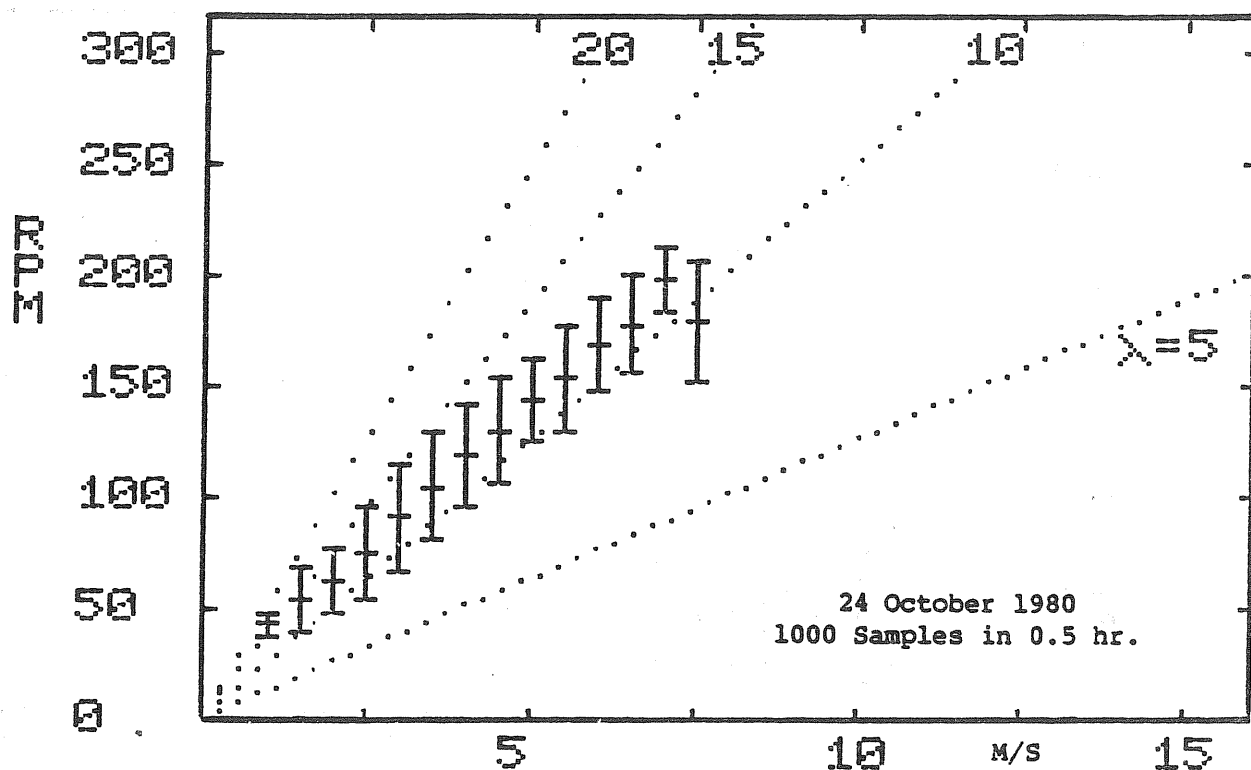SPEED FOR 15 DEGREE FURL ANGLE
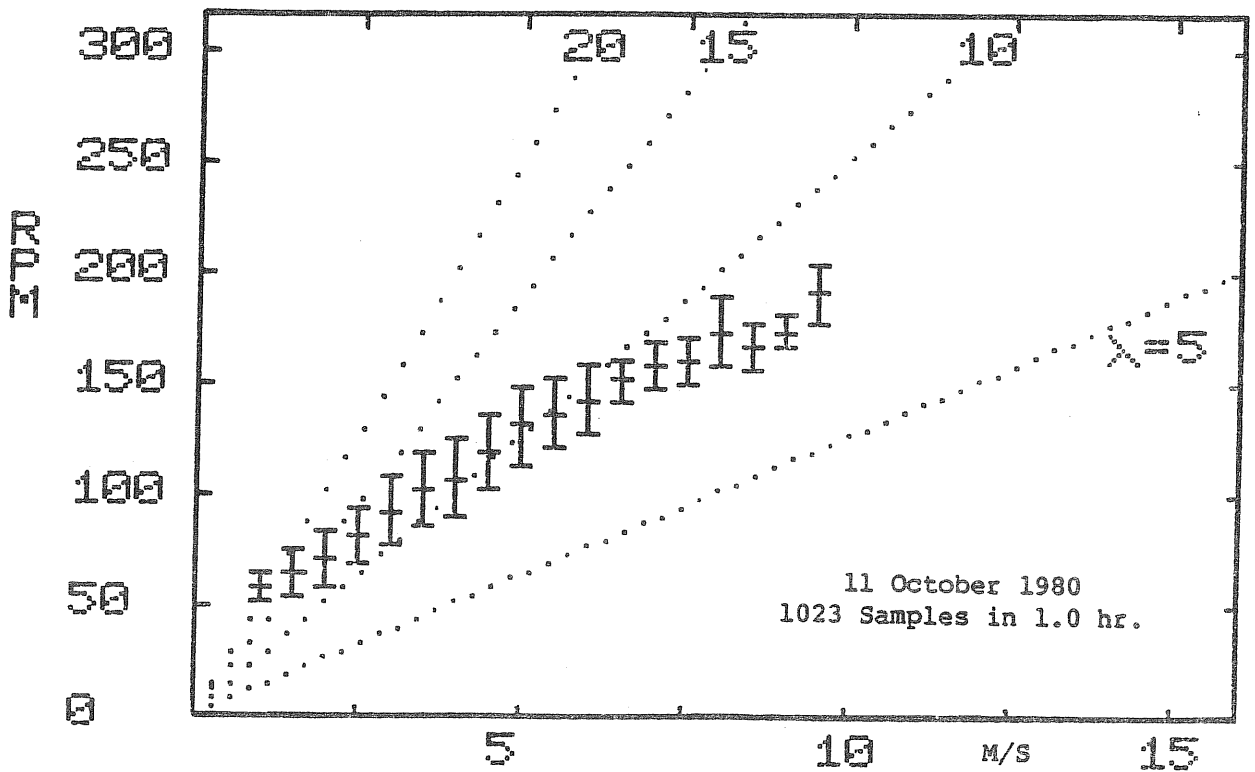
Figure 6-28b.   POWER-ON RUN, RPM VS. WIND SPEED FOR 15 DEGREE FURL ANGLE

89

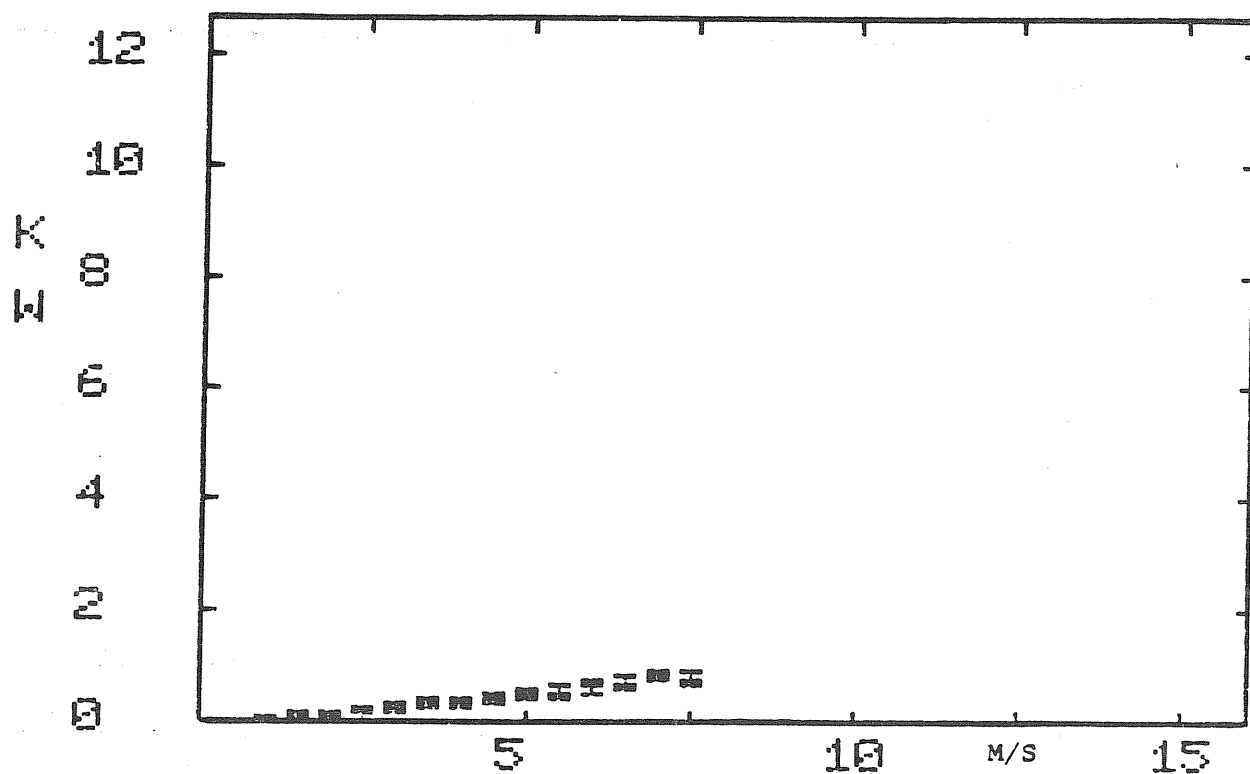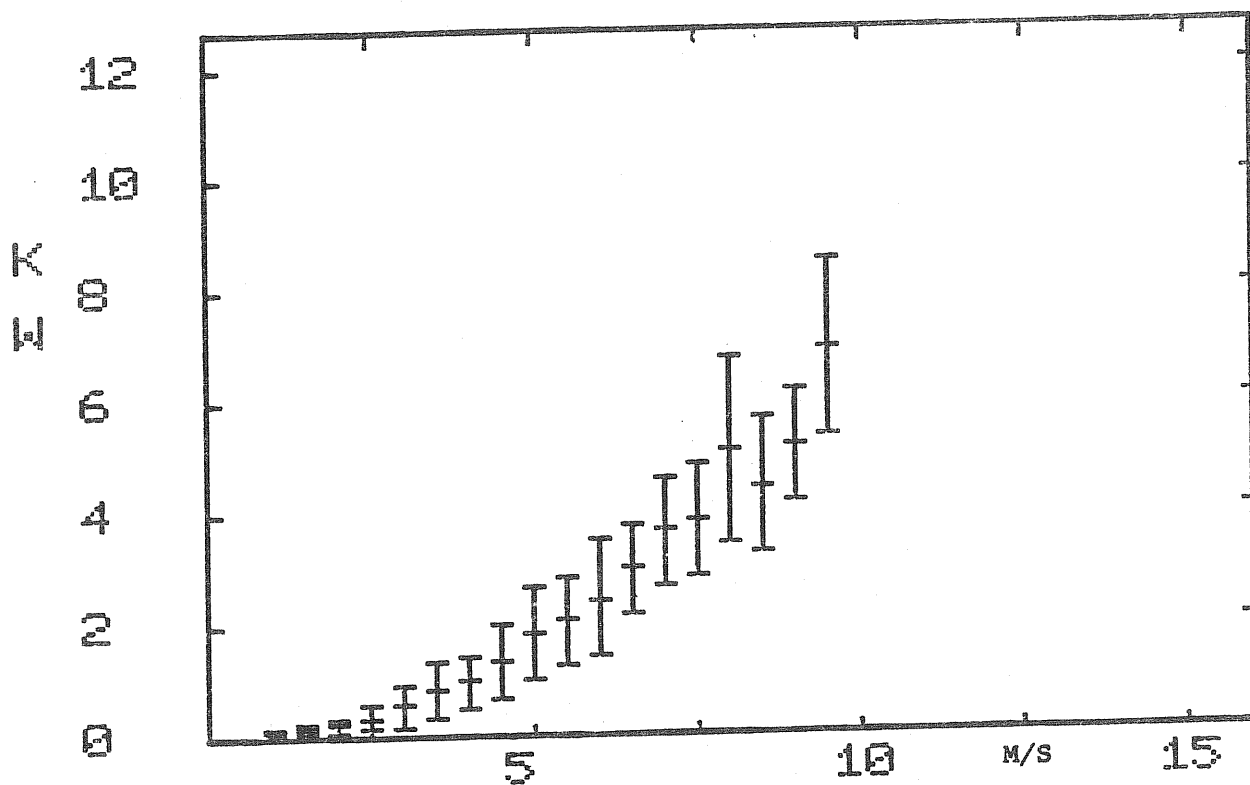Figure 6-28c.   POWER-ON RUN, ROTOR POWER VS. WIND SPEED FOR 15 DEGREE FURL
ANGLE
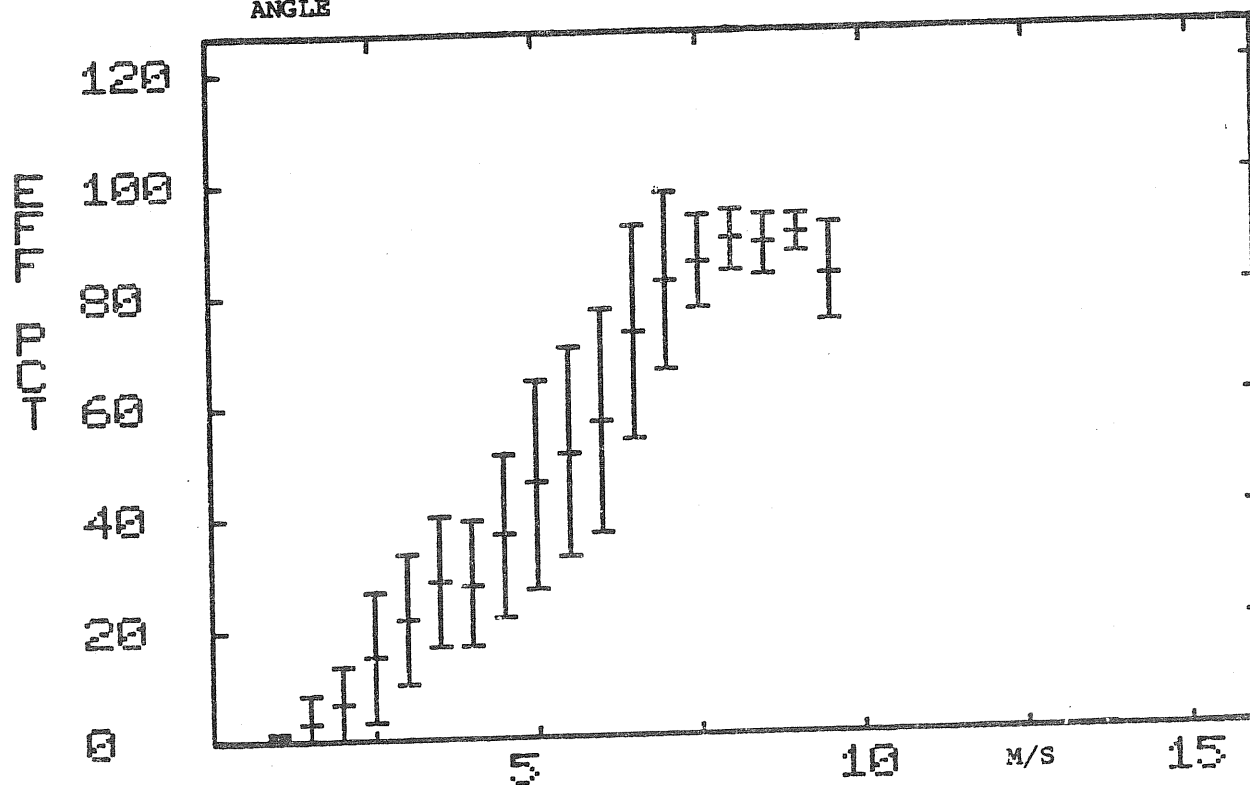
Figure 6-28d.   POWER-ON RUN, GENERATOR TO ROTOR EFFICIENCY VS. WIND SPEED
FOR 15 DEGREE FURL ANGLE

post bending moment by the distance from the upper yaw bearing to the rotor axis (205 in). From Fig. 6-28e, the rotor thrust at 9 m/sec (20 mph) is 1200 newtons (270 lb).

Figure 6-28f and 6-29d show the mean aerodynamic rotor efficiency, C_p, for each wind speed bin. At low wind speed C_p is large; at high wind speed C_p is small. The reason is that the rotor rpm and rotor power in wind gusts is lower than for steady state operation, since the rotor speed cannot follow the gust. In wind lulls the rotor rpm and rotor power is higher than for steady state operation. The mean aerodynamic efficiency, C_p, has been computed by relating the mean rotor energy during the entire run to the total energy in the wind.

$$C_p = \frac{\Sigma N \bar{P}_R}{\Sigma \frac{N}{2} A \rho \bar{V}^3} \qquad (6-4)$$

where $\bar{P}_R$ is the mean rotor power in each bin, and $\bar{V}$ is the mean wind speed in each bin.

Since the samples were taken in constant time intervals, the above expression is the ratio of the time-averaged rotor power over the time-averaged wind power. For the test run represented by Fig. 6-28, $C_p = 0.46$; for that represented Fig. 6-29, $C_p = 0.18$. ρ is the air density during the test run obtained by correcting its standard sea level value for test site ambient temperature and pressure. This correction factor was 1/1.033 for Fig. 6-28 and 1/1.043 for Fig. 6-29. The average C_p values are higher than the values of $C_p = 0.38$ and 0.12 shown in Fig. 5-7.

The correction from the wind speed measured at the anemometer site to the wind speed at the rotor center is not known and may bring the cited C_p value down. If one uses the wind profiles measured at the UMASS 25 kW wind turbine site (Ref. 12), one would conclude that the rotor center sees a 5% higher wind speed than the anemometer. The cited C_p values would then be reduced by 15%. The boundary layer profile at our test site could be quite different. In any case it appears that the storage of wind energy in the rotor during gusts and its release during lulls is quite efficient. A certain amount of loss compared to steady state operation is unavoidable. The rotor operates both above and below the tip speed ratio for maximum C_p, similar to a constant speed wind rotor, but with less variation of the tip speed ratio.

In summary, the measurements have shown that the two-bladed wind rotor with passive cyclic pitch variation performs about as expected. The cyclic pitch variation does not degrade the performance and may actually enhance it due to the rapid adaptation of the machine to changes in wind direction.

Figures 6-30 show the digital data correlation between cyclic pitch amplitude and yaw rate. It had been observed that yaw rates in the furl direction (counterclockwise seen from above) cause higher cyclic pitch amplitudes than the opposite yaw rates. The reason is that even without yaw rate there is a certain cyclic pitch amplitude with the phasing of that caused by a yaw rate in the furl direction, so that these two effects superimpose. The digital program differentiates between the two yaw rate directions. Figure 6-30a and b refer to

91
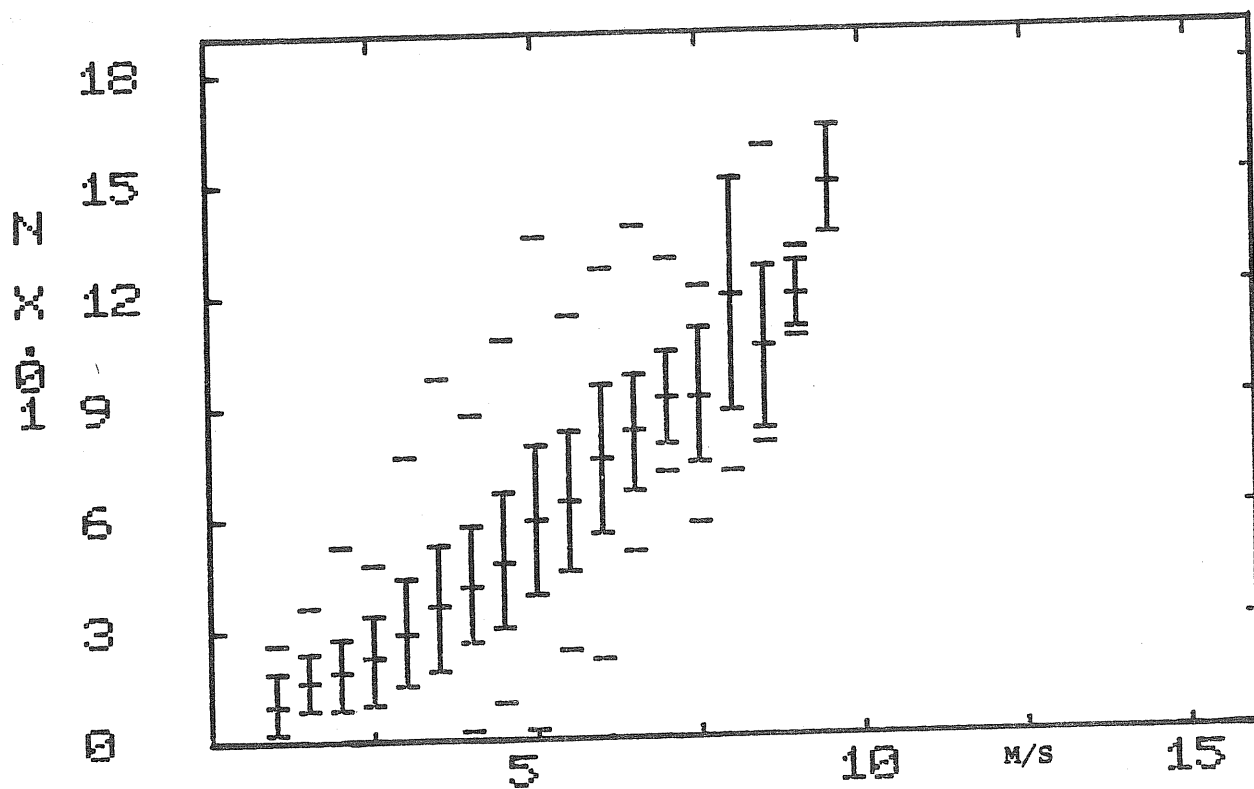
Figure 6-28e.   POWER-ON RUN, THRUST VS. WIND SPEED FOR 15 DEGREE FURL ANGLE

Average C_P = 0.46
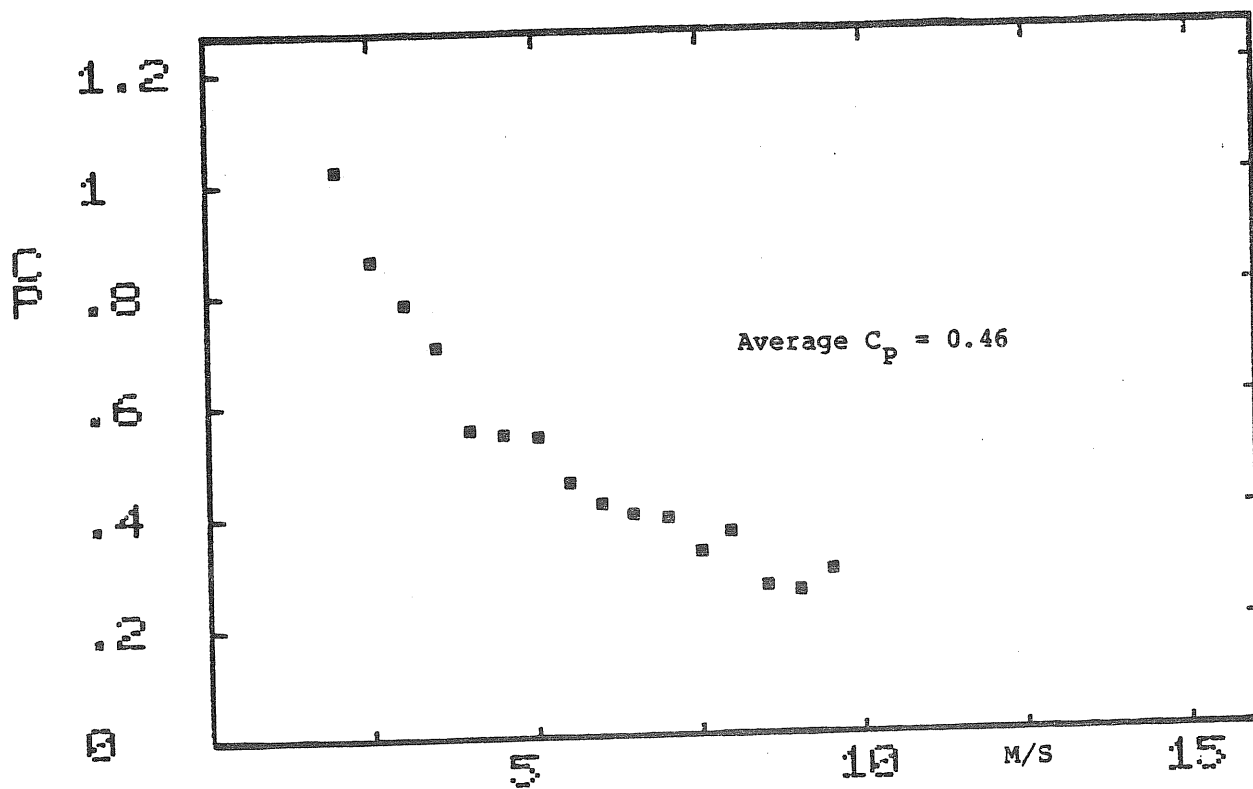
Figure 6-28f.   POWER-ON RUN, POWER COEFFICIENT VS. WIND SPEED FOR 15 DEGREE
FURL ANGLE
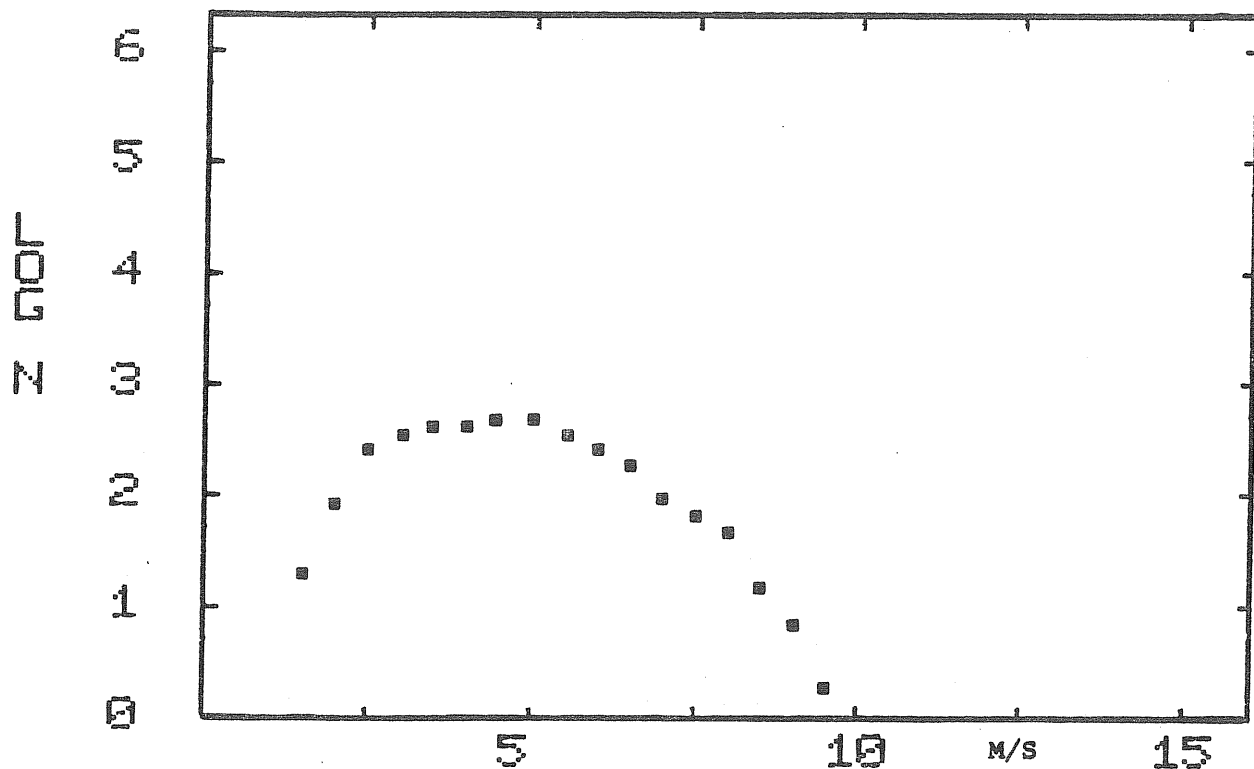
Figure 6-29a. POWER-ON RUN, SAMPLE DISTRIBUTION, LOG (N) SAMPLES VS. WIND SPEED FOR 45 DEGREE FURL ANGLE
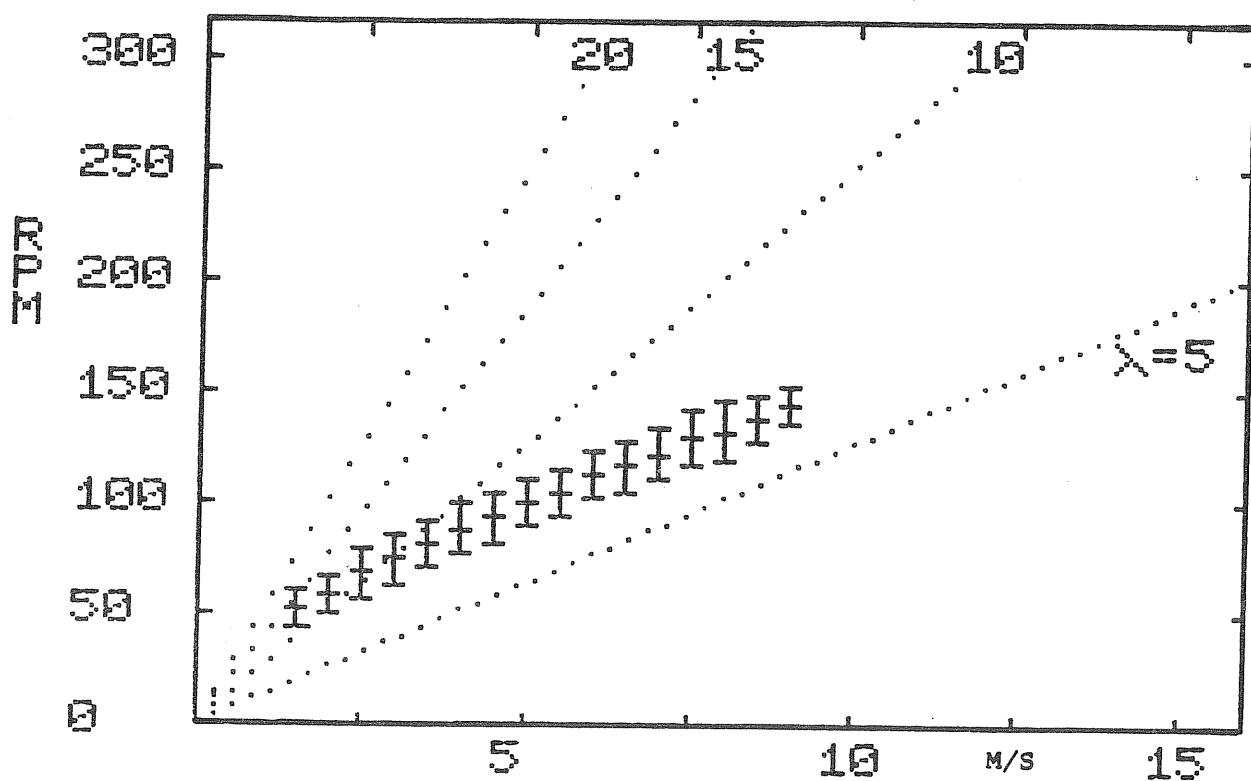
Figure 6-29b. POWER-ON RUN, RPM VS. WIND SPEED FOR 45 DEGREE FURL ANGLE

93
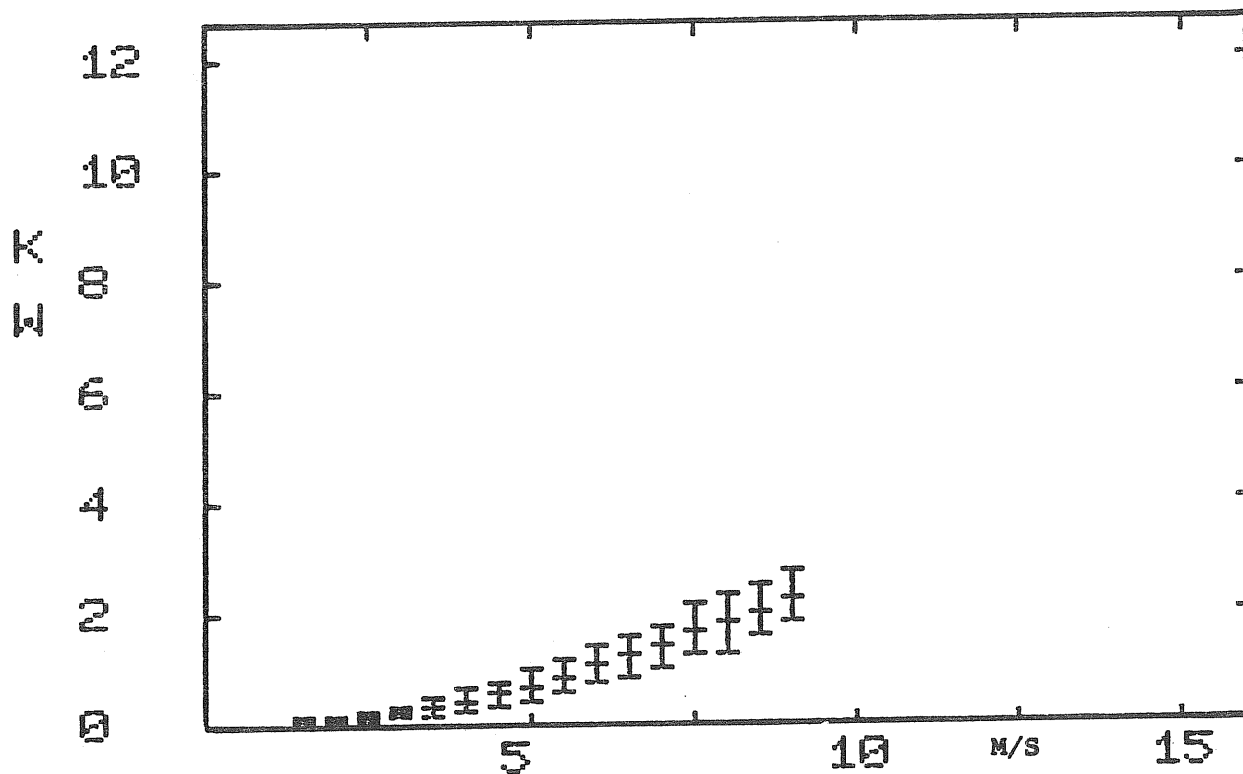
Figure 6-29c.   POWER-ON RUN, ROTOR POWER VS. WIND SPEED FOR 45 DEGREE FURL
ANGLE
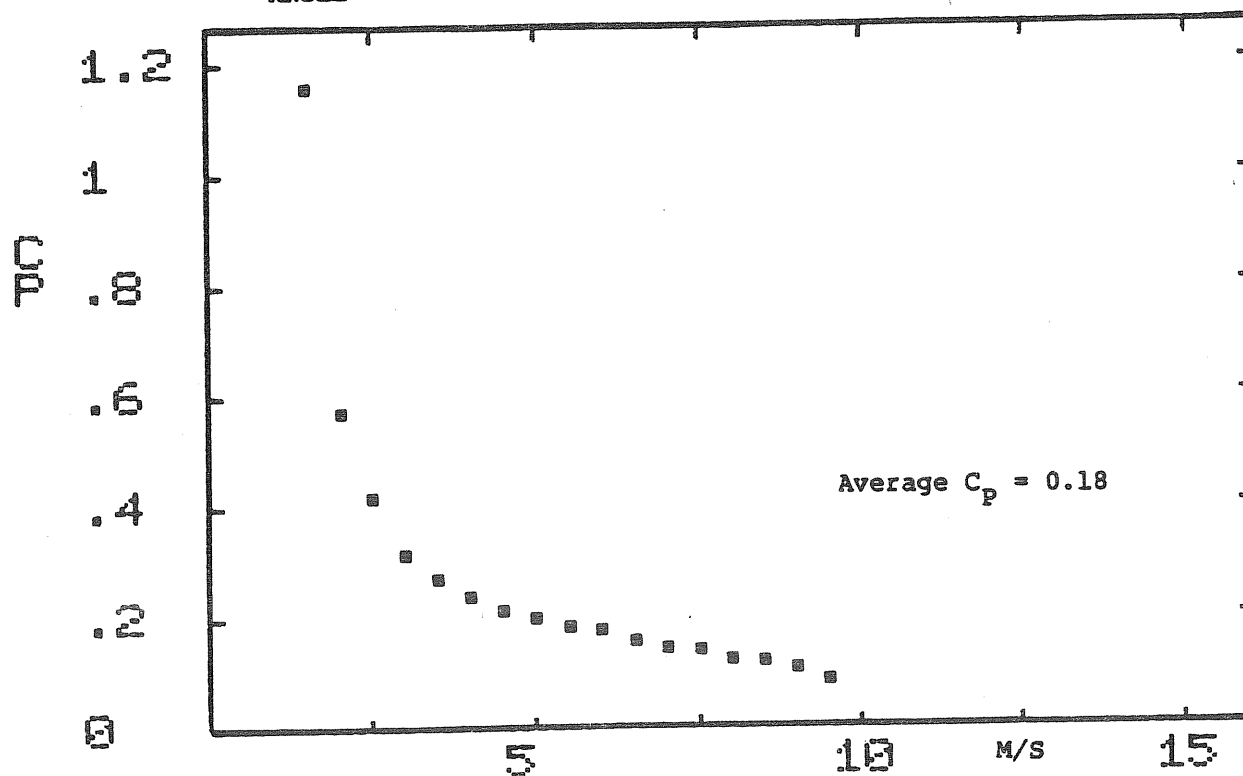
Figure 6-29d.   POWER-ON RUN, POWER COEFFICIENT VS. WIND SPEED FOR 45 DEGREE
FURL ANGLE

94

yaw rates in furl direction. Figure 6-30c and d refer to yaw rates in opposite direction. It is clearly seen that the cyclic pitch amplitude increases with yaw rate and is larger for the furl direction than for the unfurl direction.

Figures 6-31 show the results of the loads digital program for 30° furl angle. The results for 15° furl angle are almost the same and will not be presented. The fore-aft accelerometer data have been omitted since the acceleration amplitude did not exceed $\pm$ 0.1 g. Contrary to the loads from the oscillograph records, the bending moments in the digital programs are given in newton meters rather than in inch pounds. (8.85 in-lb = 1 N-m). The graphs represent volt vs. rotor rpm. The relation between the volt scale and the physical units is noted in the title of each graph. Figure 6-31a shows the sample distribution. The point to the farthest right represents only three samples and has been neglected. Figure 6-31b shows the mean flap-bending moment. The highest mean value is 4.1 x 355 = 1455 N-m. Assuming the aerodynamic center to be at 2/3 of the radius at 2.5 m, the rotor thrust is 2 X 1455/2.5 = 1164 N (260 lb), close to the rotor thrust of 1200 N from the yaw post bending shown in Fig. 6-28e at 9 m/sec wind velocity. Figure 6-31c gives the maximum mean value of the flap-bending amplitude of 276 N-m or 2440 in-lb. Figure 6-31d gives the maximum mean value of the in-plane bending amplitude of 204 N-m or 1745 in-lb. Figure 6-31e shows the vertical boom-bending amplitude which is equal to the yaw post bending amplitude at the upper yaw bearing. Its maximum occurs at the vertical boom 1P resonance, about 160 rpm and is 290 N-m or 2566 in-lb. These dynamic loads agree reasonably well with the values obtained from oscillograph records. They represent very low alternating stresses, see Table 63. Finally, Fig. 6-31f shows the cyclic pitch amplitude vs. rpm. Its mean of $\pm$ 5° at 50 rpm decreases to a mean of $\pm$ 3 at 200 rpm.

6.3.5 Loads Survey

Measured dynamic loads have been given throughout the presentations of atmospheric test results. Here these loads are summarized and discussed.

6.3.5.1 Steady States

More or less steady state conditions have been identified from the oscillograph records. For such conditions both rpm and wind speed did not change much over several seconds. From the records taken on September 9, 1980 four steady state points were selected at 125, 150, 162 and 171 rpm. The rotor was unfurled (15°). The generator to rotor gear ratio was 25:1. The second replacement generator was installed which had a different power-rpm relation than the first replacement generator used for most tests. The dynamic loads were not much affected by this difference.

Figure 6-32 shows moment amplitudes vs. rpm. The vertical boom bending moment was not plotted because it was almost equal to the yaw post bending moment. The in-plane blade bending moment was not plotted because it was almost independent of rpm and equal to about $\pm$ 1800 in-lb, see Fig. 6-31d. It orginated almost exclusively in the 1P gravitational blade moment. As mentioned before, the bending moments were not those at the location of the strain gages but rather at
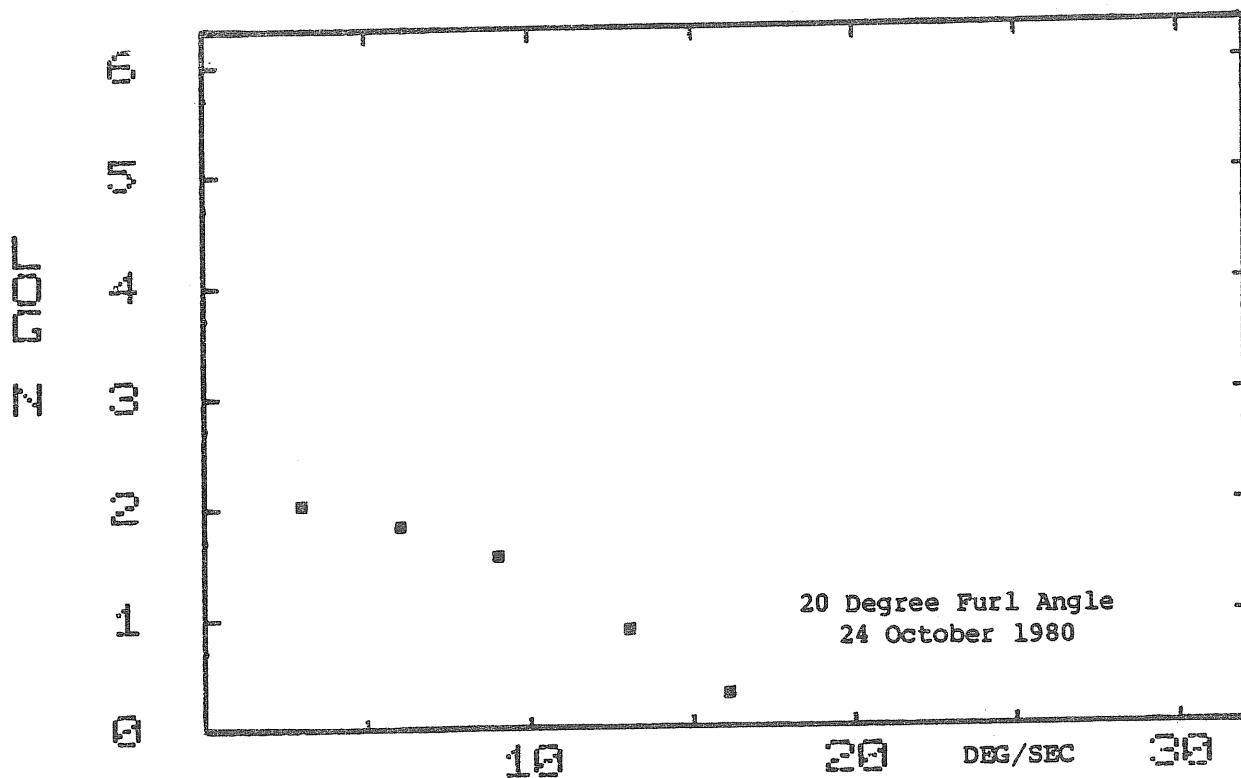
Figure 6-30al.   SAMPLE DISTRIBUTION, LOG (N) SAMPLES VS. YAW RATE; MOTION IN
FURL DIRECTION
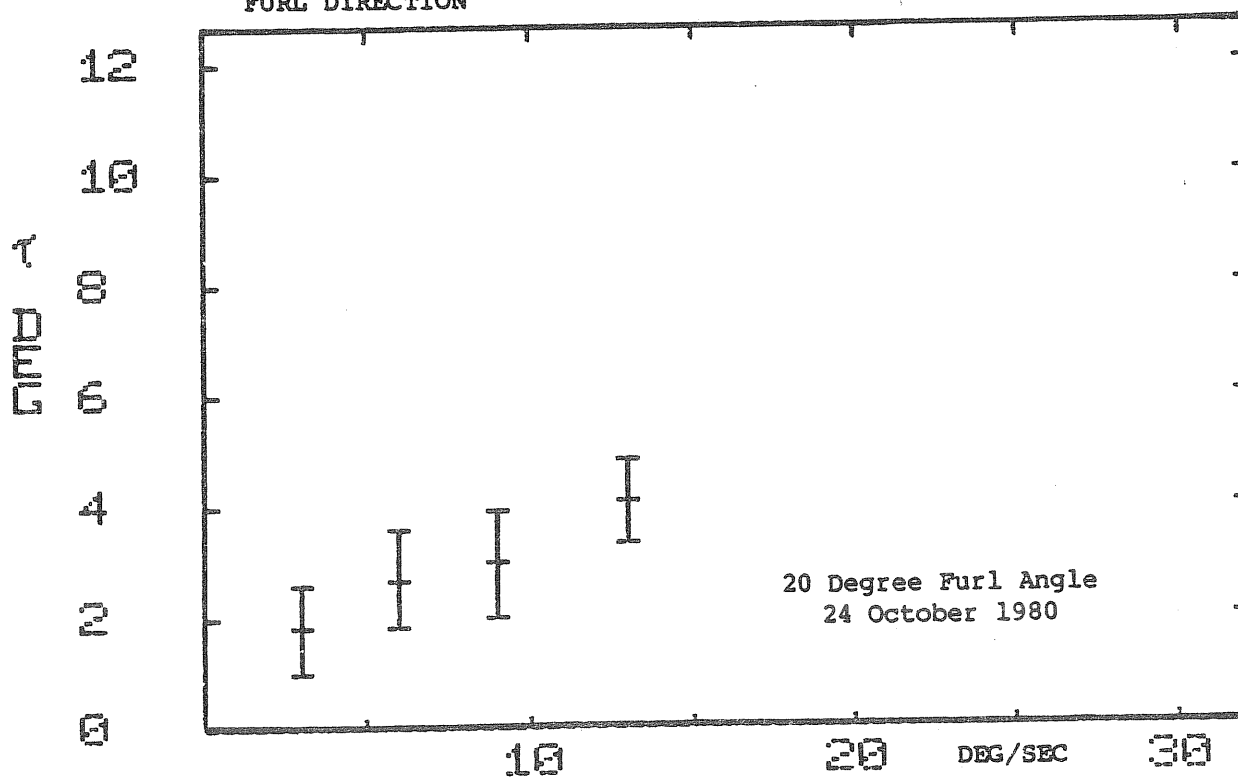
Figure 6-30a2.   CYCLIC PITCH AMPLITUDE VS. YAW RATE; MOTION IN FURL DIRE-
CTION
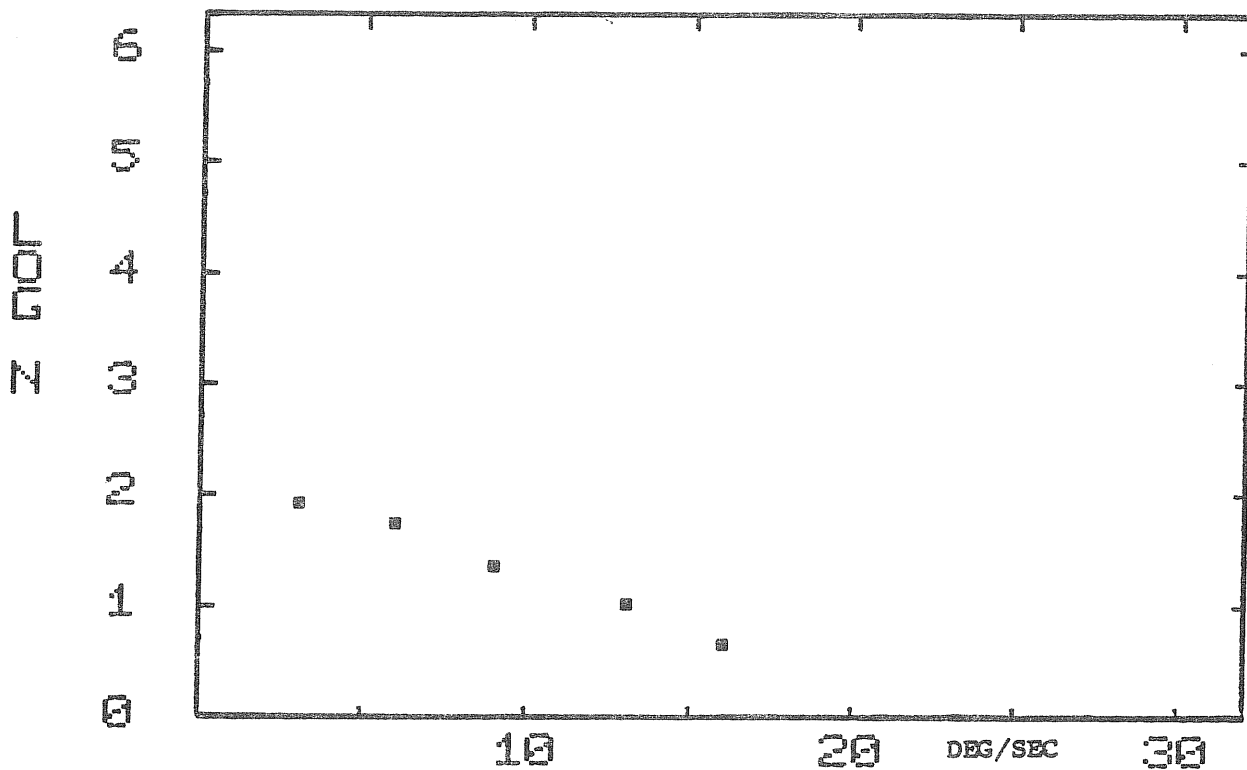
Figure 6-30bl.   SAMPLE DISTRIBUTION, LOG (N) SAMPLES VS. YAW RATE; MOTION IN UNFURL DIRECTION

20 Degree Furl Angle
24 October 1980
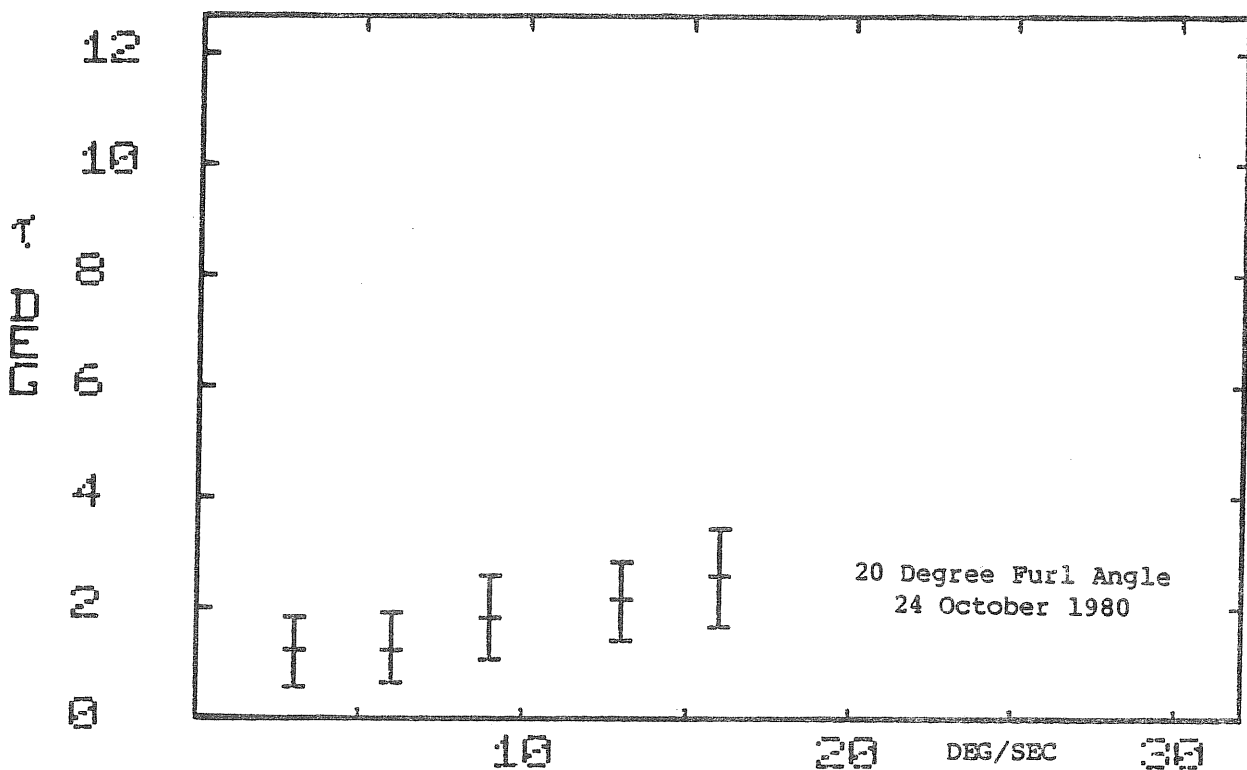
Figure 6-30b2.   CYCLIC PITCH AMPLITUDE VS. YAW RATE; MOTION IN UNFURL DIRECTION
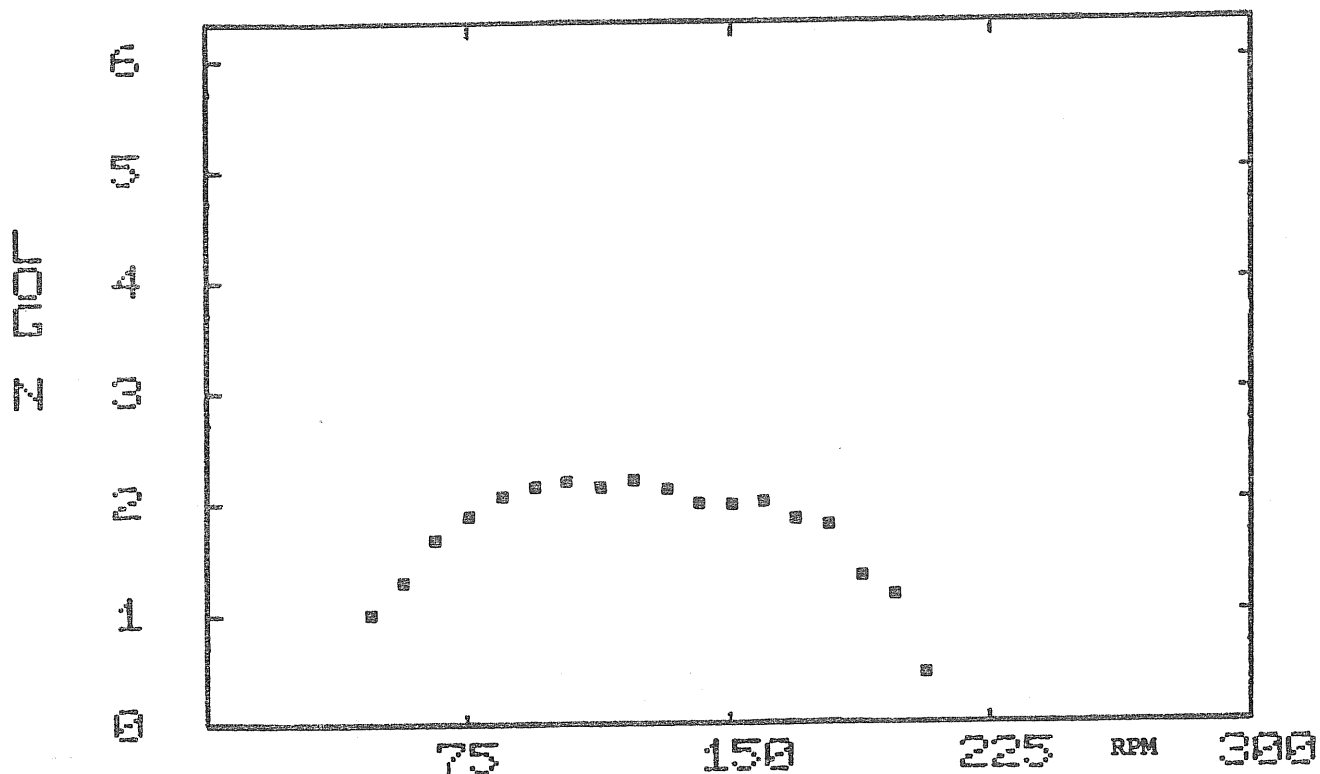
Figure 6-31a.   SAMPLE DISTRIBUTION, LOG (N) SAMPLES VS. RPM FOR 30 DEGREE
FURL ANGLE, 11 October 1980
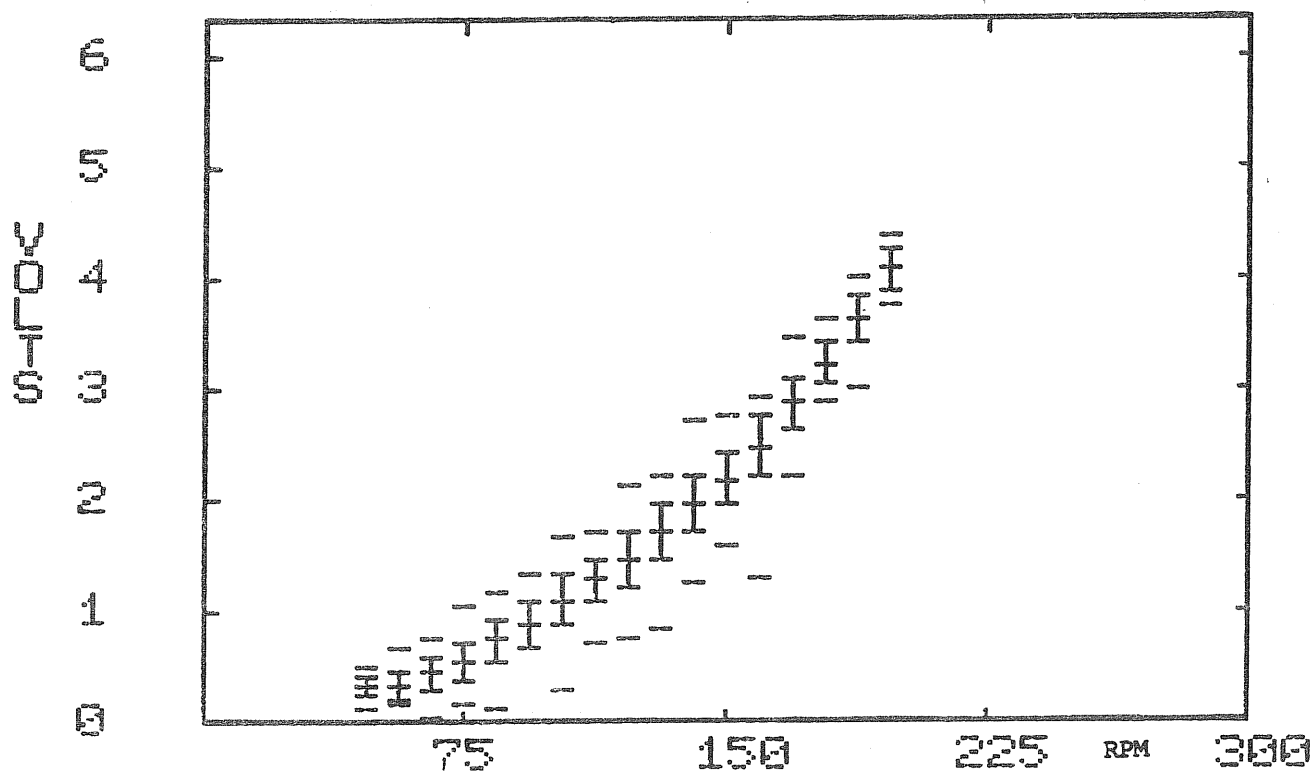
Figure 6-31b.   MEAN FLAP BENDING VS. RPM FOR 30 DEGREE FURL ANGLE,
1.0 Volt = 355 NM Flap Bending,   11 October 1980
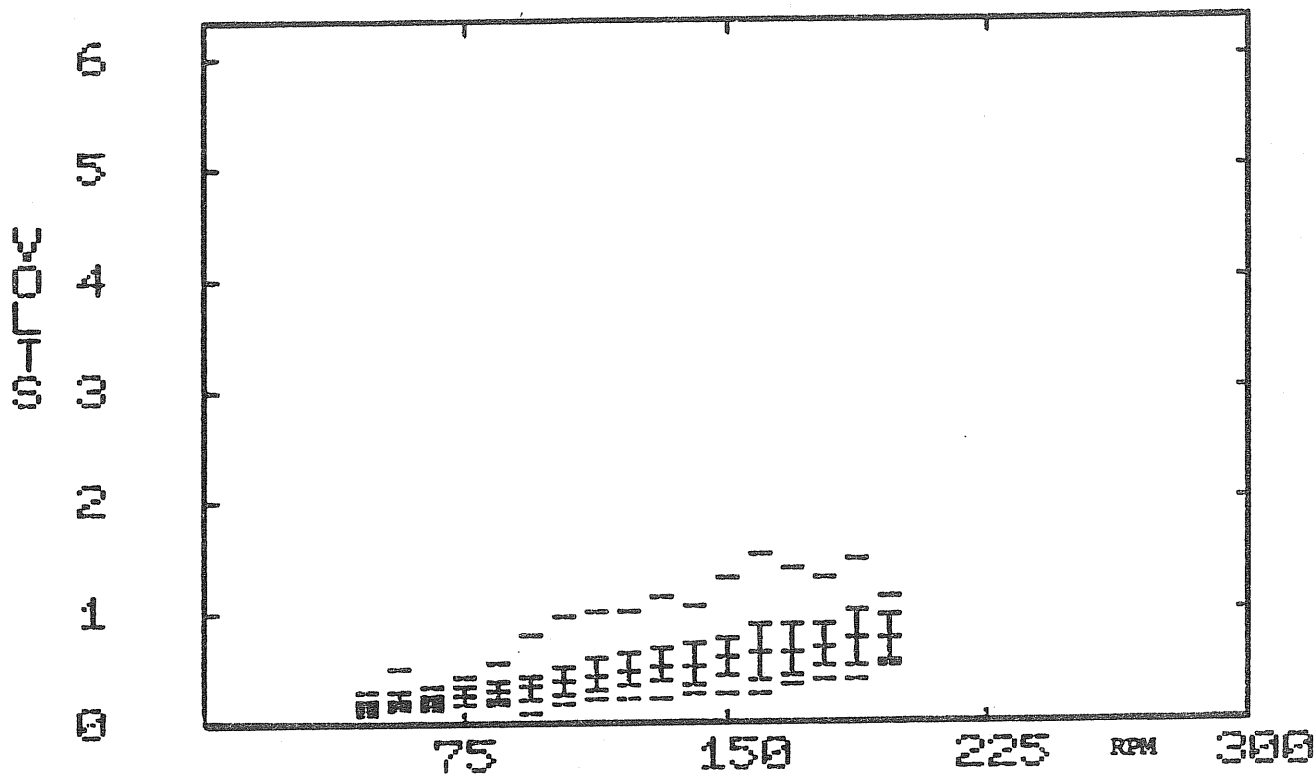
Figure 6-31c.   FLAP BENDING AMPLITUDE VS. RPM FOR 30 DEGREE FURL ANGLE,
1.0 Volt = 355 NM Flap Bending
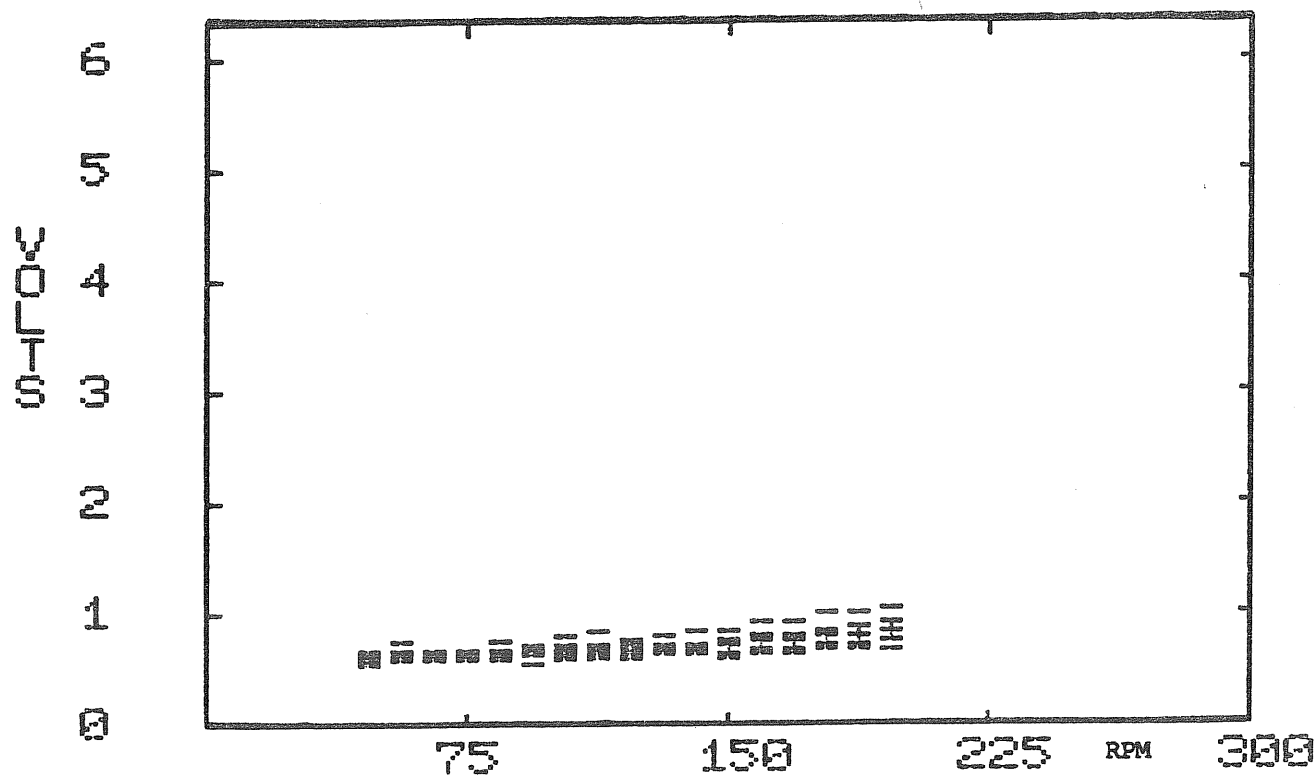
Figure 6-31d.   IN-PLANE BENDING AMPLITUDE VS. RPM FOR 30 DEGREE FURL ANGLE,
1.0 Volt = 245 NM In-Plane Bending

Figure 6-31e.   VERTICAL BOOM BENDING AMPLITUDE VS. RPM FOR 30 DEGREE FURL
ANGLE, 1.0 Volt = 290 NM Boom Bending

Figure 6-31f.   CYCLIC PITCH AMPLITUDE VS. RPM FOR 30 DEGREE FURL ANGLE,
1.0 Volt = 5.0 Degrees Cyclic Pitch Amplitude
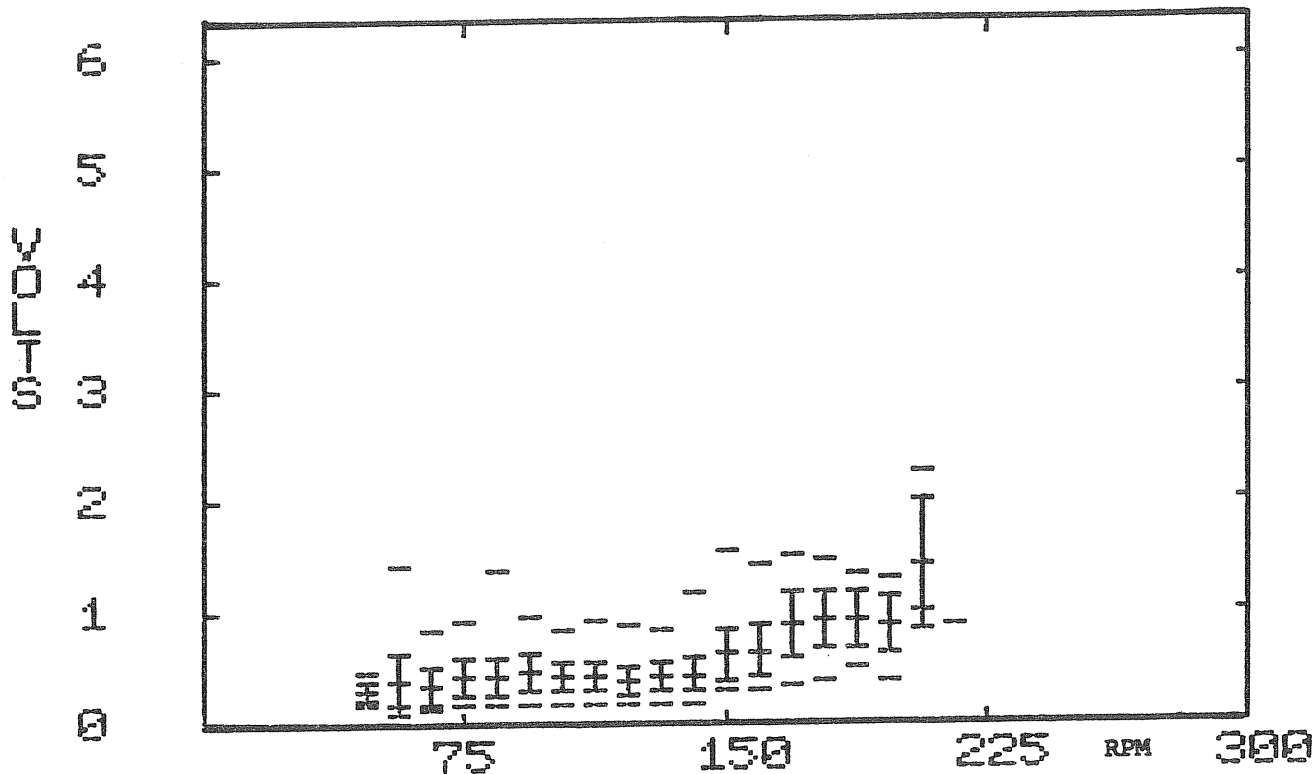
the natural reference locations. The yaw post bending moment is taken at the upper yaw bearing, the tail boom bending moment at its hinge, and the blade bending moment at the rotor center. Figure 6-32 indicates that between 125 and 171 rpm all moments peak at about 160 rpm which is the resonance rpm for vertical boom bending. Yaw post and vertical boom oscillate with 1P, and so does the in-plane blade moment not plotted in the figure. The flap-bending moment oscillates with 2P, and the horizontal boom bending moment and the shaft torque oscillate with 4P. This may indicate a coupled mode. The stresses at the strain gage locations are quite small. Using the values of Table 6-3 one obtains the maximum alternating stresses for steady conditions shown in Table 6-7.

Table 6-7. MAXIMUM LOADS FOR STEADY STATES UNFURLED (15$^{\text{o}}$)

| Component | Maximum Alternating Moment | | Maximum Steady Moment | | Yield |
	in-lb	psi	in-lb	psi	psi
Yaw post	2,700	1,100	15,000	6,150	75,000
Tail Boom	2,700	260	15,000	1,420	30,000
Blade Flap-Bending	1,900	150	20,000	1,540	30,000
Blade In-plane Bending	1,800	200	2,000	220	30,000
Rotor Shaft Torque	600	500	4,000	3,360	100,000

The maximum steady moments and stresses shown in Table 6-7 are based on the following assumptions. The maximum steady yaw post and boom moment originates in the gravity moment of the tail boom of 15,000 in-lb. The maximum blade flap-bending moment originates in the thrust. 200 lb thrust per blade acting at the 100 in station has been assumed without including centrifugal relief. The maximum steady in-plane moment originates in the torque per blade of 2000 in-lb, and the maximum steady rotor shaft torque is 4000 in-lb. The steady moments are merely rough estimates in order to see the alternating moments and stresses in perspective. Both steady and alternating stresses must be considered to determine fatigue margins. The yield limits in the last column are also approximate values. The rotor shaft is much more highly stressed from the torque arm of the shaft mounted gear box. As mentioned before, the alternating stress from this source is about $\pm$ 10,400 psi in addition to the steady 3360 psi from the torque. In view of the high strength material of the rotor shaft, the safety margin is quite high. The yaw post gravity moment is really not a steady load since it varies with furl angle so that it will occur with a certain number of load cycles.

6.3.5.2 Transients

Rather than selecting steady state conditions, we will present the maximum loads encountered for a given rpm. The effect of furl angle on the loads could only be determined at lower rotor rpm values. The high wind speeds required for sustained rated rpm at larger furl angles were not available. 30$^{\text{o}}$ furl angle
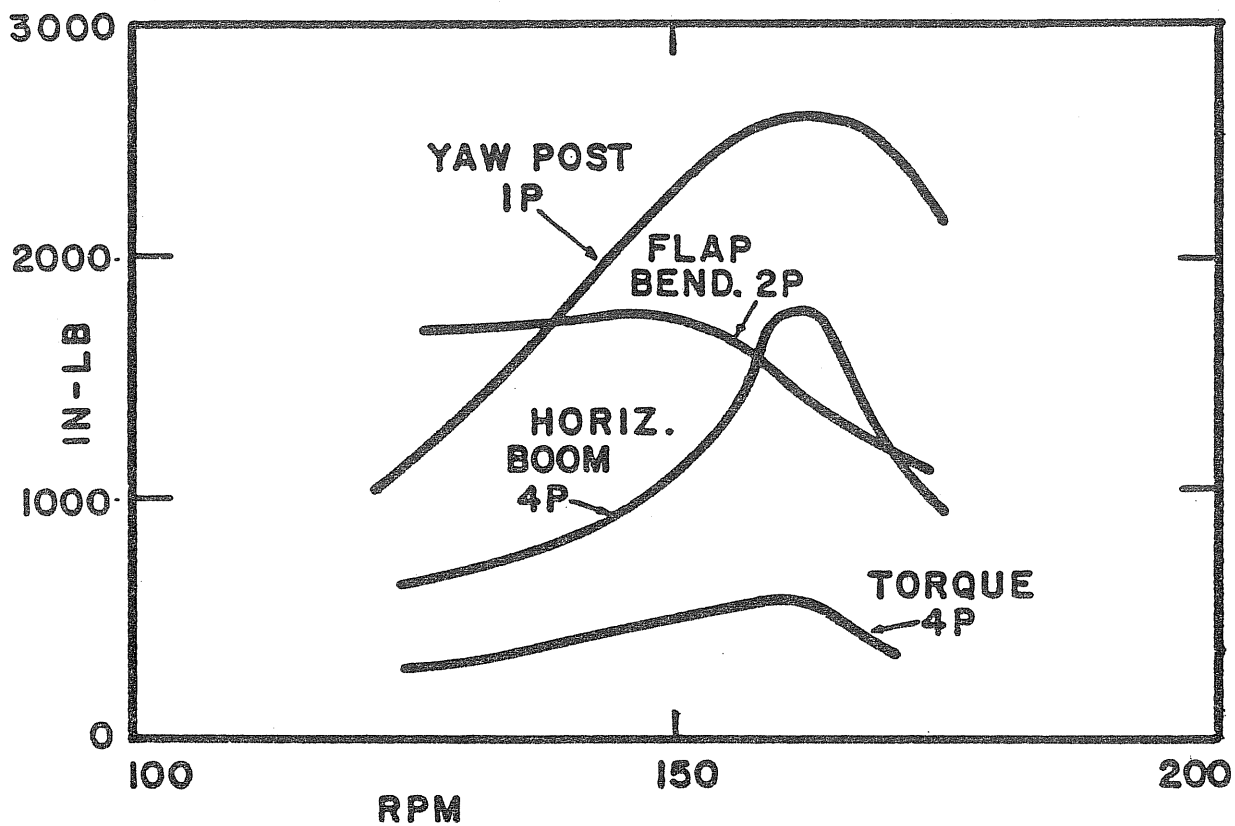
Figure 6-32.   DYNAMIC LOADS VS. ROTOR RPM FOR 15 DEGREE FURL ANGLE

was tested up to 200 rpm, and 45° furl angle up to 144 rpm. Table 6-8 gives a comparison of the maximum loads for four furl angles.

Table 6-8. EFFECT OF FURL ANGLE ON LOADS

Furl Angle	rpm	mph	Yaw Post ± in-lb	Flap-Bending ± in-lb	Torque ± in-lb	Power
15°	160	10	3500	1900	600	off
15°	160	21	2800	1900	670	on
15°	200	27	4100	2500	1170	on
30°	160	24	3500	2800	670	on
30°	200	24	3500	3100	1160	on
45°	144	22	3700	4400	670	on
80°	160	27	2800	3100		off

The in-plane bending moment remained at about ± 1800 in-lb independent of furl angle and rpm. The vertical boom bending moment was always nearly equal to the yaw post bending moment, while the horizontal boom bending moment was lower. The stresses for the maximum loads are shown in Table 6-9.

Table 6-9. MAXIMUM STRESSES

Component	Stress ± psi
Yaw post	1680
Tail Boom	390
Blade Flap Bending	340
Blade In-plane Bending	200
Rotor Shaft Torque	980

Though the stresses are in part substantially higher than for the steady states shown in Table 6-7, they should be well below the inifinite life fatigue limit.

6.3.5.3 Overspeed Conditions

Several overspeed conditions were encountered due to testing outside the normal operational envelope. Figure 6-18a shows one overspeed case where power-off operation in unfurled condition led to a 310 rpm overspeed in a strong gust. Only blade flap-bending and rotor torque were measured. They reached a maximum of ± 10,000 in-lb (2P) and ± 1660 in-lb (4P) respectively.

Another overspeed case up to 360 rpm, shown in Fig. 6-27, was caused by delayed furling in power-on operation. The only load measured during this overspeed was

the rotor torque amplitude which reached 3300 in-lb (4P) during furling. The torque amplitude was only 660 in-lb despite the high rpm prior to furling. Table 6-10 compares the known overspeed loads with the loads at 200 rpm.

Table 6-10. OVERSPEED LOADS

rpm	mph	Flap-Bending in-lb	psi	Torque in-lb	psi	Power
200	27	2,500(2P)	190	1,170(4P)	980	on
310	30	10,000(2P)	770	1,660(4P)	1,400	off
360	36			3,600(4P)	2,700	on

The large 2P flap-bending load is probably caused by the coning mode which has a 2P resonance at 280 rpm, see Fig. 5-9a. The large 4P torque may be caused by the symmetrical in-plane mode which, according to Fig. 5-9a, has a 4P resonance at 220 rpm, but which may be modified by coupling with a boom mode. Furling at all rotor speeds produces rather high 4P torque amplitudes. Even the highest overspeed stress amplitude of $\pm$ 2770 psi from torque is small compared to the rotor shaft bending stress of $\pm$ 10,400 psi caused by the torque arm of the shaft mounted speed reducer. One-half of the 3300 in-lb torque are in the blade root, causing a stress there of only 180 psi. Although the overspeed stresses during the furling are several times higher than the stresses at 200 rpm, they do not represent any structural risk.

6.4   IMPROVEMENTS FOR PROTOTYPE

Several atmospheric test equipment deficiencies have been observed which should be corrected in a prototype design. They are discussed individually in the following subsections.

6.4.1   Rotor Improvement

The rotor blade used for the test rotor was adopted from the Astral Wilcon Model 10B wind turbine. As Fig. 6-33 shows, it had a long shank section which produced drag but no torque. Also, the power output was reduced compared to the three-bladed Model 10 by using only two of the three blades, see Fig. 5-2 and 5-3. A two-bladed rotor was analyzed for the prototype that would compensate for this loss of power by using a slightly longer blade and by reducing the shank length. Figure 5-5 shows that the two-bladed prototype rotor would reach the same C_p value as the three-bladed Model 10 rotor, though at a higher tip speed ratio, thus requiring a smaller generator to rotor gear ratio. Figure 6-33 shows a comparison of the two-bladed planforms and the graphs for chord, twist and section thickness. An analysis similar to that performed for Fig. 6-7 shows that the prototype rotor has twice the starting torque of the test rotor. The increase in starting torque for the prototype rotor is due to the increased blade area close to the rotor center. While the atmospheric tests showed that a gust up to about 14 mph is needed to overcome the negative hump in Fig. 6-7, the

104
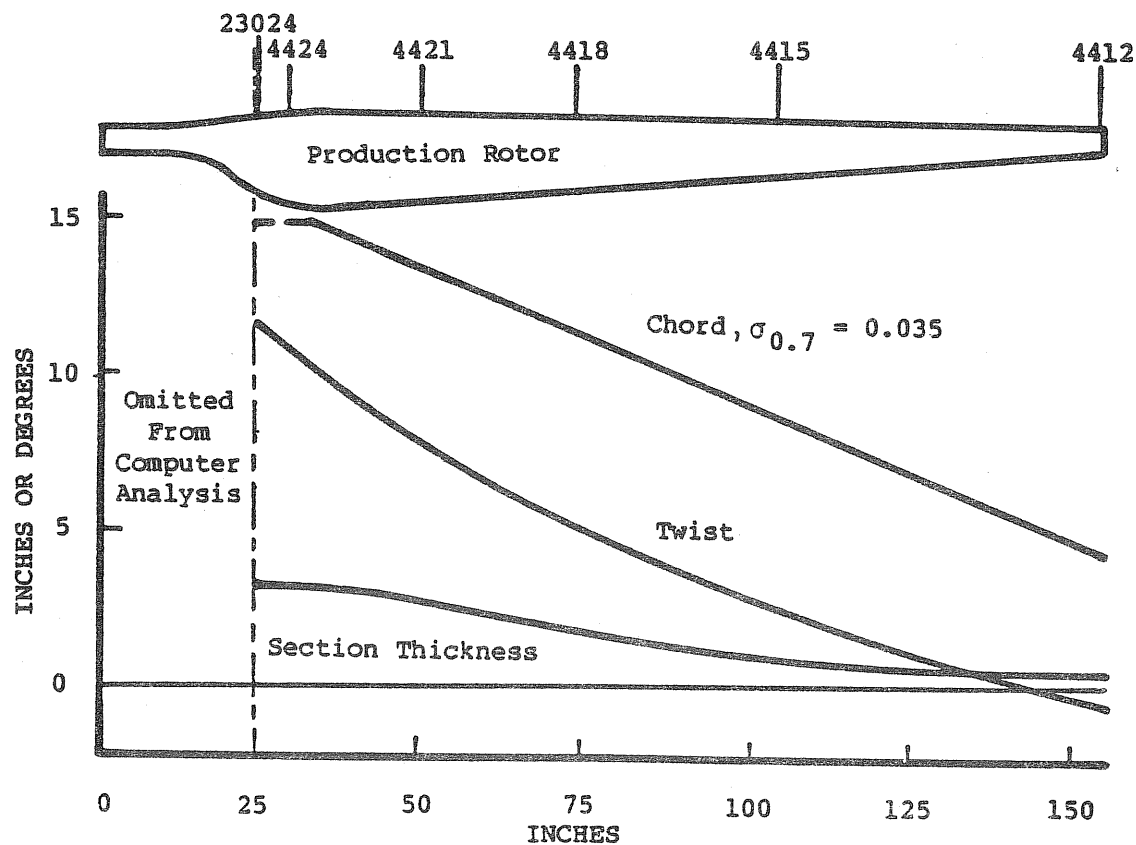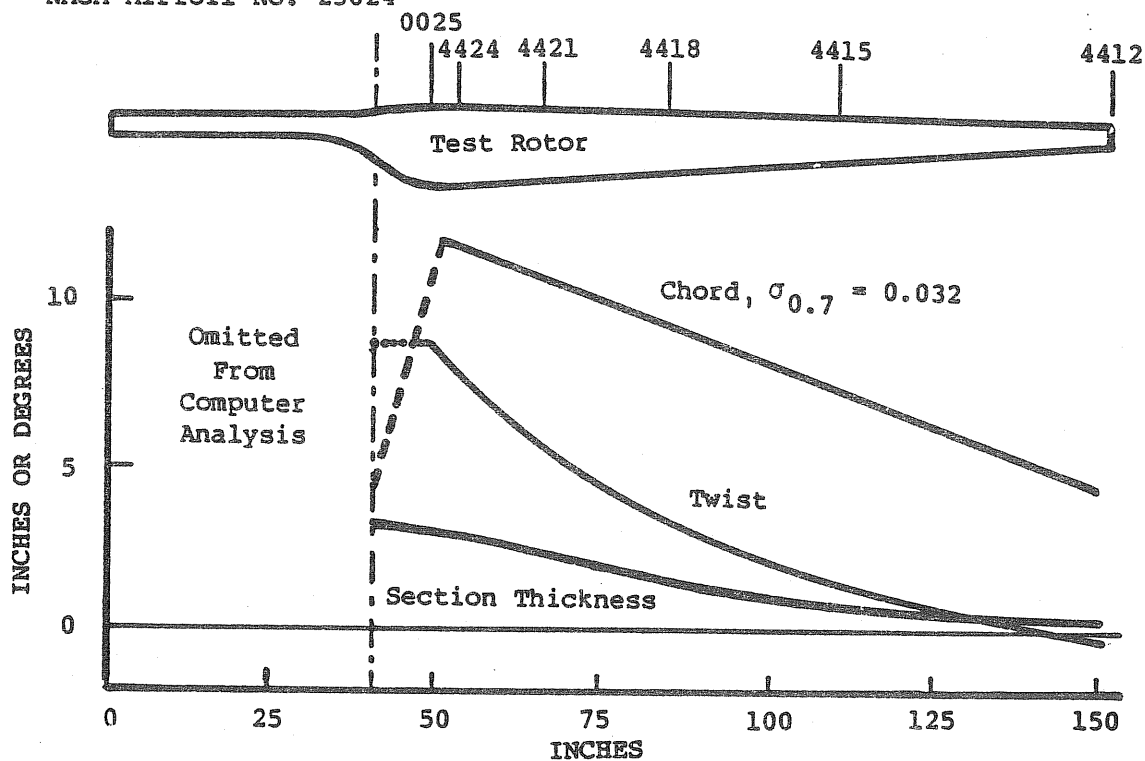
Figure 6-33.   TEST ROTOR AND PRODUCTION ROTOR BLADE

production rotor should require a gust of only 10 mph to overcome the negative hump during self-starting. The blade retention would be greatly shortened and simplified. The cast aluminum clamps would be eliminated and the rectangular blade shank would be bolted directly to the blade retention channels. The blade surface would also be greatly improved by using a metal mold rather than the reinforced epoxy mold in which the present blades were formed. One could therefore expect a greater performance increment than that indicated by the analysis in Fig. 5-4 and 5-5.

6.4.2 Generator Improvement

As Fig. 6-28d shows, the generator efficiency drops off rapidly with lower wind and rotor speed. The tuning circuit may cause this drop. A different tuning circuit could possibly be fitted to the alternator that would optimize the yearly energy output rather than maximize the peak power. Another possibility is to automatically disconnect the tuning circuit for the lower rpm values. As seen in Fig. 6-20b3, a sizeable rotor power was measured when the load resistance and the field were disconnected. The cause for this high mechanical loss should be determined. If it is the timing belt tension increase with rpm, a design with a direct drive alternator through a speed reducer with higher gear ratio would decrease the mechanical loss. This is probably a very desirable improvement anyway. We encountered cases of timing belt slippage. They were eliminated by increasing the belt tension. The need for adjustments at frequent time intervals are unacceptable in a prototype. Also, the belt would be destroyed by extended periods of slippage. It could well be that the concept of rewinding an automotive alternator to increase the output voltage and power by several hundred percent was not very sound. At the very least, the concept requires extended bench tests to optimize the configuration and to establish an acceptable time between overhaul. This was not done with the alternator used for the tests and is beyond the scope of this subcontract.

6.4.3 Tail Boom Improvement

The fiberglass reinforced plastic tail surface was bolted on to the aluminum boom. Some damage was experienced at the tail surface connection. For a prototype it probably would be cost-effective to produce both tail surface and boom from glass fiber material using a common mold. This would lighten the tail boom assembly and would provide an opportunity to shift the first natural boom frequency out of the operational rotor speed regime. Although the present vertical boom resonance at 160 rpm is not severe, it does produce relatively high stresses in the yaw post. The tail boom bearing support is rather soft and is probably responsible for the difference of the computed tail boom frequency of 280 cpm vs. the actual frequency of the 160 cpm. The tail boom bearings are custom-made Rulon flange bearings. They are very expensive and should be replaced by bronze or wood bearings in a prototype. Even Timken roller bearings would be less costly and would have much less friction. However, since the boom will assume the same position over long periods, pitting may occur in roller bearings.

6.4.4 Carrier Beam Improvement

The I-beam supplied with the machine was too soft in torsion and had to be boxed in. In a prototype, a box beam should be used instead of the I-beam. The yaw post is presently connected to only the lower flange of the I-beam. When a box beam is used, the yaw post could be connected to both the lower and upper wall, thereby stiffening the structure and probably raising the tail boom natural frequency.

6.4.5 Furl Control System Improvement

The present furl control system is adopted from the Astral Wilcon Model 10 where it serves as an emergency system in case of failure of the automatic feathering control. The Saginaw Power Pak electric actuator allows only constant speed operation, and it starts and stops with a substantial jerk, while in operation. Thus, the actuator is not suitable for an automatic control system. Instead, the development and testing of a hydraulic furl control system using a constant speed hydraulic propeller governor is recommended.

6.5 UPGRADING OF MACHINE SIZE

The contract for this work required an extension of the analytical studies to the power output, yaw characteristics and loads of a NASA MOD-0A sized machine.

6.5.1 Power Output of Upscaled Machine

The MOD-0A has a two-bladed rotor with a diameter of 125 ft (38 m). The blade solidity measured at 0.7R is 0.027, somewhat less than the 0.032 solidity of the test rotor. The 3:1 taper ratio is the same for both rotors. The blade twist between the tip and the 0.33R station is somewhat higher for the MOD-0A rotor, 12° vs. 9° twist for the test rotor. Overall, the geometries of the MOD-0A blade and the test rotor blade are nearly identical. The power output at a given wind speed should increase with the square of the linear dimension, which is 25 times. The rated power output of the test machine is 8 kW, compared to 200 kW for the MOD-0A. The ratio is 400/8 = 25. The tip speed ratio for the MOD-0A at 20 mph is 8.9 (40 rpm), the same as the test rotor with power-on. Scaling up the test rotor to the MOD-0A size should result in a machine that has approximately the performance of the MOD-0A. Differences will arise from the fact that the test rotor operates with variable rpm near the optimum C_p value, while the MOD-0A operates with constant rpm and encounters the optimum C_p value only at a specific wind speed. At other wind speeds the C_p value is lower. The same degradation of performance would occur if the test rotor were to operate at constant rotor speed, although one might suspect a loss of performance from the cyclic pitch variation. the tests have shown that no measurable loss of rotor power occurs during rapid yaw rates from wind following. One can argue to the contrary that the test rotor, when scaled up to the MOD-0A size, would avoid the loss of performance from yawed flow inherent in this machine because of the slow yaw rate of the yaw gear drive. The scaled up test rotor would respond much

faster to wind direction changes than the MOD-OA. The improvement in performance from this effect may be substantial, particularly at moderate wind speeds where wind direction changes can be large and fast.

6.5.2 Upscaling of Yaw Characteristics

The question is, how will a scaled up machine react to wind direction changes? In particular, we want to know how the cyclic pitch amplitude will change when a scaled up machine is exposed to the same wind direction change. A simple way to treat this question is to assume that the machine is exposed to an instantaneous wind direction change and to compute the yaw response and the cyclic pitch response.

The equation of yawing motion is

$$\ddot{\alpha} + \dot{\alpha}_V M_{\dot{\alpha}}/I + \alpha_V M_\alpha/I = U(t) M/I \qquad (6-5)$$

Using only the tail vane for the aerodynamic yawing moments – the rotor can be ignored because of the passive cyclic pitch mechanism – one obtains

$$M_\alpha = C_{L\alpha} qA_V h \qquad M_{\dot{\alpha}} = M_\alpha h/V \qquad (6-6)$$

The undamped natural frequency is

$$\omega = (C_{L\alpha} = qA_V h/I)^{1/2}$$

The damping ratio is

$$\zeta = \omega h/2V \qquad (6-8)$$

The damped natural frequency is

$$\omega_n = \omega(1 - \zeta^2)^{1/2} \qquad (6-9)$$

Assuming geometric similarity and assuming that masses increase with the cube of the length dimension, these equations lead to the following conclusions:

- The natural frequency increases in proportion to wind speed.

- The natural frequency is inversely proportional to the length dimension.

- The damping ratio is independent of scale.

- The damping ratio is independent of wind velocity.

- The damping ratio increases with $h(hA_V/I)^{1/2}$ and, for given geometry a light tail boom gives a high damping ratio.

108

For the test machine we have:

A_V = 12.5 ft^2, $C_{L\alpha}$ = 3.0, I = 370 slug ft^2
h^V = 15.5 ft; a wake factor 0.7 is assumed to obtain the lift slope.
For V = 21 mph (9.4 m/s) at standard sea level density (ρ = 0.00238 slugs/ft^3) one obtains:

$$\omega_n = 1.31 \text{ rad/sec} \quad \zeta = 0.33 \quad\quad\quad\quad (6\text{-}10)$$

The response to a unit step input wind direction change is shown in Fig. 6-34. The new wind direction is reached after 1.5 sec, and there is a 30% overshoot. After 4 sec the machine is practically aligned with the new wind direction. The maximum yaw rate is 0.6 α_{Vo} rad/sec, where α_{Vo} is the angle of instantaneous wind direction change.

If scaled according to our assumptions, the MOD-OA size machine would have the same yaw response but with the 5:1 expanded time scale indicated in Fig. 6-34.

In large machine design much effort is put into saving weight. Rotorcraft experience has shown that the cube law for mass does not really hold true. For many rotorcraft it was found that blade masses increase with the 2.5 power of the length dimension rather than the cube of the length dimension. This law also seems to hold for wind turbines. If test machine blade weight of 32 lb is scaled with the cube law, one obtains a MOD-OA size blade weight of machine 125 X 32 = 4000 lb; scaled with the 2.5 power, one obtains 56 X 82 = 1792 lb. The actual MOD-OA blade weighs about 2000 lb, much closer to the 2.5 power than to the cube scaling law. If the 2.5 power law were used for the masses, the time scale in Fig. 6-34 for the MOD-OA size machine would be reduced by about 2/3. The damping ratio, because of the higher ω, would increase, and less overshoot would result.

For the rotor, assuming the cube law for masses, natural frequencies are inversely proportional to the length dimension, and damping ratios are independent of scale. Thus, the rotor scaling laws match those for the tail vane. A given step change in wind direction at the same wind speed will lead to the same cyclic pitch amplitude, no matter what the scale. If the 2.5 power law for the masses applied to both tail boom and rotor blades, the scaling laws are still matched, but a higher damping ratio will result for the rotor modes.

The scaled up machine will absorb high frequency wind direction changes and will respond only to the lower frequency changes due to the longer time scale resulting in a longer response time. The power spectral density of the yawing motion is equal to the wind direction multiplied by the absolute value of the machine transfer function. For scaled up machines the transfer function is shifted to lower frequencies and cuts out the response to the higher frequencies of the wind direction spectrum. Since the yaw rates are slowed down for the scaled up machine, the cyclic pitch response for these slower rates should be about the same as for the test rotor, see Fig. 6-30. This figure should apply to a MOD-OA size machine if the yaw rate scale is divided by five.
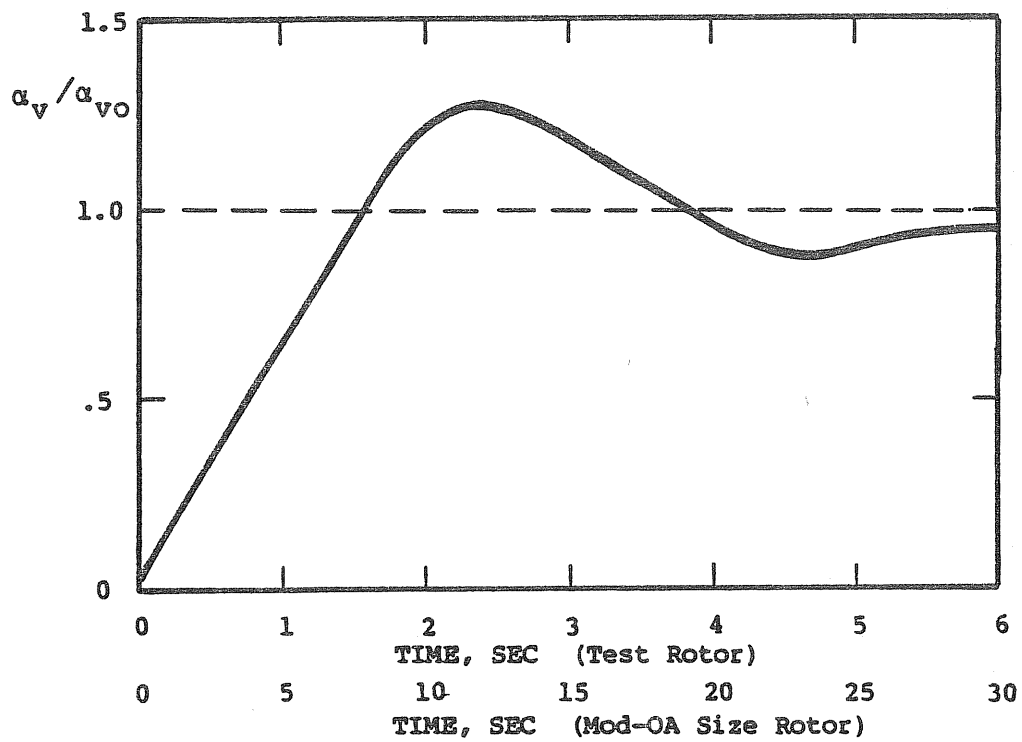
Figure 6-34.   YAW RESPONSE TO STEP WIND DIRECTION CHANGE AT 9.5 METERS/SEC
                WIND SPEED

6.5.3 Loads for Upscaled Machine

The rotor scaling laws with respect to stresses and deflections are treated in Ref. 13. If the cube law for the masses applies, all stresses from steady aerodynamic loads remain unchanged in the scaled up machine. The same is true for self-generated dynamic loads, resulting, for example, from yawing in a steady wind or from the vertical wind velocity gradient. Blade centrifugal stresses and centrifugal relief of bending stresses also remain the same. Stresses from gyroscopic effects are unchanged since the yaw rates are reduced in proportion to the inverse length dimension. Turbulence generated stresses will be different for the scaled up machine, since the machine responds to a different part of the turbulence spectrum. The turbulence related stresses are, however, small compared to the self-generated stresses and are usually neglected in a structural analysis, see Ref. 14.

Under the assumption of the cube law for the masses, the self-generated dynamic stresses remain unchanged by scale up. This is not true of gravitational stresses. The gravitational forces increase with the cube, while the aerodynamic, centrifugal and gyroscopic forces increase with the square of the linear dimension. Thus, gravitation causes stresses that increase in proportion to the linear dimension. The gravitational alternating dynamic blade stresses in a horizontal axis wind turbine become more and more dominant with increasing size. While the system under study here shares this feature with all other horizontal axis wind turbines, the tail boom and yaw post are also components subjected to increased gravitational stress with increased size. In rotor blade design the designer fights increasing gravitational blade stresses by making the blades lighter and by using materials and shapes that allow higher fatigue stresses. The gravitational stresses for blades are alternating, but are steady for the tail boom and yaw post. Therefore it should be an easier task to accommodate the increasing gravitational stresses in tail boom and yaw post than it is for the blades. The length dimensions for blades and tail boom are about the same. The design method for accommodating increasing gravitational stresses in the tail boom and yaw post is the same as for blades, namely, save weight, use higher strength materials, and use shapes that reduce the gravitational stresses. This is evidently easier for the tail boom than for a blade, since there are no aerodynamic restraints in selecting the cross section.

In scaling up the furl control system one must insure that the servo power does not increase more than the square of the linear dimension in order to keep the loss in relation to the rotor power output approximately the same. The yawing moment should not increase with more than the cube of the linear dimension. This criterion is satisfied for the yaw inertia moment I, since I increases with a^5, $\ddot{\alpha}$ with a^{-2}, a being a reference linear dimension. However, this criterion is not satisfied for the boom bearing friction moment that is proportional to the gravitational boom moment increasing with a^4. One must, therefore, use a design for the boom bearings that relieves the boom bearing friction, for example by increasing the vertical spacing between the two bearings. Also, the boom should be lightened as much as possible, whereby the 2.5 power law for its weight represents an achievable goal.

111

In summary, one encounters the same problems as for every other horizontal axis wind turbine when scaling up the size of the test machine. Scaling up the tail boom is easier than scaling up a blade. The simplicity of the rotor hub and the absence of gravity moment carrying bearings should make scale up easier than for conventional designs. In the test rotor, gravity bending moments remain inside the common blade retention beam, while in a MOD-OA type rotor, the gravity moments must be transmitted via the feathering bearings to the hub. From the point of view of loads and structural integrity, scale up of the test machine presents less severe problems than that of conventional machines with feathering control.

7.1 PERFORMANCE

Due to the hub moment free rotor with passive cyclic pitch variation, the test machine adapts rapidly to wind direction changes and develops yaw rates up to about 15°/sec. No reduction in power from rapid yawing was observed despite yaw rate-produced cyclic pitch amplitudes up to $\pm 5^{\circ}$. When relating total rotor energy output to total wind energy flow through the disk, average power coefficients C_P of over 0.4 were measured during a test run of 30 to 60 minutes in duration. Total wind energy flow was based on data from an anemometer located 13.4 m above the ground and 5.5 m below the rotor center. Performance of the test rotor was good and may be superior to conventional rotors of equal size.

7.2 YAW CHARACTERISTICS

Yaw rates from wind direction following or from the operation of the furl actuator produce cyclic pitch amplitudes in proportion to the yaw rate, thereby preventing gyroscopic moments from being transferred to the hub. When operating the machine power-on with 45° furl angle (causing about 45° yaw angle), the average C_P value during a 110 minute test run was reduced from 0.46 to 0.18. Thus, at 45° yaw angle the wind speed can be increased by a factor of $(0.46/0.18)^{1/3} = 1.35$ over rated wind speed without exceeding rated power. Rated rotor power of 10 kW is reached at about 21 mph wind speed. Operating with 45° yaw angle allows 10 kW to be produced at 28 mph. Higher yaw angles could not be tested power-on because of the absence of average winds over 28 mph. Thus, it is not known what the cut-off yaw angle and wind speed will be. Yaw angles up to 80° were tested power-off and resulted in a tip speed ratio of about 5.0. This corresponds to power-off operation at rated rotor speed of 230 rpm at 40 mph wind speed. For higher wind speeds yaw angles greater than 80° are required. One can conclude that the yaw characteristics explored so far insure rated power operation up to at least 28 mph (12.5 m/sec) and power-off operation to at least 40 mph (18 m/sec).

7.3 LOADS

Loads have been measured power-on at 15°, 30°, 45° yaw angle and power-off up to 80° yaw angle. It is expected that an expansion of the operational envelope beyond these values would be possible if higher wind speeds above 28 mph were available. Dynamic bending moments in the vertical direction of the tail boom and in the yaw post were found to be approximately equal and caused by vertical tail boom oscillations peaking at the tail boom resonance of 160 rpm. Blade dynamic in-plane bending moments are gravity produced and are almost independent of rpm and yaw angle. Blade dynamic flap-bending moments peak at 160 rpm and increase with yaw angle. Dynamic rotor shaft torque is normally insignificant except during furl operation. Linear acceleration at the rotor main bearing block is below ± 0.15 g. All dynamic stresses are well within fatigue limits.

One can conclude that the dynamic loads and vibrations in the test machine are far below the allowable level despite the two-bladed rotor which often caused unacceptable loads and vibrations in conventional designs.

7.4 STARTING

The test machine can be started at 5 mph (2.2 m/sec) wind speed with the help of the tach generator/starter motor. The rotor keeps turning at this wind speed with the generator load resistance of 6 ohm connected. The rotor self-starts at an average wind speed of 9 mph if an occasional gust to 14 mph is available to overcome the minimum driving torque at about 20 rpm. A gust of 14 mph for self-starting is required because the inner third of the rotor radius has no airfoil section. It is a box with a 6 in square cross section. This design was selected in order to use the Astral Wilcon Model 10B blades. In a prototype design with a blade airfoil extended close to the rotor hub, the starting torque should be doubled according to the analysis. Self-starting should then require only a 10 mph (4.5 m/sec) gust. With a new blade design, starting characteristics of the prototype rotor will be good and motored starting will not be required.

7.5 RECOMMENDED FURTHER WORK

The analytical and test work to date has shown the concept under study to be viable. It has the potential for cost effective wind energy conversion and a continuation of the work is recommended. Future work would require a hydraulic furl actuator to replace the electrical actuator since the latter is unsuitable for continuous furl control. The hydraulic actuator would receive oil pressure from a Woodward constant speed hydraulic propeller governor. A spring would be added to move the tail boom in the direction opposite to that of the oil pressure. When checking out the automatic furl control on the test machine, hopefully during the high wind months of March and April, 1981, there will be an opportunity to widen the operational envelope and establish the cut-off wind speed and yaw angle beyond which the rotor would be operated in the power-off condition, probably rpm controlled by the constant speed hydraulic governor.

SECTION 8.0

REFERENCES

1. Hohenemser, K. H., Some Alternative Dynamic Design Configurations for Large Horizontal Axis WECS. Wind Turbine Structural Dynamics, a workshop held at Lewis Research Center, November 15-17, 1977; DOE CONF-771148.

2. Hohenemser, K. H., Aerodynamic Aspects of the Unloaded Rotor Convertible Helicopter. Journal of American Helicopter Society; Vol. 2, No. 1; January 1957; pp 47-54.

3. Marks, M. D., Flight Test Development of XV-1 Convertiplane. Journal of American Helicopter Society; Vol. 2, No. 1; January 1957; pp 55-65.

4. Wheatley, J. B., and Bioletti, C., Wind Tunnel Tests of 10 Foot Diameter Autogiro Rotors. NACA Report No. 552; October 1935.

5. Glasgow, J. C. and Miller, D. R., Teetered, Tip Controlled Rotor: Preliminary Test Results from MOD-0 100-kW Experimental Wind Turbine. AIAA/SERI Wind Energy Conference; April 9-11, 1980; Boulder, CO; pp 261-268.

6. Wilson, R. E., and Lissaman, P. B. S., Applied Aerodynamics of Wind Power Machines. Oregon State University; May 1974.

7. Abbott, I. A., and von Doenhoff, H. E. Theory of Wing Sections. Dover Publications, Inc.; New York; 1959.

8. Gessow, A. and Tapscott, R. J. Tables and Charts for Estimating Stall Effects on Lifting Rotor Characteristics. NASA TN D-243; May 1960.

9. Norton, John H. Jr., The Development and Testing of a Variable Axis Rotor Control System with 5 Meter Rotor and Direct Drive Alternator. Proceedings of Small Wind Turbine Systems' 1979 Workshop coordinated by Rockwell International; Boulder, CO; February/March 1979; Vol. 1; pp 31-64.

10. Stoddard, F., Perkins, F. and Cromack, D., Wind Tunnel Tests for Fixed Pitch Start-up and Yaw Characteristics. Technical Report UM-WT-TR-78-1, NASA Lewis; June 1978.

11. Ko, T.W.H., Use of Tapered, Twisted Finite Elements for Dynamic Analysis of Helicopter Rotor Blades. Master Thesis prepared under the direction of Professor D. A. Peters, Washington University, Sever Institute of Technology; May 1980.

12. Kirchhoff, R. H., Measurements of the Wind Field Interaction with the UMASS 25 kW Wind Turbine. Proceedings of Small Wind Turbine System 1979 Workshop coordinated by Rockwell International; Boulder, CO; February/ March 1979; Vol. 1; pp 179-188.

REFERENCES
(continued)

13. Ormiston, R. A., <u>Dynamic Response of Wind Turbine Rotor Systems</u>.   31st
    Annual National Forum, American Helicopter Society; Washington, D.C.; May
    1975; Preprint S-993.

14. Spera, D. A., <u>Comparison of Computer Codes for Calculating Dynamic Loads in
    Wind Turbines</u>.   Wind Turbine Structural Dynamics Workshop held at Lewis
    Research Center; November 15-17, 1977; DOE CONF-77 1148.

APPENDIX A

PERFORMANCE ANALYSIS FOR ZERO YAW ANGLE

by

Andrew H. P. Swift

APPENDIX A

PERFORMANCE ANALYSIS FOR ZERO YAW ANGLE

A zero yaw angle, steady state performance program was developed based on algorithms derived in work completed by Wilson and Lissaman (Ref. 6). The program is written in Fortran IV and was run on a DEC System 20 computer at Washington University Center for Computational Mechanics.

Data inputs for blade geometry were determined from Fig. 6-33 of the main report. Data inputs for the airfoil performance were taken from ABBOT, Ref. 7 for the standard roughness curves. The data used in the analysis were corrected to infinite aspect ratio. Additional data for angles of attack beyond the steady stall limits was extrapolated from data reported in Ref. 8 for a 0015 airfoil. During program operation CL and CD values were determined by interpolating in two dimensions, between CL and CD values stored in a table for angles of attack ($\pm$ 90, 50, 20, 16, 12, 8, 4 and 0 degrees) and also for variable airfoil sections. These values are contained in an input file not shown listed here. Interpolation was accomplished using an interpolation subroutine called "TABLE", listed here.

The main program called "WILSON", used constant values for rotor radius, rotor speed, number of blade elements (10 for this analysis), number of rotor blades (2 or 3) and aerodynamic pitch setting at the 0.7 radius station. The program then iterated integer tip speed ratio values between set limits. Wind speeds were determined by the given quantities.

Next, the airfoil CL and CD data were entered as a function of blade angle of attack and airfoil section followed by a printout of the input data. Iteration over integer tip speed ratio values and blade element section then follows. The algorithm logic is outlined in the steps below.

A.1 PROGRAM LOGIC

1.   Set tip speed ratio
2.   Calculate wind speed
3.   Print output headings and initialize variables
4.   Set blade section number
5.   Calculate length of elemental blade section
6.   Calculate radius to center of elemental section
7.   Calculate chord from blade geometry
8.   Calculate local solidity
9.   Calculate geometric pitch angle based on aerodynamic pitch set as in input
10. Calculate twist at that radius from blade geometry
11. Set axial and radial induced flow factors approximately equal to zero
12. Calculate inflow angle
13. Calculate tip loss factor using the Prandtl Model (Ref. 1)
14. Check that induced flow factor is less than one-half. If it is not then print "Vortex Ring State" and go to next element
15. Add a gust factor if desired to the wind speed

```
00100     C WILSON PERFORMANCE
00150           PROGRAM WILSON
00200           COMMON TCL(15,6),TCD(15,6),A(15),RAD(6),CL,CD,ALPHAD,R
00300           COMMON BLADES,PI,RHO,RADIUS,OMEGA,ERROR,LAML,LAMU
00400           COMMON NR,LAM,WIND,V,DR,CHORD,SIGMA,N,IFLAG,THRMOM,XTR
00500           COMMON THETA,VLOC,AA,APR,PHI,F,CY,CX,APITCH,GUST,IGUST
00600           COMMON EA,EAPR,W2,THRUST,XT,TORQUE,XQR,CORR,TEST,RE
00625           COMMON XLAM,ISTART
00650           REAL LAM,MU
00700           OPEN (UNIT=6, DEVICE= 'DSK', ACCESS= 'SEQIN',
00800         1 FILE= 'WIN.DAT',RECORD SIZE=80)
00900           OPEN (UNIT=10, DEVICE= 'DSK', ACCESS= 'SEQOUT',
01000         1 FILE= 'WOUT.DAT',RECORD SIZE=130)
01200     C INPUT DATA AND INITIALIZE
01300           PI=3.1416
01400           RHO=1.23
01450           WRITE(5,99)
01475     99    FORMAT(' IF YOU WANT FRACTIONAL LAMBDA VALUES ENTER 1
01487         1 ',/,' IF NOT ENTER 0',/,' THIS DIVIDES INPUT VALUES BY 100')
01493           READ(5,*) ISTART
01500           WRITE(5,100)
01600     100   FORMAT(' INPUT RADIUS(M) OMEGA(RAD PER SEC) ERR(PER.)')
01700           READ(5,*)RADIUS,OMEGA,ERROR
01800           WRITE(5,101)
01900     101   FORMAT(' INPUT LOW LAM UP LAM NBR.OF BLADE STEPS (I)')
02000           READ(5,*)LAML,LAMU,NR
02100           WRITE(5,102)
02200     102   FORMAT(' INPUT BLADES(NO) AERODYN.PT(DEG) GUST FACTOR')
02300           READ(5,*)BLADES,APITCH,GUST
02400           READ(6,*) (A(I),I=1,15)
02500           READ(6,*) (RAD(J),J=1,6)
02600           READ(6,*) ((TCL(I,J),J=1,6),I=1,15)
02700           READ(6,*) ((TCD(I,J),J=1,6),I=1,15)
03000           THRUST=0.
03100           TORQUE=0.
03150           THRMOM=0.
03200           WRITE(10,108) BLADES,RADIUS,OMEGA,APITCH,ERROR,
03300         1 GUST
03400     108   FORMAT(/,' BLADES=',F3.0,/,' RADIUS=',F4.2,/,
03500         1 ' OMEGA=',F5.2,/,' AERODYN.PITCH=',F5.2,
03600         2 ' NOTE. -2.22 IMPLIES -.25 DEG AT TIP',/,
03700         3 ' ERROR=',F3.2,/,' GUST FACTOR=',F4.1)
03800     110   FORMAT(/,'    MU          LAM         CP        CQ/SIGMA    CT/S
03850         1IGMA   CM/SIGMA   TORQUE      THRUST     THRUST MOM.')
03900     C DO LOOP FOR MU
04000           MU=0.
04100     C DO LOOP LAM
04200           DO 400 L=LAML,LAMU
04300           LAM=L
04325           XLAM=LAM/100.
04350           IF(ISTART.EQ.1)LAM=XLAM
04400           WIND=RADIUS*OMEGA/LAM
04500           V=1./LAM
04600           THRUST=0.
04700           TORQUE=0.
04750           THRMOM=0.
04800     C DO LOOP FOR BLADE SECTIONS
04900           WRITE(10,115)
05000     115   FORMAT(///,'  R     VLOC      ALPHAD     CL      CD
05050         1 PHI     A        APR       F    TORQUE  THRUST
```

```
05150          2    TRST MOM.    RE')
05200               DO 300 IR=1,NR
05300               DR=(RADIUS-1.016)/NR
05400               R=1.016+IR*DR-.5*DR
05500               CHORD=-0.075*R+.392
05600               IF(R.LT.1.27)CHORD=0.8*R-.7112
05700               SIGMA=BLADES*CHORD/(PI*R)
05800               CORR=2.22+APITCH
05900               THETAD=-.7107*(R**3)+6.834*(R**2)-23.359*R
06000          1    +28.85+CORR
06100               IF(R.LT.1.27)THETAD=8.75
06200               THETA=THETAD/57.296
06300               VLOC=WIND/(R*OMEGA)
06400         C INITIALIZE
06500               AA=0.0001
06600               APR=0.0001
06700               IFLAG=0
06800          120  XAA=AA
06900               XAPR=APR
07000               PHI=ATAN(VLOC*(1.-AA)/(1.+APR))
07100         C CALCULATE TIP LOSS FACTOR F
07200               FX=(.5*BLADES)*(RADIUS-R)*(1./(RADIUS*SIN(PHI)))
07300               F=(2./PI)*ACOS(EXP(-1.*FX))
07400               TEST=AA*F
07500               IF(TEST.GT..5) GO TO 290
07600               IGUST=0
07700               GO TO 125
07800          124  PHI=ATAN(GUST*VLOC*(1.-AA)/(1.+APR))
07900               IGUST=1
08000          125  CONTINUE
08100               ALPHA=PHI-THETA
08200               ALPHAD=57.296*ALPHA
08400               IF(ALPHAD.LT.-90.)GO TO 126
08500               IF(ALPHAD.GT.90.)GO TO 128
08550               IF(IGUST.EQ.1)GO TO 140
08600               CALL TABLE
08605               GO TO 140
08610          126  WRITE(10,127)ALPHAD
08612               WRITE(5,127)ALPHAD
08615               GO TO 140
08620          128  WRITE(10,129)ALPHAD
08625               WRITE(5,129)ALHPAD
09000          127  FORMAT(' ALPHA BELOW RANGE, ALPHAD=',F5.1)
09500          129  FORMAT(' ALPHA ABOVE RANGE,-STALL-, ALPHAD=',F5.0)
09600               GO TO 400
10000          140  CONTINUE
10050               IF(IGUST.EQ.1)CL=.1*ALPHAD+.35
10100               CY=CL*COS(PHI)+CD*SIN(PHI)
10200               CX=CL*SIN(PHI)-CD*COS(PHI)
10300               IF(IGUST.EQ.1) GO TO 205
10400               Y1=(SIGMA*CY)/(8.*F*((SIN(PHI))**2))
10500               AA=Y1/(1.+Y1)
10600               X1=(SIGMA*CX)/(8.*F*(SIN(PHI))*(COS(PHI)))
10700               APR=X1/(1.-X1)
10800               EA=ABS(AA-XAA)/ABS(XAA)
10900               EAPR=ABS(APR-XAPR)/ABS(XAPR)
11000               IF(EA.LT.ERROR.AND.EAPR.LT.ERROR) GO TO 200
11100               IFLAG=IFLAG+1
11200               IF(IFLAG.GT.15) GO TO 190
11300               GO TO 120
```

```
11400      190      WRITE(10,195)EA,EAPR
11500      195      FORMAT(' TOO MANY ITERATIONS',/,
11600        1      'ACTL ERROR IS EA=',F6.3,'EAPR=',F5.3,/)
11700      200      CONTINUE
11750               IF(GUST.NE.1.) GO TO 124
11775      205      CONTINUE
12600    C CALCULATE W2
12700               X2=R*OMEGA*(1.+APR)
12800               Y2=GUST*WIND*(1.-AA)
12900               W2=X2**2+Y2**2
13000    C CHECK REYNOLDS NUMBER IN LIMITS
13200               W=SQRT(W2)
13300               RE=W*CHORD*1000./.01394
14200    C CALCULATE THRUST , TORQUE AND THR.MOM (INTEGRATED)
14300               XT=BLADES*CHORD*.5*RHO*W2*CY*DR
14400               THRUST=THRUST+XT
14450               XTR=XT*R
14475               THRMOM=THRMOM+XTR
14500               XQ=RHO*BLADES*CHORD*.5*W2*CX*DR
14600               XQR=XQ*R
14700               TORQUE=TORQUE+XQR
14800               WRITE(10,298)R,VLOC,ALPHAD,CL,CD,PHI,AA,APR,F,XQR,
14850        1      XT,XTR,RE
14900      298      FORMAT(F4.2,1PE9.1,11E9.1)
15000               GO TO 300
15100      290      WRITE(10,295) LAM,IR
15200      295      FORMAT(' VORTEX RNG ST ..LAM=',F3.0,' IR=',I3)
15300      300      CONTINUE
15400               POWER=TORQUE*OMEGA
15500               CP=POWER/(.5*RHO*PI*(RADIUS**2)*(WIND**3))
15505               TSIGMA=.032
15510               CQ=.5*CP/(LAM**3)
15515               CQS=CQ/TSIGMA
15520               CT=THRUST/(RHO*PI*(OMEGA**2)*(RADIUS**4))
15525               CTS=CT/TSIGMA
15530               CM=THRMOM/(RHO*PI*(OMEGA**2)*(RADIUS**5))
15535               CMS=CM/TSIGMA
15567               IF(ISTART.EQ.1)GO TO 305
15583               GO TO 310
15591      305      WRITE(10,307)
15595      307      FORMAT(' *** DIVIDE INPUT LAM VALUES BY 100 ***',//)
15597      310      CONTINUE
15600               WRITE(10,110)
15700               WRITE(10,350)MU,LAM,CP,CQS,CTS,CMS,TORQUE,THRUST,THRMOM
15800      350      FORMAT(1PE11.3,8E11.3)
15900      400      CONTINUE
16000               END
```

A.1.2 Listing For The Interpolation "TABLE" Subroutine.

```
00100              SUBROUTINE TABLE
00200              COMMON TCL(15,6),TCD(15,6),A(15),RAD(6),CL,CD,ALPHAD,R
00300              COMMON BLADES,PI,RHO,RADIUS,OMEGA,ERROR,LAML,LAMU
00400            COMMON NR,LAM,WIND,V,DR,CHORD,SIGMA,N,IFLAG,THRMOM,XTR
00500              COMMON THETA,VLOC,AA,AFR,PHI,F,CY,CX,APITCH,GUST,IGUST
00600              COMMON EA,EAPR,W2,THRUST,XT,TORQUE,XQR,CORR,TEST,RE
00700              I=1
00800      5       IF(ALPHAD-A(I)) 20,20,10
00900     10       I=I+1
01000              GO TO 5
01100     20       CONTINUE
01200              RATIOA=(A(I)-ALPHAD)/(A(I)-A(I-1))
01300              J=1
01400     25       IF(R-RAD(J)) 40,40,30
01500     30       J=J+1
01600              GO TO 25
01700     40       CONTINUE
01800              RATIOR=(RAD(J)-R)/(RAD(J)-RAD(J-1))
01900              CLR1=TCL(I,J)-RATIOA*(TCL(I,J)-TCL(I-1,J))
02000              CLR2=TCL(I,J-1)-RATIOA*(TCL(I,J-1)-TCL(I-1,J-1))
02100              CL=CLR1-RATIOR*(CLR1-CLR2)
02200              CDR1=TCD(I,J)-RATIOA*(TCD(I,J)-TCD(I-1,J))
02300              CDR2=TCD(I,J-1)-RATIOA*(TCD(I,J-1)-TCD(I-1,J-1))
02500              CD=CDR1-RATIOR*(CDR1-CDR2)
02600              RETURN
02700              END
```

A.1.3 Sample Output From "WILSON PERFORMANCE" Program.

```
BLADES= 2.
RADIUS=3.81
OMEGA= 3.00
AERODYN.PITCH=-2.00   NOTE. -2.22 IMPLIES -.25 DEG AT TIP
ERROR=.01
GUST FACTOR= 1.0
```

OUTPUT BY BLADE ELEMENT

R	VLOC	ALPHAD	CL	CD	PHI	A	APR
1.16	1.1E+00	3.8E+01	6.5E-01	3.0E-01	8.2E-01	3.7E-02	-2.9E-03
1.44	8.8E-01	3.2E+01	8.3E-01	6.6E-01	7.0E-01	5.1E-02	1.1E-03
1.71	7.4E-01	3.0E+01	8.4E-01	5.9E-01	6.1E-01	4.8E-02	1.0E-05
1.99	6.4E-01	2.7E+01	8.8E-01	5.3E-01	5.5E-01	4.8E-02	9.2E-05
2.27	5.6E-01	2.5E+01	9.4E-01	4.8E-01	4.9E-01	4.9E-02	5.2E-04
2.55	5.0E-01	2.3E+01	1.0E+00	4.3E-01	4.4E-01	5.2E-02	1.1E-03
2.83	4.5E-01	2.1E+01	1.1E+00	3.8E-01	4.0E-01	5.5E-02	1.5E-03
3.11	4.1E-01	2.0E+01	1.1E+00	3.5E-01	3.7E-01	5.7E-02	1.3E-03
3.39	3.7E-01	1.9E+01	1.1E+00	3.3E-01	3.4E-01	6.7E-02	1.3E-03
3.67	3.5E-01	1.7E+01	1.2E+00	3.1E-01	3.0E-01	1.0E-01	1.7E-03

F	TORQUE	THRUST	TRST MOM.	RE
7.5E-01	-1.6E-01	1.9E+00	2.2E+00	7.7E+04
7.5E-01	1.2E-01	3.3E+00	4.7E+00	1.1E+05
7.5E-01	1.8E-03	3.7E+00	6.3E+00	1.2E+05
7.4E-01	2.5E-02	4.2E+00	8.4E+00	1.2E+05
7.2E-01	2.1E-01	4.8E+00	1.1E+01	1.2E+05
6.9E-01	5.9E-01	5.4E+00	1.4E+01	1.2E+05
6.5E-01	1.0E+00	6.0E+00	1.7E+01	1.2E+05
5.9E-01	1.1E+00	6.2E+00	1.9E+01	1.1E+05
4.9E-01	1.2E+00	6.5E+00	2.2E+01	1.1E+05
3.1E-01	1.2E+00	6.7E+00	2.4E+01	9.7E+04

TOTALS OVER BLADE

MU	LAM	CP	CQ/SIGMA	CT/SIGMA	CM/SIGMA
0.000E+00	3.000E+00	1.013E-02	5.865E-03	2.079E-01	1.449E-01

TORQUE	THRUST	THRUST MOM.
5.240E+00	4.876E+01	1.295E+02

16. Calculate angle of attack and find CL and CD using subroutine "TABLE" unless there is a positive gust factor greater than one, in which case CL is assumed to linearly increase with angle of attack above steady state stall to simulate the effect of dynamic stall

17. Check angle of attack in range, -90 to +90 degrees

18. Calculate dimensionless thrust and torque coefficients

19. Calculate axial and radial induced flow based on momentum and blade element theory and compare with previous values. If the difference is within limits exit iteration loop. If not, go to #12 and repeat. Also, test for number of allowable iteration steps

20. Knowing inflow values, calculate thrust and torque moments and calculate local Reynolds number

21. Add elemental thrust and torque values and printout elemental values and totals over the entire blade

Listings of the program and a sample output follow. Note that all units are SI for the program and its results.

APPENDIX B

ANALYSIS OF ROTOR AND TOWER DYNAMICS BY A FINITE ELEMENT METHOD

by

David A. Peters
Timothy W-H Ko

APPENDIX B

ANALYSIS OF ROTOR AND TOWER DYNAMICS BY A FINITE ELEMENT METHOD

In this Appendix we present the results of a dynamic analysis of the rotor, tower, and boom by a finite element method. The particular program used is determined in the thesis: Ko, Timothy W-H, Use of Tapered, Twisted Finite Elements for Dynamic Analysis of Helicopter Rotor Blades, Master of Science Thesis, Washington University, May 1980. The thesis includes the derivations, mathematical techniques, extensive documentation, and various studies of the effect of blade parameters. (The thesis is available upon request.) The thesis also includes the wind-turbine results presented in this Appendix.

After most of the present computer program had been developed and documented, an opportunity arose to apply the program to an actual wind-turbine that was to be built and operated. This allowed us to test our program on a real configuration. It was these applications that motivated the addition of the teetering hinge with offset and the extension to include a flutter capability.

B.1 PHYSICAL DESCRIPTION OF BLADE

A wind-turbine generator consisting of a two-bladed horizontal axis rotor system was mounted on the top of a tower as shown in Fig. B1. The 150 inch-radius, hingeless blade had mass and stiffness distributions shown in Fig. B2 and B3.

The data in the figures were obtained from static tests of mass, inertia, and deflection under loading. These data, along with the blade geometry were used to develop a consistent mass and stiffness distribution. Subsequently, frequency measurements in bending and torsion were used to further modify these values. The stiffnesses (GJ and EI) were modified so that the frequencies calculated from the program could match the measured frequencies.

$$\text{modified} \begin{Bmatrix} EI_{yy} \\ EI_{zz} \end{Bmatrix} = 0.77 \text{ X} \quad \text{measured} \begin{Bmatrix} EI_{yy} \\ EI_{zz} \end{Bmatrix}$$

modified GJ = 0.08 X measured EI.

modified I_o (torsional mass-moment of inertia)

$$= 1.5 \text{ X calculated } I_o$$

(calculated as $I_o = 0.034 \text{ mc}^2$)

and where 0.77 is the ratio of the square of measured flapping natural frequency to the square of the calculated flapping natural frequency, and 0.67 is the ratio of the measured torsional frequency to the calculated torsional frequency.
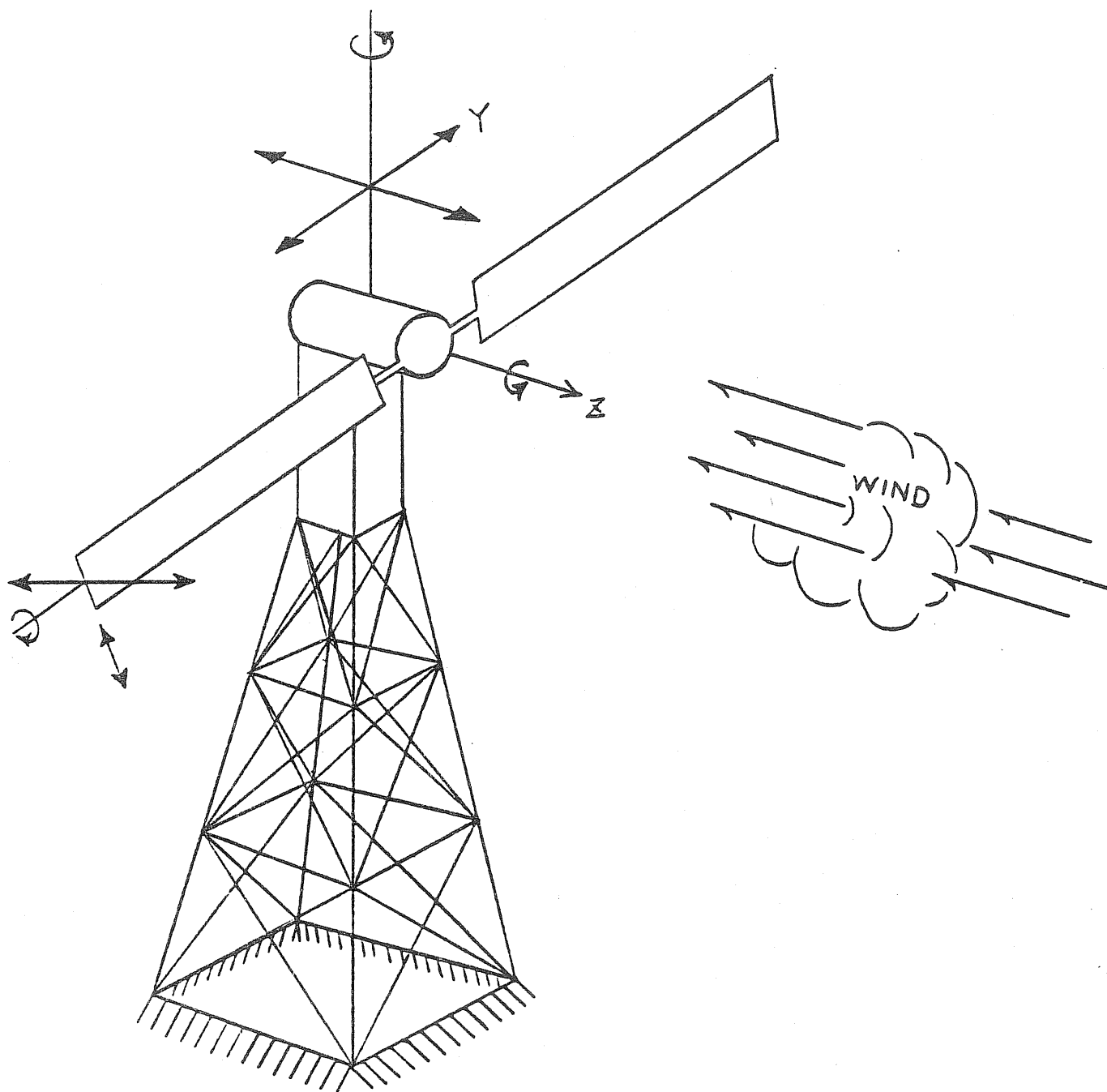
Figure B-1. WIND TURBINE SYSTEM
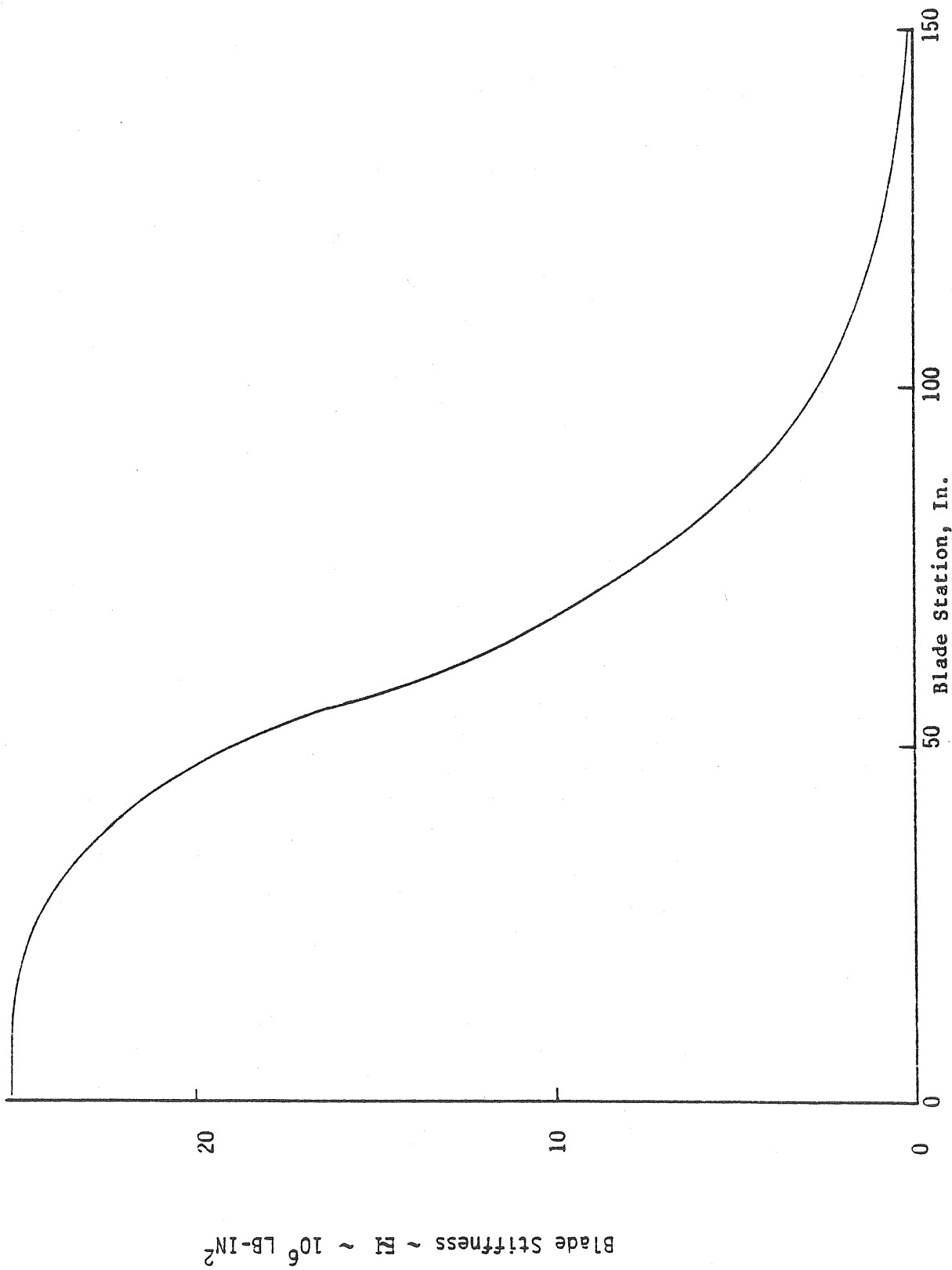
Figure B-2. WIND TURBINE BLADE STIFFNESS DISTRIBUTION
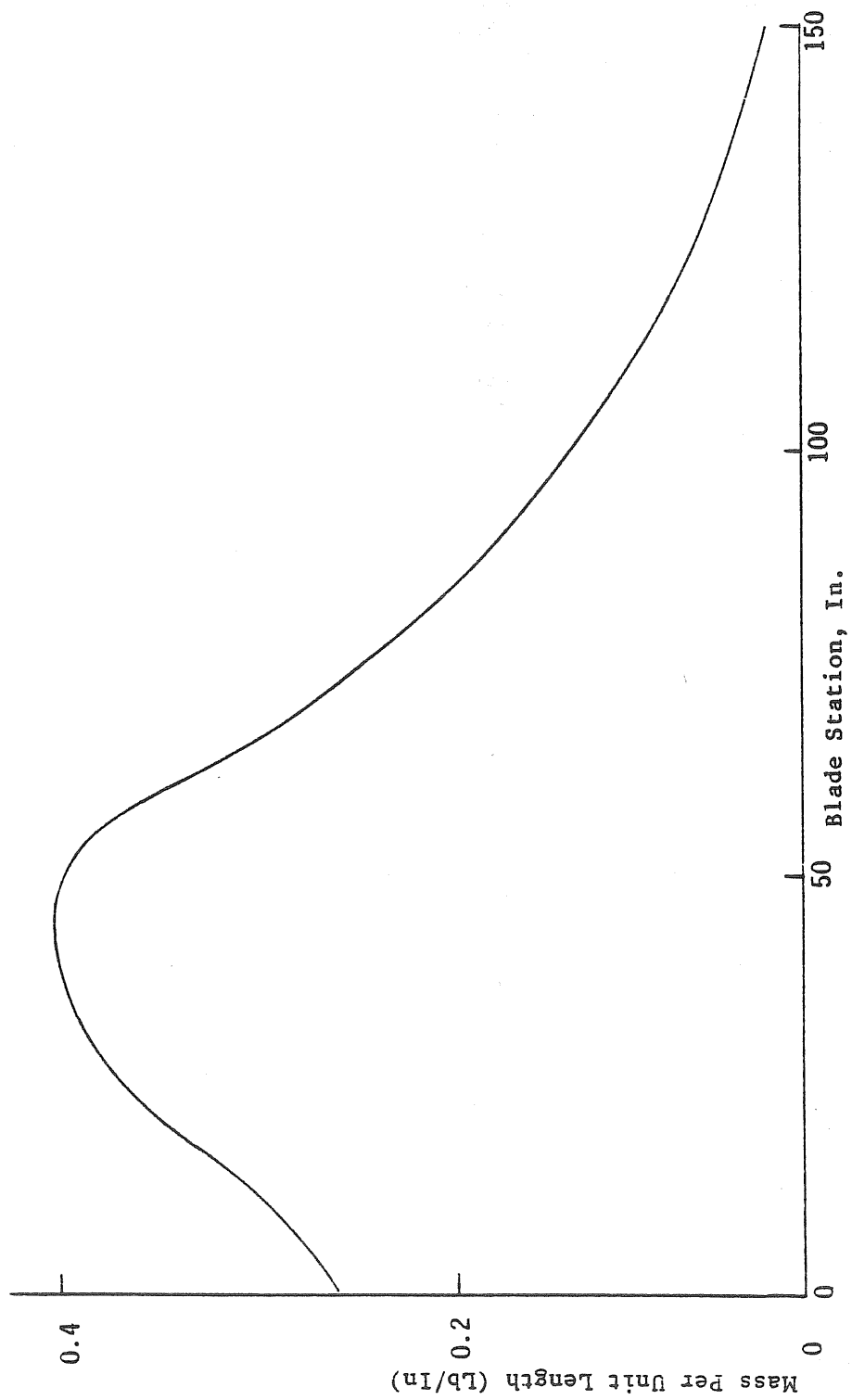
Figure B-3. WIND TURBINE BLADE MASS DISTRIBUTION

In order to correctly model the experiment, the blade must be treated in the following way. A steel collar is cantilevered to the center of rotation and is 25 in long. The blade has 17 in cut-off at the end and is pinned to the collar at r = 17 in and r = 25 in as shown in Fig. B4. This configuration was chosen to model the true hub as closely as possible.

The stiffnesses (GJ and EI) of the collar were assumed to be constant and equal to 87.5×10^6 lb/in, and the mass distribution was 0.423 lb/in.

For this particular problem, the old program was modified as described in the following. First, the mass and stiffness matrices were obtained separately for the cantilever collar and for the cut-off blade. After coordinate condensation (U_3, U_4, U_5 were reduced out), the matrices of the two parts were combined together at the corresponding pinned points.

The modal displacement and frequencies of the first and second flapping mode are shown in Fig. B5 and B6 for 200 rpm. The actual rotor was teetering, however, so that both symmetric and asymmetric modes were considered.

B.2 MODES AND FREQUENCIES

Two separate fan-plots are presented for the teetering rotor. One describes symmetric modes for which each blade performs an identical, in-phase motion. This was calculated by taking the blade to be cantilevered inflap but pinned inplane. Thus, the teetering mode did not enter the analysis, Fig. B7. A second plot described asymmetric modes for which each blade performs identical, but 180° out-of-phase, motion. Thus, the blade was cantilevered inplane and the teetering degree of freedom are included, Fig. B8. In either case, torsion was neglected. As a further approximation, the lift forces due to teetering were included, but coriolis terms and lift due to rates (i.e. the damping matrix) were neglected. Also, the nonsymmetric stiffness terms due to δ_3 (the last column in (K)) were balanced by an identical row in the equation to make the matrix symmetric. Although these terms are, strictly speaking, incorrect, in practice they do not appreciably alter the frequencies. The computational advantage of a symmetric matrix was chosen over the slightly improved accuracy of an exact stiffness matrix. Stated in another way, the aerodynamic terms were allowed to couple the flapping modes, but were not allowed to add or subtract energy. The offset e is 3.5 in and δ_3 is 67°. It is interesting to note that the teetering and inplane modes couple at 350 rpm for the asymmetric plot as shown in Fig. B8. Within the normal operational range of the machine, several possible resonances are identified. First, there is the asymmetric inplace crossing 3/rev at 150 rpm. Second, there is the second symmetric inplace crossing 4/rev at 200 rpm. Third, there is the first symmetric flap crossing 3/rev at 300 rpm.

B. 3 FLUTTER ANALYSIS

The flutter analysis for the wind-turbine blade was performed by including the mass offset and the lift due to elastic deflection, U_5. Thus, each elemental stiffness matrix was modified by the term $U_5 LW_i$.
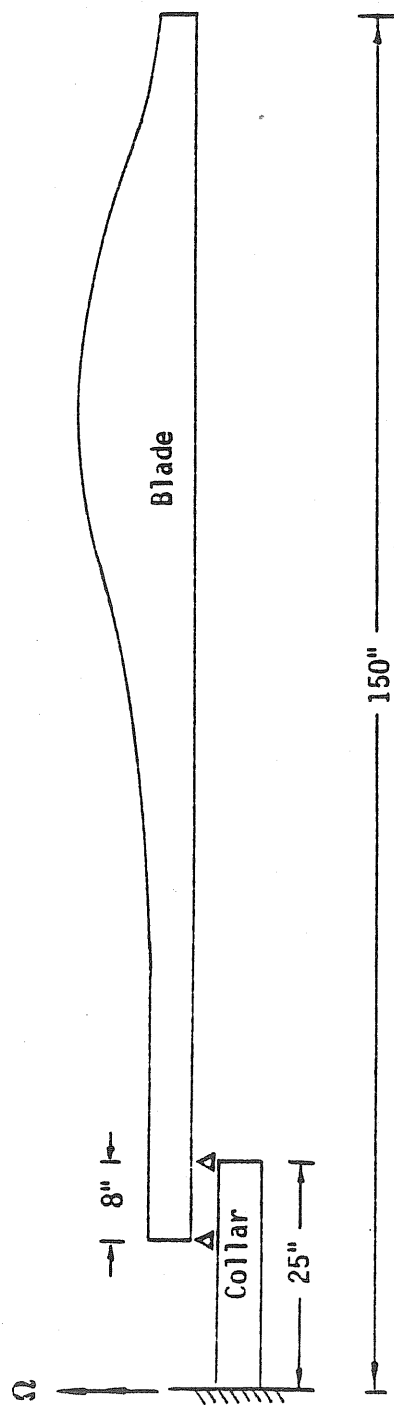
Figure B-4. AN ILLUSTRATION OF WIND TURBINE BLADE
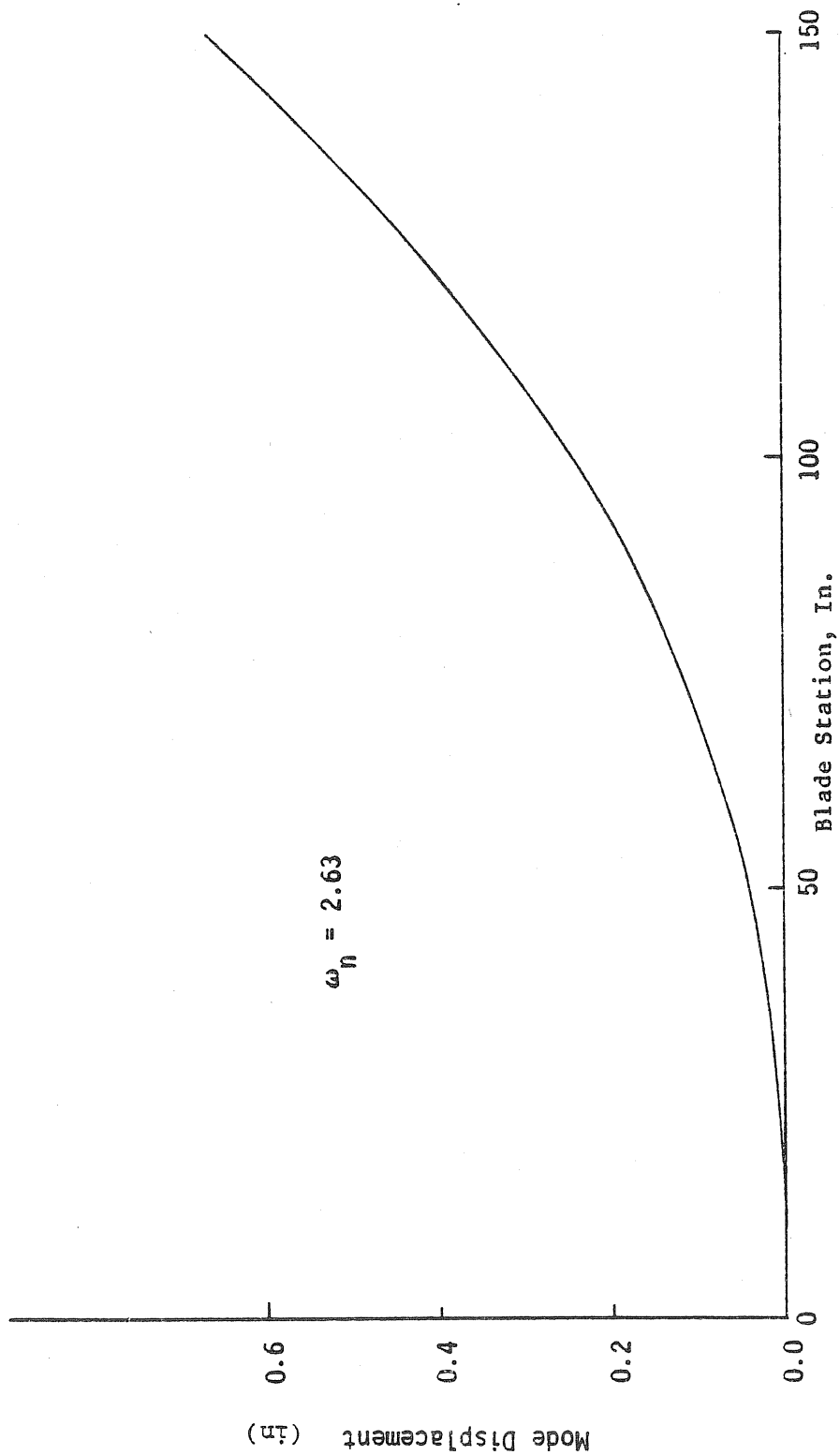
Figure B-5. WIND TURBINE BLADE FIRST FLAP MODE

$\omega_n = 6.74$

Mode Displacement (in)

Blade Station, In.
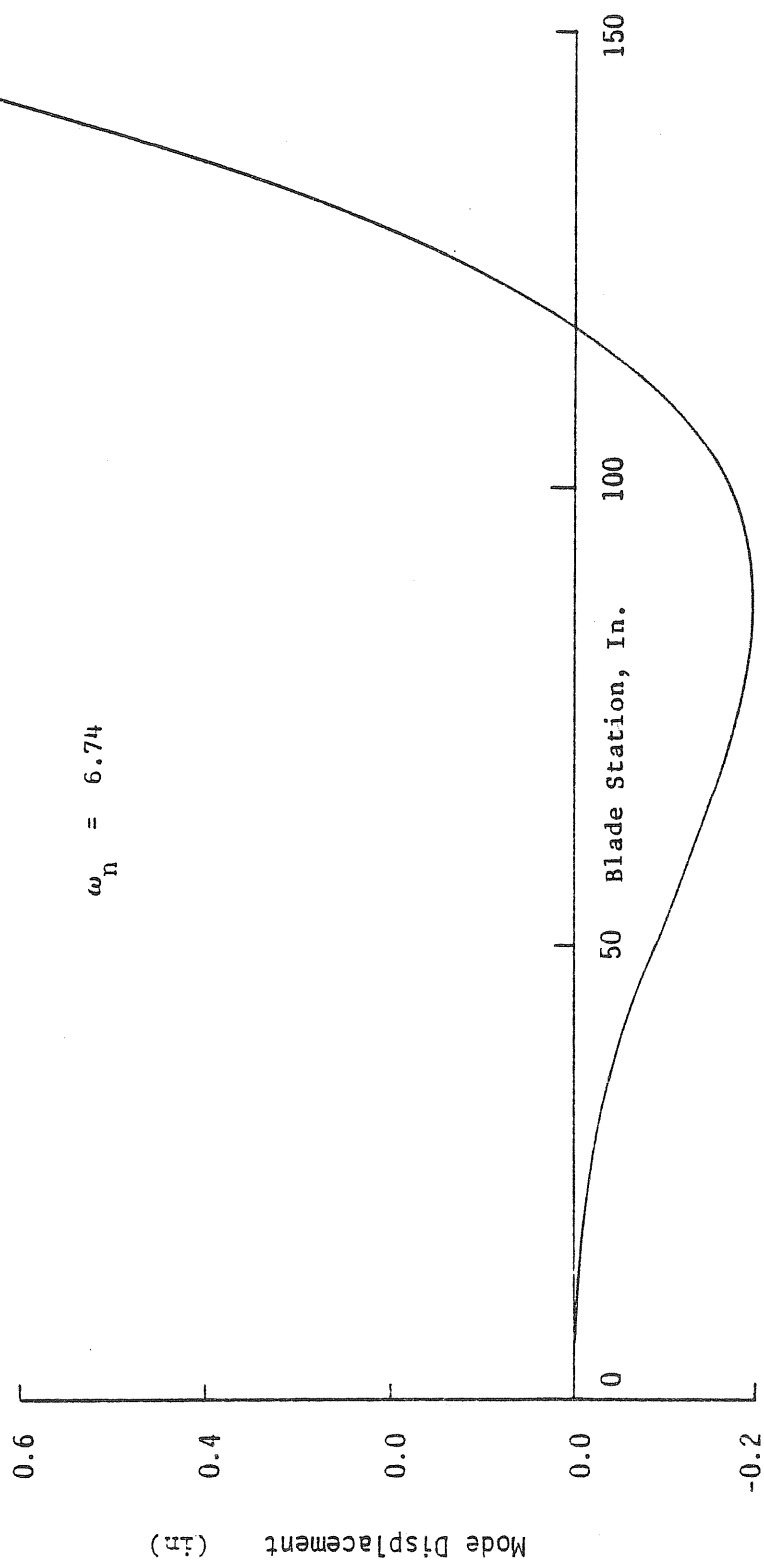
Figure B-6. WIND TURBINE BLADE SECOND FLAP MODE

$$
\begin{bmatrix}
& \vdots & \\
& \vdots & -L_{W_i} \\
---&---+&--- \\
& \vdots & \\
& \vdots & \\
& \vdots &
\end{bmatrix}
\begin{Bmatrix}
U_1 \\
\\
\\
U_5
\end{Bmatrix}
$$

In this case, no symmetric term occurred (no aerodynamic moment due to bending) and a nonconservative system developed.

Results are shown in Fig. B9 for the blade in Section 1, cantilevered at $r = 25$ in, with $e = 0.13$ C. The torsion first coalesced with the second flap, but no flutter occurred. Of further interest, the first flap coupled with torsion while the torsion was still coupled to the first flap. Thus, no flutter at all occurred. It should also be noted that, due to the high torsional frequency, all of these couplings only occured at unrealistically high rpm. Thus, flutter is not significant for this blade.

B.4   FORCED RESPONSE

Forced response under a given load for a wind-turbine blade was investigated to avoid interference between the tower and the blades when blades are rotating.

The forcing load is described in Fig. B10 and the displacement of the wind-turbine blade under the given load is shown in Fig. B11.

B.5   MODES OF TOWER

The present approach actually is not restricted to the modes and frequencies of rotor blades, but may also be used for those of the tower. Thus, the program can be of use in the design and analysis of the entire rotor-body system.

The tower is shown in Fig. B12. The information concerning stiffness and mass distribution of parts of the tower is also shown.

A point mass of 1.35 mugs (1 mug = 12 slugs) to model the transmission was assumed to be at the 60 ft station of the tower. The mass of the rotor was assumed to be 15 in above the 60 ft station of the tower and 20 in forward of the tower center. The structure between the upper end of the yaw post and the point mass was assumed rigid. The flexible tail boom had a 200 in length and 0.22 mug mass, resulting in a mass per unit length of 0.0011 mugs/ in. The tail boom stiffness was EI = 400 X 10^5 lb-in^2. At the end of the tail boom there was a mass of 0.05 mugs. The yaw

B11
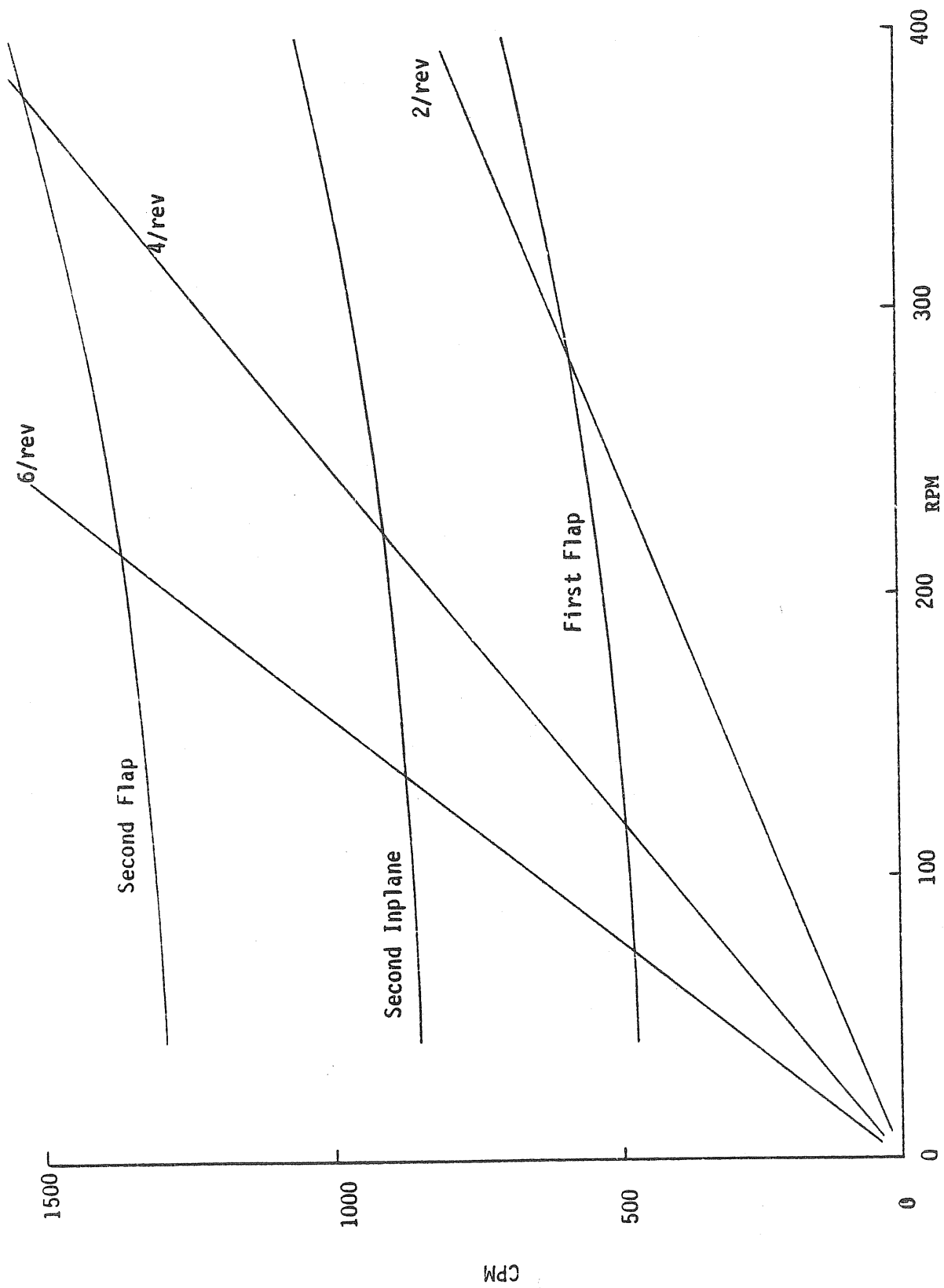
Figure B-7. FAN PLOT OF SYMMETRIC MODE FOR TEETERING
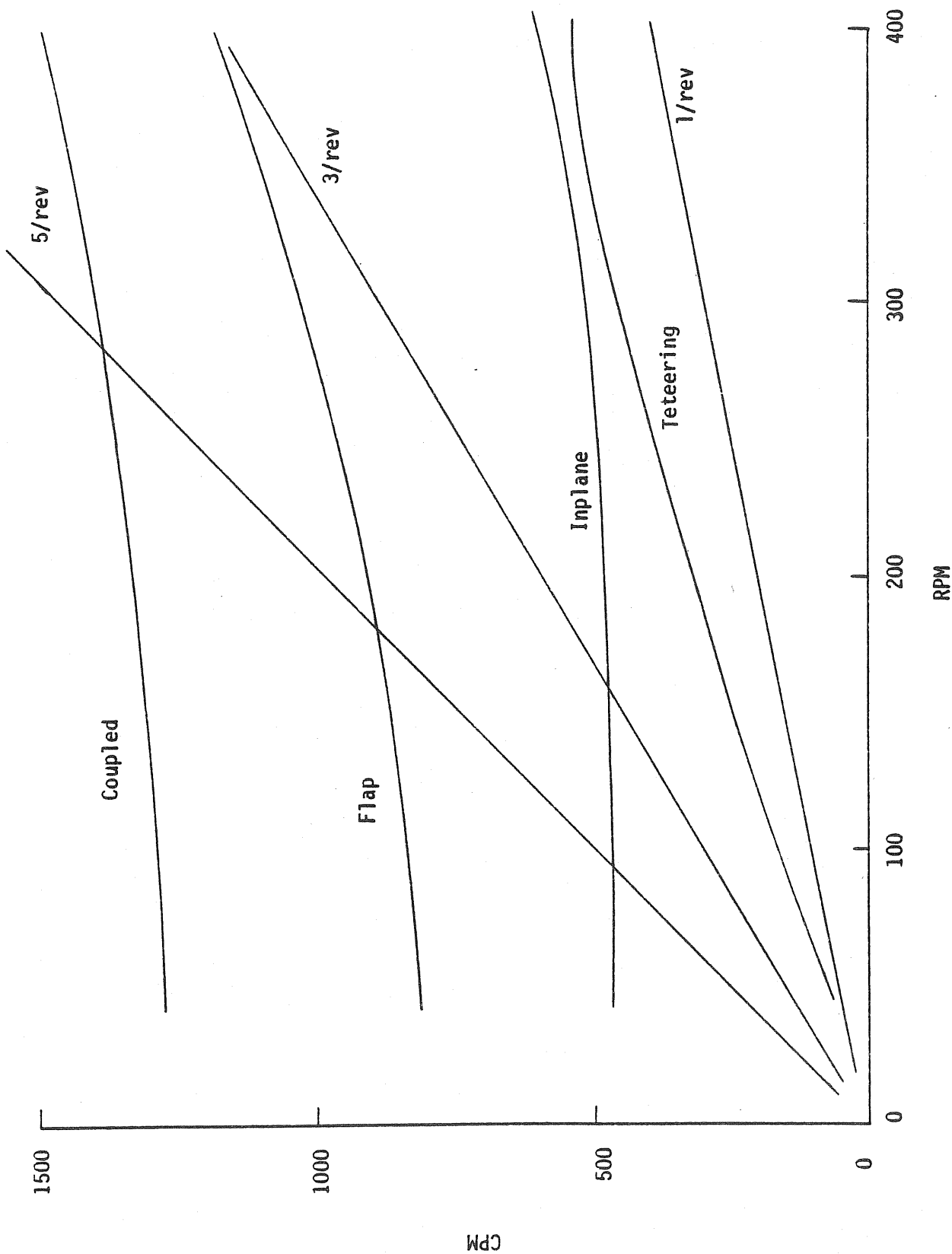
Figure B-8.   FAN PLOT OF ASYMMETRIC MODE FOR TEETERING

post was slender, with 20 in length and bending stiffness of 50×10^6 lb-in^2. The upper yaw bearing was self-aligning, so that the yaw post was treated as beam on the pinned points. The mass and stiffness distribution of the tower proper are given in Fig. B13 and B14.

The computer program developed in the past had to be modified for the coupled tower-boom. Tower and boom stiffness K_T and K_B were calculated respectively in the usual way. The V_1 coordinate at the root of the boom was eliminated. The signs of the rows and columns of the V_4 coordinates were also reversed. After the switch of rows and columns between V_4 and U_5 of the boom, and the two stiffness matrices K_T and K_B were overlapped on (U_2, V_2), (U_3, V_3), (U_4, V_5), (U_5, V_4). The mass matrices M_T^B and M_O were treated in a similar way but the lumped mass of the whole boom was added to in the U_1 coordinate at the end of the tower.

Table B1 gives the natural frequencies of the first few modes. Figure B16 and B17 show the mode shape of the tower normal to the rotor.

Table B1. FREQUENCIES OF TOWER

Type of Modes	Natural Frequencies (cpm)
Rigid-body yaw	0
Tower normal to rotor	134
Tower lateral	158
First boom vertical	280
First boom lateral	796

B14
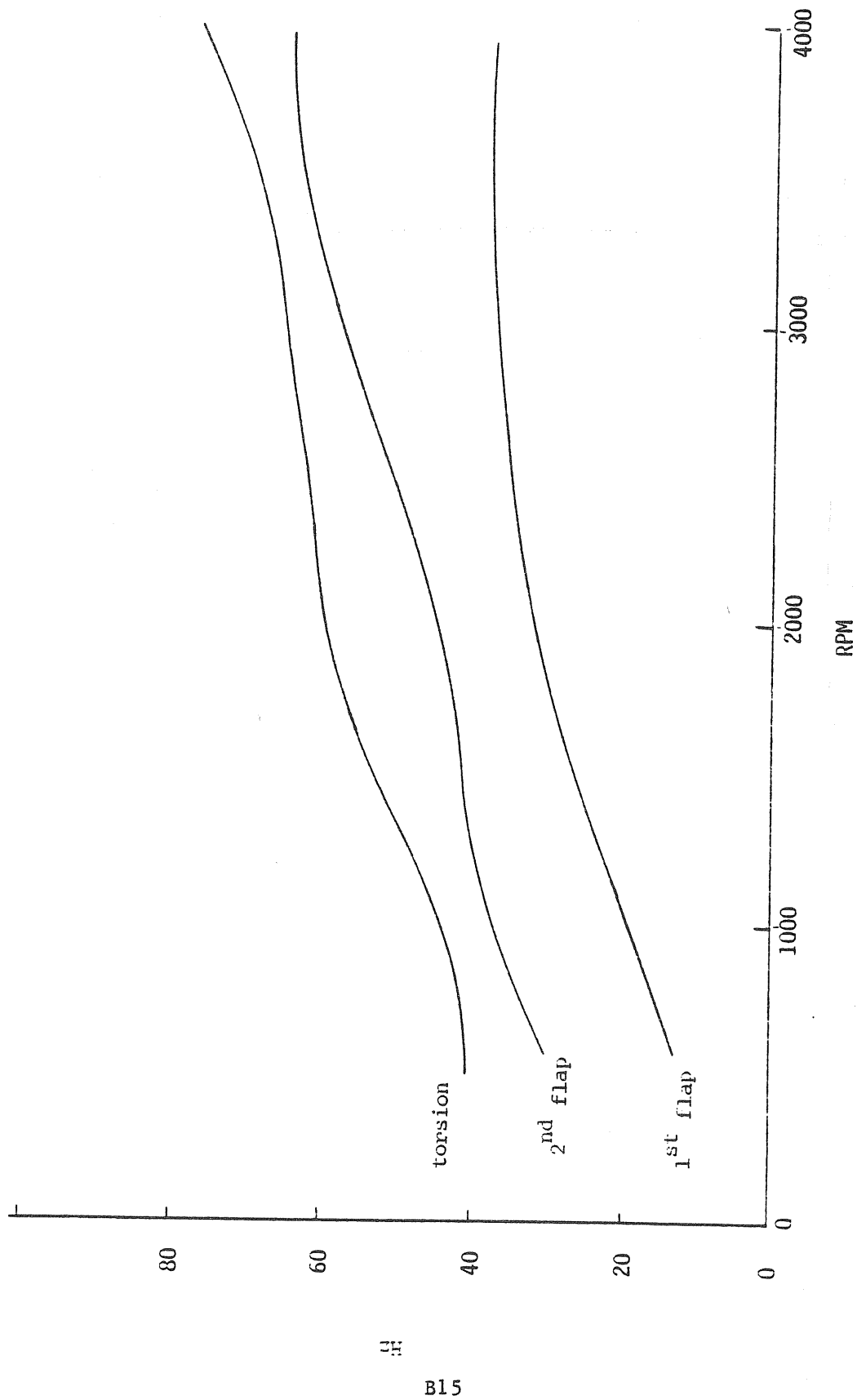
Figure B-9. FAN PLOT FOR FLUTTER

B15
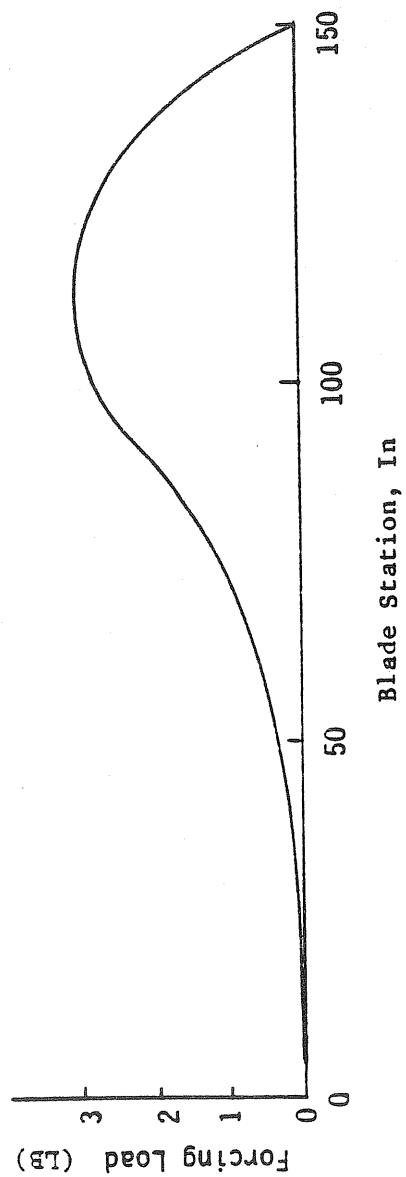
Figure B-10. LOAD DISTRIBUTION

n = 8.79

Mode Displacement (in)

Blade Station, In
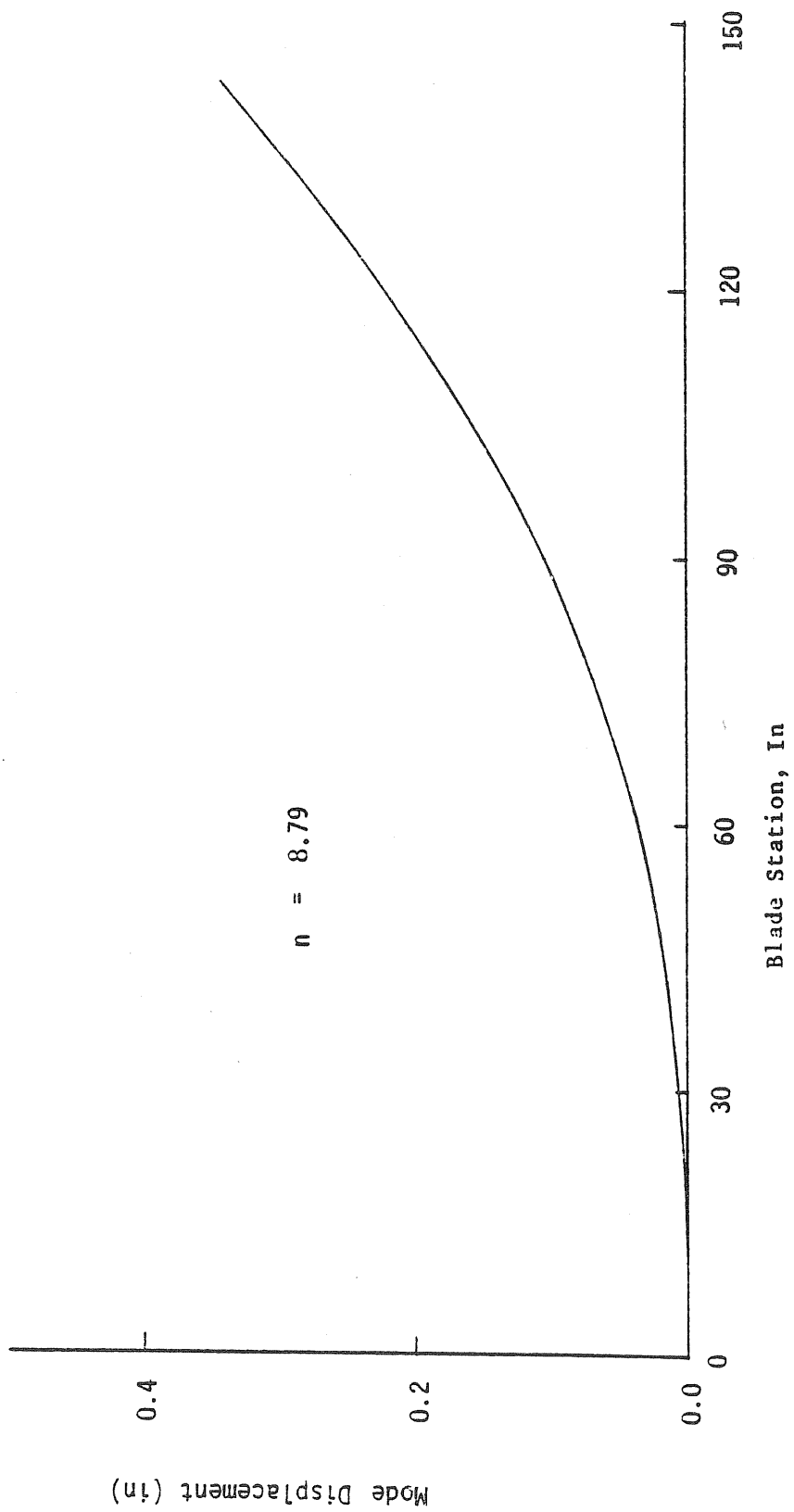
Figure B-11. FIRST FLAP MODE UNDER GIVEN LOAD

200"   20"

1.16 mugs

15"

0.05mugs

rigid structure,no mass

pinned

BOOM

0.011mugs/in

$EI = 400 \times 10^6 LB\text{-}IN^2$

yaw post,no mass

$EI = 50 \times 10^6 LB\text{-}IN^2$

pinned

720"
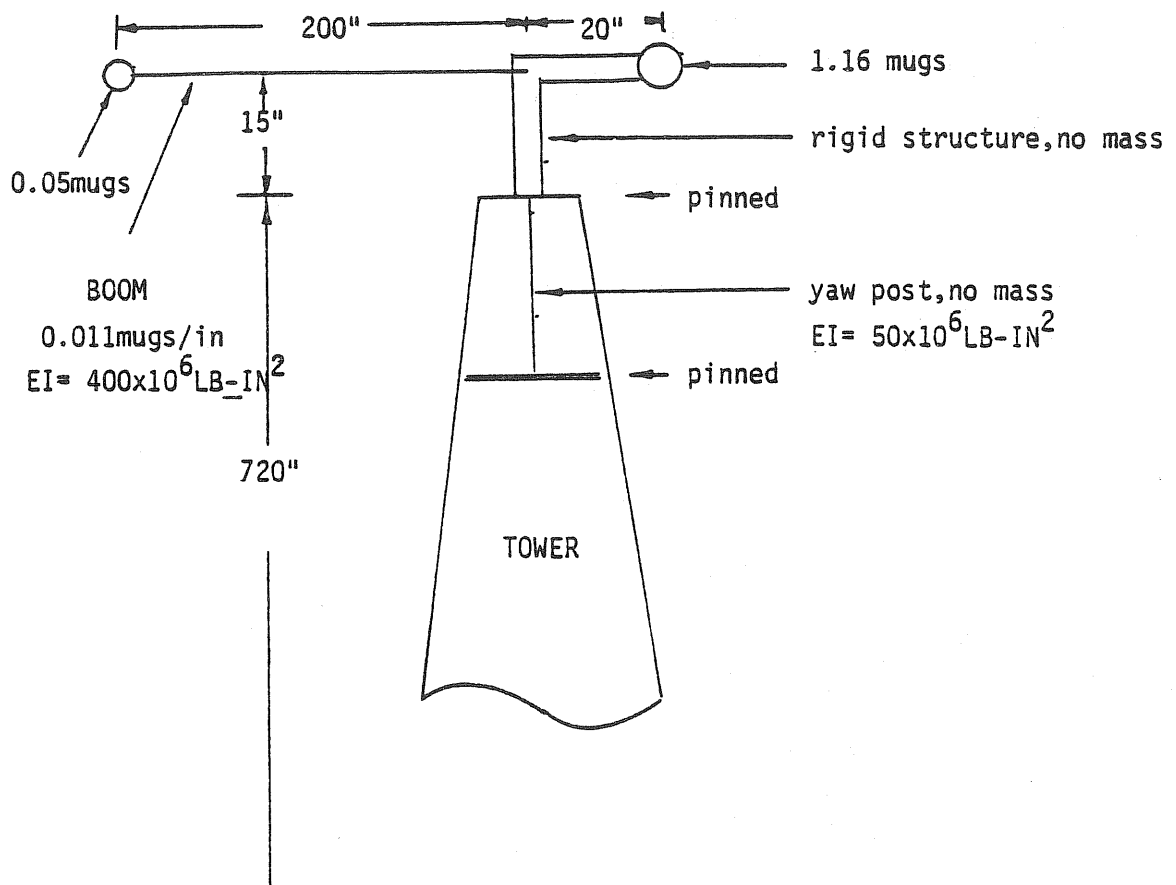
TOWER
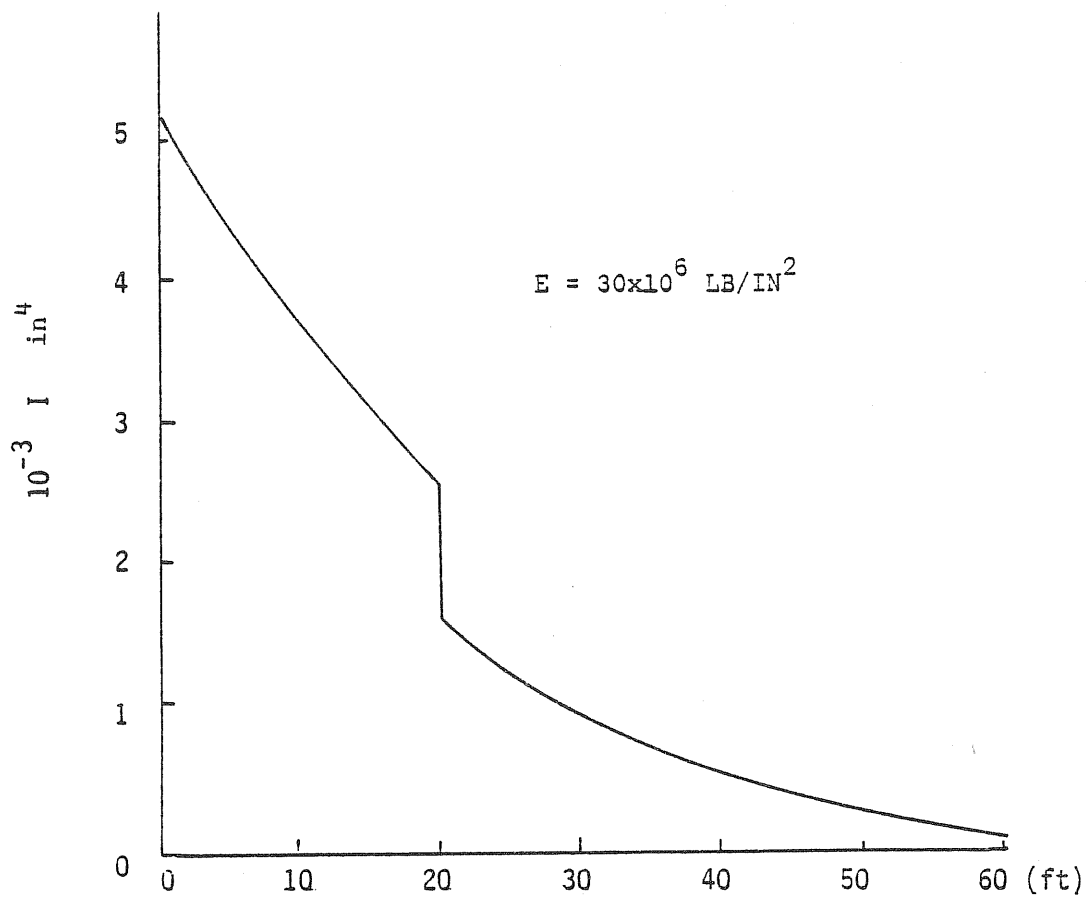
Figure B-12.   TOWER

Figure B-13. TOWER STIFFNESS DISTRIBUTION

$E = 30 \times 10^6 \ LB/IN^2$
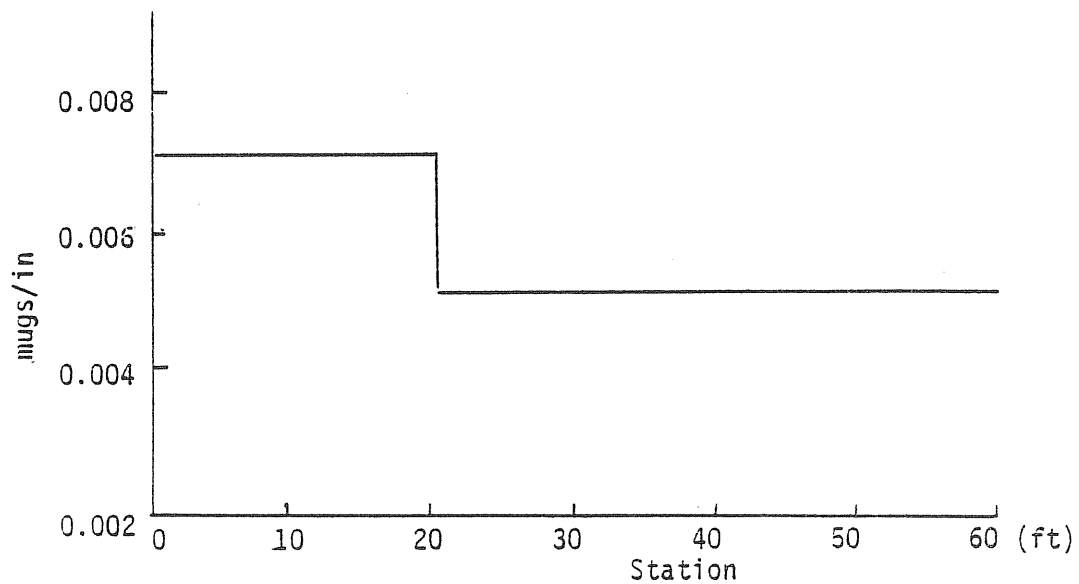
Figure B-14. TOWER MASS DISTRIBUTION

B19
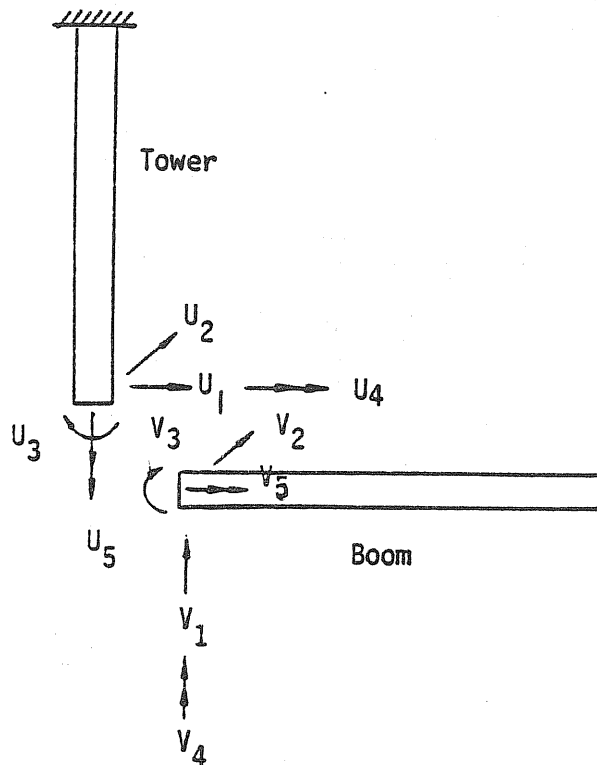
Figure B-20. COORDINATE RELATIONSHIP BETWEEN TOWER
AND BOOM
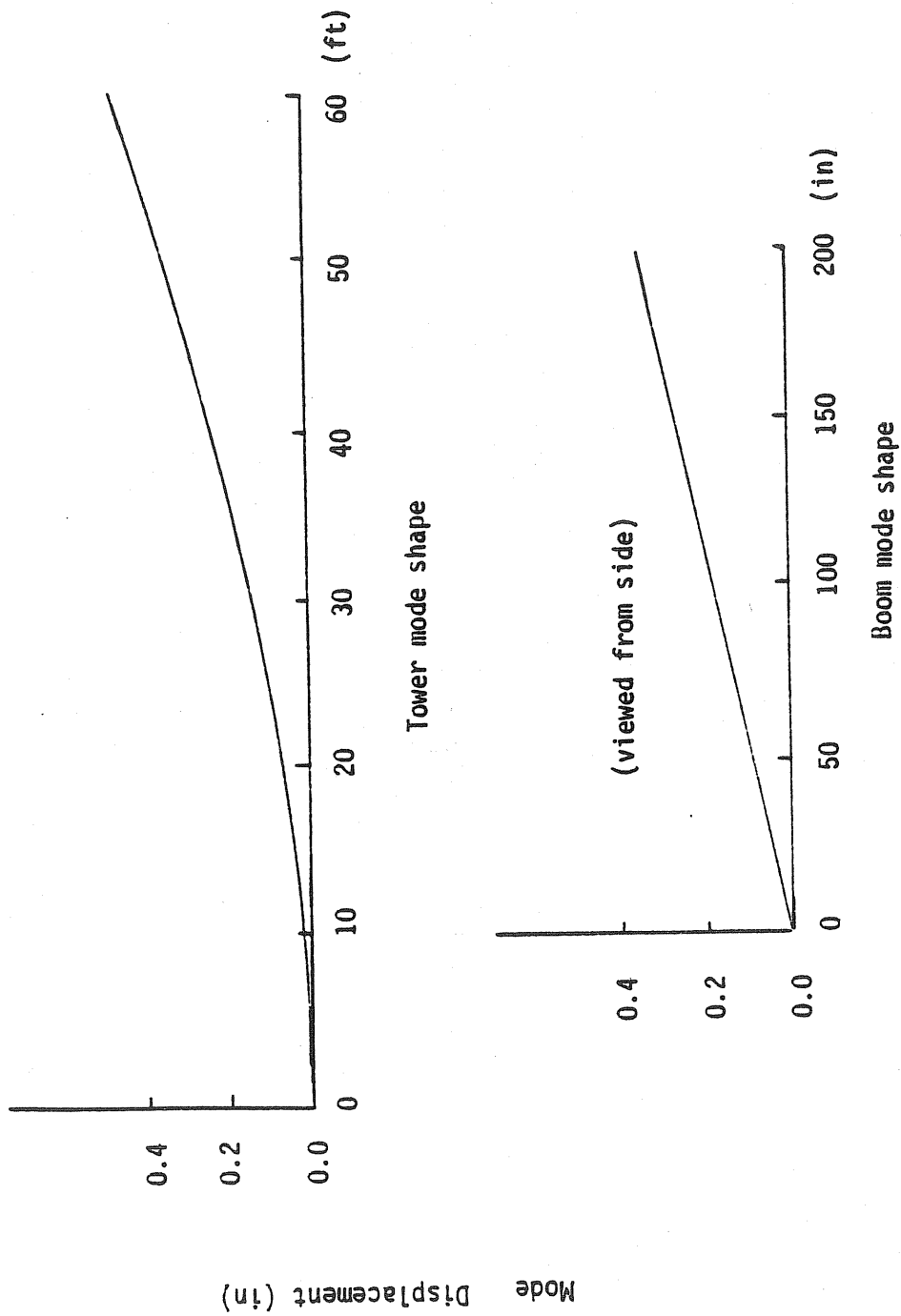
Figure B-16. TOWER NORMAL TO ROTOR MODE

Tower mode shape

Boom mode shape

(looking down)

0.4
0.4
0.2
0.0

0.0 50 100 150 200 (in)

0 10 20 30 40 50 60 (ft)

0.4
0.2
0.0

Mode Displacement (inch)
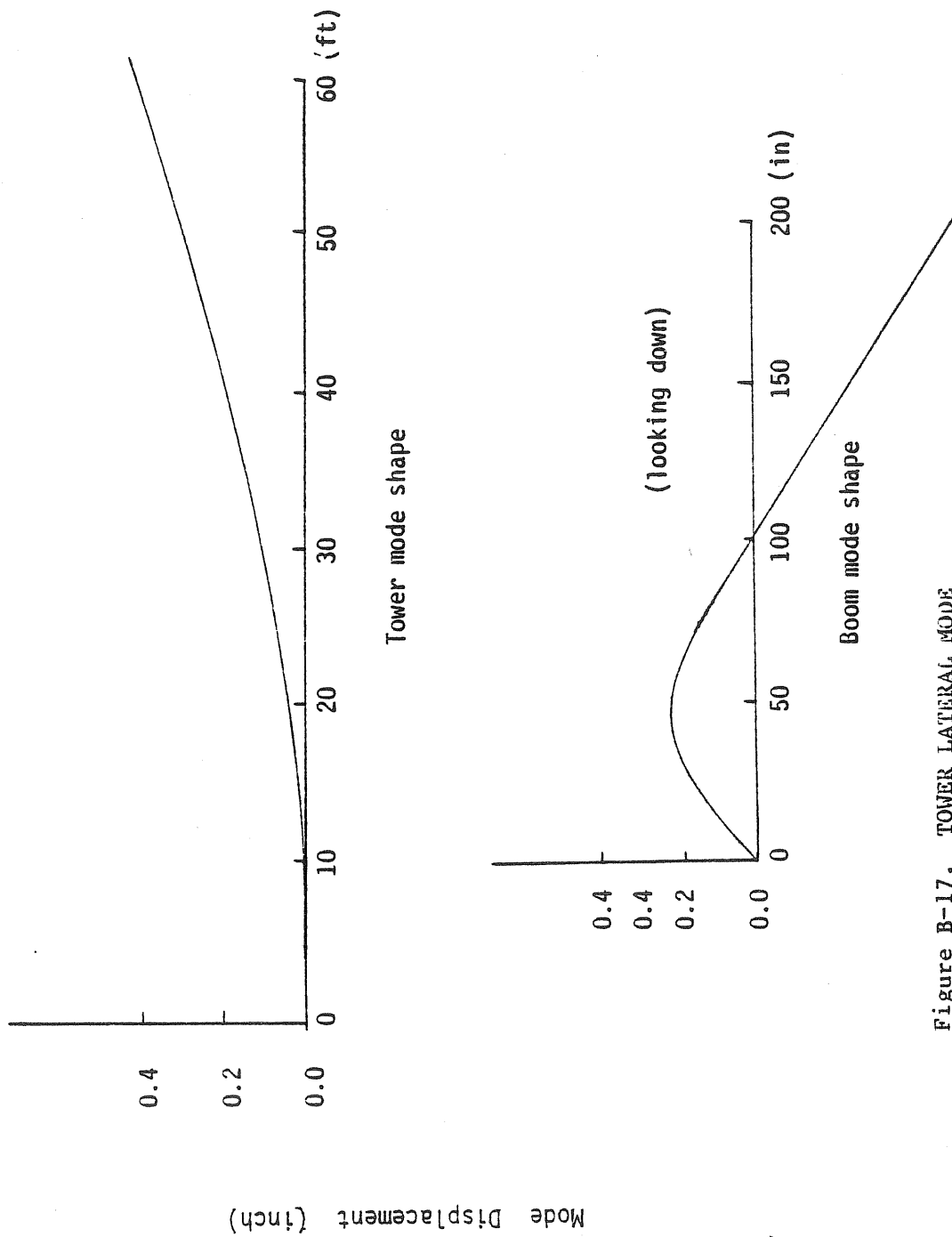
Figure B-17. TOWER LATERAL MODE

B22

APPENDIX C

ANALYSIS OF POTENTIAL WHIRL INSTABILITY

by

David A. Peters

S. Y. Chen

APPENDIX C

ANALYSIS OF POTENTIAL WHIRL INSTABILITY

In this Appendix we present the results of two independent
analyses for the critical speed of the wind-turbine, tower
system. The first analysis was a greatly simplified analysis
with many simplifying assumptions. The purpose of this
preliminary analysis was to give an early indication of any
potential problems. The second analysis was a more sophisticated
method, including four blade degrees of freedom.

C.1 SIMPLIFIED ANALYSIS

We considered a simple, two-degree-of-freedom model as shown
in Fig. C 1. In terms of rotating coordinates, (X, Y), the

potential and kinetic energies may be written as

$$V = 1/2\ Ky^2 + 1/2 \left(\frac{K\,K_R}{K+K_R}\right)\ x^2$$

$$T = 1/2m(\dot{x}-\Omega y)^2 + 1/2m(\dot{y}+\Omega x)^2$$

If one includes dampers, C, in the nonrotating system, the Rayleigh dissipation, function is

$$R = 1/2/C(\dot{x}-\Omega y)^2 + 1/2C(\dot{y}+\Omega x)^2$$

The resultant equations of motion are,

$$m\ddot{x} - 2m\Omega\dot{y} - m\Omega^2 x + C\dot{x} - C\Omega y + \frac{K\,K_R}{K+K_R}\ x = 0$$

$$m\ddot{y} + 2m\Omega\dot{x} - m\Omega^2 y + C\dot{y} + C\Omega x + Ky = 0$$

These may be nondimensionalized in terms of

$$y = \Omega t, \quad (\ )^* = d(\ )/d\psi, \quad \omega_y^2 = K/m\Omega^2, \quad \omega_R^2 = \frac{K_R}{m\Omega^2}$$

$$\omega_x^2 = (1/\omega_y^2 + 1/\omega_R^2)^{-1}, \quad \zeta = \frac{C}{2\sqrt{Km}}$$

$$\overset{**}{x} - 2\overset{*}{y} + (\omega_x^2 -1)x + 2\zeta\omega_y\overset{*}{x} - 2\zeta\omega_y y = 0$$

$$\overset{**}{y} + 2\overset{*}{x} + (\omega_y^2 -1)y + 2\zeta\omega_y\overset{*}{y} + 2\zeta\omega_y x = 0$$

For $\begin{Bmatrix} x \\ y \end{Bmatrix} = \begin{Bmatrix} a \\ b \end{Bmatrix} e^{st}$, we have in matrix form

$$\begin{bmatrix} s^2 + 2\zeta\omega_y S + (\omega_x^2 -1) & -2S - 2\zeta\omega_y \\ 2S + 2\zeta\omega_y & s^2 + 2\zeta\omega_y S + (\omega_y^2 -1) \end{bmatrix} \begin{Bmatrix} a \\ b \end{Bmatrix} = \begin{Bmatrix} 0 \\ 0 \end{Bmatrix}$$

C4

We now examine the above equation for $\zeta = 0$ and find that the unstable whirl region occurs between the points for which $S = 0$. The condition $S = 0$ gives

$$(\omega_x^2 - 1)(\omega_y^2 - 1) = 0 , \quad \omega_x = 1 , \quad \omega_y = 1$$

The second critical speed is $\omega_y = 1$, or $\Omega_2^2 = \frac{K}{m}$.

The first critical speed is

$$\frac{1}{\omega_x^2} = \frac{1}{\omega_y^2} + \frac{1}{\omega_R^2} = 1 , \quad \omega_y^2 = \frac{\omega_R^2}{1 + \omega_R^2} ,$$

or

$$\frac{1}{\Omega_1^2} = \frac{m}{K} + \frac{m}{K_R}$$

Now, to apply this to the wind turbine, we take $\sqrt{K/m}$ to be the tower frequency which is about 162 cpm. We take $\sqrt{K_R/m}$ to be the asymmetric inplane frequency which is about 440 cpm. Thus,

$$\Omega_1 = \frac{(162)(440)}{\sqrt{(162)^2 + (440)^2}} = 152 \text{ rpm}$$

$$\Omega_2 = 162 \text{ rpm}$$

Therefore, the critical whirl speeds (for symmetric tower) would be roughly 152-162 rpm.

Now we turn to the question of how much damping would be necessary to suppress the whirl. In other words, what value of ζ would prevent the determinant from becoming negative? The critical condition is

$$(\omega_x^2 - 1)(\omega_y^2 - 1) + 4\zeta^2 \omega_y^2 = 0$$

C5

The worst case should be near the center of the whirl region for which $\Omega = 157$ rpm,

$$\omega_x = \frac{152}{157} \;, \quad \omega_y = \frac{162}{157}$$

$$4\zeta^2 \left(\frac{162}{157}\right)^2 = (.0627)(.0647)$$

$$\zeta = \frac{.0637}{(1.03)(2)} = .031$$

Thus, for this simplified case, 3% structural damping would be required.

C.2 DETAILED ANALYSIS

We now describe a more detailed rotor-tower dynamic analysis. The model is sketched in Figure C 2. The rotor consists of two blades having both flap and inplane degrees of freedom. Thus, the rotor has a total of four degrees of freedom: a teetering (or asymmetric) flapping mode, a coning (or symmetric) flapping mode, a wind-up (or symmetric) inplane mode, and center-of-mass (or asymmetric) inplane mode. The rotor model includes a linear, quasi-steady strip-theory representation of aerodynamics including a uniform induced flow.

The rotor is attached to the tower by a rigid boom which has mass and mass moment-of-inertia. The tower has three degrees of freedom represented by two bending modes (in the z and y directions) and one yaw mode (about the x axis). The bending modes are simple parabolas, and the yaw mode is a linear, torsional deflection.

C6

Equations for the rotor are written in the rotating coordinate system, and those for the tower are written in the nonrotating system. A set of constraint equations (including boom geometry) couples the system.

Some of the more basic rotor parameters used in this study are:

$$C_{do} = .015, \; C_T = .004, \; C_Q = .00025, \; \sigma = .032,$$

Other parameters are as in Appendix B.

The nondimensional frequencies, also taken from the fan-plots of Appendix B of this report, are

$$\omega_\beta^2 = 1.77 + 5.2/\eta^2 \qquad \text{(symmetric)}$$

$$\omega_\zeta^2 = .75 + 5.2/\eta^2 \qquad \text{(asymmetric)}$$

$$\omega_\beta^2 = 3.17 \qquad \text{(asymmetric)}$$

$$\omega_q^2 = 0 \qquad \text{(symmetric)}$$

$$\omega_{tower} = .81/\eta \qquad \text{(both bendings)}$$

$$\omega_{tower} = 0 \qquad \text{(yaw)}$$

where η is a nondimensional rotor speed, RPM/250. The zero values of ω_q and ω_{tower} imply freely-yawing and auto-rotating.

The results of this analysis are shown in Figure C 3. The plot gives frequencies (nondimensionalized on RPM) as a function of 250/RPM, or $1/\eta$. We notice that the flap and lag coalesce at $1/\eta = 3.45$ (72 RPM) but the crossing is stable. The whirl speed is reached at $1/\eta = 1.23$ (200 RPM) but the system is stable. It is

the unequalness of the support springs (rather than structural
damping) which stabilizes this whirl. There is an unstable
ground resonance at $1/\eta = .1$ (2500 RPM) which is far above the
operating speed and beyond the limits of physical possibility.
Thus, the model shows the system to be stable at all speeds.

C.3 METHOD OF ANALYSIS

The analysis used to obtain the above results is based on stan-
dard techniques in the literature. The blade equations are those
of Ref. 1 with a root spring to account for teetering. The tower
equations are those for a cantilever beam, Ref. 2. The method of
solution is Floquet theory as described in Ref. 3.

C.4 REFERENCES

1. Wei, John Fu-Shang, <u>Flap-Lag Stability of Helicopter and</u>
    <u>Windmill Rotor Blades in Powered Flight and Autorotation</u>
    <u>by a Perturbation Method</u>, Doctor of Science Thesis,
    Washington University in St. Louis, August 1978.

2. Meirovitch, Leonard, <u>Analytical Methods in Vibrations</u>,
    Macmillan Co., New York, 1967, pp. 207-211.

3. Peters, D.A. and Hohenemser, K.H., "Application of the
    Floquet Transition Matrix to Problems of Lifting Rotor
    Stability", <u>Journal of the American Helicopter Society</u>,
    April 1971.
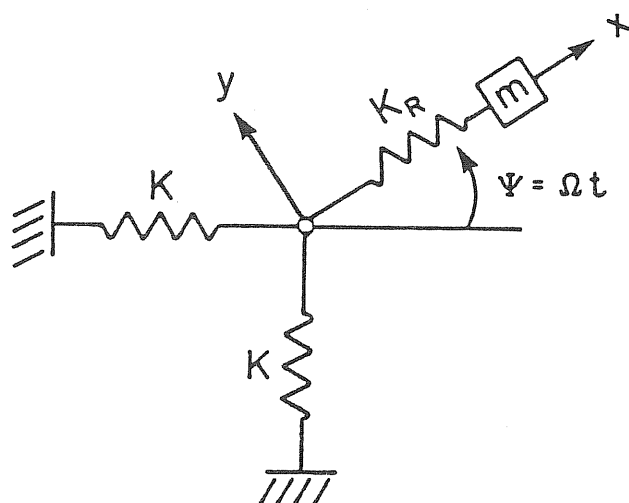
Figure C-1.   SIMPLIFIED SCHEMATIC
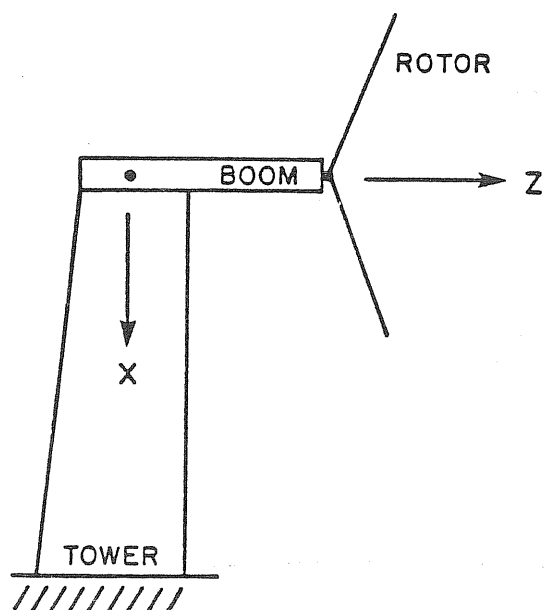
Figure C-2.   ROTOR-TOWER CONFIGURATION
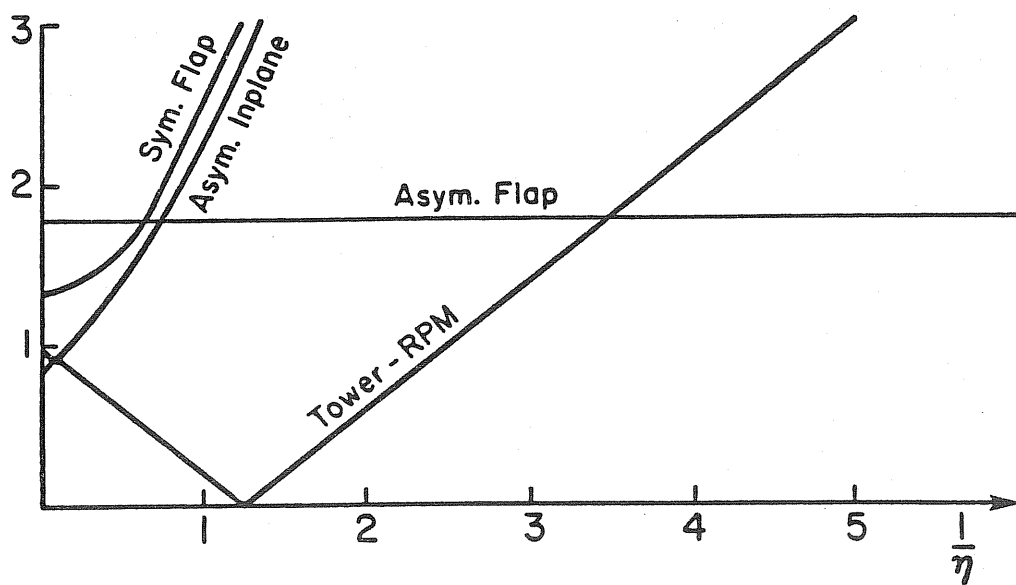
Figure C-3. FREQUENCIES VS. INVERSE OF RPM

APPENDIX D

DATA ANALYSIS SOFTWARE

by

Andrew H. P. Swift

APPENDIX D

DATA ANALYSIS SOFTWARE

D.   INTRODUCTION

Nine computer programs were developed to evaluate and analyze the performance of the experimental wind turbine.   Brief logical descriptions along with the program listing are presented here.

D.1   THE "WIND-2" PROGRAM

D.1.1   Program Logic

1.   Type operator instructions.
2.   Check variable conversion constants and desired values of cyclic pitch amplitude limits and furl angle.
3.   Calculate required furl set angle to account for rotor tilt and display result.
4.   Read clock – store start time.
5.   Sample wind speed and rpm twice consecutively and calculate mean value.
6.   Sample furl angle.
7.   Calculate current value of average rpm during test.
8.   Test rpm greater than preset value to avoid operation in starting regime.   If test fails go to #16.
9.   Test furl angle in limits.   If test fails go to #15.
10.   Sample cyclic pitch position 47 times (approximately 1 sec), store the values, calculate the amplitude of the signal and store the value.
11.   Test cyclic pitch within limits; if test fails, print warning on screen, toggle speaker and continue.
12.   Calculate bin number based on sampled wind speed and 0.5 m/s bin width.
13.   For each bin array, rpm and cyclic pitch amplitude, update the following values at the current bin number.   Maximum value in the bin, minimum value, number of samples, mean value, and standard deviation.
14.   Go to #17.
15.   Print furl angle out of limits, pause and go to #17.
16.   Print rpm out of limits and pause.
17.   Test wind ≠ 0, if test fails, go to #20.
18.   Calculate current wind speed, rpm, cyclic pitch amplitude and tip to wind speed ratio and print out values on the monitor.
19.   Go to #21.
20.   Print "wind is calm".
21.   Test to see if operator wishes to pause or stop sampling program.   If pause is desired, go to pause subroutine; if neither, go to #5 and repeat sampling.
22.   Read clock, calculate elapsed time of test and total rotor revolutions using current average rpm value.
23.   Print out bin arrays.
24.   Store bin array data on disk along with other pertinent test data.
25.   End.

D.1.2 Documentation for Sampling Programs

Documentation used for Wind 2, Wind 6, Rpm 6, Wind 2 Fast, Yawrate, and Binplot Programs:

AR	Average Rotor Speed.
B%	Bin Number (integer).
CB	Boom Calculation, Per Volt.
CC	Cyclic Pitch Calibration, Per Volt.
CF	Flap Bending Calibration, Per Volt.
COLLECT 5	
OBJECT	Assembly Language Sampling Program.
CR	Rpm Calibration, Per Volt.
CT	Torque Calibration, Per Volt.
CV	Generator Volts Calibration, Per Volt.
CW	Wind Calibration, Per Volt.
CY	Yaw Post Bending Calibration, Per Volt.
DAT.BINS	File Name for Bin Data or Disk.
D1	Ambient Temperature (^{o}C).
D2	Ambient Pressure (atm).
D3	Wind Direction (degrees).
D4	Generator Load (ohms).
D5	Gear Ratio, Rotor to Generator.
D6	Furl Angle, (degrees) Desired.
FC	Density Correction Factor

$$\rho_{(standard)} * \frac{1}{FC} = \rho_{(corrected)}$$

FS	Furl Set Angle Correcting for Rotor Tilt.
FV	Fast Variable Address Counter for Getting Sampled Data. See Collect 5 Program.
I	Sampled Variable Number.
J	Bin Number Counter.
K	Channel Number Counter.
K-$	Channel Names.
MAX	Maximum Value in Bin.
MEAN	Mean Value in Bin.
MN	Minimum Value in Bin.
N	Number of Samples in Bin.
NR	Number of rpm Samples for Average.
OS	Furl Voltage for Controlling Data Collection at Proper Furl Angle.
PM	Maximum Cyclic Pitch Voltage (0-255).
PN	Minimum Cyclic Pitch Voltage (0-255).
REV	Revolution Counter.
RPM	Rotor rpm.
S	Sampled Variable for Bin Data.
SBAR	Dummy Variable for Bin Data.
SE	Standard Deviation in Bin.
SLW	Slow Variable Address Counter (See Collect 5 Program).
ST	Number of Data Sets Counter.
TABLE	Pointer for Collect 5 Program.

TIME	Elapsed Time.
TSR	Tip Speed Ratio, R/v.
T-$	Clock Variables.
V1	Number of Digital Units Equivalent to One Volt for Analog Board.
WIND	Wind Speed (m/s).
Z$	Data File Name.

USED FOR WIND 2 ONLY

BP	Desired Furl Angle.
CCYCP	Same as CC.
CRPM	Same as CR.
CWIND	Same as CW.
F1	Sampled Furl Angle.
XS	Sampled Cyclic Pitch.
VF	Same as OS.

USED FOR YAWRATE ONLY

CDYN	Dynamic Channel Number
CYAW	Yaw Position Channel Number.
DH	Maximum Dynamic Value Sampled.
DL	Minimum Dynamic Value Sampled.
ET	Elapsed Time.
FURL	Furl Angle.
HS	Maximum rpm for Test.
LS	Minimum rpm for Test.
QP	Yaw Direction 0 = CCW, 1 = CW.
Y1P	1st Yaw Position.
Y2P	2nd Yaw Position.
Y%	Yaw Rate Bin (integer).

```
5    REM   THE WIND2 PROGRAM
6    REM   *****
10   D$ =  CHR$ (4)
20   PRINT D$;"MON C,I,O"
30   PRINT D$;"OPEN DAT.W2"
40   PRINT D$;"DELETE DAT.W2"
50   PRINT D$;"OPEN DAT.W2"
60   PRINT D$;"CLOSE DAT.W2"
61   REM   FILE DAT.W2 ON DISK IS CYCLIC PITCH DATA FILE.
65   HOME : VTAB 5: PRINT "THERE ARE 4 CONTROL INSTRUCTIONS:"
66   PRINT "1. 'O' PUTS CYCLIC PITCH DATA ON DISK": PRINT "   ANY KEY RECOVERS":
PRINT "2. 'CNTRL W' IS A WAIT ROUTINE": PRINT "3. 'CNTRL G' RECOVERS FOR DATA SA
MPLING": PRINT "4. 'CNTRL Z' STOPS PROG. AND STORES DATA"
67   PRINT : PRINT : INPUT "   PRESS RETURN TO CONT.";W$
71   V1 = 54
72   HOME : VTAB 5: PRINT " CHANNEL ASSIGNMENTS": PRINT ,"0 = WIND": PRINT ,"1 =
RPM": PRINT ,"2 = CYCLIC PITCH": PRINT : PRINT
73   PRINT ,"3=BOOM POTENT.": PRINT : PRINT
75   PRINT " PRESENTLY ONE VOLT = ";V1
76   PRINT "   CHANGE LINE 71 IF DESIRED"
77   PRINT : PRINT "CHECK VARIABLE CALIBRATION CONSTANTS IN LINE 85  IF REQUIRED
BEFORE RUNNING PROGRAM."
78   PRINT : INPUT "       PRESS RETURN TO CONT.";W$
79   HOME : VTAB 5
80   INPUT "INPUT MAX AND MIN CYCLIC PITCH CONTROL NUMBERS.. NORMAL VALUES ARE- 2
45 AND 4 ? ";PM,PN
85   CWIND = 6.705:CRPM = 60.0:CCYCP = 5
90   XR = CRPM / V1:NR = 0:AR = 0
100  DIM S(3),MAX(56,2),MN(56,2),MEAN(56,2),N(56,2),SE(56,2),SBAR(56,2)
110  DIM XS(50)
115  PRINT : PRINT : INPUT " ENTER FURL ANGLE INCLUDING ROTOR TILT > ";BP
117  XZ = ( COS (BP * 3.14159 / 180)) / ( COS (.14))
118  FS = - ATN (XZ / SQR ( - XZ * XZ + 1)) + 1.5708
119  PRINT : PRINT "FURL SET ANGLE IS ";FS * 180 / 3.14159;" DEGREES": PRINT
120  VF = FS * 6 * V1 * .95 / 3.14159
125  PRINT : PRINT : INPUT "   PRESS RETURN TO CONT.";W$
131  HOME : VTAB 12: INPUT "  PRESS RETURN TO START DATA SAMPLING";W$
132  GOSUB 2000:H$ = T$:T1$ = T$
140  FOR J = 1 TO 56: FOR K = 0 TO 2
150  MN(J,K) = 255
160  NEXT K
170  NEXT J
180  LL = 47
190  FOR I = 0 TO 1: REM SAMPLE WIND AND RPM
200  POKE  - 15871,I
202  P1 =  PEEK ( - 15872)
204  POKE  - 15871,I
206  P2 =  PEEK ( - 15872)
210  S(I) = .5 * (P1 + P2)
220  NEXT I
225  POKE  - 15871,3
226  F1 =  PEEK ( - 15872)
230  NR = NR + 1
240  AR = S(1) * XR / NR + (NR - 1) * AR / NR
245  IF S(1) < 15 THEN 660
246  IF F1 > (VF + 7) THEN 656
247  IF F1 < (VF - 4) THEN 656
250  REM   SAMPLE CYCLIC PITCH
260  FOR L = 1 TO LL
270  POKE  - 15871,2
280  XS(L) =  PEEK ( - 15872)
290  NEXT L
300  REM   CALC CYC.PIT AMP.
```

```
310 MM = 0
320 XN = 255
330 FOR L = 1 TO LL
340 IF XS(L) > MM THEN MM = XS(L)
350 IF XS(L) < XN THEN XN = XS(L)
360 NEXT L
370 IF MM > PM OR XN < PN THEN GOTO 390
380 GOTO 430
390 PRINT "CYCLIC PITCH OUT OF LIMITS!"
400 FOR B = 1 TO 140
410 S = PEEK ( - 16336)
420 NEXT B
430 S(2) = .5 * (MM - XN): REM S(2)=HALF TOTAL AMPL.
450 REM   BIN CALC, 56 BINS, .090           V/BIN
460 B% = (2.015 + S(0)) / 4.0268
470 REM  UPDATE BIN ARRAYS
480 FOR I = 1 TO 2
490 IF S(I) > MAX(B%,I) THEN MAX(B%,I) = S(I)
500 IF S(I) < MN(B%,I) THEN MN(B%,I) = S(I)
510 N(B%,I) = N(B%,I) + 1
520 MEAN(B%,I) = (S(I) + ((N(B%,I) - 1) * MEAN(B%,I))) / N(B%,I)
530 SBAR(B%,I) = (SBAR(B%,I) * (N(B%,I) - 1) + S(I) ^ 2) / N(B%,I)
540 SE(B%,I) = SQR (SBAR(B%,I) - MEAN(B%,I) ^ 2)
550 NEXT I
560 WW = PEEK ( - 16384)
570 IF WW < > (128 + 68) THEN GOTO 675
580 REM  PUSHING THE D KEY CAUSES THE
590 REM  CYCLIC PITCH DATA TO BE STORED ON DISK. PUSH ANY OTHER KEY TO STOP.
600 PRINT D$;"APPEND DAT.W2"
610 PRINT D$;"WRITE DAT.W2"
620 FOR MM = 1 TO LL
630 PRINT XS(MM)
640 NEXT MM
650 PRINT D$;"CLOSE DAT.W2"
655 GOTO 675
656 PRINT : PRINT "FURL ANGLE OUT OF LIMITS - RESET"
657 PRINT : PRINT "  BIN DATA NOT UPDATED"
658 FOR IM = 1 TO 1200: NEXT IM
659 GOTO 675
660 PRINT : PRINT : PRINT ,"RPM TOO LOW"
665 PRINT : PRINT ,"BIN DATA NOT UPDATED"
666 PRINT : PRINT
670 FOR WQ = 1 TO 1000: NEXT WQ
675 IF S(0) = 0 THEN GOTO 760
680 WIND = CWIND * S(0) / V1:RPM = CRPM * S(1) / V1:CYP = CCYCP * S(2) / V1
690 TSR = .4 * RPM / WIND
700 TSR = .1 * INT (TSR * 10 + .5)
710 RPM = INT (RPM + .5):CYP = .1 * INT (10 * CYP + .5)
720 PRINT "TIP SPEED R","RPM","CYC PTCH"
730 PRINT TSR,RPM,CYP
740 WIND = .1 * INT (WIND * 10 + .5): PRINT : PRINT "WIND,M/S": PRINT WIND: PRI
NT : PRINT : PRINT
750 GOTO 770
760 PRINT "WIND IS CALM"
770 REM
780 REM  LOGIC FOR STOPPING PROGRAM
785 REM  WAIT SUBR..PRESS CNTRL W
786 Q6 = PEEK ( - 16384)
787 IF Q6 = 151 THEN GOSUB 1500
790 REM  TO STOP SAMPLING PRESS CNTRL Z
800 XX = PEEK ( - 16384)
810 IF XX < > (128 + 26) THEN 190
```

```
811  GOSUB 2000
812  HOME : VTAB 5
814  GOSUB 3000:H2 = STD
816  T$ = T1$: GOSUB 3000:H1 = STD
818  TIME = (H2 - H1) / 3600
820  ST = 0: FOR K = 1 TO 2: FOR J = 1 TO 56
830  IF M(J,K) = 0 THEN 850
840  ST = ST + 1
850  NEXT J: NEXT K
860  PRINT "TIME OF TEST START WAS:": PRINT : PRINT H$
870  PRINT "  ELAPSED TIME OF TEST WAS": PRINT ,TIME;" HOURS"
880  REV =  INT (AR * 60 * TIME + .5)
885  PRINT : PRINT "TOTAL ROTOR REV.= ";REV;" REVS."
886  PRINT : PRINT " INSERT DATA DISK IF DESIRED"
887  PRINT : INPUT "PRESS RETURN TO CONT.";H$
890  PRINT D$;"OPEN DAT.BINS"
900  PRINT D$;"DELETE DAT.BINS"
910  PRINT D$;"OPEN DAT.BINS"
920  PRINT D$;"WRITE DAT.BINS"
925  PRINT V1: PRINT CWIND: PRINT CRPM: PRINT CCYCP
930  PRINT ST: PRINT H$
940  PRINT TIME
950  PRINT BP: PRINT REV
960  FOR K = 1 TO 2: FOR J = 1 TO 56
970  IF M(J,K) = 0 THEN 1060
980  PRINT K
990  PRINT J
1000  PRINT M(J,K)
1010  PRINT MAX(J,K)
1020  PRINT MEAN(J,K)
1030  PRINT MN(J,K)
1040  PRINT SE(J,K)
1050  PRINT SBAR(J,K)
1060  NEXT J
1070  NEXT K
1080  PRINT D$;"CLOSE DAT.BINS"
1090  PRINT D$;"PR#1"
1100  PRINT "START TIME= ";H$
1110  PRINT "ELAPSED TIME= ";TIME;" HOURS": PRINT
1120  PRINT "FURL ANGLE = ";BP;" DEGREES"
1130  PRINT "ROTOR REV.(CALC.)= ";REV: PRINT : PRINT
1150  PRINT "CH#/BIN#/N#/MEAN/STD.DEV/MAX/MIN"
1160  PRINT
1170  FOR K = 1 TO 2: FOR J = 1 TO 56
1180  IF M(J,K) = 0 THEN 1220
1190  PRINT K;"   ";J;"   ";M(J,K);"   ";MEAN(J,K);"   ";SE(J,K);"   ";MAX(J,K);"   ";
MN(J,K)
1220  NEXT J
1230  NEXT K
1240  PRINT D$;"PR#0"
1250  HOME : VTAB 5: PRINT "DONT FORGET TO RENAME DAT.BINS. DATA IS DELETED WHEN
PROGRAM IS RUN AGAIN.!!!!!"
1260  END
1500  REM   SUBR WAIT. CNTRL G RETURNS TO PROGRAM
1510  POKE  - 16368,0
1517 SZ =  - 16336
1520  FOR QZ = 1 TO 90:AZ =  PEEK (SZ): NEXT QZ
1530 Q7 =  PEEK ( - 16384)
1540  IF Q7 <  > (135) THEN 1520
1545  POKE  - 16368,0
1550  RETURN
2000  REM
2005  REM  *** SUBR - GET THE TIME
```

```
2010  REM *** THESE NEED TO BE CHANGED IF DISK IS NOT USED
2025  REM  FOR SLOT 4 CLOCK ONLY ***
2030  PRINT D$;"IN#4"
2040  PRINT D$;"PR#4"
2050  INPUT " ";T$
2060  PRINT D$;"IN#0"
2070  PRINT D$;"PR#0"
2080  RETURN
3000  REM
3001  REM  FOR LEAP YEAR***:L=1
3005  REM  SUBR - STD
3006  REM
3010  REM  CALCULATE SECONDS TO DATE FOR EACH TIME (STD)
3020  REM  THIS IS THE NUMBER OF SECONDS SINCE JANUARY 1
3030  REM  DO THIS FOR STRING TIME T$
3040  REM    RETURN A NUMBER - STD
3050  REM
3060  REM  FIND #'S FOR DATE AND TIME
3070  MT =  VAL ( MID$ (T$,1,2))
3080  D =  VAL ( MID$ (T$,4,2))
3090  H =  VAL ( MID$ (T$,7,2))
3100  M =  VAL ( MID$ (T$,10,2))
3110  S =  VAL ( MID$ (T$,13,6))
3130  REM  CALCULATE DAYS TO DATE - DTD
3135  RESTORE
3140  DTD = 0
3150  FOR I = 1 TO MT
3160  READ J
3170  DTD = DTD + J
3180  NEXT I
3200  DATA  0,31,28,31,30,31,30,31,31,30,31,30,31
3205  REM   ADD IN DAYS AND LEAP YEAR DAY
3210  DTD = DTD + D
3230  IF MT > 2 AND L = 1 THEN DTD = DTD + 1
3240  REM  FIND SECONDS TO DATE - STD
3250  STD = DTD * 86400 + H * 3600 + M * 60 + S
3300  RETURN
```

D.2. THE "COLLECT 5" SUBROUTINE BY MICRO SYSTEMS DEVELOPMENT

The following narrative and flow chart (Fig. D-1) describe the task accomplished by the machine language program developed by Micro Systems Development Company. They are designed to give an overview and a logical description of the program. They do not describe the actual sequence of events which was optimized for CPU/memory efficiency.

Upon call, the machine language program performs initialization and bookkeeping functions, sets flags, etc. It checks for user interrupts, and services them on a first in first out basis. Then the A/D board fast channels are processed and the local data table updated. This process is repeated until a data set (128 values for each variable) is collected at which point the less rapidly changing variables are read once.

If the rotor speed is below a preset value data are not desired, and control is returned to the calling program; otherwise, a test for critical loads is conducted. Next the global data bank is updated and mean and axial amplitude values are calculated completing the task of a single call.

When an unacceptable load condition is confirmed, the data buffers are transferred to random access memory, and rapid read/dump-to-disk cycle initiated. This will result in each of the fast variable values being written to disk at a rate of approximately 128 values/second until the disk is filled, which should give extremely detailed time histories for about 2 minutes following detection of a critical load.
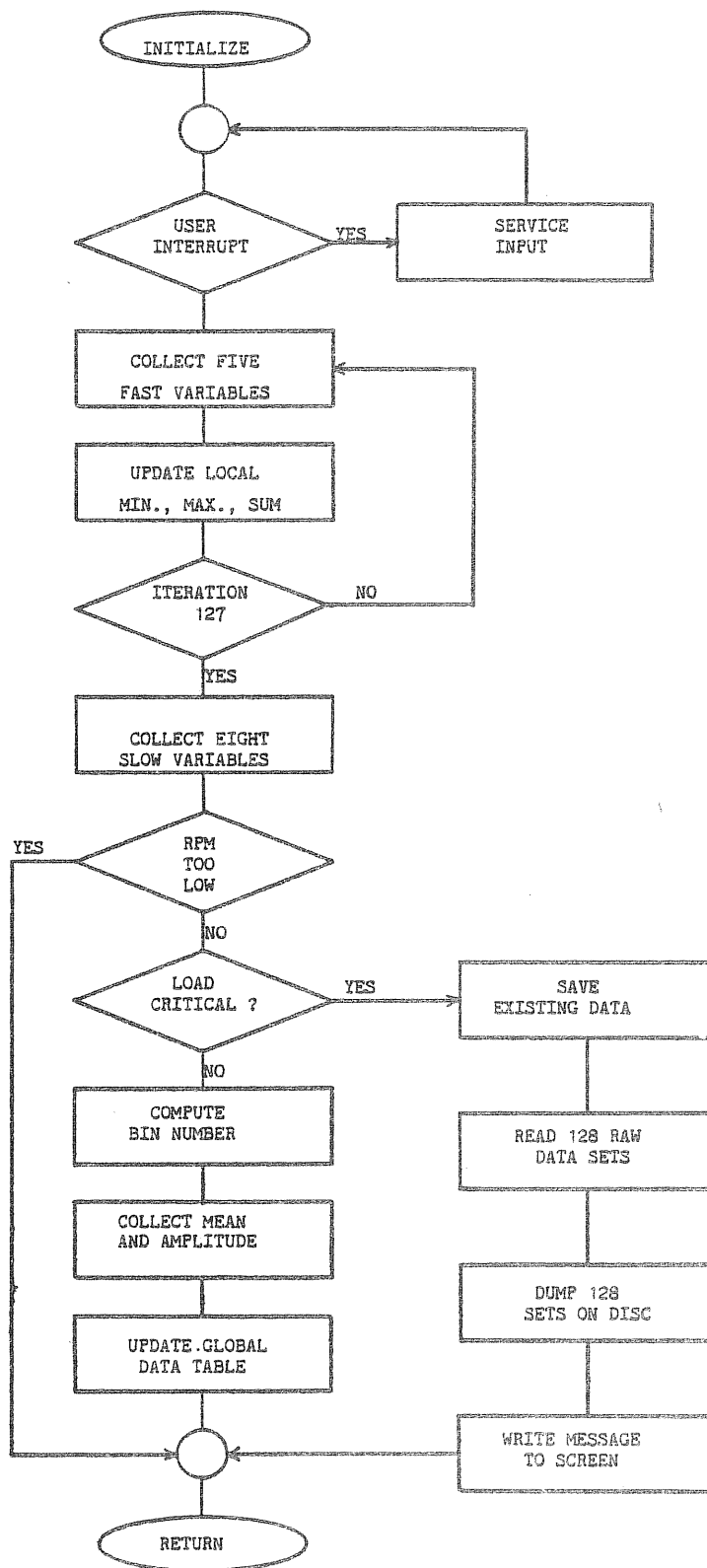
Figure D-1.   FLOW CHART FOR "COLLECTIVE FIVE" SUBROUTINE

```
1000 * DATA COLLECTION
1010 * MICRO SYS DEV CO
1020 * 5/24/80
1030 *
1040 * COLLECT5 SOURCE
1050 *
1060 * REVISION 8/30/80
1070 *
1080 * ORIGIN = 9000
1090 * PROGRAM SPACE = 768 BYTES
1100 *     $9000 - $92FF
1110 * GLOBAL DATA TABLE = 768 BYTES
1120 *     $9300 - $95FF
1130 * DOS SPACE = 10752 BYTES
1140 *     $9600 - $BFFF
1150 * DISK APLSFT SPACE = 10243 BYTES
1160 *     $0800 - $3003
1170 * HARDWARE SPACE = 2047 BYTES
1180 *     $0000 - $07FF
1190 *
1200 * SPACE REMAINING = 25341 BYTES
1210 *
1220 * INDIRECT INDEX POINTERS
1230 *    $FC/$FD - GLOBAL   "BTBL"
1240 *    $FE/$FF - DATA     "DPNT"
1250 *
1260       .OR $9000
1270       .TA $0800
1280 *
1290 * DATA TABLE BASE ADDRESS
1300 *    HIGH BYTE ONLY  LOW = $00
1310 DPNT .EQ $00FE
1320 BTBL .EQ $00FC
1330 LTBL .EQ $02A2
1340 BUFR .EQ $0200
1350 *
1360 CHNL .EQ $C201      A-D PORTS
1370 STDM .EQ $C202
1380 INTM .EQ $C203
1390 DATA .EQ $C200
1400 EOCF .EQ $C202
1410 INTF .EQ $C203
1420 *
1430 SPCK .EQ $C0C6      CLOCK PORTS
1440 STCK .EQ $C0C5
1450 TME1 .EQ $C0C4
1460 TME2 .EQ $C0C3
1470 TME3 .EQ $C0C2
1480 TME4 .EQ $C0C1
1490 TME5 .EQ $C0C0
1500 *
1510 RWTS .EQ $03D9      FIRMWARE
1520 KYBD .EQ $C000      SUBROUTINES
1530 STRB .EQ $C010
1540 SPKR .EQ $FBDD
1550 YAWN .EQ $FCA8
1560 IORS .EQ $FF3F
1570 IOSV .EQ $FF4A
1580 *
```

```
                        1590 *
                        1600 *
9000- 20 4A FF          1610 WUTA JSR IOSV      SAVE REGISTERS
9003- 20 0A 90          1620      JSR MODE      PROGRAM
9006- 20 3F FF          1630      JSR IORS      RESTORE REG'S
9009- 60                1640      RTS
                        1650 *
900A- AD EC 92          1660 MODE LDA CRIT      CRITICAL?
900D- F0 0E             1670      BEQ MOD2      NO!
900F- AD CE 92          1680      LDA CMND
9012- C9 02             1690      CMP #02       CMND=WRITE?
9014- D0 03             1700      BNE MOD1      NO!
9016- 4C 4F 92          1710      JMP CRI0
9019- 8D EC 92          1720 MOD1 STA CRIT      THEN CMND=3
901C- 60                1730      RTS
                        1740 *
901D- AD CE 92          1750 MOD2 LDA CMND      INITIALIZE
9020- D0 03             1760      BNE MOD3      PROGRAM?
9022- 4C 09 92          1770      JMP INIT
                        1780 *
9025- C9 04             1790 MOD3 CMP #04       INITIALIZE
9027- D0 09             1800      BNE STRT      DISK?
9029- 20 BA 92          1810      JSR DISK
902C- A9 02             1820      LDA #02       SET CMND
902E- 8D CE 92          1830      STA CMND      TO WRITE
9031- 60                1840      RTS
                        1850 *
9032- AD 00 C0          1860 STRT LDA KYBD      TEST FOR
9035- 10 18             1870      BPL ENTR      USER
9037- 2C 10 C0          1880      BIT STRB      INTERRUPT
903A- C9 DA             1890      CMP #218      'Z'       + 128
903C- D0 06             1900      BNE ENT0
903E- A9 02             1910      LDA #02
9040- 8D F6 92          1920      STA ABRT
9043- 60                1930      RTS
                        1940 *
9044- 20 DD FB          1950 ENT0 JSR SPKR      HALT PROGRAM
9047- 2C 00 C0          1960      BIT KYBD
904A- 10 F8             1970      BPL ENT0
904C- 2C 10 C0          1980      BIT STRB
                        1990 *
904F- AE E8 92          2000 ENTR LDX FVAR      INITIALIZE
9052- A0 00             2010      LDY #00       LOCAL DATA
9054- 98                2020      TYA           TABLE
9055- 99 A2 02          2030 ENT3 STA LTBL,Y
9058- C8                2040      INY
9059- A9 FF             2050      LDA #$FF
905B- 99 A2 02          2060      STA LTBL,Y
905E- C8                2070      INY
905F- A9 00             2080      LDA #00
9061- 99 A2 02          2090      STA LTBL,Y
9064- C8                2100      INY
9065- 99 A2 02          2110      STA LTBL,Y
9068- C8                2120      INY
9069- 99 A2 02          2130      STA LTBL,Y
906C- C8                2140      INY
```

```
906D- CA       2150       DEX
906E- D0 E5    2160       BNE ENT3
9070- AD EA 92 2170       LDA ASET
9073- CD E7 92 2171       CMP MSET
9076- D0 0C    2172       BNE ENT4
9078- A9 00    2173       LDA #00
907A- 8D EA 92 2174       STA ASET
907D- 85 FE    2175       STA DPNT
907F- AD CB 92 2176       LDA BUFL+1
9082- 85 FF    2177       STA DPNT+1
9084- 20 D9 90 2180 ENT4  JSR PNTB
9087- 20 8D 90 2190       JSR FAST
908A- 4C E6 90 2200       JMP NEXT
               2210 *
908D- 20 A3 90 2220 FAST  JSR FAS1        FAST VARIABLES
9090- AD EC 92 2230       LDA CRIT
9093- D0 03    2240       BNE FAS0
9095- 20 65 91 2250       JSR MXMN
9098- C8       2260 FAS0  INY
9099- C0 80    2270       CPY #128
909B- F0 26    2280       BEQ SLOW
909D- 20 B5 90 2290       JSR FAS2
90A0- 4C 8D 90 2300       JMP FAST
               2310 *
90A3- 20 49 91 2340 FAS1  JSR GET
90A6- 9D 00 02 2350       STA BUFR,X
90A9- A9 80    2355       LDA #128
90AB- 20 5B 91 2356       JSR UPAD
90AE- E8       2360       INX
90AF- EC E8 92 2370       CPX FVAR
90B2- D0 EF    2380       BNE FAS1
90B4- 60       2390       RTS
               2400 *
90B5- A2 00    2410 FAS2  LDX #00
90B7- 20 0E 91 2420       JSR NEX1
90BA- AD EB 92 2440       LDA DLY1
90BD- F0 03    2450       BEQ FAS3
90BF- 20 A8 FC 2460       JSR YAWN
90C2- 60       2470 FAS3  RTS
               2480 *
90C3- A0 00    2490 SLOW  LDY #00         SLOW VARIABLES
90C5- A0 00    2510       LDY #00
90C7- 20 49 91 2520 SLO1  JSR GET
90CA- 99 00 02 2530       STA BUFR,Y
90CD- E8       2540       INX
90CE- C8       2550       INY
90CF- CC E9 92 2560       CPY SVAR
90D2- D0 F3    2570       BNE SLO1
90D4- 98       2575       TYA             PLUS 8
90D5- 20 5B 91 2577       JSR UPAD        TO INDIR ADDRES
90D8- 60       2580       RTS
               2590 *
90D9- A0 00    2600 PNTB  LDY #00
90DB- A5 FE    2610       LDA DPNT        SET
90DD- 8D EF 92 2620       STA PBSE        BASE
90E0- A5 FF    2630       LDA DPNT+1      POINTER
90E2- 8D F0 92 2640       STA PBSE+1
90E5- 60       2650       RTS
```

D14

```
                2660 *
90E6- AD FA 92  2670 NEXT LDA TCRI
90E9- 8D EC 92  2680      STA CRIT
90EC- A2 00     2690      LDX #00
90EE- A0 00     2700      LDY #00
90F0- BD 00 02  2710      LDA BUFR,X     COMPUTE BIN #
90F3- 29 FC     2720      AND #$FC
90F5- 8D ED 92  2730      STA WIND
90F8- 4A        2740      LSR
90F9- 4A        2750      LSR
90FA- 8D EE 92  2760      STA BINN
90FD- 20 F1 91  2770      JSR GBIN
9100- E8        2780      INX
9101- BD 00 02  2790      LDA BUFR,X
9104- CD F9 92  2800      CMP LRPM       RPM TEST
9107- B0 10     2810      BCS LAS0
9109- A9 01     2820      LDA #01        SET FLAG & RET
910B- 8D F6 92  2830      STA ABRT       IF TOO SLOW
910E- AD EF 92  2831 NEX1 LDA PBSE
9111- 85 FE     2832      STA DPNT
9113- AD F0 92  2833      LDA PBSE+1
9116- 85 FF     2834      STA DPNT+1
9118- 60        2840      RTS
9119- D1 FC     2850 LAS0 CMP (BTBL),Y
911B- 90 06     2860      BCC LAS1
911D- 91 FC     2870      STA (BTBL),Y   MAX GLOBAL RPM
911F- C8        2880      INY
9120- 4C 2A 91  2890      JMP LAS2
9123- C8        2900 LAS1 INY
9124- D1 FC     2910      CMP (BTBL),Y
9126- B0 02     2920      BCS LAS2
9128- 91 FC     2930      STA (BTBL),Y   MIN GLOBAL RPM
912A- E8        2940 LAS2 INX
912B- BD 00 02  2950      LDA BUFR,X
912E- CD F4 92  2960      CMP ALTH       MAX ALT TEMP
9131- 90 06     2970      BCC LAS3
9133- 8D F4 92  2980      STA ALTH
9136- 4C 41 91  2990      JMP LAS4
9139- CD F5 92  3000 LAS3 CMP ALTL       MIN ALT TEMP
913C- B0 03     3010      BCS LAS4
913E- 8D F5 92  3020      STA ALTL
9141- C8        3030 LAS4 INY
9142- 20 B6 91  3040      JSR MEAN
9145- EE EA 92  3130      INC ASET
9148- 60        3160 END  RTS
                3170 *
9149- BD 07 92  3180 GET  LDA VCHN,X     A-D ACCESS
914C- 8D 01 C2  3190      STA CHNL
914F- AD FB 92  3200      LDA DLY2
9152- 20 A8 FC  3210      JSR YAWN
9155- AD 00 C2  3220      LDA DATA
9158- 91 FE     3230      STA (DPNT),Y
915A- 60        3240      RTS
                3250 *
915B- 18        3260 UPAD CLC            UPDATE POINTER
915C- 65 FE     3270      ADC DPNT
915E- 85 FE     3280      STA DPNT
9160- 90 02     3290      BCC NOCY
9162- E6 FF     3300      INC DPNT+1
9164- 60        3310 NOCY RTS
```

```
                       3320  *
9165- 98               3330  MXMN  TYA              LOCAL DATA MAX
9166- 48               3340        PHA              MIN MEAN TEST
9167- 8A               3345        TXA
9168- 48               3347        PHA
9169- A2 00            3350        LDX  #00
916B- A0 00            3360        LDY  #00
916D- B9 00 02         3370  MXM1  LDA  BUFR,Y
9170- DD A2 02         3380        CMP  LTBL,X
9173- 90 1F            3390        BCC  MXM5
9175- F0 03            3400        BEQ  MXM2
9177- 9D A2 02         3410        STA  LTBL,X
917A- E8               3420  MXM2  INX
917B- E8               3430  MXM3  INX
917C- E8               3435        INX
917D- 18               3440        CLC
917E- 7D A2 02         3450        ADC  LTBL,X
9181- 9D A2 02         3460        STA  LTBL,X
9184- 90 1A            3470        BCC  MXM7
9186- E8               3480        INX
9187- FE A2 02         3490        INC  LTBL,X
918A- C8               3500  MXM4  INY
918B- CC E8 92         3510        CPY  FVAR
918E- F0 14            3520        BEQ  MXM8
9190- E8               3530        INX
9191- 4C 6D 91         3540        JMP  MXM1
9194- E8               3550  MXM5  INX
9195- DD A2 02         3560        CMP  LTBL,X
9198- B0 03            3570        BCS  MXM6
919A- 9D A2 02         3580        STA  LTBL,X
919D- 4C 7B 91         3590  MXM6  JMP  MXM3
91A0- E8               3600  MXM7  INX
91A1- 4C 8A 91         3610        JMP  MXM4
91A4- 68               3620  MXM8  PLA
91A5- AA               3625        TAX
91A6- 68               3627        PLA
91A7- A8               3630        TAY
91A8- AD F8 92         3640        LDA  CRIV
91AB- CD 00 02         3650        CMP  BUFR
91AE- B0 05            3660        BCS  MXM9
91B0- A9 01            3670        LDA  #01
91B2- 8D FA 92         3680        STA  TCRI
91B5- 60               3690  MXM9  RTS
                       3700  *
91B6- A2 00            3710  MEAN  LDX  #00         COMPUTE MEAN &
91B8- BD A2 02         3720  MEA1  LDA  LTBL,X      UPDATE GLOBAL
91BB- 48               3730        PHA              MAX/MIN
91BC- D1 FC            3740        CMP  (BTBL),Y
91BE- 90 07            3750        BCC  MEA2
91C0- 91 FC            3760        STA  (BTBL),Y    GLOBAL MAX
91C2- C8               3770        INY
91C3- E8               3780        INX
91C4- 4C 02 91         3790        JMP  MEA3
91C7- C8               3800  MEA2  INY
91C8- E8               3810        INX
91C9- BD A2 02         3820        LDA  LTBL,X
91CC- D1 FC            3830        CMP  (BTBL),Y
91CE- B0 02            3840        BCS  MEA3
91D0- 91 FC            3850        STA  (BTBL),Y    GLOBAL MIN
91D2- C8               3860  MEA3  INY
91D3- 68               3870        PLA
```

```
91D4- 38          3880        SEC
91D5- FD A2 02 3890        SBC LTBL,X
91D8- 4A          3900        LSR
91D9- E8          3910        INX
91DA- 9D A2 02 3920        STA LTBL,X      LOCAL
91DD- E8          3930        INX             AMPLITUDE
91DE- 1E A2 02 3940        ASL LTBL,X
91E1- E8          3950        INX
91E2- 3E A2 02 3960        ROL LTBL,X      MEAN-INTEGER
91E5- CA          3970        DEX
91E6- 5E A2 02 3980        LSR LTBL,X      MEAN-REMAINDER
91E9- E8          3990        INX
91EA- E8          4000        INX
91EB- CC F1 92 4010        CPY FUR1
91EE- D0 C8       4020        BNE MEA1
91F0- 60          4030        RTS
                  4040 *
                  4050 * COMPUTE GLOBAL BIN ADDRESS
                  4060 *
91F1- AD F3 92 4070 GBIN LDA GTBL
91F4- 85 FD       4080        STA BTBL+1
91F6- AD ED 92 4090        LDA WIND        BIN # X 4
91F9- 48          4100        PHA
91FA- 0A          4110        ASL             BIN # X 8
91FB- 20 02 92 4120        JSR GBI1
91FE- 68          4130        PLA
91FF- 18          4140        CLC
9200- 65 FC       4150        ADC BTBL        (X 4) + (X 8)
9202- 85 FC       4160 GBI1 STA BTBL
9204- 90 02       4170        BCC GBI2
9206- E6 FD       4180        INC BTBL+1
9208- 60          4190 GBI2 RTS
                  4200 *
9209- AD F2 92 4210 INIT LDA BASE        INITIALIZE
920C- 8D CB 92 4220        STA BUFL+1
920F- 8D F0 92 4230        STA PBSE+1
9212- 85 FF       4240        STA DPNT+1
9214- A9 C2       4250        LDA #TBL0       VARIABLE
9216- 85 06       4260        STA $06         REFERENCE
9218- A9 92       4270        LDA /TBL0       ADDRESS
921A- 85 07       4280        STA $07
921C- A9 00       4290        LDA #00
921E- 85 FE       4300        STA DPNT
9220- 85 FC       4310        STA BTBL
9222- AD F3 92 4320        LDA GTBL
9225- 85 FD       4330        STA BTBL+1
9227- A2 03       4340        LDX #03         INITIALIZE
9229- A0 00       4350        LDY #00         GLOBAL DATA
922B- A9 00       4360 INI1 LDA #00          TABLE
922D- 91 FC       4370        STA (BTBL),Y
922F- C8          4380        INY
9230- A9 FF       4390        LDA #$FF
9232- 91 FC       4400        STA (BTBL),Y
9234- C8          4410        INY
9235- D0 F4       4420        BNE INI1
9237- CA          4430        DEX
9238- F0 05       4440        BEQ INI2
923A- E6 FD       4450        INC BTBL+1
923C- 4C 2B 92 4460        JMP INI1
```

```
923F- A9 03     4470 INI2 LDA #03
9241- 8D CE 92  4480      STA CMND
9244- AD E8 92  4490      LDA FVAR
9247- 0A        4500      ASL
9248- 18        4505      CLC
9249- 69 02     4507      ADC #02
924B- 8D F1 92  4510      STA FVR1
924E- 60        4520      RTS
                4530 *
924F- AD F7 92  4540 CRI0 LDA CRIL     CRITICAL
9252- 8D E7 92  4550      STA MSET     PROCESSING
9255- AD EA 92  4560      LDA ASET     ROUTINE
9258- 8D 00 02  4600      STA BUFR
925B- AD 01 02  4610      LDA BUFR+1
925E- 8D CB 92  4620      STA BUFL+1
9261- 20 BA 92  4630      JSR DISK     SAVE.INP BUFR
9264- 20 96 92  4640      JSR RITE     SAVE PRE DATA
9267- A9 00     4650 CRI1 LDA #00
9269- 85 FE     4660      STA DPNT
926B- AD F2 92  4670      LDA BASE
926E- 85 FF     4680      STA DPNT+1
9270- A9 20     4690      LDA #32
9272- 8D EA 92  4700      STA ASET
9275- 20 D9 90  4710 CRI2 JSR PNTB     SET BASE ADDR
9278- A2 00     4720      LDX #00
927A- 20 8D 90  4730 CRI3 JSR FAST     GET 32
927D- CE EA 92  4750      DEC ASET
9280- AD EA 92  4760      LDA ASET
9283- D0 F0     4770      BNE CRI2
9285- 20 96 92  4780      JSR RITE
9288- CE E7 92  4790      DEC MSET
928B- AD E7 92  4800      LDA MSET
928E- D0 D7     4810      BNE CRI1
9290- A9 02     4820      LDA #02
9292- 8D EC 92  4830      STA CRIT
9295- 60        4840      RTS
                4850 *
9296- AD F2 92  4860 RITE LDA BASE     DISK BUFFER
9299- 8D CB 92  4870      STA BUFL+1   = RAW DATA TBL
929C- A2 51     4880      LDX #81
929E- EE C7 92  4890 CRI4 INC SECT
92A1- AD C7 92  4900      LDA SECT
92A4- C9 0D     4910      CMP #13
92A6- D0 08     4920      BNE CRI5
92A8- A9 00     4930      LDA #00
92AA- 8D C7 92  4940      STA SECT
92AD- EE C6 92  4950      INC TRAK
92B0- 20 BA 92  4960 CRI5 JSR DISK     SAVE DATA TABL
92B3- EE CB 92  4970      INC BUFL+1
92B6- CA        4980      DEX
92B7- D0 E5     4990      BNE CRI4
92B9- 60        5000      RTS
                5010 *
                5020 *
92BA- A0 C2     5030 DISK LDY #TBL0
92BC- A9 92     5040      LDA /TBL0
92BE- 20 D9 03  5050      JSR RWTS
92C1- 60        5060 DONE RTS
                5070 *
                5080 *
                5090 *
```

D18

```
92C2- 01 60 01
92C5- 00          5100 TBL0 .HS 01600100
92C6- 00          5110 TRAK .DA #00
92C7- 00          5120 SECT .DA #00
92C8- D3          5130 DCTL .DA #DCTA
92C9- 92          5140 DCTH .DA /DCTA
92CA- 00 3F       5150 BUFL .DA $3F00
92CC- 00 00       5160 TBL1 .HS 0000
92CE- 00          5170 CMND .DA #00
92CF- 00 00 60
92D2- 01          5180 TBL2 .HS 00006001
92D3- 00 01 EF
92D6- D8          5190 DCTA .HS 0001EFD8
                  5200 *
                  5210 * CHANNEL ASSIGNMENT-SEQUENCE
                  5220 *
92D7- 00 01 02
92DA- 03          5230 VCHN .HS 00010203
92DB- 04 05 06
92DE- 07          5240      .HS 04050607
92DF- 08 09 0A
92E2- 0B          5250      .HS 08090A0B
92E3- 0C 0D 0E
92E6- 0F          5260      .HS 0C0D0E0F
                  5270 *
92E7- 20          5280 MSET .DA #32       VARIABLES &
92E8- 05          5290 FVAR .DA #05       CONSTANTS
92E9- 08          5300 SVAR .DA #08
92EA- 00          5310 ASET .DA #00
92EB- 2E          5320 DLY1 .DA #46
92EC- 00          5330 CRIT .DA #00
92ED- 00          5340 WIND .DA #00
92EE- 00          5350 BINN .DA #00 ~
92EF- 00 3F       5360 PBSE .DA $3F00
92F1- 00          5370 FVR1 .DA #00
92F2- 3F          5380 BASE .DA #$3F
92F3- 93          5390 GTBL .DA #$93
92F4- 00          5400 ALTH .DA #00
92F5- FF          5410 ALTL .DA #$FF
92F6- 00          5420 ABRT .DA #00       0-OK  $FF-SLOW
92F7- 04          5430 CRIL .DA #04
92F8- E6          5440 CRIV .DA #230
92F9- 00          5450 LRPM .DA #00
92FA- 00          5460 TCRI .DA #00
92FB- 09          5465 DLY2 .DA #09
                  5470 *
                  5480 *
                  5490 * LOCAL DATA TABLE ADDRESSES
                  5500 *
                  5510 * $02A2 FV1 MAX
                  5520 * $02A3 FV1 MIN
                  5530 * $02A4 FV1 AMPLITUDE
                  5540 * $02A5 FV1 MEAN-REMAINDER
                  5550 * $02A6 FV1 MEAN-INTEGER
                  5560 *
                  5570 * $02A7 FV2 MAX
                  5580 * $02A8 FV2 MIN
                  5590 * $02A9 FV2 AMPLITUDE
                  5600 * $02AA FV2 MEAN-REMAINDER
                  5610 * $02AB FV2 MEAN-INTEGER
```

```
5620 *
5630 *  $02AC  FV3  MAX
5640 *  $02AD  FV3  MIN
5650 *  $02AE  FV3  AMPLITUDE
5660 *  $02AF  FV3  MEAN-REMAINDER
5670 *  $02B0  FV3  MEAN-INTEGER
5680 *
5690 *  $02B1  FV4  MAX
5700 *  $02B2  FV4  MIN
5710 *  $02B3  FV4  AMPLITUDE
5720 *  $02B4  FV4  MEAN-REMAINDER
5730 *  $02B5  FV4  MEAN-INTEGER
5740 *
5750 *  $02B6  FV5  MAX
5760 *  $02B7  FV5  MIN
5770 *  $02B8  FV5  AMPLITUDE
5780 *  $02B9  FV5  MEAN-REMAINDER
5790 *  $02BA  FV5  MEAN-INTEGER
5800 *
5810 *
5820 *  CHANNEL SEQUENCE / VARIABLE
5830 *
5840 *    1   CYCLIC PITCH
5850 *    2   DYNAMIC VARIABLE
5860 *    3   DYNAMIC VARIABLE
5870 *    4   DYNAMIC VARIABLE
5880 *    5   DYNAMIC VARIABLE
5890 *
5900 *    6   WIND SPEED
5910 *    7   RPM
5920 *    8   ALTERNATOR TEMP
5930 *
5940 *    9   SLOW VARIABLE
5950 *   10   SLOW VARIABLE
5960 *   11   SLOW VARIABLE
5970 *   12   SLOW VARIABLE
5980 *   13   SLOW VARIABLE
```

SYMBOL TABLE

DPNT	00FE	BTBL	00FC	LTBL	02A2
BUFR	0200	CHNL	C201	STDM	C202
INTH	C203	DATA	C200	EOCF	C202
INTF	C203	SPCK	C0C6	STCK	C0C5
TME1	C0C4	TME2	C0C3	TME3	C0C2
TME4	C0C1	TME5	C0C0	RWTS	03D9
KYBD	C000	STRB	C010	SPKR	FBDD
YAWN	FCA8	IORS	FF3F	IOSV	FF4A
WUTA	9000	MODE	900A	MOD1	9019
MOD2	901D	MOD3	9025	STRT	9032
ENT0	9044	ENTR	904F	ENT3	9055
ENT4	9084	FAST	908D	FAS0	9098
FAS1	90A3	FAS2	90B5	FAS3	90C2
SLOW	90C3	SLO1	90C7	PNTB	90D9
NEXT	90E6	NEX1	910E	LAS0	9119
LAS1	9123	LAS2	912A	LAS3	9139
LAS4	9141	END	9148	GET	9149
UPAD	915B	NOCY	9164	MXMN	9165
MXM1	916D	MXM2	917A	MXM3	917B
MXM4	918A	MXM5	9194	MXM6	919D
MXM7	91A0	MXM8	91A4	MXM9	91B5
MEAN	91B6	MEA1	91B8	MEA2	91C7
MEA3	91D2	GBIN	91F1	GBI1	9202
GBI2	9208	INIT	9209	INI1	922B
INI2	923F	CRI0	924F	CRI1	9267
CRI2	9275	CRI3	927A	RITE	9296
CRI4	929E	CRI5	92B0	DISK	92BA
DONE	92C1	TBL0	92C2	TRAK	92C6
SECT	92C7	DCTL	92C8	DCTH	92C9
BUFL	92CA	TBL1	92CC	CMND	92CE
TBL2	92CF	DCTA	92D3	VCHN	92D7
MSET	92E7	FVAR	92E8	SVAR	92E9
ASET	92EA	DLY1	92EB	CRIT	92EC
WIND	92ED	BINN	92EE	PBSE	92EF
FVR1	92F1	BASE	92F2	GTBL	92F3
ALTH	92F4	ALTL	92F5	ABRT	92F6
CRIL	92F7	CRIV	92F8	LRPM	92F9
TCRI	92FA	DLY2	92FB		

D.3. THE "WIND 6" PROGRAM

D.3.1 Program Logic

1. List operating instructions and initialize data
2. Calculate correction to standard atmosphere based on pressure and temperature.
3. Enter desired yaw angle for test.
4. Calculate furl set angle based on desired yaw angle and 8 degree rotor tilt.
5. Calculate offset for yaw post signal based on furl set angle. This compensates for the changing boom gravity loads at various furl angles.
6. Load "COLLECT 5" subroutine and initialize.
7. Calculate base data addresses and name data channel variables.
8. Disable critical dump and abort feature of the subroutine.
9. Call "COLLECT 5" subroutine and sample data for 1 sec.
10. Calculate current values of the six performance variables and furl angle based on the data stored from the "COLLECT 5" subroutine.
11. Update average rpm value.
12. Test rpm. If below limit go to #21.
13. Test cyclic pitch amplitude. If out of limits then go to #16.
14. Test furl angle. If out of limits then go to #20.
15. Skip to #17.
16. Toggle speaker and print cyclic pitch warning on screen.
17. Read bin number, and check if within limits.
18. Update 6 bin arrays based on current bin number and variable value. Update maximum, minimum, mean, standard deviation, and number of samples.
19. Skip to #22.
20. Print furl angle out of limits warning, then go to #22.
21. Print rpm out of limits warning, pause, then go to #22.
22. Test for zero wind speed. If zero then go to #25.
23. Print wind speed, RPM, cyclic pitch amplitude, and tip to wind speed ratio.
24. Skip to #26.
25. Print "Wind is Calm".
26. Check for operator signal to stop data sampling. If no stop signal then go to #9 and repeat sampling.
27. Print test time and rotor revolutions of test based on average rpm and elapsed time.
28. Store bin data and test parameters on disk.
29. Print out bin data and test parameters on printer.
30. End.

```
5   REM   THE WIND6 PROGRAM
6   REM   *****
10  D$ =  CHR$ (4)
11   PRINT D$;"MON C,I,O"
12  HIMEM: 16127
15   HOME : VTAB 1: PRINT "  DYNAMIC SAMPLING PROGRAM-WIND5"
16   PRINT : PRINT : PRINT
17   PRINT : PRINT "CHANNEL ASSIGNMENTS"
18   PRINT ,"0.CYCLIC PITCH": PRINT ,"1.TORQUE"
19   PRINT ,"2.FLAP": PRINT ,"3.YAWPOST BENDING"
20   PRINT ,"4.OPTIONAL FAST VARIABLE"
21   PRINT ,"5.WIND SPEED": PRINT ,"6.RPM"
22   PRINT ,"7.ALT.TEMP.": PRINT ,"8.ALT.VOLTS"
23   PRINT ,"9.BOOM POTENT."
24   PRINT ,"10,11,12.OPT."
25   PRINT : INPUT "PRESS RETURN TO CONT.";H$
27   READ V1,CH,CR,CC,CT,CF,CY,CV
28   DATA  54,6.705,60,5.94,2,355,1428,100
30   HOME : VTAB 5: PRINT "PRESENT CALIBRATION FACTORS ARE-": PRINT ,"ONE VOLT=";
V1
31   PRINT ,"WIND=";CH: PRINT ,"RPM=";CR
32   PRINT ,"CYCLIC PITCH= ";CC: PRINT ,"TORQUE=";CT
33   PRINT ,"FLAP=";CF: PRINT ,"YAWPOST=";CY
34   PRINT ,"ALT.VOLTS=";CV
35   PRINT "GO TO LINE 28 FOR CHANGES IF REQUIRED": INPUT "  PRESS RETURN TO CONT
.";H$
36   HOME : VTAB 2: PRINT "   TEST PARAMETERS": PRINT : PRINT "INPUT WEATHER VARI
ABLES"
37   PRINT : INPUT "ENTER AMB.TEMP.(C) > ";O1: INPUT "     AMB.PRESSURE (ATM) >
";O2: INPUT "    WIND DIRECTION (DEG) > ";O3
38  FC = ((O1 + 273) / 288) * (1 / O2)
39   PRINT : PRINT : PRINT " CORRECTION FACTOR= ";FC: PRINT : INPUT " \ PRESS RET
URN TO CONT.";H$
40   HOME : VTAB 10: INPUT "ENTER TOTAL GEN. LOAD (OHMS) > ";O4: INPUT "     GEA
R RATIO (IE 25 FOR 25:1) > ";O5
41  PM = 245:PN = 4: HOME : VTAB 10
42   PRINT : PRINT : PRINT "MAX AND MIN CYCLIC PITCH CONTROL NUMBERS ARE ";PM;"
AND  ";PN: PRINT "CHANGE LINE 41 IF REQUIRED"
43   PRINT : PRINT : INPUT "  PRESS RETURN TO CONT.";H$
45   HOME : VTAB 10: PRINT "ENTER FURL ANGLE INCLUDING ROTOR TILT.": PRINT : PRIN
T
46   INPUT "  ENTER FURL (DEG) > ";O6
47  XZ = ( COS (O6 * 6.283 / 360)) / ( COS (.14)):FS =  - ATN (XZ / SQR ( - XZ
* XZ + 1)) + 1.5708
48   PRINT : PRINT " FURL SET ANGLE IS ";FS * 180 / 3.14159;" DEGREES":VF = FS *
6 * .95 * 54 / 3.14159
49  OS = V1 * (2.95 - (FS * 4.5 / 3.14159))
50   INPUT "PRESS RETURN TO CONT. ";H$: HOME : VTAB 5: PRINT "   CONTROL FUNCTION
S"
51   PRINT : PRINT "ANY KEY PUTS PROGRAM IN TEMP. HOLD...ANY KEY RECOVERS"
52   PRINT : PRINT "CNTRL Z STOPS PROGRAM AND SENDS DATA TO PRINTER AND DISK"
53   PRINT : PRINT : INPUT "  PRESS RETURN TO CONT.";H$
90  XR = CRPM / V1:NR = 0:AR = 0
145  HOME : HTAB 4: VTAB 12: PRINT "PROGRAM LOADING INTO MEMORY"
150 PRG = 36864
152  PRINT D$;"BLOAD COLLECT5 OBJECT,A$9000"
154  CALL PRG
155  PRINT : PRINT : PRINT "   PROGRAM INITIALIZED"
156  DIM S(10),MEAN(35,6),M(35,6),SE(35,6),SBAR(35,6),MAX(35,6),MN(35,6)
157  FOR K = 1 TO 6: FOR J = 1 TO 35
158 MN(J,K) = 255 ^ 2
159  NEXT J: NEXT K
160 TABLE = (256 * PEEK (7)) + PEEK (6)
165 FV = 673:SLW = 16768: REM  FIRST SLOW VBL
166 GBL = 37632: REM  FIRST GLOBAL DATA
170 IX = 0:NR = 0:AR = 0
172 ACRIT = TABLE + 42:AABRT = TABLE + 52
173 BIN = TABLE + 44
175 K1$ = "CH.1=RPM":K2$ = "CH.2=GEN.VOLTS"
```

D23

```
176 K3$ = "CH.3=CYCLIC PITCH AMPL.":K4$ = "CH.4=ROTOR POWER"
177 K5$ = "CH.5=EFF.":K6$ = "CH.6=THRUST(N)"
178  HOME : VTAB 12: INPUT "   PRESS RETURN TO START DATA SAMPLING";H$
179  PRINT : PRINT : INPUT " ENTER START TIME AND DATE > ";H$
180  POKE ACRIT,0: POKE AABRT,0
185  CALL PRG
187 JX = IX * 648
190 S(0) =  PEEK (SLH + JX): REM  WIND
191 S(1) =  PEEK (SLH + 1 + JX): REM  RPM
192 S(2) =  PEEK (SLH + 3 + JX):S(2) = S(2) ^ 2: REM  GEN. POWER
193 S(3) =  PEEK (FV + 3): REM  CY.P.AMPL.
194 S(4) = S(1) *  PEEK (FV + 10): REM  ROTOR POWER
204  IF S(4) = 0 THEN 210
205 S(5) = S(2) / S(4): REM  EFFICIENCY
208  GOTO 215
210 S(5) = 0
215  REM  CONTINUE
217 S(6) =  PEEK (FV + 20)
218 S(6) = S(6) - OS
219 S(7) =  PEEK (SLH + 4 + JX): REM  FURL ANGLE
220 IX = IX + 1
225  IF  INT (IX / 32) > 0 THEN IX = 0
230 NR = NR + 1
240 AR = S(1) * XR / NR + (NR - 1) * AR / NR
245  IF S(1) < 14 THEN 660
370  IF S(3) > (PM - PN) THEN 390
375  IF S(7) > (VF + 7) THEN 656
376  IF S(7) < (VF - 4) THEN 656
380  GOTO 450
390  PRINT "CYCLIC PITCH OUT OF LIMITS!"
400  FOR B = 1 TO 140
410 BZ =  PEEK ( - 16336)
420  NEXT B
450 B% =  PEEK (BIN)
451  PRINT "BIN= ";B%
452  IF B% > 35 THEN B% = 0
480  FOR I = 1 TO 6
490  IF S(I) > MAX(B%,I) THEN MAX(B%,I) = S(I)
500  IF S(I) < MN(B%,I) THEN MN(B%,I) = S(I)
510 NK(B%,I) = NK(B%,I) + 1
520 MEAN(B%,I) = (S(I) + ((NK(B%,I) - 1) * MEAN(B%,I))) / NK(B%,I)
530 SBAR(B%,I) = (SBAR(B%,I) * (NK(B%,I) - 1) + S(I) ^ 2) / NK(B%,I)
540 SE(B%,I) =  SQR (SBAR(B%,I) - MEAN(B%,I) ^ 2)
550  NEXT I
655  GOTO 675
656  PRINT : PRINT "FURL ANGLE OUT OF LIMITS - RESET"
657  PRINT : PRINT "BIN DATA NOT UPDATED"
658  GOTO 675
660  PRINT : PRINT : PRINT ,"RPM TOO LOW"
665  PRINT : PRINT ,"BIN DATA NOT UPDATED"
666  PRINT : PRINT
670  FOR WQ = 1 TO 1000: NEXT WQ
675  IF S(0) = 0 THEN  GOTO 760
680 WIND = CWIND * S(0) / V1:RPM = CRPM * S(1) / V1:PTH = CC * S(3) / V1
690 TSR = .4 * RPM / WIND
700 TSR = .1 * INT (TSR * 10 + .5)
710 RPM =  INT (RPM + .5):PTH = .1 *  INT (10 * PTH + .5)
720  PRINT "TIP SPEED R","RPM","CYC PTCH"
730  PRINT TSR,RPM,PTH
740 WIND = .1 *  INT (WIND * 10 + .5): PRINT : PRINT "WIND,M/S": PRINT WIND: PRI
NT : PRINT : PRINT
750  GOTO 800
```

D24

```
760   PRINT "WIND IS CALM"
790   REM   TO STOP SAMPLING PRESS CNTRL Z
800 XX =  PEEK ( - 16384)
810   IF XX <  > (154) THEN 180
811   HOME : VTAB 5: PRINT "  START TIME WAS  ";H$
814   PRINT : PRINT : INPUT "ENTER ELAPSED TIME IN HRS. > ";TIME
816   HOME : VTAB 3
820 ST = 0: FOR K = 1 TO 6: FOR J = 1 TO 35
830   IF N(J,K) = 0 THEN 850
840 ST = ST + 1
850   NEXT J: NEXT K
860   PRINT "TIME OF TEST START WAS:": PRINT : PRINT H$
870   PRINT "  ELAPSED TIME OF TEST WAS": PRINT ,TIME;" HOURS"
880 REV =  INT (AR * 60 * TIME + .5)
885   PRINT : PRINT "TOTAL ROTOR REV.= ";REV;" REVS."
886   PRINT : PRINT " INSERT DATA DISK IF DESIRED"
887   PRINT : INPUT "PRESS RETURN TO CONT.";H$
889 D$ =  CHR$ (4)
890   PRINT D$;"OPEN DAT.BINS"
900   PRINT D$;"DELETE DAT.BINS"
910   PRINT D$;"OPEN DAT.BINS"
920   PRINT D$;"WRITE DAT.BINS"
924   REM   1 VOLT,CHIND,CRPM,CCYCP
925   PRINT V1: PRINT CH: PRINT CR: PRINT CC
926   REM   CTORQUE(NN),CFLAP,CYAWPOST,CGEN.VOLTS
927   PRINT CT: PRINT CF: PRINT CV: PRINT CU
928   REM   AMB.TEMP,PRESS,WIND DIR.,GEN LOAD
930   PRINT D1: PRINT D2: PRINT D3: PRINT D4
931   REM   GEAR RATIO, FURL ANGLE, CORREC. FACTOR
933   PRINT D5: PRINT D6: PRINT FC
934   REM   CHANNEL TITLES FOR BIN DATA
935   PRINT K1$: PRINT K2$: PRINT K3$: PRINT K4$: PRINT K5$: PRINT K6$
936   REM   SETS, START TIME, ET, REV
940   PRINT ST: PRINT H$: PRINT TIME: PRINT REV
960   FOR K = 1 TO 6: FOR J = 1 TO 35
970   IF N(J,K) = 0 THEN 1060
980   PRINT K
990   PRINT J
1000   PRINT N(J,K)
1010   PRINT MAX(J,K)
1020   PRINT MEAN(J,K)
1030   PRINT MN(J,K)
1040   PRINT SE(J,K)
1050   PRINT SBAR(J,K)
1060   NEXT J
1070   NEXT K
1080   PRINT D$;"CLOSE DAT.BINS"
1085   HOME : VTAB 10: INPUT " ENTER NAME OF TEST > ";N1$
1090   PRINT D$;"PR#1"
1095   PRINT : PRINT "TEST NAME IS ";N1$
1100   PRINT "START TIME= ";H$
1110   PRINT "ELAPSED TIME= ";TIME;" HOURS"
1130   PRINT "ROTOR REV.(CALC.)= ";REV
1132   PRINT "CALIBRATIONS AND TEST PARAMETERS"
1133   PRINT "FURL ANGLE (INCL. TILT)= ";D6
1134   PRINT "ONE VOLT=";V1;"  CHIND=";CH;"  CRPM=";CR;"  CCYPTCH=";CC
1135   PRINT "CTORQUE=";CT;"  CFLAP=";CF;"  CYAWPOST=";CY;"  CGEN.V=";CU
1136   PRINT "TEMP(DEG C)=";D1;"  PRESS(ATM)=";D2;"  CORR.FAC.=";FC;"  WIND DIR="
;D3
1137   PRINT "GEN LOAD(OHMS)=";D4;"        GEAR RATIO = ";D5;" TO 1"
1140   PRINT K1$;"   ";K2$;"   ";K3$
1141   PRINT K4$;"   ";K5$;"   ";K6$
```

```
1145   PRINT
1150   PRINT "CH#/BIN#/N#/MEAN/S.DEV/MAX/MIN"
1170   FOR K = 1 TO 6: FOR J = 1 TO 35
1180   IF N(J,K) = 0 THEN 1220
1190   PRINT K;"   ";J;"   ";N(J,K);"   ";MEAN(J,K);"   ";SE(J,K);"   ";MAX(J,K);"   ";
MN(J,K)
1220   NEXT J
1230   NEXT K
1240   PRINT D$;"PR#0"
1250   HOME : VTAB 5: PRINT "DONT FORGET TO RENAME DAT.BINS. DATA IS DELETED WHEN
 PROGRAM IS RUN AGAIN,!!!!!"
1260   END
```

D.4   "WIND 2, FAST"

D.4.1   Program Logic

1 to 9.	The first 9 steps are identical to the "WIND 6" program logic.
10.	Read data for two "fast" variables at appropriate addresses.
11.	Update average rpm value.
12.	Read bin number at appropriate address.
13.	Print current variable values to screen.
14.	Test bin number in limits.
15.	Update bin arrays for the two variables as in the "WIND 6" program.
16.	Test for stop sampling signal. If none, then go to #9 and repeat sampling.
17,18,19.	Same as steps 27, 28, 29 for "WIND 6" program.
20.	End.

```
5   REM   THE WIND2.FAST PROGRAM
6   REM   *****
7   REM   APPROXIMATELY 1.4 SECONDS PER SAMPLE
10  D$ =  CHR$ (4)
11   PRINT D$;"MON C,I,O"
12  HIMEM: 16127
15  HOME : VTAB 1: PRINT "   DYNAMIC SAMPLING PROGRAM -WIND2.FAST"
16   PRINT : PRINT : PRINT
17   PRINT : PRINT "CHANNEL ASSIGNMENTS"
18   PRINT ,"1.TORQUE": PRINT ,"2.RPM"
19   PRINT ,"5.WIND SPEED"
24   PRINT ,"10,11,12.OPT."
25   PRINT : INPUT "PRESS RETURN TO CONT.";H$
27   READ V1,CH,CR,CT
28   DATA  54,6.705,60,94.2
29  ZR = CR / V1:ZT = .105 * CR * CT / (V1 ^ 2)
30   HOME : VTAB 5: PRINT "PRESENT CALIBRATION FACTORS ARE-": PRINT ,"ONE VOLT=";V1
31   PRINT ,"WIND=";CH: PRINT ,"RPM=";CR
32   PRINT ,"TORQUE=";CT
35   PRINT "GO TO LINE 28 FOR CHANGES IF REQUIRED": INPUT "  PRESS RETURN TO CONT.";H$
36   HOME : VTAB 2: PRINT "   TEST PARAMETERS": PRINT : PRINT "INPUT WEATHER VARIABLES"
37   PRINT : INPUT "ENTER AMB.TEMP.(C) > ";O1: INPUT "     AMB.PRESSURE (ATM) > ";O2: INPUT "     WIND DIRECTION (DEG) > ";O3
38  FC = ((O1 + 273) / 288) * (1 / O2)
39   PRINT : PRINT " CORRECTION FACTOR= ";FC: PRINT : INPUT "   PRESS RETURN TO CONT.";H$
40   HOME : VTAB 10: INPUT "ENTER TOTAL GEN. LOAD (OHMS) > ";O4: INPUT "    GEAR RATIO (IE 25 FOR 25:1) > ";O5
43   PRINT : PRINT : INPUT "  PRESS RETURN TO CONT.";H$
45   HOME : VTAB 10: PRINT "ENTER FURL ANGLE INCLUDING ROTOR TILT.": PRINT : PRINT
46   INPUT "  ENTER FURL (DEG) > ";O6
47  XZ = ( COS (O6 * 6.283 / 360)) / ( COS (.14)):FS =  - ATN (XZ / SQR ( - XZ * XZ + 1)) + 1.5708
48   PRINT : PRINT " FURL SET ANGLE IS ";FS * 180 / 3.14159;" DEGREES":VF = FS * 6 * .95 * 54 / 3.14159
50   INPUT "PRESS RETURN TO CONT. ";H$: HOME : VTAB 5: PRINT "   CONTROL FUNCTIONS"
51   PRINT : PRINT "ANY KEY PUTS PROGRAM IN TEMP. HOLD...ANY KEY RECOVERS"
52   PRINT : PRINT "CNTRL Z STOPS PROGRAM AND SENDS DATA TO PRINTER AND DISK"
53   PRINT : INPUT "  PRESS RETURN TO CONT.";H$
90  XR = CRPM / V1:NR = 0:AR = 0
145  HOME : HTAB 4: VTAB 12: PRINT "PROGRAM LOADING INTO MEMORY"
150  PRG = 36864
152   PRINT D$;"BLOAD COLLECT5 OBJECT,A$9000"
154   CALL PRG
155   PRINT : PRINT : PRINT "    PROGRAM INITIALIZED"
156   DIM S(10),MEAN(35,2),M(35,2),SE(35,2),SBAR(35,2),MAX(35,2),MN(35,2)
157   FOR K = 1 TO 2: FOR J = 1 TO 35
158  MN(J,K) = 255 ^ 2
159   NEXT J: NEXT K
160  TABLE = (256 * PEEK (7)) + PEEK (6)
165  FV = 673:SLW = 16768: REM  FIRST SLOW VBL
166  GBL = 37632: REM  FIRST GLOBAL DATA
170  IX = 0:NR = 0:AR = 0
172  ACRIT = TABLE + 42:AABRT = TABLE + 52
173  BIN = TABLE + 44
175  K1$ = "CH.1=RPM":K2$ = "CH.2=ROTOR POWER"
178   HOME : VTAB 12: INPUT "   PRESS RETURN TO START DATA SAMPLING";H$
179   PRINT : PRINT : INPUT " ENTER START TIME AND DATE > ";H$
180   POKE ACRIT,0: POKE AABRT,0
185   CALL PRG
191  S(1) =  PEEK (FV + 15)
192  S(2) = S(1) +  PEEK (FV + 10)
230  NR = NR + 1
```

```
240 AR = S(1) * XR / NR + (NR - 1) * AR / NR
440 B% = PEEK (BIN):R% = S(1) * ZR:H% = S(2) * ZT
445  PRINT "BIN=";B%;"  RPM=";R%;"  R.PHR=";H%
452  IF B% > 35 THEN B% = 0
480  FOR I = 1 TO 2
490  IF S(I) > MAX(B%,I) THEN MAX(B%,I) = S(I)
500  IF S(I) < MN(B%,I) THEN MN(B%,I) = S(I)
510 N(B%,I) = N(B%,I) + 1
520 MEAN(B%,I) = (S(I) + ((N(B%,I) - 1) * MEAN(B%,I))) / N(B%,I)
530 SBAR(B%,I) = (SBAR(B%,I) * (N(B%,I) - 1) + S(I) ^ 2) / N(B%,I)
540 SE(B%,I) =  SQR (SBAR(B%,I) - MEAN(B%,I) ^ 2)
550  NEXT I
800 XX =  PEEK ( - 16384)
810  IF XX < > (154) THEN 180
811  HOME : VTAB 5: PRINT "  START TIME WAS  ";H$
814  PRINT : PRINT : INPUT "ENTER ELAPSED TIME IN HRS. > ";TIME
816  HOME : VTAB 3
820 ST = 0: FOR K = 1 TO 2: FOR J = 1 TO 35
830  IF N(J,K) = 0 THEN 850
840 ST = ST + 1
850  NEXT J: NEXT K
860  PRINT "TIME OF TEST START WAS:": PRINT : PRINT H$
870  PRINT "  ELAPSED TIME OF TEST WAS": PRINT ,TIME;" HOURS"
880 REV =  INT (AR * 60 * TIME + .5)
885  PRINT : PRINT "TOTAL ROTOR REV.= ";REV;" REVS."
886  PRINT : PRINT " INSERT DATA DISK IF DESIRED"
887  PRINT : INPUT "PRESS RETURN TO CONT.";H$
889 D$ =  CHR$ (4)
890  PRINT D$;"OPEN DAT.BINS"
900  PRINT D$;"DELETE DAT.BINS"
910  PRINT D$;"OPEN DAT.BINS"
920  PRINT D$;"WRITE DAT.BINS"
924  REM  1 VOLT,CHIND,CRPM,CCYCP
925  PRINT V1: PRINT CH: PRINT CR: PRINT CC
926  REM  CTORQUE(NM),CFLAP,CYAWPOST,CGEN.VOLTS
927  PRINT CT: PRINT CF: PRINT CY: PRINT CV
928  REM  AMB.TEMP,PRESS,WIND DIR.,GEN LOAD
930  PRINT D1: PRINT D2: PRINT D3: PRINT D4
931  REM  GEAR RATIO, FURL ANGLE, CORREC. FACTOR
933  PRINT D5: PRINT D6: PRINT FC
934  REM  CHANNEL TITLES FOR BIN DATA
935  PRINT K1$: PRINT K2$: PRINT K3$: PRINT K4$: PRINT K5$: PRINT K6$
936  REM  SETS, START TIME, ET, REV
940  PRINT ST: PRINT H$: PRINT TIME: PRINT REV
960  FOR K = 1 TO 2: FOR J = 1 TO 35
970  IF N(J,K) = 0 THEN 1060
980  PRINT K
990  PRINT J
1000  PRINT N(J,K)
1010  PRINT MAX(J,K)
1020  PRINT MEAN(J,K)
1030  PRINT MN(J,K)
1040  PRINT SE(J,K)
1050  PRINT SBAR(J,K)
1060  NEXT J
1070  NEXT K
1080  PRINT D$;"CLOSE DAT.BINS"
1085  HOME : VTAB 10: INPUT " ENTER NAME OF TEST > ";N1$
1090  PRINT D$;"PR#1"
1095  PRINT : PRINT "TEST NAME IS ";N1$
1100  PRINT "START TIME= ";H$
```

```
1110   PRINT "ELAPSED TIME= ";TIME;" HOURS"
1130   PRINT "ROTOR REV.(CALC.)= ";REV
1132   PRINT "CALIBRATIONS AND TEST PARAMETERS"
1133   PRINT "FURL ANGLE (INCL. TILT)= ";O6
1134   PRINT "ONE VOLT=";V1;"   CWIND=";CW;"   CRPM=";CR;"   CCYPTCH=";CC
1135   PRINT "CTORQUE=";CT;"   CFLAP=";CF;"   CYAWPOST=";CY;"   CGEN.V=";CV
1136   PRINT "TEMP(DEG C)=";O1;"   PRESS(ATM)=";O2;"   CORR.FAC.=";FC;"   WIND DIR="
       ;O3
1137   PRINT "GEN LOAD(OHMS)=";O4;"      GEAR RATIO = ";O5;" TO 1"
1140   PRINT K1$;"    ";K2$;"    ";K3$
1141   PRINT K4$;"    ";K5$;"    ";K6$
1145   PRINT
1150   PRINT "CH#/BIN#/N#/MEAN/S.DEV/MAX/MIN"
1170   FOR K = 1 TO 2: FOR J = 1 TO 35
1180   IF N(J,K) = 0 THEN 1220
1190   PRINT K;"    ";J;"    ";N(J,K);"    ";MEAN(J,K);"    ";SE(J,K);"    ";MAX(J,K);"    ";
       MN(J,K)
1220   NEXT J
1230   NEXT K
1240   PRINT D$;"PR#0"
1250   HOME : VTAB 5: PRINT "DONT FORGET TO RENAME DAT.BINS. DATA IS DELETED WHEN
       PROGRAM IS RUN AGAIN,!!!!!"
1260   END
```

D.5 "RPM-6"

D.5.1 Program Logic

The program logic for the "RPM-6" program is identical to that of the "WIND 6"
program.   Channel assignments and conversion constants are changed so that
desired variables are related to rpm bins rather than wind speed bins, but the
logic remains the same.

```
5   REM   THE RPM6 PROGRAM
6   REM   *****
10  D$ =  CHR$ (4)
11  PRINT D$;"MON C,I,O"
12  HIMEM: 16127
15  HOME : VTAB 1: PRINT "   DYNAMIC SAMPLING PROGRAM-RPM6"
16  PRINT : PRINT : PRINT
17  PRINT : PRINT "CHANNEL ASSIGNMENTS"
18  PRINT ,"0.CYCLIC PITCH": PRINT ,"1.TORQUE"
19  PRINT ,"2.FLAP": PRINT ,"3.YAWPOST BENDING"
20  PRINT ,"4.VERTICAL BOOM"
21  PRINT ,"5.RPM"
22  PRINT ,"6,7,8.OPEN"
23  PRINT ,"9.BOOM POTENT."
24  PRINT ,"10,11,12.OPT."
25  PRINT : INPUT "PRESS RETURN TO CONT.";W$
27  READ V1,CB,CR,CC,CT,CF,CY,CV
28  DATA   54,290,60,5,94.2,355,1420,100
30  HOME : VTAB 5: PRINT "PRESENT CALIBRATION FACTORS ARE-": PRINT ,"ONE VOLT=";
V1
31  PRINT ,"BOOM=";CB: PRINT ,"RPM=";CR
32  PRINT ,"CYCLIC PITCH= ";CC: PRINT ,"TORQUE=";CT
33  PRINT ,"FLAP=";CF: PRINT ,"YAWPOST=";CY
34  PRINT ,"ALT.VOLTS=";CV
35  PRINT "GO TO LINE 28 FOR CHANGES IF REQUIRED": INPUT "  PRESS RETURN TO CONT
.";W$
36  HOME : VTAB 2: PRINT "   TEST PARAMETERS": PRINT : PRINT "INPUT WEATHER VARI
ABLES"
37  PRINT : INPUT "ENTER AMB.TEMP.(C) > ";O1: INPUT "     AMB.PRESSURE (ATM) >
";O2: INPUT "      WIND DIRECTION (DEG) > ";O3
38  FC = ((O1 + 273) / 288) * (1 / O2)
39  PRINT : PRINT : PRINT " CORRECTION FACTOR= ";FC: PRINT : INPUT "   PRESS RET
URN TO CONT.";W$
40  HOME : VTAB 10: INPUT "ENTER TOTAL GEN. LOAD (OHMS) > ";O4: INPUT "      GEA
R RATIO (IE 25 FOR 25:1) > ";O5
41  PH = 245:PN = 4: HOME : VTAB 10
42  PRINT : PRINT : PRINT "MAX AND MIN CYCLIC PITCH CONTROL NUMBERS ARE ";PH;"
AND  ";PN: PRINT "CHANGE LINE 41 IF REQUIRED"
43  PRINT : INPUT "  PRESS RETURN TO CONT.";W$
45  HOME : VTAB 10: PRINT "ENTER FURL ANGLE INCLUDING ROTOR TILT.": PRINT : PRIN
T
46  INPUT "  ENTER FURL (DEG) > ";O6
47  XZ = ( COS (O6 * 6.283 / 360)) / ( COS (.14)):FS =  -  ATN (XZ /  SQR ( - XZ
 * XZ + 1)) + 1.5708
48  PRINT : PRINT " FURL SET ANGLE IS ";FS * 180 / 3.14159;" DEGREES":UF = FS *
6 * .95 * 54 / 3.14159
49  OS = V1 * (2.95 - (FS * 4.5 / 3.14159)): PRINT : PRINT "YAWPOST OFFSET= ";OS
 / V1;" VOLTS"
50  INPUT "PRESS RETURN TO CONT. ";W$: HOME : VTAB 5: PRINT "   CONTROL FUNCTION
S"
51  PRINT : PRINT "ANY KEY PUTS PROGRAM IN TEMP. HOLD...ANY KEY RECOVERS"
52  PRINT : PRINT "CNTRL Z STOPS PROGRAM AND SENDS DATA TO PRINTER AND DISK"
53  PRINT : PRINT : INPUT "   PRESS RETURN TO CONT.";W$
90  XR = CRPM / V1:NR = 0:AR = 0
145 HOME : HTAB 4: VTAB 12: PRINT "PROGRAM LOADING INTO MEMORY"
150 PRG = 36864
152 PRINT D$;"BLOAD COLLECT5 OBJECT,A$9000"
154 CALL PRG
155 PRINT : PRINT : PRINT "    PROGRAM INITIALIZED"
156 DIM S(10),MEAN(35,6),M(35,6),SE(35,6),SBAR(35,6),MAX(35,6),MN(35,6)
157 FOR K = 1 TO 6: FOR J = 1 TO 35
158 MN(J,K) = 255 ^ 2
159 NEXT J: NEXT K
160 TABLE = (256 * PEEK (7)) + PEEK (6)
165 FV = 673:SLW = 16768: REM  FIRST SLOW VBL
166 GBL = 37632: REM  FIRST GLOBAL DATA
170 IX = 0:NR = 0:AR = 0
172 ACRIT = TABLE + 42:AABRT = TABLE + 52
173 BIN = TABLE + 44
175 K1$ = "CH.1=MEAN FLAP":K2$ = "CH.2=FLAP AMPL."
```

```
176 K3$ = "CH.3=YAWPOST AMPL.(THRUST)";K4$ = "CH.4=TORQUE AMPL."
177 K5$ = "CH.5=V.BOOM AMPL.";K6$ = "CH.6=CYCLIC PITCH AMPL."
178  HOME : VTAB 12: INPUT "   PRESS RETURN TO START DATA SAMPLING";H$
179  PRINT : PRINT : INPUT " ENTER START TIME AND DATE > ";H$
180  POKE ACRIT,0: POKE AABRT,0
185  CALL PR6
187 JX = IX * 648
190 S(0) =  PEEK (SLH + JX): REM  RPM
191 S(1) =  PEEK (FV + 15): REM  MEAN FLAP
192 S(2) =  PEEK (FV + 13): REM  FLAP AMPL.
193 S(3) =  PEEK (FV + 18): REM  YAWPOST AMPL.
195 S(4) =  PEEK (FV + 8): REM  TORQUE AMPL.
196 S(5) =  PEEK (FV + 23): REM  V. BOOM AMPL.
197 S(6) =  PEEK (FV + 3): REM  CYCLIC PITCH AMPL.
219 S(7) =  PEEK (SLH + 4 + JX): REM  FURL ANGLE
220 IX = IX + 1
225  IF  INT (IX / 32) > 0 THEN IX = 0
230 NR = NR + 1
240 AR = S(1) * XR / NR + (NR - 1) * AR / NR
245  IF S(0) < 14 THEN 660
370  IF S(6) > (PM - PN) THEN 390
375  IF S(7) > (VF + 7) THEN 656
376  IF S(7) < (VF - 4) THEN 656
380  GOTO 450
390  PRINT "CYCLIC PITCH OUT OF LIMITS!"
400  FOR B = 1 TO 140
410 BZ =  PEEK ( - 16336)
420  NEXT B
450 B% = .5 *  PEEK (BIN)
451  PRINT "BIN= ";B%
452  IF B% > 35 THEN B% = 0
480  FOR I = 1 TO 6
490  IF S(I) > MAX(B%,I) THEN MAX(B%,I) = S(I)
500  IF S(I) < MN(B%,I) THEN MN(B%,I) = S(I)
510 N(B%,I) = N(B%,I) + 1
520 MEAN(B%,I) = (S(I) + ((N(B%,I) - 1) * MEAN(B%,I))) / N(B%,I)
530 SBAR(B%,I) = (SBAR(B%,I) + (N(B%,I) - 1) + S(I) ^ 2) / N(B%,I)
540 SE(B%,I) =  SQR (SBAR(B%,I) - MEAN(B%,I) ^ 2)
550  NEXT I
655  GOTO 675
656  PRINT : PRINT "FURL ANGLE OUT OF LIMITS - RESET"
657  PRINT : PRINT "BIN DATA NOT UPDATED"
658  GOTO 675
660  PRINT : PRINT : PRINT ,"RPM TOO LOW"
665  PRINT : PRINT ,"BIN DATA NOT UPDATED"
666  PRINT : PRINT
670  FOR WQ = 1 TO 1000: NEXT WQ
675  PRINT : PRINT ,"RPM = ";60 * S(0) / V1: PRINT
790  REM  TO STOP SAMPLING PRESS CNTRL Z
800 XX =  PEEK ( - 16384)
810  IF XX < > (154) THEN 180
811  HOME : VTAB 5: PRINT "  START TIME WAS  ";H$
814  PRINT : PRINT : INPUT "ENTER ELAPSED TIME IN HRS. > ";TIME
816  HOME : VTAB 3
820 ST = 0: FOR K = 1 TO 6: FOR J = 1 TO 35
830  IF N(J,K) = 0 THEN 850
840 ST = ST + 1
850  NEXT J: NEXT K
860  PRINT "TIME OF TEST START WAS:": PRINT : PRINT H$
870  PRINT "  ELAPSED TIME OF TEST WAS": PRINT ,TIME;" HOURS"
880 REV =  INT (AR * 60 * TIME + .5)
```

```
885    PRINT : PRINT "TOTAL ROTOR REV.= ";REV;" REVS."
886    PRINT : PRINT " INSERT DATA DISK IF DESIRED"
887    PRINT : INPUT "PRESS RETURN TO CONT.";H$
889  D$ =  CHR$ (4)
890    PRINT D$;"OPEN DAT.BINS"
900    PRINT D$;"DELETE DAT.BINS"
910    PRINT D$;"OPEN DAT.BINS"
920    PRINT D$;"WRITE DAT.BINS"
924  REM    1 VOLT,CBOOM,CRPH,CCYCP
925    PRINT V1: PRINT CB: PRINT CR: PRINT CC
926  REM   CTORQUE(NM),CFLAP,CYAWPOST,CGEN.VOLTS
927    PRINT CT: PRINT CF: PRINT CY: PRINT CV
928  REM   AMB.TEMP,PRESS,WIND DIR.,GEN LOAD
930    PRINT D1: PRINT D2: PRINT D3: PRINT D4
931  REM   GEAR RATIO, FURL ANGLE, CORREC. FACTOR
933    PRINT D5: PRINT D6: PRINT FC
934  REM   CHANNEL TITLES FOR BIN DATA
935    PRINT K1$: PRINT K2$: PRINT K3$: PRINT K4$: PRINT K5$: PRINT K6$
936  REM   SETS, START TIME, ET, REV
940    PRINT ST: PRINT H$: PRINT TIME: PRINT REV
960    FOR K = 1 TO 6: FOR J = 1 TO 35
970    IF N(J,K) = 0 THEN 1060
980    PRINT K
990    PRINT J
1000   PRINT N(J,K)
1010   PRINT MAX(J,K)
1020   PRINT MEAN(J,K)
1030   PRINT MN(J,K)
1040   PRINT SE(J,K)
1050   PRINT SBAR(J,K)
1060   NEXT J
1070   NEXT K
1080   PRINT D$;"CLOSE DAT.BINS"
1085   HOME : VTAB 10: INPUT " ENTER NAME OF TEST > ";N1$
1090   PRINT D$;"PR#1"
1095   PRINT : PRINT "TEST NAME IS ";N1$
1100   PRINT "START TIME= ";H$
1110   PRINT "ELAPSED TIME= ";TIME;" HOURS"
1130   PRINT "ROTOR REV.(CALC.)= ";REV
1132   PRINT "CALIBRATIONS AND TEST PARAMETERS"
1133   PRINT "FURL ANGLE (INCL. TILT)= ";D6
1134   PRINT "ONE VOLT=";V1;" CBOOM=";CB;"   CRPH=";CR;"  CCYPTCH=";CC
1135   PRINT "CTORQUE=";CT;"  CFLAP=";CF;"  CYAWPOST=";CY;"  CGEN.V=";CV
1136   PRINT "TEMP(DEG C)=";D1;"  PRESS(ATM)=";D2;"  CORR.FAC.=";FC;"  WIND DIR="
       ;D3
1137   PRINT "GEN LOAD(OHMS)=";D4;"      GEAR RATIO = ";D5;" TO 1"
1140   PRINT K1$;"   ";K2$;"   ";K3$
1141   PRINT K4$;"   ";K5$;"   ";K6$
1145   PRINT
1150   PRINT "CH#/BIN#/N#/MEAN/S.DEV/MAX/MIN"
1170   FOR K = 1 TO 6: FOR J = 1 TO 35
1180   IF N(J,K) = 0 THEN 1220
1190   PRINT K;"   ";J;"   ";N(J,K);"   ";MEAN(J,K);"   ";SE(J,K);"   ";MAX(J,K);"   ";
       MN(J,K)
1220   NEXT J
1230   NEXT K
1240   PRINT D$;"PR#0"
1250   HOME : VTAB 5: PRINT "DONT FORGET TO RENAME DAT.BINS. DATA IS DELETED WHEN
       PROGRAM IS RUN AGAIN,!!!!!"
1260   END
```

D.6 "YAWRATE" PROGRAM

D.6.1 Program Logic

1. Provide operator instructions and initialize data.
2. Define directional code (i.e. clockwise or counterclockwise yaw rates).
3. Read clock for test start time.
4. Sample yaw position.
5. Sample clock.
6. Sample dynamic variable, usually cyclic pitch, for 0.5 sec (24 samples).
7. Sample yaw position.
8. Sample clock.
9. Calculate elapsed time.
10. Calculate yaw rate.
11. Check yaw rate within limits. If not then go to #13.
12. Skip to #14.
13. Print yaw rate out of limits. Go to #17.
14. Calculate amplitude of dynamic signal.
15. Calculate yaw rate bin.
16. Update bin array with current value to include maximum, minimum, mean, standard deviation and number of samples.
17. Sample and test rpm in limits. If not, pause and test again until within limits.
18. Check for operator stop signal. If none, then go to #4 and repeat sampling.
19. Output bin array data to disk and printer.
20. End.

```
5   REM   THE YAWRATE CORRELATION PROGRAM
6   REM   *****
10  REM   THIS PROGRAM IS USED TO CALCULATE A YAW RATE AND CORRELATE IT TO A DYNA
MIC VARIABLE
12  REM   *** CLOCK IN SLOT 4
14  REM   *** PRINTER IN SLOT 1
16  REM   *** LEAP YEAR (L=1)
17  HOME : VTAB 2: PRINT "  DO NOT TEST WITH NORTHERLY WINDS ": PRINT : PRINT :
PRINT
18  REM   FOLLOWING TESTS LIMITS OF TEST
19  PRINT " THIS PROGRAM CORRELATES YAW": PRINT " RATES TO A DYNAMIC VARIABLE":
PRINT " YAW RATE BIN # IS 1 DEG PER SEC": PRINT " MAX VALUE IS 35 DEG PER SEC."
20  PRINT : INPUT " INPUT LOW AND HIGH RPM VALUES FOR TEST ? ";LS,HS
21  PRINT : PRINT : INPUT " INPUT  1 VOLT=? AND CRPM=? ";V1,CRPM
22  INPUT " INPUT TEST FURL ANGLE ? ";FURL
23  HOME : VTAB 2: PRINT "RPM IS CHANNEL 1": PRINT : PRINT
30  PRINT : PRINT "DIRECTION OF ROTATION FOR TEST"
35  PRINT "    ENTER A '1' FOR CLOCKWISE"
36  PRINT "    ENTER A '0' FOR COUNTERCLOCKWISE"
37  PRINT : INPUT "    ENTER > ";QP
50  INPUT " INPUT YAW POSITION CHANNEL ?";CYAW
51  INPUT " INPUT DYNAMIC POSITION CHANNEL ? ";CDYN
60  REM   24 POINTS ARE SAMPLED AND SAMPLE TIME IS APPROXIMATELY 0.5 SEC.
80  D$ = CHR$ (4): REM   SETS CNTRL D
81  PRINT D$;"NOMON C,I,O"
82  INPUT "INPUT NAME OF DYN VARIABLE ? ";U$
83  PRINT D$;"PR#1"
84  PRINT "  CORRELATION OF YAW RATE VS ";U$: PRINT : PRINT D$;"PR#0"
85  GOSUB 2000: GOSUB 3000:BEGIN = STD
90  DIM DV(47),MAX(35),MN(35),N(35),SBAR(35),MEAN(35),SE(35)
95  FOR I = 0 TO 35:MN(I) = 255: NEXT I
100 POKE  - 15871,CYAW
110 Y1P =  PEEK ( - 15872)
120 GOSUB 2000: REM   GET TIME AS T$
130 FOR I = 1 TO 24: POKE  - 15871,CDYN:DV(I) =  PEEK ( - 15872): NEXT I
140 POKE  - 15871,CYAW
150 Y2P =  PEEK ( - 15872)
160 T1$ = T$: GOSUB 2000
170 REM   GET ELAPSED TIME
180 GOSUB 3000:S2 = STD
190 T$ = T1$: GOSUB 3000:S1 = STD
200 ET = S2 - S1
220 REM   CONVERT YAWRATE TO DEG PER SEC.
221 YQ = Y2P - Y1P
222 IF QP = 1 AND YQ < 0 THEN 100
223 IF QP = 0 AND YQ > 0 THEN 100
224 YQ =  ABS (YQ)
230 Y% = (YQ) * (100 / V1) * (1 / ET) + .5
236 IF Y% > 35 THEN 238
237 GOTO 240
238 PRINT " YAW RATE OUT OF RANGE": PRINT "   YAW RATE = ";Y%
239 GOTO 100
240 REM   CALC DYN VARIABLE
245 DH = 0:DL = 255
250 FOR I = 1 TO 24
260 IF DV(I) > DH THEN DH = DV(I)
270 IF DV(I) < DL THEN DL = DV(I)
280 NEXT I
290 AMPL = (DH - DL) / 2
291 PRINT : PRINT "YAW RATE= ";Y%,"AMPL= ";AMPL
300 REM   UPDATE BINS
```

```
310  IF AMPL > MAX(Y%) THEN MAX(Y%) = AMPL
320  IF AMPL < MIN(Y%) THEN MIN(Y%) = AMPL
330  N(Y%) = N(Y%) + 1
340  MEAN(Y%) = (AMPL + ((N(Y%) - 1) * MEAN(Y%))) / N(Y%)
350  SBAR(Y%) = (SBAR(Y%) * (N(Y%) - 1) + AMPL ^ 2) / N(Y%)
358  QQ =  ABS (SBAR(Y%) - MEAN(Y%) ^ 2)
360  SE(Y%) =  SQR (QQ)
370  REM  RPM TEST
375  POKE  - 15871,1
377  RPM = (CRPM / V1) *  PEEK ( - 15872)
380  IF RPM < LS OR RPM > HS THEN 382
381  GOTO 390
382  PRINT : PRINT "RPM OUT OF LIMITS": PRINT : PRINT " BIN DATA NOT UPDATED"
383  FOR WZ = 1 TO 2000: NEXT WZ
384  GOTO 375
390  REM  STOP***PRESS CNTRL Z
392 XX =  PEEK ( - 16384)
393  IF XX <  > (128 + 26) THEN 100
400  REM  PRINT OUTS
402  HOME : VTAB 12: INPUT "INPUT CONVERSION FACTOR FOR DYNAMIC VARIABLE. I.E. C
ONVERTS DIGITAL DATA TO DESIRED VALUE ? (USE 1 IF DIGITAL DATA DESIRED) ? ";CG
405  REM  GET DATE AND TIME OF TEST
406  GOSUB 5000: PRINT
407  GOSUB 4000
408  PRINT D$;"PR#1"
409  PRINT "RPM FOR TEST WAS BETWEEN ";LS;" AND ";HS: PRINT "FURL ANGLE FOR TEST
 WAS ";FURL;" DEG"
410  IF QP = 1 THEN  PRINT "ROTATION WAS CLOCKWISE"
411  IF QP = 0 THEN  PRINT "ROTATION WAS COUNTERCLOCKWISE"
412  PRINT
415  FOR I = 0 TO 35
420  IF N(I) = 0 THEN 450
430  PRINT " YAWRATE (DEG/S)= ";I
435  PRINT "N= ";N(I);" MAX=";CG * MAX(I);" MIN=";CG * MIN(I);" MEAN=";CG * MEAN(
I);" STD DEV=";CG * SE(I)
440  PRINT
450  NEXT I
455  PRINT D$;"PR#0"
460  END
2000  REM
2005  REM  *** SUBR - GET THE TIME
2010  REM *** THESE NEED TO BE CHANGED IF DISK IS NOT USED
2024 SLOT = 4
2025  REM  FOR SLOT 4 ONLY***
2030  PRINT D$;"IN#";SLOT
2040  PRINT D$;"PR#";SLOT
2050  INPUT " ";T$
2060  PRINT D$;"IN#0"
2070  PRINT D$;"PR#0"
2080  RETURN
3000  REM
3001  REM  FOR LEAP YEAR***:L=1
3005  REM  SUBR - STD
3006  REM
3010  REM  CALCULATE SECONDS TO DATE FOR EACH TIME (STD)
3020  REM  THIS IS THE NUMBER OF SECONDS SINCE JANUARY 1
3030  REM  DO THIS FOR STRING TIME T$
3040  REM   RETURN A NUMBER - STD
3050  REM
3060  REM  FIND #'S FOR DATE AND TIME
3070 MT =  VAL ( MID$ (T$,1,2))
3080 D =  VAL ( MID$ (T$,4,2))
3090 H =  VAL ( MID$ (T$,7,2))
3100 M =  VAL ( MID$ (T$,10,2))
```

```
3110 S =   VAL ( MID$ (T$,13,6))
3130  REM   CALCULATE DAYS TO DATE - DTD
3135  RESTORE
3140 DTD = 0
3150  FOR I = 1 TO MT
3160  READ J
3170 DTD = DTD + J
3180  NEXT I
3200  DATA  0,31,28,31,30,31,30,31,31,30,31,30,31
3205  REM    ADD IN DAYS AND LEAP YEAR DAY
3210 DTD = DTD + D
3230  IF MT > 2 AND L = 1 THEN DTD = DTD + 1
3240  REM  FIND SECONDS TO DATE - STD
3250 STD = DTD * 86400 + H * 3600 + M * 60 + S
3300  RETURN
4000  REM
4010  REM  SUBR - PUT SECONDS INTO DAYS, HOURS, MINUTES, SECONDS
4020  REM   GIVEN ET IN SECONDS
4025  PRINT D$;"PR#1"
4030 ET = STD + ET - BEGIN
4040 D =   INT (ET / 86400)
4050 ET = ET - D * 86400
4060 H =   INT (ET / 3600)
4070 ET = ET - H * 3600
4080 M =   INT (ET / 60)
4090 S = ET - M * 60
4091  PRINT : PRINT : PRINT "ELAPSED TIME OF TEST WAS: ": PRINT
4092  PRINT ,D;" DAYS"
4093  PRINT ,H;" HOURS"
4094  PRINT ,M;" MINUTES"
4095  PRINT ,S;" SECONDS"
4096  PRINT : PRINT : PRINT
4097  PRINT D$;"PR#0"
4100  RETURN
5000  REM   SUBROUTINE FOR DATE AND TIME
5001  REM   WILL PRINT TO SCREEN OR PRINTER
5010  REM   *** APPLESOFT DATE AND TIME ***
5020  REM
5030  REM    ******* BY SHERI MUHONEN *******
5040  REM
5050  REM
5060 D$ =   CHR$ (4)
5070  PRINT D$;"NOMON I,O,C": REM   PREVENT DISK COMMANDS FROM PRINTING ON SCREEN
5080 SLOT = 4: REM   FOR CLOCK IN SLOT 4***
5090 YEAR$ = "1900"
5120  REM   READ THE TIME
5130  REM
5140  PRINT D$;"IN#";SLOT: REM   SET INPUT TO CLOCK
5150  PRINT D$;"PR#";SLOT: REM   SET OUPUT TO CLOCK
5170  INPUT " ";T$: REM   OBTAIN TIME
5180  PRINT D$;"IN#0": REM   RESTORE INPUT TO KEYBOARD
5190  PRINT D$;"PR#0": REM   RESTORE OUTPUT TO CRT
5200  REM
5210  REM   OBTAIN MONTH, DAY, HOUR,...ECT
5220  REM
5230 MTH$ =   LEFT$ (T$,2)
5240 DAY$ =   MID$ (T$,4,2)
5250 HOUR$ =   MID$ (T$,7,2)
5260 MINUTE$ =   MID$ (T$,10,2)
5270 SEC$ =   MID$ (T$,13,2)
5280 FRAC$ =   RIGHT$ (T$,3)
```

```
5290  REM
5300  REM    OBTAIN MONTH (JANUARY, FEBRUARY...)
5310  REM
5320  MTH =  VAL (MTH$): REM  FIND DECIMAL # FOR MONTH
5330  RESTORE : FOR I = 0 TO 12: READ DD: NEXT I
5340  FOR I = 1 TO MTH
5350  READ MTH$: REM  FIND NAME OF MONTH
5360  NEXT I
5370  DATA  "JANUARY","FEBRUARY","MARCH","APRIL","MAY","JUNE"
5380  DATA  "JULY","AUGUST","SEPTEMBER","OCTOBER","NOVEMBER","DECEMBER"
5390  REM
5400  REM   OUTPUT DATE AND TIME
5410  REM
5420  PRINT D$;"PR#1"
5430  PRINT "DATE: ";MTH$;" ";DAY$;", ";YEAR$
5450  PRINT "TIME: ";HOUR$;":";MINUTE$;":";SEC$;".";FRAC$
5455  PRINT D$;"PR#0"
5460  RETURN
```

D.7 "BINPLOT" PROGRAMS

D.7.1 Program Logic

1. Provide operator instructions.
2. Name data test file to be plotted.
3. Display menu.
4. Select plot.
5. Read data.

   Note: Steps 4 and 5 may be reversed depending on the plotting program used.

6. Calculate "X" position based on bin number.
7. Calculate "Y" position based on scaling factor and bin data, to include maximum, minimum, mean, standard deviation and number of samples as desired.
8. Plot data on axis scale which was previously loaded in graphics memory.
9. Go to #4 and repeat.
10. End.

```
3   REM   THE BINPLOT.WIND2 PROGRAM
4   REM   *****
5   DIM N(35,2),MAX(35,2),MEAN(35,2),MN(35,2),SE(35,2)
7   HOME : VTAB 5
8   PRINT : PRINT " TYPE -CONT- AFTER PLOT IS DRAWN": PRINT : INPUT "   PRESS RET
URN TO CONT.";W$
9   HOME : VTAB 5
10  D$ = CHR$ (4)
20  INPUT "NAME TEXT FILE FOR PLOTTING? ";Z$
21  PRINT : INPUT "   INPUT DATA DISK";W$
22  PRINT D$;"MON C,I,O"
24  PRINT D$;"OPEN ";Z$: PRINT D$;"READ ";Z$
40  INPUT V1,CHINO,CRPM,CCYCP
50  INPUT SETS,W$,TIME,BP,REV
80  FOR S = 1 TO SETS
90  INPUT K,J,N(J,K),MAX(J,K),MEAN(J,K),MN(J,K),SE(J,K),SBAR
100  NEXT S
105  PRINT D$;"CLOSE ";Z$
107  PRINT : INPUT "   INPUT BINPLOT DISK";W$
110  HOME : VTAB 5: PRINT " SELECT PLOT": PRINT
111  PRINT ,"RPM=1": PRINT ,"CYCLIC PITCH=2": PRINT ,"SAMPLE FREQUENCY=3"
112  PRINT ,"PRINT GRAPH=4"
114  PRINT : INPUT "   ENTER SELECTION > ";QP
115  ON QP GOTO 120,300,1000,7000
120 K = 1
124  HGR
125  POKE - 16302,0
126  HCOLOR= 3
127  PRINT D$;"BLOAD AXIS-RPM"
128 CR = CRPM / V1
130  FOR J = 1 TO 35
140  IF N(J,K) < 10 THEN 250
145 X = 42 + J * 7
170 R = MEAN(J,K) * CR
180  GOSUB 500
210 R = MEAN(J,K) * CR + SE(J,K) * CR: GOSUB 500
215 R1 = R
220 R = MEAN(J,K) * CR - SE(J,K) * CR: GOSUB 500
225 R2 = R
226 Y1 = INT ( - .4677 * R1 + 156.5)
227 Y2 = INT ( - .4677 * R2 + 156.5)
230  IF Y2 > 156 THEN Y2 = 156
232  HPLOT X,Y1 TO X,Y2
250  NEXT J
260  STOP
270  TEXT
280  GOTO 110
300 K = 2
310  HGR : HCOLOR= 3
315  POKE - 16302,0
320  PRINT D$;"BLOAD AXIS-TAU"
330 CC = CCYCP / V1
340  FOR J = 1 TO 35
350  IF N(J,K) = 0 THEN 470
360 X = 42 + J * 7
370 C = MAX(J,K) * CC: GOSUB 600
380 C = MEAN(J,K) * CC: GOSUB 600
390 C = MN(J,K) * CC: GOSUB 600
400 C = MEAN(J,K) * CC + SE(J,K) * CC: GOSUB 600
```

```
410 C1 = C
420 C = MEAN(J,K) * CC - SE(J,K) * CC: GOSUB 600
430 C2 = C
440 Y1 =  INT ( - 12.000 * C1 + 156.5)
450 Y2 =  INT ( - 12.000 * C2 + 156.5)
455  IF Y2 > 156 THEN Y2 = 156
460  HPLOT X,Y1 TO X,Y2
470  NEXT J
480  STOP
485  TEXT
490  GOTO 110
500 Y =  INT ( - .4677 * R + 156.5)
505  IF Y > 156 THEN Y = 156
506  IF Y < 4 THEN Y = 0
510  HPLOT X - 2,Y TO X + 2,Y
520  RETURN
600 Y =  INT ( - 12.000 * C + 156.5)
605  IF Y > 156 THEN Y = 156
606  IF Y < 4 THEN Y = 0
610  HPLOT X - 2,Y TO X + 2,Y
620  RETURN
700  PRINT D$;"PR#1"
705  PRINT : PRINT
707  PRINT "NAME OF TEST FILE IS ";Z$
710  PRINT "START TIME=  ";H$
715  PRINT "  (MTH/DY HR;MIN;SEC.FRAC)"
716  PRINT
720  PRINT "ELAPSED TIME= ";TIME;" HOURS": PRINT
730  PRINT "YAW ANGLE= ";BP;" DEGREES": PRINT
735  PRINT "  AUTOROTATION DATA"
740  PRINT " ROTOR REV.(CALC)= ";REV;" REV.
750  PRINT : PRINT : PRINT
755  PRINT D$;"PR#0"
760  RETURN
1000  REM  SUBR FOR SAMPLES PLOT
1010  GOSUB 700
1020  HGR : HCOLOR= 3: POKE  - 16302,0
1030  PRINT D$;"BLOAD AXIS-SAMPLES"
1040 K = 1
1050  FOR J = 1 TO 35
1055  IF N(J,K) = 0 THEN 1240
1060 X = 42 + J * 7
1100  REM  CALC LOG N
1110 I1 = 1
1120 E1 = 10 ^ I1
1130  IF (N(J,K) - E1) < 0 THEN 1170
1140 I1 = I1 + 1
1145  IF I1 > 6 THEN  STOP
1150  GOTO 1120
1170 I2 = 1
1180 E2 = 10 ^ ((I1 - 1) + (I2 / 24))
1190  IF (N(J,K) - E2) < 0 THEN 1220
1200 I2 = I2 + 1
1205  IF I2 > 24 THEN  STOP
1210  GOTO 1180
1220 Y = 156 - (24 * (I1 - 1) + (I2 - 1))
1230  HPLOT X,Y
1240  NEXT J
1250  STOP
1260  TEXT
1270  GOTO 110
```

```
3    REM   THE BINPLOT.WIND6 PROGRAM
4    REM   *****
5    DIM N(35),MAX(35),MEAN(35),MN(35),SE(35),SBAR(35)
6    HOME : VTAB 5
7    PRINT "    RESET HIMEM IF REQUIRED": PRINT : PRINT
8    PRINT : PRINT " TYPE -CONT- AFTER PLOT IS DRAWN": PRINT : INPUT "    PRESS RET
URN TO CONT.";H$
9    HOME : VTAB 5
10   D$ =  CHR$ (4)
15   PRINT D$;"MON C,I,O"
17   RZ% = 0
20   INPUT "NAME TEXT FILE FOR PLOTTING? ";Z$
25   HOME : VTAB 5: PRINT "SELECT PLOT": PRINT "   ALWAYS SELECT TITLE FIRST": PRI
NT
26   PRINT ,"0.PRINT GRAPH (SMALL)": PRINT ,"1.TITLE PAGE": PRINT ,"2.SAMPLE FREQ
UENCY": PRINT ,"3.RPM": PRINT ,"4.CYCLIC PITCH AMPLE."
27   PRINT ,"5.GEN. POWER": PRINT ,"6.ROTOR POWER": PRINT ,"7.EFFICIENCY": PRINT
,"8.THRUST": PRINT : INPUT "    ENTER SELECTION > ";QP
28   IF QP = 1 THEN 55
29   IF QP = 8 THEN K = 6
30   IF QP = 2 THEN K = 1
31   IF QP = 3 THEN K = 1
32   IF QP = 4 THEN K = 3
33   IF QP = 5 THEN K = 2
34   IF QP = 6 THEN K = 4
35   IF QP = 7 THEN K = 5
36   IF QP = 0 THEN 7000
39   PRINT "SETS= ";ST
40   RZ% = 25 + (K - 1) * (ST / 6) * 8
41   PRINT "RZ= ";RZ%
55   PRINT : INPUT "   INPUT DATA DISK";H$: PRINT D$;"OPEN ";Z$
56   PRINT D$;"POSITION ";Z$;",R ";RZ%
57   PRINT D$;"READ ";Z$
58   IF RZ% > 0 THEN 80
60   INPUT U1,UH,UR,UC,UT,UF,UY,UU
65   INPUT D1,D2,D3,D4,D5,D6,FC
70   INPUT K1$,K2$,K3$,K4$,K5$,K6$
75   INPUT ST,H$,TIME,REV
76   IF RZ% = 0 THEN 105
80   FOR S = 1 TO ST
81   ONERR  GOTO 105
82   INPUT KT
85   IF KT > K THEN 105
86   IF KT < > K THEN  STOP
90   INPUT J,N(J),MAX(J),MEAN(J),MN(J),SE(J),SBAR(J)
100  NEXT S
105  PRINT D$;"CLOSE ";Z$
106  INPUT "   INPUT BINPLOT DISK";H$
107  ON QP GOTO 700,1000,120,300,2000,3000,4000,5000
120  REM  RPM
124  HGR
125  POKE  - 16302,0
126  HCOLOR= 3
127  PRINT D$;"BLOAD AXIS-RPM"
128  CR = UR / U1
130  FOR J = 1 TO 32
140  IF N(J) = 0 THEN 250
145  X = 42 + J * 7
170  R = MEAN(J) * CR
180   GOSUB 500
210  R = MEAN(J) * CR + SE(J) * CR: GOSUB 500
215  R1 = R
```

```
220 R = MEAN(J) * CR - SE(J) * CR: GOSUB 500
225 R2 = R
226 Y1 =   INT ( - .4677 * R1 + 156.5)
227 Y2 =   INT ( - .4677 * R2 + 156.5)
230  IF Y2 > 156 THEN Y2 = 156
232  HPLOT X,Y1 TO X,Y2
250  NEXT J
260  STOP
270  TEXT
280  GOTO 25
300  REM  PLOT ROUTINE
310  HGR : HCOLOR= 3
315  POKE  - 16302,0
320  PRINT D$;"BLOAD AXIS-TAU"
330 CC = UC / U1
340  FOR J = 1 TO 32
350  IF N(J) = 0 THEN 470
360 X = 42 + J * 7
370 C = MAX(J) * CC: GOSUB 600
380 C = MEAN(J) * CC: GOSUB 600
390 C = MIN(J) * CC: GOSUB 600
400 C = MEAN(J) * CC + SE(J) * CC: GOSUB 600
410 C1 = C
420 C = MEAN(J) * CC - SE(J) * CC: GOSUB 600
430 C2 = C
440 Y1 =   INT ( - 12.000 * C1 + 156.5)
445  IF Y1 < 4 THEN Y1 = 4
450 Y2 =   INT ( - 12.000 * C2 + 156.5)
455  IF Y2 > 156 THEN Y2 = 156
460  HPLOT X,Y1 TO X,Y2
470  NEXT J
480  STOP
485  TEXT
490  GOTO 25
500 Y =   INT ( - .4677 * R + 156.5)
505  IF Y > 156 THEN Y = 156
506  IF Y < 4 THEN Y = 0
510  HPLOT X - 2,Y TO X + 2,Y
520  RETURN
600 Y =   INT ( - 12.000 * C + 156.5)
605  IF Y > 156 THEN Y = 156
606  IF Y < 4 THEN Y = 0
610  HPLOT X - 2,Y TO X + 2,Y
620  RETURN
700  PRINT D$;"PR#1"
705  PRINT
707  PRINT "FILE NAME IS  ";Z$
710  PRINT "START TIME=  ";H$
720  PRINT "ELAPSED TIME= ";TIME;" HOURS"
730  PRINT "FURL ANGLE(INCL. TILT OF ROTOR) =";D6;" DEG"
740  PRINT " ROTOR REV.(CALC)= ";REV;" REV.
750  PRINT "ONE VOLT=";U1;"  CWIND=";UH;"  CRPM=";UR;"  CCYPTCH=";UC
760  PRINT "CTORQUE=";UT;"  CFLAP=";UF;"  CYAWPOST=";UY;"  CGEN.VOLTS=";UV
770  PRINT "TEMP (DEG C)=";O1;"  PRESS(ATM)=";O2;"  CORR.FAC.=";FC;"  WIND DIR="
;O3
780  PRINT "GEN. LOAD (OHMS)=";O4;"  GEAR RATIO=";O5;" TO 1"
790  PRINT K1$;"  ";K2$;"  ";K3$
800  PRINT K4$;"  ";K5$;"  ";K6$
810  PRINT
820  PRINT D$;"PR#0"
830  GOTO 25
1000  REM  SUBR FOR SAMPLES PLOT
```

```
1020  HGR : HCOLOR= 3: POKE  - 16302,0
1030  PRINT D$;"BLOAD AXIS-SAMPLES"
1050  FOR J = 1 TO 32
1055  IF N(J) = 0 THEN 1240
1060 X = 42 + J * 7
1100  REM  CALC LOG N
1110  I1 = 1
1120 E1 = 10 ^ I1
1130  IF (N(J) - E1) < 0 THEN 1170
1140 I1 = I1 + 1
1145  IF I1 > 6 THEN  STOP
1150  GOTO 1120
1170 I2 = 1
1180 E2 = 10 ^ ((I1 - 1) + (I2 / 24))
1190  IF (N(J) - E2) < 0 THEN 1220
1200 I2 = I2 + 1
1205  IF I2 > 24 THEN  STOP
1210  GOTO 1180
1220 Y = 156 - (24 * (I1 - 1) + (I2 - 1))
1230  HPLOT X,Y
1240  NEXT J
1250  STOP
1260  TEXT
1270  GOTO 25
2000  REM  GEN POWER PLOT
2010  HGR : HCOLOR= 3: POKE  - 16302,0
2020  PRINT D$;"BLOAD AXIS-G.PWR"
2022  FOR J = 1 TO 32
2024 MAX(J) = 0:MN(J) = 0
2025  NEXT J
2030 CC = (((UV * 1.03) / U1) ^ 2) / D4
2035 CC = CC / 1000
2040  GOTO 340
3000  REM  ROTOR POWER
3010  HGR : HCOLOR= 3: POKE  - 16302,0
3020  PRINT D$;"BLOAD AXIS-R.PWR"
3022  FOR J = 1 TO 32
3024 MAX(J) = 0:MN(J) = 0
3025  NEXT J
3030 CC = (UT * UR * .105) / (U1 ^ 2)
3035 CC = CC / 1000
3040  GOTO 340
4000  REM  EFFICIENCY
4010  HGR : HCOLOR= 3: POKE  - 16302,0
4020  PRINT D$;"BLOAD AXIS-EFF."
4022  FOR J = 1 TO 32
4024 MAX(J) = 0:MN(J) = 0
4025  NEXT J
4030 CC = ((UV * 1.03) ^ 2) / (UT * UR * .105 * D4)
4035 CC = CC * 10
4040  GOTO 340
5000  REM  THRUST
5010  HGR : HCOLOR= 3: POKE  - 16302,0
5020  PRINT D$;"BLOAD AXIS-THRUST"
5030 CC = UV / U1
5035 CC = CC / 150
5040  GOTO 340
7000  REM  PLOT SUBROUTINE
7010  HOME : VTAB 10
7020  PRINT "LARGE OR SMALL (L/S)"
7030  INPUT "  ENTER > ";ANS$
```

```
7040   IF ANS$ = "S" THEN 7500
7050   REM   PRINT LARGE PICTURE
7055   REM   PRINTER IN SLOT 1
7060   POKE 1272,0
7061   POKE 1144,32
7062   POKE 1400,1
7063   POKE 1528,128
7064   POKE 1656,1
7065   CALL  - 16000
7080   GOTO 25
7500   CALL  - 16046
7510   GOTO 25
```

```
3   REM   THE BINPLOT.WIND2.FAST PROGRAM
4   REM   *****
5   DIM N(35),MAX(35),MEAN(35),HM(35),SE(35),SBAR(35)
6   HOME : VTAB 5
7   PRINT "   RESET HIMEM IF REQUIRED": PRINT : PRINT
8   PRINT : PRINT " TYPE -CONT- AFTER PLOT IS DRAWN": PRINT : INPUT "    PRESS RET
URN TO CONT.";H$
9   HOME : VTAB 5
10  D$ =  CHR$ (4)
15   PRINT D$;"MON C,I,O"
17  RZ% = 0
20   INPUT "NAME TEXT FILE FOR PLOTTING? ";Z$
25   HOME : VTAB 5: PRINT "SELECT PLOT": PRINT "  ALWAYS SELECT TITLE FIRST": PRI
NT
26   PRINT ,"0.PRINT GRAPH (SMALL)": PRINT ,"1.TITLE PAGE": PRINT ,"2.SAMPLE FREQ
UENCY": PRINT ,"3.RPM": PRINT ,"4.ROTOR POWER"
27   PRINT : INPUT "    ENTER SELECTION > ";QP
28   IF QP = 1 THEN 55
30   IF QP = 2 THEN K = 1
31   IF QP = 3 THEN K = 1
32   IF QP = 4 THEN K = 2
36   IF QP = 0 THEN 7000
39   PRINT "SETS= ";ST
40  RZ% = 25 + (K - 1) * (ST / 2) * 8
41   PRINT "RZ= ";RZ%
55   PRINT : INPUT "  INPUT DATA DISK";H$: PRINT D$;"OPEN ";Z$
56   PRINT D$;"POSITION ";Z$;",R ";RZ%
57   PRINT D$;"READ ";Z$
58   IF RZ% > 0 THEN 80
60   INPUT U1,UH,UR,UC,UT,UF,UY,UU
65   INPUT D1,D2,D3,D4,D5,D6,FC
70   INPUT K1$,K2$,K3$,K4$,K5$,K6$
75   INPUT ST,H$,TIME,REV
76   IF RZ% = 0 THEN 105
80   FOR S = 1 TO ST
81   ONERR  GOTO 105
82   INPUT KT
85   IF KT > K THEN 105
86   IF KT <  > K THEN  STOP
90   INPUT J,N(J),MAX(J),MEAN(J),HM(J),SE(J),SBAR(J)
100   NEXT S
105   PRINT D$;"CLOSE ";Z$
106   INPUT "  INPUT BINPLOT DISK";H$
107   ON QP GOTO 700,1000,120,3000
120   REM   RPM
124   HGR
125   POKE  - 16302,0
126   HCOLOR= 3
127   PRINT D$;"BLOAD AXIS-RPM"
128  CR = UR / U1
130   FOR J = 1 TO 32
140   IF N(J) = 0 THEN 250
145  X = 42 + J * 7
170  R = MEAN(J) * CR
180   GOSUB 500
210  R = MEAN(J) * CR + SE(J) * CR: GOSUB 500
215  R1 = R
220  R = MEAN(J) * CR - SE(J) * CR: GOSUB 500
225  R2 = R
226  Y1 =  INT ( - .4677 * R1 + 156.5)
227  Y2 =  INT ( - .4677 * R2 + 156.5)
```

```
230   IF Y2 > 156 THEN Y2 = 156
232   HPLOT X,Y1 TO X,Y2
250   NEXT J
260   STOP
270   TEXT
280   GOTO 25
300   REM   PLOT ROUTINE
310   HGR : HCOLOR= 3
315   POKE  - 16302,0
320   PRINT D$;"BLOAD AXIS-TAU"
330 CC = UC / U1
340   FOR J = 1 TO 32
350   IF N(J) = 0 THEN 470
360 X = 42 + J * 7
370 C = MAX(J) * CC: GOSUB 600
380 C = MEAN(J) * CC: GOSUB 600
390 C = MN(J) * CC: GOSUB 600
400 C = MEAN(J) * CC + SE(J) * CC: GOSUB 600
410 C1 = C
420 C = MEAN(J) * CC - SE(J) * CC: GOSUB 600
430 C2 = C
440 Y1 =   INT ( - 12.000 * C1 + 156.5)
445   IF Y1 < 4 THEN Y1 = 4
450 Y2 =   INT ( - 12.000 * C2 + 156.5)
455   IF Y2 > 156 THEN Y2 = 156
460   HPLOT X,Y1 TO X,Y2
470   NEXT J
480   STOP
485   TEXT
490   GOTO 25
500   Y =   INT ( - .4677 * R + 156.5)
505   IF Y > 156 THEN Y = 156
506   IF Y < 4 THEN Y = 0
510   HPLOT X - 2,Y TO X + 2,Y
520   RETURN
600   Y =   INT ( - 12.000 * C + 156.5)
605   IF Y > 156 THEN Y = 156
606   IF Y < 4 THEN Y = 0
610   HPLOT X - 2,Y TO X + 2,Y
620   RETURN
700   PRINT D$;"PR#1"
705   PRINT
707   PRINT "FILE NAME IS   ";Z$
710   PRINT "START TIME=   ";H$
720   PRINT "ELAPSED TIME= ";TIME;" HOURS"
730   PRINT "FURL ANGLE(INCL. TILT OF ROTOR) =";O6;" DEG"
740   PRINT " ROTOR REV.(CALC)= ";REV;" REV.
750   PRINT "ONE VOLT=";U1;"   CWIND=";UH;"   CRPM=";UR;"   CCYPTCH=";UC
760   PRINT "CTORQUE=";UT;"   CFLAP=";UF;"   CYAWPOST=";UY;"   CGEN.VOLTS=";UV
770   PRINT "TEMP (DEG C)=";O1;"   PRESS(ATM)=";O2;"   CORR.FAC.=";FC;"   WIND DIR="
;O3
780   PRINT "GEN. LOAD (OHMS)=";O4;"   GEAR RATIO=";O5;" TO 1"
790   PRINT K1$;"   ";K2$;"   ";K3$
800   PRINT K4$;"   ";K5$;"   ";K6$
810   PRINT
820   PRINT D$;"PR#0"
830   GOTO 25
1000   REM   SUBR FOR SAMPLES PLOT
1020   HGR : HCOLOR= 3: POKE  - 16302,0
1030   PRINT D$;"BLOAD AXIS-SAMPLES"
1050   FOR J = 1 TO 32
1055   IF N(J) = 0 THEN 1240
```

D48

```
1060 X = 42 + J * 7
1100  REM   CALC LOG N
1110 I1 = 1
1120 E1 = 10 ^ I1
1130  IF (N(J) - E1) < 0 THEN 1170
1140 I1 = I1 + 1
1145  IF I1 > 6 THEN  STOP
1150  GOTO 1120
1170 I2 = 1
1180 E2 = 10 ^ ((I1 - 1) + (I2 / 24))
1190  IF (N(J) - E2) < 0 THEN 1220
1200 I2 = I2 + 1
1205  IF I2 > 24 THEN  STOP
1210  GOTO 1180
1220 Y = 156 - (24 * (I1 - 1) + (I2 - 1))
1230  HPLOT X,Y
1240  NEXT J
1250  STOP
1260  TEXT
1270  GOTO 25
2000  REM   GEN POWER PLOT
2010  HGR : HCOLOR= 3: POKE  - 16302,0
2020  PRINT D$;"BLOAD AXIS-G.PWR"
2022  FOR J = 1 TO 32
2024 MAX(J) = 0:MN(J) = 0
2025  NEXT J
2030 CC = (((UV * 1.03) / U1) ^ 2) / D4
2035 CC = CC / 1000
2040  GOTO 340
3000  REM   ROTOR POWER
3010  HGR : HCOLOR= 3: POKE  - 16302,0
3020  PRINT D$;"BLOAD AXIS-R.PWR"
3022  FOR J = 1 TO 32
3024 MAX(J) = 0:MN(J) = 0
3025  NEXT J
3030 CC = (UT * UR * .105) / (U1 ^ 2)
3035 CC = CC / 1000
3040  GOTO 340
4000  REM   EFFICIENCY
4010  HGR : HCOLOR= 3: POKE  - 16302,0
4020  PRINT D$;"BLOAD AXIS-EFF."
4022  FOR J = 1 TO 32
4024 MAX(J) = 0:MN(J) = 0
4025  NEXT J
4030 CC = ((UV * 1.03) ^ 2) / (UT * UR * .105 * D4)
4035 CC = CC * 10
4040  GOTO 340
5000  REM   THRUST
5010  HGR : HCOLOR= 3: POKE  - 16302,0
5020  PRINT D$;"BLOAD AXIS-THRUST"
5030 CC = UY / U1
5035 CC = CC / 150
5040  GOTO 340
7000  REM   PLOT PICTURE
7010  HOME : VTAB 10
7020  PRINT "LARGE OR SMALL (L/S)"
7030  INPUT "  ENTER > ";ANS$
7040  IF ANS$ = "S" THEN 7500
7050  REM   PRINT LARGE PICTURE
7055  REM   PRINTER IN SLOT 1
7060  POKE 1272,0
```

```
7061  POKE 1144,32
7062  POKE 1400,1
7063  POKE 1528,128
7064  POKE 1656,1
7065  CALL - 16000
7080  GOTO 25
7500  CALL - 16046
7510  GOTO 25
```

```
3   REM   THE BINPLOT.RPM6 PROGRAM
4   REM   ****
5   DIM N(35),MAX(35),MEAN(35),MN(35),SE(35),SBAR(35)
6   HOME : VTAB 5
7   PRINT "    RESET MIMEM IF REQUIRED": PRINT : PRINT
8   PRINT : PRINT " TYPE -CONT- AFTER PLOT IS DRAWN": PRINT : INPUT "    PRESS RET
URN TO CONT.";H$
9   HOME : VTAB 5
10  D$ =  CHR$ (4)
15   PRINT D$;"MON C,I,O"
17  RZ% = 0
20   INPUT "NAME TEXT FILE FOR PLOTTING? ";Z$
25   HOME : VTAB 5: PRINT "SELECT PLOT": PRINT "  ALWAYS SELECT TITLE FIRST": PRI
NT
26   PRINT ,"0.PRINT GRAPH (SMALL)": PRINT ,"1.TITLE PAGE": PRINT ,"2.SAMPLE FREQ
UENCY": PRINT ,"3.MEAN FLAP": PRINT ,"4.FLAP AMPL."
27   PRINT ,"5.FRONT ACCEL. ": PRINT ,"6.IN PLANE AMPL.": PRINT ,"7.V. BOOM AMPL.
": PRINT ,"8.CYCLIC PITCH AMPL.": PRINT : INPUT "     ENTER SELECTION > ";QP
28   IF QP = 1 THEN 55
29   IF QP = 8 THEN K = 6
30   IF QP = 2 THEN K = 1
31   IF QP = 3 THEN K = 1
32   IF QP = 4 THEN K = 2
33   IF QP = 5 THEN K = 3
34   IF QP = 6 THEN K = 4
35   IF QP = 7 THEN K = 5
36   IF QP = 0 THEN 7000
39   PRINT "SETS= ";ST
40  RZ% = 25 + (K - 1) * (ST / 6) * 8
41   PRINT "RZ= ";RZ%
55   PRINT : INPUT "  INPUT DATA DISK";H$: PRINT D$;"OPEN ";Z$
56   PRINT D$;"POSITION ";Z$;",R ";RZ%
57   PRINT D$;"READ ";Z$
58   IF RZ% > 0 THEN 80
60   INPUT U1,UB,UR,UC,UT,UF,UY,UU
65   INPUT D1,D2,D3,D4,D5,D6,FC
70   INPUT K1$,K2$,K3$,K4$,K5$,K6$
75   INPUT ST,H$,TIME,REV
76   IF RZ% = 0 THEN 105
80   FOR S = 1 TO ST
81   ONERR  GOTO 105
82   INPUT KT
85   IF KT > K THEN 105
86   IF KT < > K THEN  STOP
90   INPUT J,N(J),MAX(J),MEAN(J),MN(J),SE(J),SBAR(J)
100   NEXT S
105   PRINT D$;"CLOSE ";Z$
106   PRINT : INPUT "  INPUT BINPLOT DISK";H$
107   ON QP GOTO 700,1000,2000,3000,4000,5000,6000,300:
300   REM   PLOT ROUTINE
310   HGR : HCOLOR= 3
315   POKE  - 16302,0
320   PRINT D$;"PR#1"
322   PRINT "     PLOT OF CYCLIC PITCH AMPLITUDE VS RPM FOLLOWS"
324   PRINT "     ONE VOLT = ";UC;" DEGREES"
325   PRINT D$;"PR#0"
327   PRINT D$;"BLOAD AXIS-VOLTS/RPM"
330 CC = 2 / U1
340   FOR J = 1 TO 32
350   IF N(J) = 0 THEN 470
360 X = 42 + J * 7
370 C = MAX(J) * CC: GOSUB 600
```

```
380 C = MEAN(J) * CC: GOSUB 600
390 C = HN(J) * CC: GOSUB 600
400 C = MEAN(J) * CC + SE(J) * CC: GOSUB 600
410 C1 = C
420 C = MEAN(J) * CC - SE(J) * CC: GOSUB 600
430 C2 = C
440 Y1 =  INT ( - 12.000 * C1 + 156.5)
450 Y2 =  INT ( - 12.000 * C2 + 156.5)
455  IF Y2 > 156 THEN Y2 = 156
460  HPLOT X,Y1 TO X,Y2
470  NEXT J
480  STOP
485  TEXT
490  GOTO 25
500 Y =  INT ( - .4677 * R + 156.5)
505  IF Y > 156 THEN Y = 156
506  IF Y < 4 THEN Y = 0
510  HPLOT X - 2,Y TO X + 2,Y
520  RETURN
600 Y =  INT ( - 12.000 * C + 156.5)
605  IF Y > 156 THEN Y = 156
606  IF Y < 4 THEN Y = 0
610  HPLOT X - 2,Y TO X + 2,Y
620  RETURN
700  PRINT D$;"PR#1"
705  PRINT
707  PRINT "FILE NAME IS  ";Z$
710  PRINT "START TIME=  ";H$
720  PRINT "ELAPSED TIME= ";TIME;" HOURS"
730  PRINT "FURL ANGLE(INCL. TILT OF ROTOR) =";D6;" DEG"
740  PRINT " ROTOR REV.(CALC)= ";REV;" REV.
750  PRINT "ONE VOLT=";U1;"  CBOOM=";U8;"  CCYLCPTCH=";UC
760  PRINT "CINPLNE=";UT;"  CFLAP=";UF;"  CF.ACCEL=";UV
770  PRINT "TEMP (DEG C)=";D1;"  PRESS(ATM)=";D2;"  CORR.FAC.=";FC;"  WIND DIR="
;D3
780  PRINT "GEN. LOAD (OHMS)=";D4;"  GEAR RATIO=";D5;" TO 1"
790  PRINT K1$;"  ";K2$;"  ";K3$
800  PRINT K4$;"  ";K5$;"  ";K6$
810  PRINT
820  PRINT D$;"PR#0"
830  GOTO 25
1000  REM  SUBR FOR SAMPLES PLOT
1020  HGR : HCOLOR= 3: POKE  - 16302,0
1030  PRINT D$;"BLOAD AXIS-SAMPLES/RPH"
1050  FOR J = 1 TO 32
1055  IF N(J) = 0 THEN 1240
1060 X = 42 + J * 7
1100  REM  CALC LOG N
1110  I1 = 1
1120  E1 = 10 ^ I1
1130  IF (N(J) - E1) < 0 THEN 1170
1140  I1 = I1 + 1
1145  IF I1 > 6 THEN  STOP
1150  GOTO 1120
1170  I2 = 1
1180  E2 = 10 ^ ((I1 - 1) + (I2 / 24))
1190  IF (N(J) - E2) < 0 THEN 1220
1200  I2 = I2 + 1
1205  IF I2 > 24 THEN  STOP
1210  GOTO 1180
1220  Y = 156 - (24 * (I1 - 1) + (I2 - 1))
1230  HPLOT X,Y
```

```
1240   NEXT J
1250   STOP
1260   TEXT
1270   GOTO 25
2000   REM   MEAN FLAP
2010   HGR : HCOLOR= 3: POKE   - 16302,0
2025   PRINT D$;"PR#1"
2026   PRINT "    PLOT OF MEAN FLAP VS RPM FOLLOWS"
2027   PRINT "      ONE VOLT = ";UF;" NM FLAP BENDING"
2030 CC = 2 / U1
2035   PRINT D$;"PR#0"
2039   PRINT D$;"BLOAD AXIS-VOLTS/RPM"
2040   GOTO 340
3000   REM   FLAP AMPL.
3010   HGR : HCOLOR= 3: POKE   - 16302,0
3020   PRINT D$"PR#1"
3022   PRINT "    PLOT OF FLAP AMPLITUDE VS RPM FOLLOWS"
3024   PRINT "      ONE VOLT = ";UF;" NM FLAP BENDING"
3025   PRINT D$;"PR#0"
3030 CC = 2 / U1
3035   PRINT D$;"BLOAD AXIS-VOLTS/RPM"
3040   GOTO 340
4000   REM   YAWPOST AMPL.
4010   HGR : HCOLOR= 3: POKE   - 16302,0
4020   PRINT D$"PR#1"
4022   PRINT "    PLOT OF FRONT ACCELEROMETER AMPLITUDE VS RPM FOLLOWS"
4025   PRINT "      ONE VOLT = ";UY;" .2 G"
4028   PRINT D$;"PR#0"
4030 CC = 2 / U1
4035   PRINT D$;"BLOAD AXIS-VOLTS/RPM"
4040   GOTO 340
5000   REM   TORQUE AMPL.
5010   HGR : HCOLOR= 3: POKE   - 16302,0
5020   PRINT D$;"PR#1"
5022   PRINT "    PLOT OF IN PLANE AMPLITUDE VS RPM FOLLOWS"
5024   PRINT "      ONE VOLT = ";UT;" NM IN PLANE BENDING"
5028   PRINT D$;"PR#0"
5030 CC = 2 / U1
5035   PRINT D$;"BLOAD AXIS-VOLTS/RPM"
5040   GOTO 340
6000   REM   V. BOOM AMPL.
6010   HGR : HCOLOR= 3: POKE   - 16302,0
6020   PRINT D$;"PR#1"
6022   PRINT "    PLOT OF VERTICAL BOOM BENDING AMPLITUDE VS RPM FOLLOWS"
6024   PRINT "      ONE VOLT = ";UB;" NM BOOM BENDING"
6028   PRINT D$;"PR#0"
6030 CC = 2 / U1
6035   PRINT D$;"BLOAD AXIS-VOLTS/RPM"
6040   GOTO 340
7000   REM   PLOT SUBROUTINE
7010   HOME : VTAB 10
7020   PRINT "LARGE OR SMALL (L/S)
7030   INPUT "  ENTER > ";ANS$
7040   IF ANS$ = "S" THEN 7500
7050   REM   PRINT LARGE PICTURE
7055   REM   PRINTER IN SLOT 1
7060   POKE 1272,0
7061   POKE 1144,32
7062   POKE 1400,1
7063   POKE 1528,128
7064   POKE 1656,1
7065   CALL   - 16000
7080   GOTO 25
7500   CALL   - 16046
7510   GOTO 25
```

D.7.6 Listing For "BINPLOT-YAWRATE" Program

```
3   REM   THE BINPLOT.YAWRATE PROGRAM
4   REM   *****
5   DIM N(35,2),MAX(35,2),MEAN(35,2),MN(35,2),SE(35,2)
7   HOME : VTAB 5
8   PRINT : PRINT " TYPE -CONT- AFTER PLOT IS DRAWN": PRINT : INPUT "    PRESS RET
URN TO CONT.";W$
9   HOME : VTAB 5
10  D$ =  CHR$ (4)
20   INPUT "NAME TEXT FILE FOR PLOTTING? ";Z$
21   PRINT : INPUT "    INPUT DATA DISK";W$
22   PRINT D$;"MON C,I,O"
24   PRINT D$;"OPEN ";Z$: PRINT D$;"READ ";Z$
40   INPUT SETS,FURL,C6,V1,NAS$,FL$,LS,HS
50   INPUT MTHS$,DAYS$,YEARS$,HOURS$,MINUTE$
60   INPUT SECS$,H,M,S
65  SD = S
80   FOR S = 1 TO SETS
90   INPUT K,J,N(J,K),MAX(J,K),MEAN(J,K),MN(J,K),SE(J,K),SBAR
100   NEXT S
105   PRINT D$;"CLOSE ";Z$
107   PRINT : INPUT "    INPUT BINPLOT DISK";W$
110   HOME : VTAB 5: PRINT " SELECT PLOT": PRINT
111   PRINT ,"0.PRINT GRAPH": PRINT ,"1.TITLE": PRINT ,"2.CCW SAMPLES": PRINT ,"3
.CW SAMPLES": PRINT ,"4.CCW": PRINT ,"5.CW"
112   PRINT : INPUT "    ENTER SELECTION > ";QP
114   IF QP = 0 THEN 1500
115   ON QP GOTO 700,1000,1000,300,300
300   IF QP = 4 THEN K = 1
301   IF QP = 5 THEN K = 2
310   HGR : HCOLOR= 3
315   POKE  - 16302,0
320   PRINT D$;"BLOAD AXIS-YAWRATE"
330  CC = C6 / V1
340   FOR J = 1 TO 32
350   IF N(J,K) < 5 THEN 470
360  X = 42 + J * 7
380  C = MEAN(J,K) * CC: GOSUB 600
400  C = MEAN(J,K) * CC + SE(J,K) * CC: GOSUB 600
410  C1 = C
420  C = MEAN(J,K) * CC - SE(J,K) * CC: GOSUB 600
430  C2 = C
440  Y1 =  INT ( - 12.000 * C1 + 156.5)
450  Y2 =  INT ( - 12.000 * C2 + 156.5)
455   IF Y2 > 156 THEN Y2 = 156
456   IF Y1 < 4 THEN Y1 = 4
460   HPLOT X,Y1 TO X,Y2
470   NEXT J
480   STOP
485   TEXT
490   GOTO 110
600  Y =  INT ( - 12.000 * C + 156.5)
605   IF Y > 156 THEN Y = 156
606   IF Y < 4 THEN Y = 0
610   HPLOT X - 2,Y TO X + 2,Y
620   RETURN
700   PRINT D$;"PR#1"
705   PRINT : PRINT
707   PRINT "NAME OF TEST FILE IS ";FL$
708   PRINT "NAME OF TEST IS ";NA$
710   PRINT : PRINT "START TIME WAS ";MTH$;" ";DAYS$;", ";YEARS$
```

```
715  PRINT ,HOURS;":";MINUTES;" HOURS"
720  PRINT "ELAPSED TIME="
721  PRINT ,H;" HOURS"
722  PRINT ,M;" MINUTES"
723  PRINT ,SD;" SECONDS"
730  PRINT "FURL ANGLE= ";FURL;" DEGREES"
740  PRINT "CALIBRATION CONSTANTS  : CG=";CG;"   ONE VOLT=";V1
750  PRINT : PRINT : PRINT
755  PRINT D$;"PR#0"
760  GOTO 110
1000 REM   SUBR FOR SAMPLES PLOT
1010 IF QP = 2 THEN K = 1
1011 IF QP = 3 THEN K = 2
1020 HGR : HCOLOR= 3: POKE  - 16302,0
1030  PRINT D$;"BLOAD AXIS-SAMPLES/YAWRATE"
1050 FOR J = 1 TO 32
1055 IF N(J,K) = 0 THEN 1240
1060 X = 42 + J * 7
1100 REM   CALC LOG N
1110 I1 = 1
1120 E1 = 10 ^ I1
1130 IF (N(J,K) - E1) < 0 THEN 1170
1140 I1 = I1 + 1
1145 IF I1 > 6 THEN  STOP
1150  GOTO 1120
1170 I2 = 1
1180 E2 = 10 ^ ((I1 - 1) + (I2 / 24))
1190 IF (N(J,K) - E2) < 0 THEN 1220
1200 I2 = I2 + 1
1205 IF I2 > 24 THEN  STOP
1210  GOTO 1180
1220 Y = 156 - (24 * (I1 - 1) + (I2 - 1))
1230  HPLOT X,Y
1240  NEXT J
1250  STOP
1260  TEXT
1270  GOTO 110
1500 REM   PRINTER
1510 CALL  - 16046
1520  GOTO 110
```

D.8 COEFFICIENT OF PERFORMANCE ANALYSIS; "CP" PROGRAM

D.8.1 Program Logic

1.   Provide user instructions.
2.   Determine data source.
3.   Read data (i.e., rotor power and number of samples vs. bin number).
4.   Enter bin limits for analysis.
5.   Calculate total data points in all bins.
6.   Calculate mean wind speed.
7.   Calculate mean wind power and speed at which it occurs based on air density corrected for pressure and temperature.
8.   Calculate average CP using mean rotor power over all bins and corrected air density.
9.   Print results.
10. Calculate CP by bin number with mean rotor power and corrected air density.
11. Print results.
12. Load CP axis vs. bin number.
13. Plot CP vs. bin number, if desired.
14. Plot rotor power vs. bin number if desired.
15. End.

D.8.2 Documentation for CP Program

I1	Rotor Power Per Bin.
I2	Wind Power Per Bin.
I3	Rotor Performance Coefficient Per Bin.
JL	Lower Bin Used for Analysis.
JU	Upper Bin Used for Analysis.
MP	Mean Wind Power Over All Bins.
MR	Mean Rotor Power Over All Bins.
M3	Average Cube of Wind Speed or Wind Speed at Mean Wind Power.
PC	Rotor Coefficient of Performance, C_p.
QP	File Selector.
RZ%	Position Selector on Disk.
SB	Array of C_p Values Per Bin.
SUM	Number of Sample Points, Total.
SW	Average Wind Speed for Test.
Z$	Bin Plot Data File Name.

```
3   REM   THE CP PROGRAM
4   REM   *****
5   DIM N(35),MAX(35),MEAN(35),HN(35),SE(35),SBAR(35)
6   HOME : VTAB 5
7   PRINT "   RESET HIMEM IF REQUIRED": PRINT : PRINT
8   PRINT : PRINT " TYPE -CONT- AFTER PLOT IS DRAWN": PRINT : INPUT "   PRESS RET
URN TO CONT.";H$
9   HOME : VTAB 5
10  D$ =  CHR$ (4)
15  PRINT D$;"MON C,I,O"
17  RZ% = 0
20  INPUT "NAME TEXT FILE FOR PLOTTING? ";Z$
25  HOME : VTAB 5: PRINT "IS THIS A WIND6 OR WIND2.FAST PROGRAM ?": PRINT : PRIN
T "WIND6 = 1": PRINT "WIND2.FAST = 2"
27  PRINT : INPUT "   ENTER SELECTION > ";QP
28  IF QP = 1 THEN K = 4
29  IF QP = 1 THEN OP = 6
30  IF QP = 2 THEN K = 2
31  IF QP = 2 THEN OP = 2
35  GOTO 55
38  PRINT D$;"CLOSE ";Z$
39  PRINT "SETS= ";ST
40  RZ% = 25 + (K - 1) * (ST / OP) * 8
41  PRINT "RZ= ";RZ%
55  PRINT : INPUT "  INPUT DATA DISK";H$: PRINT D$;"OPEN ";Z$
56  PRINT D$;"POSITION ";Z$;",R ";RZ%
57  PRINT D$;"READ ";Z$
58  IF RZ% > 0 THEN 80
60  INPUT U1,UH,UR,UC,UT,UF,UY,UU
65  INPUT O1,O2,O3,O4,O5,O6,FC
70  INPUT K1$,K2$,K3$,K4$,K5$,K6$
75  INPUT ST,H$,TIME,REV
76  GOTO 38
80  FOR S = 1 TO ST
81  ONERR  GOTO 105
82  INPUT KT
85  IF KT > K THEN 105
86  IF KT < > K THEN  STOP
90  INPUT J,N(J),MAX(J),MEAN(J),HN(J),SE(J),SBAR(J)
100  NEXT S
105  PRINT D$;"CLOSE ";Z$
106  INPUT "  INPUT BINPLOT DISK";H$
107  GOSUB 700
140  INPUT "ENTER LOWER AND UPPER BIN LIMITS FOR CALCULATIONS > ";JL,JU
150  REM   SUM POINTS
160  FOR J = JL TO JU
170  SUM = SUM + N(J)
175  NEXT J
180  REM   FIND MEAN WIND SPEED
185  FOR J = JL TO JU
190  SW = SW + J * N(J) * .5
195  NEXT J
200  SW = SW / SUM
210  REM   MEAN WIND^3
215  FOR J = JL TO JU
220  M3 = M3 + N(J) * (J / 2) ^ 3
230  NEXT J
235  M3 = M3 / SUM
236  MP = M3 * .5 * 1.23 * 3.14159 * (3.81 ^ 2) / FC
240  M3 = M3 ^ .3333
```

```
245  FOR J = JL TO JU
246 MR = MR + MEAN(J) * N(J)
247  NEXT J
248 MR = MR / SUM
249 MR = MR * (UT * UR * .105 / (U1 ^ 2))
250 PC = MR / MP
251  PRINT D$;"PR#1"
252  PRINT "   DATA ANALYSIS FOR FILE  ";Z$
253  PRINT
255  PRINT "MEAN WIND SPEED(M/S)=";SW
256  PRINT "MEAN WIND PWR (WATTS)=";MP
257  PRINT "SPEED AT MEAN WIND POWER=";M3
258  PRINT "MEAN ROTOR POWER(WATTS)=";MR
259  PRINT "AVERAGE CP=";PC
260  PRINT "TOTAL SAMPLES=";SUM
262  FOR J = JL TO JU
264 I1 = MEAN(J) * (UT * UR * .105) / (U1 ^ 2)
266 I2 = 1.23 * 3.14159 * (3.81 ^ 2) * ((J / 2) ^ 3) / (2 * FC)
268 I3 = I1 / I2
270  PRINT "WIND SPEED (M/S)=";J / 2;"  CP=";I3
272 SB(J) = I3
273  NEXT J
275  PRINT D$;"PR#0"
276  INPUT "DO YOU WISH TO PLOT CP VS WIND SPEED (Y/N)";W$
278  IF W$ = "N" THEN  STOP
279  HGR :HCOLR = 3: POKE  - 16302,0
282  PRINT D$;"BLOAD AXIS-CP"
284  FOR J = JL TO JU
286 X = 42 + J * 7
288 C = SB(J) * 10
290 Y =  INT ( - 12 * C + 156.5)
292  IF Y > 156 THEN Y = 156
293  IF Y < 4 THEN Y = 0
294  HPLOT X,Y
295  NEXT J
296  STOP
298  TEXT
300  INPUT "DO YOU WANT TO PRINT GRAPH?";W$
302  IF W$ = "Y" THEN  CALL  - 16046
304  INPUT "DO YOU WANT TO PLOT ROTOR POWER BINPLOT? (Y/N)";W$
306  IF W$ = "Y" THEN  GOTO 3000
308  STOP
330  REM  PLOT ROUTINE
340  FOR J = 1 TO 32
350  IF N(J) = 0 THEN 470
360 X = 42 + J * 7
370 C = MAX(J) * CC: GOSUB 600
380 C = MEAN(J) * CC: GOSUB 600
390 C = MN(J) * CC: GOSUB 600
400 C = MEAN(J) * CC + SE(J) * CC: GOSUB 600
410 C1 = C
420 C = MEAN(J) * CC - SE(J) * CC: GOSUB 600
430 C2 = C
440 Y1 =  INT ( - 12.000 * C1 + 156.5)
445  IF Y1 < 4 THEN Y1 = 4
450 Y2 =  INT ( - 12.000 * C2 + 156.5)
455  IF Y2 > 156 THEN Y2 = 156
460  HPLOT X,Y1 TO X,Y2
470  NEXT J
480  STOP
485  TEXT
```

```
496    INPUT " DO YOU WISH TO PRINT GRAPH?";H$
497    IF H$ = "Y" THEN  CALL  - 16046
499    END
600 Y =  INT ( - 12.000 * C + 156.5)
605    IF Y > 156 THEN Y = 156
606    IF Y < 4 THEN Y = 0
610    HPLOT X - 2,Y TO X + 2,Y
620    RETURN
700    PRINT D$;"PR#1"
705    PRINT
707    PRINT "FILE NAME IS   ";Z$
710    PRINT "START TIME=   ";H$
720    PRINT "ELAPSED TIME= ";TIME;" HOURS"
730    PRINT "FURL ANGLE(INCL. TILT OF ROTOR) =";O6;" DEG"
740    PRINT " ROTOR REV.(CALC)= ";REV;" REV.
750    PRINT "ONE VOLT=";U1;"  CHIND=";UH;"  CRPM=";UR;"  CCYPTCH=";UC
760    PRINT "CTORQUE=";UT;"  CFLAP=";UF;"  CYAWPOST=";UY;"  CGEN.VOLTS=";UV
770    PRINT "TEMP (DEG C)=";O1;"  PRESS(ATM)=";O2;"  CORR.FAC.=";FC;"  WIND DIR="
;O3
780    PRINT "GEN. LOAD (OHMS)=";O4;"  GEAR RATIO=";O5;" TO 1"
790    PRINT K1$;"   ";K2$;"   ";K3$
800    PRINT K4$;"   ";K5$;"   ";K6$
810    PRINT
820    PRINT D$;"PR#0"
830    RETURN
3000   REM  ROTOR POWER
3010   HGR : HCOLOR= 3: POKE  - 16302,0
3020   PRINT D$;"BLOAD AXIS-R.PWR"
3022   FOR J = 1 TO 32
3024 HAX(J) = 0:HMX(J) = 0
3025   NEXT J
3030 CC = (UT * UR * .105) / (U1 ^ 2)
3035 CC = CC / 1000
3040   GOTO 340
```

D.9 AXIS PLOTTING ROUTINES

All axis plots are based on these programs with minor changes in axis labelling
or scaling.

D.9.1 Program Logic

1.   Load graphics character generator.
2.   Print vertical scale.
3.   Print horizontal scale.
4.   Draw axis lines.
5.   Print vertical label.
6.   Print horizontal label.
7.   Print grid scale lines.
8.   Plot constant tip speed ratio lines (rpm only).
9.   Save Axis as a binary file.
10.   End.

D.9.2 Listing For "RPM AXIS PLOT" Program

```
5   REM   THE RPM AXIS PLOT PROGRAM
6   REM   *****
10  D$ =   CHR$ (4)
15   HGR : HCOLOR= 3
20   PRINT D$;"BRUN HI-RES CHARACTER GENERATOR"
26   PRINT D$;"BLOAD GREEK LETTERS"
40   FOR I = 1 TO 7:: HTAB 3: VTAB 3 * I - 1: PRINT 350 - 50 * I: NEXT I
60   FOR I = 1 TO 3: VTAB 21: HTAB 6 + 10 * I: PRINT 5 * I: NEXT I
70   HPLOT 42,4 TO 266,4 TO 266,156 TO 42,156 TO 42,4
80   FOR I = 1 TO 3: HTAB 1: VTAB 6 + I
81   IF I = 1 THEN  PRINT "R"
82   IF I = 2 THEN  PRINT "P"
83   IF I = 3 THEN  PRINT "M"
84   NEXT I
90   VTAB 24: HTAB 8: PRINT "RPM US WIND SPEED (M/S)"
100  FOR Y = 4 TO 153 STEP 149: FOR X = 77 TO 266 STEP 35
110  HPLOT X,Y + 1 TO X,Y + 3
120  NEXT X: NEXT Y
130  FOR X = 42 TO 263 STEP 221: FOR Y = 12 TO 132 STEP 24
140  HPLOT X + 1,Y TO X + 3,Y
150  NEXT Y: NEXT X
160  FOR LAM = 5 TO 20 STEP 5: FOR X = 46 TO 266 STEP 4
170  Y = 156 - .086 * (X - 42) * LAM
175  IF Y < 4 THEN Y = 4
180  HPLOT X,Y
190  NEXT X: NEXT LAM
200  VTAB 10: HTAB 35: PRINT "%=5"
210  VTAB 2: HTAB 30: PRINT "10"
220  VTAB 2: HTAB 22: PRINT "15"
230  VTAB 2: HTAB 18: PRINT "20"
240  PRINT D$;"BSAVE AXIS-RPM,A$2000,L$2000"
250  END
```

D.9.3 Listing For "TAU AXIS PLOT" Program

```
5   REM   THE TAU AXIS PLOT PROGRAM
6   REM   *****
10  D$ =   CHR$ (4)
15   HGR : HCOLOR= 3
17   POKE  - 16302,0
20   PRINT D$;"BRUN HI-RES CHARACTER GENERATOR"
26   PRINT D$;"BLOAD GREEK LETTERS"
40   FOR I = 1 TO 7:: HTAB 3: VTAB 3 * I - 1: PRINT 14 - 2 * I: NEXT I
60   FOR I = 1 TO 3: VTAB 21: HTAB 6 + 10 * I: PRINT 5 * I: NEXT I
70   HPLOT 42,4 TO 266,4 TO 266,156 TO 42,156 TO 42,4
80   FOR I = 1 TO 5: HTAB 1: VTAB 6 + I
81   IF I = 1 THEN  PRINT "*"
82   IF I = 2 THEN  PRINT " "
83   IF I = 3 THEN  PRINT "O"
84   IF I = 4 THEN  PRINT "E"
85   IF I = 5 THEN  PRINT "G"
86   NEXT I
90   VTAB 24: HTAB 5: PRINT "CYCLIC PITCH US WIND SPEED (M/S)"
100  FOR Y = 4 TO 153 STEP 149: FOR X = 77 TO 266 STEP 35
110  HPLOT X,Y + 1 TO X,Y + 3
120  NEXT X: NEXT Y
130  FOR X = 42 TO 263 STEP 221: FOR Y = 12 TO 132 STEP 24
140  HPLOT X + 1,Y TO X + 3,Y
150  NEXT Y: NEXT X
240  END
```

D.9.4 Listing For "VOLTS AXIS PLOT" Program

```
5   REM   THE VOLTS AXIS PLOT PROGRAM
6   REM   *****
10  D$ =  CHR$ (4)
15  HGR : HCOLOR= 3
17  POKE  - 16302,0
20  PRINT D$;"BRUN HI-RES CHARACTER GENERATOR"
26  PRINT D$;"BLOAD GREEK LETTERS"
40  FOR I = 1 TO 7:: HTAB 3: VTAB 3 * I - 1: PRINT 7 - I: NEXT I
60  FOR I = 1 TO 4: VTAB 21: HTAB 6 + 8 * I: PRINT 75 * I: NEXT I
70  HPLOT 42,4 TO 266,4 TO 266,156 TO 42,156 TO 42,4
80  FOR I = 1 TO 5: HTAB 1: VTAB 6 + I
81  IF I = 1 THEN  PRINT "V"
82  IF I = 2 THEN  PRINT "O"
83  IF I = 3 THEN  PRINT "L"
84  IF I = 4 THEN  PRINT "T"
85  IF I = 5 THEN  PRINT "S"
86  NEXT I
90  VTAB 24: HTAB 12: PRINT " VOLTS  US  RPM"
100  FOR Y = 4 TO 153 STEP 149: FOR X = 98 TO 266 STEP 56
110  HPLOT X,Y + 1 TO X,Y + 3
120  NEXT X: NEXT Y
130  FOR X = 42 TO 263 STEP 221: FOR Y = 12 TO 132 STEP 24
140  HPLOT X + 1,Y TO X + 3,Y
150  NEXT Y: NEXT X
160  PRINT D$;"BSAVE AXIS-VOLTS/RPM,A$2000,L$2000"
240  END
```

D.9.5 Listing For "SAMPLES AXIS PLOT" Program

```
5   REM   THE SAMPLES AXIS PLOT PROGRAM
6   REM   *****
10  D$ =  CHR$ (4)
12  PRINT D$;"NOMON C,I,O"
15  HGR : HCOLOR= 3
16  POKE  - 16302,0
20  PRINT D$;"BRUN HI-RES CHARACTER GENERATOR"
26  PRINT D$;"BLOAD GREEK LETTERS"
40  FOR I = 1 TO 7:: HTAB 4: VTAB 3 * I - 1: PRINT 7 - I: NEXT I
60  FOR I = 1 TO 3: VTAB 21: HTAB 6 + 10 * I: PRINT 5 * I: NEXT I
70  HPLOT 42,4 TO 266,4 TO 266,156 TO 42,156 TO 42,4
80  FOR I = 1 TO 5: HTAB 1: VTAB 6 + I
81  IF I = 1 THEN  PRINT "L"
82  IF I = 2 THEN  PRINT "O"
83  IF I = 3 THEN  PRINT "G"
84  IF I = 4 THEN  PRINT " "
85  IF I = 5 THEN  PRINT "N"
86  NEXT I
90  VTAB 24: HTAB 3: PRINT "LOG SAMPLES (N) US WIND SPEED (M/S)"
100  FOR Y = 4 TO 153 STEP 149: FOR X = 77 TO 266 STEP 35
110  HPLOT X,Y + 1 TO X,Y + 3
120  NEXT X: NEXT Y
130  FOR X = 42 TO 263 STEP 221: FOR Y = 12 TO 132 STEP 24
140  HPLOT X + 1,Y TO X + 3,Y
150  NEXT Y: NEXT X
160  FOR X = 42 TO 263 STEP 221: FOR Y = 19 TO 139 STEP 24
170  HPLOT X + 1,Y TO X + 2,Y
180  NEXT Y: NEXT X
200  PRINT D$;"BSAVE AXIS-SAMPLES,A$2000,L$2000"
240  END
```

APPENDIX E

TEST WIND TURBINE ASSEMBLY DRAWINGS

VIEW A-A

5703552 ACTUATOR
12VDC 12.0 STROKE
PERFORMANCE PAK
SAGINAW STEERING
GEAR

A

MODEL E-95 ALTERNATOR
(REWOUND) MAREMONT

TORQUE ARM

E.V B-B

- WIRING LEAD THRU

- 115 DIA MORSE SHAFT MOUNTED REDUCER

-ING ASSY

- TACH. GENERATOR

A   B

-ASTRAL WILCON
 MODIFIED AW-10B MACHINE

MRC 48 SEALMASTER

ROHN VS-19 TOWER SECTION

ASTRAL WILCON AW-10B
GLASS FIBER-EPOXY
COMPOSITE BLADES

NUTA, INC.	
REPORT NO: SERI/TR-8085-15	
TEST WIND TURBINE	
NACELL AND ROTOR ASSEMBLY	
DWG. NO: E-8008-WG 25-2	DEC 1980

NG-25-2

E-3

204.0

100.0

60 FT.

TOWER HINGE
1/10 SIZE

WUTA, INC

REPORT NO. SERI/TR-8085-15

TEST WIND TURBINE
GENERAL ARRANGEMENT

DWG. NO. C 8008-WG-25-1   DEC. 1980

E-4

APPENDIX F

SIGNAL AND POWER DISTRIBUTION SCHEMATIC DIAGRAMS

ROTATING SYSTEM

YAW POST

BOOM

FRONT ACCELEROMETER

THERMOCOUPLES

MAGNETIC PICKUP

ALTERNATOR

ANEMOMETER

STARTER MOTOR DC TACH GENERATOR

CYCLIC PITCH AMPLITUDE
IN PLANE STRAIN
FLAP STRAIN
TORQUE

YAW POST POSITION
FOR-AFT YAW POST STRAIN
SIDE YAW POST STRAIN

BOOM POSITION
HORIZONTAL BOOM STRAIN
VERTICAL BOOM STRAIN

AMBIENT TEMPERATURE
GENERATOR/ACTUATOR TEMPERATURE

ROTOR RPM

STATOR
FIELD

WIND SPEED

STARTER MOTOR
FORWARD/REVERSE SWITCH

VISHAY MODEL 2120

SIGNAL CONDITIONING, BUFFER ISOLATION

MULTIPLE OUTPUTS >> COMPUTER INPUT

MULTIPLE OUTPUTS >> OSCILLOGRAPH INPUT

MULTIPLE OUTPUTS >> METER INPUT

>> OSCILLOGRAPH INPUT

RESISTIVE LOAD BANK

LOAD SWITCH

RECTIFIER & CAPACITOR CIRCUIT

LOAD VOLTAGE

SIGNAL CONDITIONING, FILTERING, BUFFER ISOLATION

ROTOR RPM OUTPUT

MULTIPLE OUTPUTS >> COMPUTER INPUT

MULTIPLE OUTPUTS >> OSCILLOGRAPH INPUT

MULTIPLE OUTPUTS >> METER INPUT

O2

O1

STARTER/DC. TACH SWITCH

WUTA, INC.
REPORT NO:
SERI/TR-8085-15
SIGNAL AND POWER
DISTRIBUTION SCHEMATIC
DIAGRAM —— PAGE 1 OF 2
DWG. NO: B8008-F1 | DEC. 1987.

F-2

FURL/UNFURL
ACTUATOR

ACTUATOR
INDICATOR

S TO ABT SYSTEM INVERTER

S TO FURL/UNFURL
CONTROL RELAYS

FURL/UNFURL
AUTO-MANUAL
MODE
SELECT SW.

FURL/UNFURL
CONTROL
RELAYS
MAIN SW.

12V.

EMERGENCY
OVERRIDE
FURL/UNFURL
CONTROL SW.

MAIN POWER SW.
TO FURL/UNFURL
ACTUATOR AND
INVERTER

12V.

FURL/UNFURL
MANUAL
CONTROL
SYSTEM

BATTERY PACK

FURL/UNFURL
AUTOMATIC
SAFETY
SYSTEM

24V.

STARTER SYSTEM
MAIN SWITCH

FROM A/C CONDITIONING
SYSTEM

12V. BATTERY
CHARGER

12V. BATTERY
CHARGER

12V A.C.
LINE

WUTA, INC.		
REPORT NO:	SERI/TR-8085-15	
	SIGNAL AND POWER	
	DISTRIBUTION SCHEMATIC	
	DIAGRAM-----PAGE 2 OF 2	
DWG. NO: B-8008-F2	DEC. 1982	

F-3

APPENDIX G

SHORT ABSTRACT

ROTATING SYSTEM
— CYCLIC PITCH AMPLITUDE
— IN PLANE STRAIN
— FLAP STRAIN
— TORQUE

YAW POST
— YAW POST POSITION
— FOR-AFT YAW POST STRAIN
— SIDE YAW POST STRAIN

BOOM
— BOOM POSITION
— HORIZONTAL BOOM STRAIN
— VERTICAL BOOM STRAIN

FRONT ACCELEROMETER

THERMOCOUPLES
— AMBIENT TEMPERATURE
— GENERATOR/ACTUATOR TEMPERATURE

MAGNETIC PICK-UP
— ROTOR RPM

VISHAY MODEL 2120

SIGNAL CONDITIONING BUFFER ISOLATION

MULTIPLE OUTPUTS > COMPUTER INPUT

MULTIPLE OUTPUTS > OSCILLOGRAPH INPUT

MULTIPLE OUTPUTS > METER INPUT

> OSCILLOGRAPH INPUT

ALTERNATOR
STATOR
FIELD

ANEMOMETER
WIND SPEED

STARTER MOTOR
D.C. TACH GENERATOR

RECTIFIER & CAPACITOR CIRCUIT

STARTER MOTOR FORWARD/REVERSE SWITCH

RESISTIVE LOAD BANK

LOAD SWITCH

LOAD VOLTAGE

STARTER/D.C. TACH SWITCH

SIGNAL CONDITIONING, FILTERING, BUFFER ISOLATION

ROTOR RPM OUTPUT

MULTIPLE OUTPUTS > COMPUTER INPUT

MULTIPLE OUTPUTS > OSCILLOGRAPH INPUT

MULTIPLE OUTPUTS > METER INPUT

O2

O2

O1

O1

WUTA, INC.
REPORT NO.
SERI/TR-80185-14
SIGNAL AND POWER
DISTRIBUTION SCHEMATIC
DIAGRAM —— PAGE 1 OF 2
DWG NO. B8008-F1 | DEC 1981

FURL/UNFURL ACTUATOR

ACTUATOR INDICATOR

TO ABT SYSTEM INVERTER

TO FURL/UNFURL CONTROL RELAYS

FURL/UNFURL CONTROL RELAYS MAIN SW.

FURL/UNFURL AUTO-MANUAL MODE SELECT SW

FURL/UNFURL AUTOMATIC SAFETY SYSTEM

FURL/UNFURL MANUAL CONTROL SYSTEM

EMERGENCY OVERRIDE FURL/UNFURL CONTROL SW.

MAIN POWER SW. TO FURL/UNFURL ACTUATOR AND INVERTER

12V

12V

BATTERY PACK

24V

STARTER SYSTEM MAIN SWITCH

12 V BATTERY CHARGER

12 V BATTERY CHARGER

12 V AC LINE

FROM SIGNAL CONDITIONING SYSTEM

O2

O1

WUTA, INC.

REPORT NO:
SERI/TR-8085-15

SIGNAL AND POWER DISTRIBUTION SCHEMATIC DIAGRAM-----PAGE 2 of 2

DWG. NO: B 8076-F2